FACULTY OF Bioscience Engineering
DEPARTMENT OF BIOSYSTEMS.
CROP BIOTECHNICS DIVISION
Willem De Croylaan 42
B-3001 HEVERLEE, BELGIUM
tel. + 32 16 37 70 12
bert.stvns@gmail.com

Bert Stevens

ADDRESSING WATER STRESS IN BANANA-BASED CROPPING SYSTEMS

January 2021

KU LEUVEN

ARENBERG DOCTORAL SCHOOL
FACULTY OF BIOSCIENCE ENGINEERING

ADDRESSING WATER STRESS IN BANANA-BASED CROPPING SYSTEMS

Evaluating the applicability of the *AquaCrop* computer simulation model for banana plantations

Bert Stevens

Supervisor(s):
Prof. Rony Swennen
Prof. Jan Diels
Prof. Patrick Ndakidemi
Dr. Eline Vanuytrecht

Dissertation presented in partial fulfilment of the requirements for the degree of Doctor of Bioscience Engineering (PhD)
January 2021

ADDRESSING WATER STRESS IN BANANA-BASED CROPPING SYSTEMS

Evaluating the applicability of the AquaCrop computer simulation model for banana plantations

Bert STEVENS

Supervisor(s):
Prof. Dr. Ir. R. Swennen
Prof. Dr. Ir. J. Diels
Prof. Dr. P. Ndakidemi
Dr. Ir. E. Vanuytrecht

Dissertation presented in partial fulfilment of the requirements for the degree of Doctor of Bioscience Engineering (PhD)

Members of the Examination Committee:
Prof. Dr. Ir. V. Van Noort (Chair)
Prof. Dr. Ir. D. Raes
Prof. Dr. Ir. B. Muys
Dr. Ir. S. Carpentier
Dr. Ir. P. Schmitter
International Water Management Institute, Myanmar
Prof. Dr. K. Mtei
Nelson Mandela African Institute of Science and Technology, Tanzania

January 2021

Doctoraatsproefschrift nr. 1671 aan de faculteit Bio-ingenieurswetenschappen van de KU Leuven

© 2021 KULeuven – Faculty of Bioscience Engineering
Uitgegeven in eigen beheer, Bert Stevens, Willem de Croylaan 42 - box 2427, 3001 Leuven

Alle rechten voorbehouden. Niets uit deze uitgave mag worden vermenigvuldigd en/of openbaar gemaakt worden door middel van druk, fotokopie, microfilm, elektronisch of op welke andere wijze ook zonder voorafgaandelijke schriftelijke toestemming van de uitgever.

All rights reserved. No part of the publication may be reproduced in any form by print, photoprint, microfilm, electronic or any other means without written permission from the publisher.

Acknowledgements

No man is an island.

I could not have written this thesis without the support of those surrounding me. It seems impossible to thank all the people who consciously or subconsciously drove my PhD to fruition. Their shoulders are the foundation upon which this thesis rests.

Firstly, I would like to thank Rony Swennen, my supervisor, for providing me with the opportunity of doing a PhD. Thanks for guiding and accompanying me on this journey through the world of bananas. I appreciate the trust you put in me, the passion with which you have always given feedback and I sincerely value our open conversations. From the initial conception of the research plan to the very end, thanks for being there at every step of the way and teaching me the merits of assertiveness.

Secondly, I would like to thank my co-supervisors Jan Diels, Eline Vanuytrecht and assessor Dirk Raes. Their critical eye helped me to focus on the crop modelling aspect when I could no longer see through the banana forest. Also, thanks to my co-supervisor Patrick Ndakidemi, who brought me back to the banana forest when modelling was all I could see.

To all my colleagues at KULeuven and the Laboratory of Tropical Crop Improvement, it was a pleasure to work amongst you. David and Clara, thanks for sharing the office, and always watering my plants when I was away. For someone working on drought, such a small gesture is highly regarded.

Many thanks to my colleagues at NM-AIST and IITA. Thanks, Allan Brown, for hosting me in the fields, and thanks to the field team for making me feel at home there. Erick Wangaely, Salim Ramadhani, Joshua Jackson, Emanuel Nasolwa and Stanley Bayo, you are the engine behind this project, and I am forever grateful. Asante Sana. Thanks to Hassan Mduma and Veronica Massawe for their practical guidance and Scola Ponera and Joyce Rugakingila for administrative support.

Friends and family, I love you all very dearly… more than words can express. Thanks for your continuous support and belief.

A special thanks goes out to the entire Tanzanian people, whose hospitality, good cheer, and life lessons I can never repay.

And lastly, thanks to the donors for making this project possible. Primarily the VLIR-UOS VLADOC scholarship but also those who supported this work through their contributions to the CGIAR Fund and in particular to the CGIAR Research Program for Roots, Tubers, and Bananas.

We are who we surround ourselves with, and I have been surrounded by the best. I can only hope their wisdom, passion, work ethic, humor, empathy, congeniality, … rubbed off on me.

Bert Stevens

Summary

Bananas and plantains are the 12th most produced crops worldwide (in tons), the fourth most produced crops in Africa, and as such the world's most popular fruits. Water is considered the most important abiotic factor threatening production. Banana production needs to increase to feed a growing and wealthier population, under increasingly variable climatic conditions whilst simultaneously reducing water footprints to enhance environmental sustainability. To achieve this, proper plantation management is crucial. Crop simulation models can act as tools to guide management in reducing water footprints, yet despite bananas' popularity, no widely used model exists that accurately simulates biomass and yield in relation to soil moisture and irrigation. Previous banana simulation models (e.g. CENTURY, STICS, LINTUL, SIMBA, AAB plantain model) were either empirical, and not based on underlying physiology, or based on physiological principles, but requiring too extensive knowledge on calibration processes to lead to accurate simulation and/or widespread adoption. Of the plethora of current simulation models, the water driven AquaCrop model, developed by the Food and Agricultural Organization of the United Nations, shows promise. It has been calibrated and used accurately for over 15 different annual crops in multiple environments characterized by differences in climates, soil, and management schemes. So far, banana (a multi-cycle perennial crop) has not been included in this model.

The general aim of this PhD research was to assess the applicability of the AquaCrop simulation model for a banana field over the course of two crop (harvest) cycles (C1 and C2).

A field experiment was set up in Arusha, Tanzania using two cultivars: the diploid Mchare - Huti Green Bell (HG) and the triploid Cavendish - Grande Naine (GN), to assess growth and production under fully irrigated (FI) and water-limited rainfed (RF) conditions to act as a database for AquaCrop modelling. The design was a blocked design with drip irrigation as treatment. All plots received irrigation for the first four months post-transplant, after which irrigation treatments were applied based on daily soil water contents (SWC), as measured by time domain reflectometry. FI plots received irrigation whenever more than 25% of total available water was about to be depleted. No supplemental irrigation was provided to the RF plots after the establishment period, except from December 2018 to February 2019 to limit plant death in the field.

Field observations showed SWC in the FI plots was close to field capacity over the course of the entire field experiment whilst in RF plots soil moisture closely followed the seasonal variation in rainfall, leading to differences in SWC between FI and RF plots, affecting production.

As canopy cover (CC) is used as a system variable in AquaCrop modelling, both CC and the leaf area index (LAI) were studied at the plantation level as an indicator for growth and drought. Results indicate CC and LAI were reduced 8-9 weeks after the start of SWC divergence between RF and FI treatments in both cultivars, leading to a reduction in CC growth rate (r and cgc) and maximum CC (CC_x) in RF plots. CC varied diurnally under conditions of high evaporative demand (ET_0 > 3 mm day^{-1}) following the diurnal leaf folding pattern. This diurnal pattern was increased under increased soil moisture depletion levels. To be able to calculate CC values based on LAI, cultivar-specific CC-LAI curves were created following the Lambert-Beer equation. Curves were different between cultivars, whereby HG had a lower extinction coefficient (0.52) than GN (0.67), which might be related to their respective ploidy. As CC growth over time deviated between FI and RF plots, CC seems a promising indicator for water deficit in the field in the presence of a fully irrigated plot acting as a reference.

Diurnally, CC was more affected by evaporative demand than soil moisture depletion. Leaf folding on its own can thereby also occur in optimally irrigated plots, although soil moisture depletion might still enhance these CC diurnal drops.

In studying biomass (B) and yield (Y), weighted least square regression models were built for (1) estimating aboveground vegetative dry biomass ($ABGVD$) and corm dry biomass ($cormD$) and (2) forecasting bunch fresh weight ($bunchF$), based on non-destructive parameters for our two cultivars, whereby it was checked whether relationships differed under different irrigation regimes. Generally, irrigation sped up phenology and improved growth and yield, indicating soil moisture affected production. Pseudostem volume (V_{pseudo}) proved a good predictor for estimating $ABGVD$, but was suboptimal for $cormD$ estimation due to its subterranean position. $ABGVD$ and $cormD$ models were not different for FI and RF plots. V_{pseudo} at flowering ($V_{pseudo,flower}$) proved to be a good predictor for $bunchF$ in FI plots. Significant differences were observed between cultivars and between treatments indicating allometric plasticity under drought during bunch filling. As such, bunch allometry was affected by irrigation, proving $bunchF$ forecasting needs to include information on moisture stress during bunch filling or information on bunch parameters at harvest.

Using the insights and database from this field trial, AquaCrop was calibrated and evaluated for the first two crop cycles of GN, whereby phenology, CC, SWC, B and Y data were used for calibration. The AquaCrop model scheme was adjusted to simulate (1) C1 and C2 cycles of banana successively and (2) drip irrigation. Goodness-of-fit indicators used were *R^2, relative root mean square error, Nash and Sutcliffe model performance and Willmott's index of Agreement*. Based on these indicators, FI and RF plots were simulated with good to moderate good accuracy for all parameters: CC, SWC, B and Y. Slight underestimations of B in RF plots could have resulted from differences in root extension in the dry season which led to lower SWC in the root zone during simulations than were observed. Even so, our adjustments to AquaCrop proved capable in modelling initial plantations of banana under drip irrigation, and our research provided first estimates of parameter calibration for crop files of C1 and C2 banana plantations to be used in AquaCrop. Successive modelling of banana cycles as a fruit crop, can be used in initial plantations characterized by a narrow flowering and harvest timeframe. Our calibrated crop files can be used for model assistance in setting up plantations (considering slight adjustment to local conditions and cultivars). This is handy as commercial growers often replant to achieve harvest peaks when necessary. Further validation and evaluation in young banana fields (using different cultivars) is necessary to test our calibrated crop parameters, especially under drought and nutrient stress. Additionally, the proposed AquaCrop adjustment to model drip irrigation needs to be further fine-tuned, and the phenological delay under drought (as observed in banana plantations) can be included in AquaCrop to achieve better model simulations and a better model performance for banana plantations.

Future AquaCrop research needs to focus on mature plantations (i.e. beyond C2) when the banana population structure will become even more heterogeneous. AquaCrop still seems useful for simulating mature plantations. In such plantations, the only additional requirement will be to estimate harvest dynamics over the course of a year and assess how this will be influenced by soil moisture. As such, our research shows the clear promise of modelling banana plantations (both initial cycles as mature plantations) with AquaCrop.

Samenvatting

Banaan (en plantaan) is het twaalfde meest geproduceerde gewas (in ton) in de wereld, het vierde in Afrika, en daarbij ook het belangrijkste fruitgewas. De geschatte bevolkingsgroei, het veranderende klimaat en een toenemende duurzaamheidszin in het gebruik van water, zetten toekomstige bananenproductie onder druk. De grootste abiotische stress in de bananenproductie is watertekort. In gebieden waar neerslag onvoldoende is, biedt irrigatie een oplossing, maar momenteel wordt wereldwijd 70% van het zoetwater al gebruikt in de landbouwsector. Een goed irrigatiebeheer is cruciaal, maar eenvoudige beslissingsondersteunende hulpmiddelen om watergebruik in een plantage te verminderen en productie te verhogen bestaan momenteel niet.

Tot op heden bestaat er geen eenvoudig, accuraat, en universeel gebruikt gewasmodel om de groei van bananenplantages en hun bodemvochtdynamiek te simuleren. Van de hele resem aan huidige modellen (e.g. CENTURY, STICS, LINTUL, SIMBA, AAB plantain model) - die veelal enkel bruikbaar zijn door onderzoekers, of niet praktisch bruikbaar door een gebrek aan accuraatheid of onderliggende fysiologische wetmatigheden - lijkt het AquaCrop model de beste kandidaat. Dit model werd in 2009 gecreëerd door de Wereldvoedselorganisatie van de Verenigde Naties. AquaCrop werd al voor meer dan 15 éénjarige gewassen gekalibreerd en toont goede simulaties in verschillende omgevingen, dit onder verschillende weersomstandigheden, bodems, gewassen en veldbeheer. Van alle gewassen is banaan het meest geproduceerde gewas ter wereld waarvoor AquaCrop nog niet gekalibreerd is.

Deze thesis tracht als eerste het AquaCrop model te gebruiken voor het simuleren van de groei van bananenplantages in de eerste twee groeicycli.

Een veldexperiment werd opgezet in Arusha, Tanzania. Twee verschillende bananencultivars: Mchare-Huti Green Bell (HG) en Cavendish-Grande Naine (GN) werden onderworpen aan twee verschillende irrigatieregimes: optimale druppelirrigatie gebaseerd op bodemvochtgehaltes (*full irrigation*, FI) en regen-gevoede productie (*rainfed,* RF). Groei en fenologie van de cultivars werden opgevolgd gedurende twee groeicycli (C1 en C2) en vergeleken met de onderliggende vochtregimes om een database aan te leggen voor kalibratie van AquaCrop. Bodemvochtgehaltes ($Soil\ water\ content, SWC$) werden dagelijks opgevolgd met tijdsdomeinreflectometrie-sensoren. Bodemvocht in de FI behandeling bleef gedurende het hele experiment voornamelijk nabij veldcapaciteit, terwijl bodemvocht in de RF behandeling de seizoenale variatie in neerslag volgde, en tot verwelkingspunt daalde in de droge seizoenen. Plantgroei werd opgevolgd in termen van fenologie (bloei en oogsttijdstip), bodembedekkingsgraad ($Canopy\ Cover, CC$), bladoppervlakte-index ($Leaf\ Area\ Index,\ LAI$), biomassa (B) en trosopbrengst ($Yield,\ Y$).

Irrigatie versnelde fenologie en verbeterde groei en opbrengst in het veld. CC en LAI in RF behandelingen daalden 8-9 weken nadat bodemvochtgehaltes voor de eerste keer verschilden van FI behandelingen. Lagere bodemvochtgehaltes reduceerden groei snelheden (r en cgc) en maximum CC (CC_x) in RF proefvlakken. CC toonde bovendien een dagelijks patroon, ten gevolge van bladvouwing, onder een grote verdampingsvraag. CC bereikte maximale waarden 's ochtends, nam af tot minimale waarden 's middags, en klom terug naar maximale waarden in de late namiddag/avond. Dit patroon werd versterkt onder toenemende vochtstress. CC-LAI curves werden opgesteld voor de verschillende cultivars volgens de Lambert-Beer vergelijking, waarbij HG een lagere extinctie-coëfficiënt toonde dan GN, wat mogelijks gelinkt is aan hun ploidie.

Gewogen kleinste-kwadraten regressie-modellen werden vervolgens opgesteld om (1) B op niet-destructieve wijze te monitoren over de tijd en om (2) Y te voorspellen alvorens planten oogstrijp waren. Parameters die op niet-destructieve wijze bepaald konden worden, werden gebruikt als predictoren in de modellen. Aparte B modellen werd opgesteld voor bovengrondse vegetatieve biomassa ($ABGVD$) en ondergrondse cormus biomassa ($cormD$). Het effect van irrigatie op de modellen, allometrische plasticiteit, werd gecontroleerd. Pseudostamvolume (V_{pseudo}) was een goede predictor voor $ABGVD$, maar niet voor $cormD$, waarschijnlijk door diens ondergrondse positie. Modellen verschilden niet tussen irrigatieregimes. Om vers trosgewicht ($bunchF$) te voorspellen, bleek pseudostam volume bij bloei ($V_{pseudo,flower}$) een goede predictor. $bunchF$ modellen verschilden significant tussen irrigatieregimes, en cultivars omdat indicatoren bij bloei geen informatie bevatten over het vochtregime en groei tijdens de trosvulling die het uiteindelijke trosgewicht zullen bepalen. Onze $bunchF$ modellen voor FI behandelingen kunnen gebruikt worden om optimale trosgewichten bij oogst te schatten bij optimaal beheer tijdens de trosvulling. Om effectieve trosgewichten te bekomen is informatie nodig over het vochtregime tijdens trosvulling of dienen parameters bij oogst in de modellen opgenomen te worden.

Met de verzamelde data en inzichten van het veld, werd voor de eerste maal het AquaCrop model gekalibreerd en geëvalueerd voor de eerste twee groeicycli van de Cavendish GN cultivar. Fenologie, CC, SWC, B en Y data werden gebruikt voor kalibratie. Een aanpassing aan het AquaCrop model werd voorgesteld voor het modelleren van (1) de eerste twee groeicycli van banaan en (2) druppelirrigatie. Statistische indicatoren die gebruikt werden waren: *R²*, *relative root mean square error*, *Nash and Sutcliffe model performance* en *Willmot's index of Agreement*. Afgaande op deze indicatoren en bijhorende grafische analyse, bekwamen we een goede simulatie van alle parameters (CC, SWC, B en Y) in RF en FI behandelingen over de twee groeicycli. B werd lichtjes onderschat in de RF behandeling wat te wijten kon zijn aan een ondersimulatie van het SWC in vergelijking met geobserveerde SWC waarden. Deze onderschatting was echter minimaal waardoor we kunnen concluderen dat AquaCrop in staat was om de eerste twee groeicycli van een plantage correct te simuleren. Ons onderzoek heeft daarbij voor de eerste maal de kalibratie van gewasbestanden van C1 en C2 bananenplantages kunnen doen voor gebruik in AquaCrop. Door gewascycli achtereenvolgens te simuleren is er aldus een nieuwe stap gezet voor het simuleren van meerjarige gewassen in AquaCrop. Jonge en hernieuwde plantages, gekarakteriseerd door smalle bloei- en oogsttijdstippen, kunnen gebruik maken van het AquaCrop model, en de gekalibreerde crop parameters in ons onderzoek (aangepast aan lokale omstandigheden) als leidraad gebruiken voor simulaties.

Verder onderzoek in jonge plantages is noodzakelijk om deze gewasparameters voor C1 en C2 te testen en verder aan te passen, vooral onder droogte – en - nutriëntstress. Een betere inclusie van druppelirrigatie en de invoeging van de fenologische vertraging onder droogtestress kunnen eveneens leiden tot een betere simulatie met AquaCrop. Volwassen plantages verschillen qua samenstelling van jonge plantages (meer heterogeen, planten van verschillende leeftijden). In zulke scenario's is er wellicht een kleine aanpassing van onze vooropgestelde AquaCrop simulatie en kalibratie nodig. AquaCrop wordt verwacht bruikbaar te blijven voor heterogene plantages, waarbij de enige extra parameter een schatting van de oogstfrequenties in het veld doorheen het jaar is, en hoe deze beïnvloed wordt door bodemvochtgehaltes. Ons onderzoek toont hierbij de geschiktheid van AquaCrop aan in het modelleren van bananenplantages.

Abbreviations and symbols

$ABGVD$	Aboveground vegetative dry weight
A_{drip}	Horizontal area wetted by drippers
A_{field}	Horizontal area of the field surface
A_{Root}	Horizontal area of the root zone container
b	Extinction coefficient Lambert-Beer equation
B	Dry above-ground crop biomass
B_{rate}	Bunch growth rate
$bunchF$	Bunch fresh weight
$C1$	Cycle 1
$C2$	Cycle 2
$C3$	Cycle 3
CC	Green canopy cover
CC_0	Initial green canopy cover
CC_{rel}	Relative canopy cover
CC_x	Maximum green canopy cover
cdc	Canopy decline coefficient
cgc	Canopy growth coefficient
CO_2	Carbon dioxide
$cormD$	Corm dry weight
CR	Capillary rise
DAP	Days after planting
$deadL$	Dead leaves
DM	Dry matter
DP	Deep percolation
Dr	Root zone moisture depletion
DTF	Days to flower emergence
$DTFI$	Days to flower initiation
DTH	Days to harvest
E	Soil evaporation
EAH	East African Highlands
$EAHB$	East African Highland Banana
ECA	East and Central Africa
ET	Evapotranspiration

ET_0	Reference evapotranspiration
FAO	Food and agricultural organization of the united nations
FC	Field capacity
FCD	Flower cycle duration
f_{drip}	Fraction of the wetted area by the drippers
FI	Full Irrigation
$fingerF$	Individual finger weight
f_{root}	fraction of the root zone container
f_{sink}	Crop performance under elevated atmospheric CO2 conditions
$functL$	Functional leaves
G_{base}	Girth of pseudostem at base of pseudostem
GDD	Growing degree days
$GDDF$	Growing degree days from planting/selection to flower emergence
$GDDFI$	Growing degree days from planting/selection to flower initiation
$GDDH$	Growing degree days from planting/selection to harvest
G_{mid}	Girth of pseudostem at middle of pseudostem
GN	Cavendish - Grande Naine
$Grade$	Bunch maturity grade
H	Height of pseudostem
HCD	Harvest cycle duration
HG	Mchare - Huti Green Bell
HI	Harvest index
HI_0	Reference harvest index
$IITA$	International Institute of Tropical Agriculture
$IPCC$	Intergovernmental Panel on Climate Change
Kc_{Tr}	Crop transpiration coefficient
K_E	Soil evaporation coefficient
K_{ET}	Evapotranspiration coefficient
Ks	Stress coefficient
K_{sat}	Saturated hydraulic conductivity
Ks_{aer}	Vol% for anaerobiotic point at which deficient aeration occurs
Ks_b	Cold stress coefficient for biomass production
Ks_{CCx}	Soil fertility stress coefficient for maximum canopy cover
l	Light extinction coefficient
LA	Leaf area

LA_{plant}	Leaf area plant
LA_{mat}	Leaf area mat
laf	Leaf area factor
LAI	Leaf Area Index
LAI_{flower}	Leaf area index at flowering
$LAI_{flowerS}$	Leaf area index of the follower at flowering of the mother
$leafD$	Leaf dry weight
L_{finger}	Finger length
LGP	Length of the growing period
$LINTUL$	Light Interception and Utilization model
LL	Leaf length
$LL3$	Leaf length of third functional leaf
LUE	Light use efficiency
LW	Leaf width
$LW3$	Leaf width of third functional leaf
MAP	Month after planting
N_{Finger}	Number of fingers on bunch
N_{hand}	Number of hands on bunch
nls	Nonlinear least squares
$NM-AIST$	Nelson Mandela African Institution of Science and Technology
NSE	Nash-Sutcliffe model efficiency
P	Precipitation
p	Depletion factor
PAR	Photosynthetic Active Radiation
$petioleD$	Petiole dry weight
p_{exp-up}	Soil water depletion factor for canopy expansion - Upper threshold
$p_{exp-\mathrm{low}}$	Soil water depletion factor for canopy expansion - Lower threshold
$p_{exp-shp}$	Shape factor for water stress coefficient for canopy expansion
$p_{sto-\mathrm{up}}$	Soil water depletion fraction for stomatal control - Upper threshold
$p_{\mathrm{sto}-shp}$	Shape factor for water stress coefficient for stomatal
$p_{\mathrm{sen}-\mathrm{up}}$	Soil water depletion factor for canopy senescence - Upper threshold
$p_{\mathrm{sen}-\mathrm{shp}}$	Shape factor for water stress coefficient for canopy senescence
pol_{mn}	Minimum air temperature below which pollination starts to fail
pol_{mx}	Maximum air temperature above which pollination starts to fail

$pseudostemD$	Pseudostem dry weight
PWP	Permanent wilting point
r	Growth coefficient of nls curve
R	Ratio of cumulative water added and cumulative ET0
R^2	Coefficient of determination
R^2_{adj}	Adjusted coefficient of determination
$Ratio_{finger}$	Ratio $r_{finger}$to L_{finger}
RAW	Readily available water
R_{base}	Radius of pseudostem at base
REW	Readily evaporable water
RF	Rainfed
R_{FH}	R between flower emergence and harvest
R_{FIF}	R between flower initiation and flower emergence
r_{finger}	Finger radius
RME	Relative model error
$RMSE$	Root-mean-square error
RO	Surface runoff
R_{PF}	R between planting/sucker selection and flower emergence
R_{PH}	R between planting/sucker selection and harvest
$RRMSE$	Relative root-mean-square error
Rs_{int}	Intercepted solar radiation
RUE	Radiation Use Efficiency
R_{up}	Radius of pseudostem at top
SD	Standard deviation
SE	Standard error
SSA	Sub Saharan Africa
$STICS$	Simulateur mulTIdisciplinaire pour les Culture Standards
SWB	Soil water balance
SWC	Soil water content
TAW	Total Available Water
T_{base}	Base temperature below which crop development does not progress
T_{max}	Daily maximum temperature
T_{min}	Daily minimum temperature
T_r	Crop transpiration

T_{up}	Upper temperature above which crop development no longer increases with an increase in temperature
UN	United Nations
$USDA$	United States Department of Agriculture
V_{drip}	Volume wetted by the drippers
V_{finger}	Volume of a finger
$vol\%$	Volume percentage
V_{pseudo}	Pseudostem volume
$V_{pseudo,flower}$	Pseudostem volume at flowering
$V_{pseudo,flowerS}$	Pseudostem volume of the follower at flowering of the mother
V_{rate}	Pseudostem growth rate
V_{root}	Volume of the root zone container
VWC	Volumetric water content
WAP	Weeks after planting
WHC	Water Holding Capacity
WP	Water Productivity
WP^*	Normalized Water Productivity
WP_B	Water Biomass Productivity
WP_B^*	Normalized Biomass Water Productivity
WP_{ET}	ET crop water productivity
WUE	Water Use Efficiency
Y	Dry crop yield
Z_r	Effective rooting depth
$Z_{r,min}$	Minimum effective rooting depth
$Z_{r,max}$	Maximum effective rooting depth
θ	Volumetric soil water content
θ_{AD}	Air dry volumetric soil water content
θ_{crit}	Critical volumetric soil water content
θ_{FC}	Volumetric soil water content at field capacity
θ_{OS}	Oxygen stress volumetric soil water content
θ_{PWP}	Volumetric soil water content at permanent wilting point
θ_{SAT}	Volumetric soil water content at saturation
τ	Drainage coefficient

Contents

Acknowledgements ..... **i**

Summary ..... **iii**

Samenvatting ..... **v**

Abbreviations and symbols ..... **vii**

Contents ..... **xiii**

1 Introduction, objectives, and outline **1**

1.1 General introduction *1*

1.2 Research objectives *3*

1.3 Dissertation outline *4*

2 Banana production: overview, practices, and challenges **5**

2.1 Importance *5*

2.2 Classification *5*

2.3 Morphology *6*

2.4 Phenological development and plantation heterogeneity *9*

2.5 Heterogeneity: structure of a banana plantation *11*

2.6 Banana abiotic growth requirements and limitations *12*

2.7 Banana response to moisture *15*

2.8 Improving water use efficiencies in banana plantations through crop modelling *16*

3 Banana crop modelling efforts **19**

3.1 Crop modelling introduction *19*

3.2 Simulated processes in crop models *20*

3.2.1 Modelling crop phenology 20

3.2.2 Modelling biomass production through growth engines 21

3.2.3 Modelling dry matter partitioning 23

3.2.4 Modelling attainable production: soil moisture balance and stress 24

3.3 Banana crop production models *25*

3.3.1 Leaf production model 25

3.3.2 CENTURY 25

3.3.3 STICS 26

3.3.4 SIMBA models 26

3.3.5 Individual plant growth model 29

3.3.6 LINTUL models 29

3.3.7 AAB plantain model 32

3.4 Modelling the banana plant: towards an AquaCrop growth model 33

4 AquaCrop modelling scheme 35

4.1 Introduction 35

4.2 Input requirements 35

4.3 Crop development 37

4.4 Soil water balance 39

4.5 Crop response to abiotic factors 40

4.6 Evaluation of model outputs 41

4.7 Model performance assessment and uncertainty 42

5 Canopy cover evolution, diurnal patterns, and leaf area index relationships in a Mchare and Cavendish banana cultivar under different soil moisture regimes 45

5.1 Introduction 45

5.2 Material and methods 47

5.2.1 Experimental site and conditions 47
5.2.2 Plant material 48
5.2.3 Experimental design 48
5.2.4 Management 48
5.2.5 Banana growth measurements 50
5.2.6 Statistical analysis 52
5.2.7 CC-LAI curve 54
5.2.8 Goodness of Fit characteristics 54
5.2.9 Software and used packages 54

5.3 Results 54

5.3.1 Soil moisture depletion 54
5.3.2 Canopy growth over time 55
5.3.3 Standard logistical regression 57
5.3.4 AquaCrop logistical regression 57
5.3.5 Diurnal CC variation 61
5.3.6 CC-LAI relationship 63

5.4 Discussion 65

5.4.1 Canopy growth over time 65
5.4.2 Standard logistical growth curve 66
5.4.3 AquaCrop logistical growth curve 66
5.4.4 Diurnal CC variation 67
5.4.5 CC-LAI relationship 69

5.5 Conclusion 69

6 Banana biomass estimation and yield forecasting from non-destructive measurements for two contrasting cultivars and water regimes 71

6.1 Introduction 71

6.2 Material and methods ... *74*
6.2.1 Experimental design ... 74
6.2.2 Plant data collection ... 77
6.2.3 Moisture effect on plant growth ... 81
6.2.4 Allometric regression ... 81
6.2.5 Software and used packages ... 83

6.3 Results ... *83*
6.3.1 Moisture effect on phenology, vegetative growth, and bunch parameters ... 83
6.3.2 Aboveground vegetative dry matter estimation ... 89
6.3.3 Corm dry matter estimation ... 93
6.3.4 Bunch weight forecast ... 94

6.4 Discussion ... *97*
6.4.1 Moisture effect on phenology, vegetative growth, and bunch parameters ... 97
6.4.2 ABGVD estimation from non-destructive observations ... 98
6.4.3 $\boldsymbol{CormD}$ estimation from non-destructive observations ... 99
6.4.4 Bunch yield forecast ... 101

6.5 Conclusion ... *102*

7 Parameterization and evaluation of the AquaCrop model for two crop cycles of a Grande Naine banana (Musa spp.) cultivar under irrigated and rainfed conditions ... 105

7.1 Introduction ... *105*

7.2 Material and methods ... *107*
7.2.1 Field experiments ... 107
7.2.2 Weather and soil data ... 107
7.2.3 Irrigation infrastructure and soil moisture measurements ... 108
7.2.4 Crop data ... 109
7.2.5 AquaCrop model ... 110
7.2.6 Crop parameter calibration ... 112
7.2.7 Adjustment of AquaCrop model for localized drip irrigation ... 113
7.2.8 Model evaluation ... 119

7.3 Results ... *119*
7.3.1 Canopy cover ... 120
7.3.2 Soil water content ... 121
7.3.3 Biomass ... 121
7.3.4 Yield ... 122

7.4 Discussion ... *122*
7.4.1 Comparison calibrated parameters with literature ... 123
7.4.2 Evaluation of model outputs ... 124
7.4.3 Towards an AquaCrop banana growth model ... 127

7.5 Conclusion and recommendation ... *128*

8 General discussion and conclusions ... 131

8.1 Introduction ... *131*

8.2 Effect of drought on field grown banana ... *131*

8.2.1 Effect of drought on canopy cover 132
8.2.2 Effect of drought on other vegetative, generative and phenological parameters 134
8.2.3 How to spot and address drought stress in smallholder fields? 136

8.3 AquaCrop calibration of irrigated and drought stressed banana 138
8.3.1 Drip irrigation adjustments 139
8.3.2 Crop parameter sets for the first two cycles of a banana plantation 140
8.3.3 Modelling mature banana plantations 143

8.4 AquaCrop usefulness and applicability 145
8.4.1 AquaCrop validation and performance 145
8.4.2 AquaCrop-banana usefulness for agriculture in SSA 146
8.4.3 AquaCrop versus other banana models 146
8.4.4 Recommendations for future research on AquaCrop 152

References 155

Annex I: AquaCrop Parameters 173

Annex II: Experimental design overview 177

Annex III: Canopy cover supplementary data 187

Annex IV: Allometry supplementary data 197

Annex V: AquaCrop model supplementary data 201

Annex VI: Adjustment for simulating drip irrigation 203

1 Introduction, objectives, and outline

1.1 General introduction

By 2050, the global population level will rise to 9.8 billion, with nearly all of this increase occurring in developing countries (United Nations, 2019). These population levels, combined with a wealthier population with changing consumption preferences, will put higher demands on food, feed, fiber and fuel (Foley et al., 2011). Agricultural production needs to increase 25-70% by 2050 to satisfy demands (Hunter et al., 2017). This production needs to occur under a changing climate (IPCC, 2019). Climate variability and extremes are the biggest drivers causing the recent surge in undernourishment indicating current agriculture is not adapted to changing climate conditions (FAO et al., 2018). Extreme weather events, weather variability and failure to adapt to a changing climate are among the top five impactful risks for the future (World Economic Forum, 2018). Previously, agriculture focused on using more inputs (land, fertilizers, and water) to reach more outputs, often detrimental to the environment leading to rising greenhouse gas emissions, loss of natural ecosystems and declining biodiversity. Current agriculture covers 38% of global land area, uses 70% of all global freshwater and emits 30-35% of global greenhouse gasses (Foley et al., 2011; IPCC, 2019). The limits of planetary boundaries within which humans can safely operate are being reached as critical thresholds for biodiversity loss, climate change and nitrogen cycle are already surpassed, and boundaries for global freshwater use and land use will be reached soon (Rockström et al., 2009). Only 10% of the necessary production increase can come from an expansion of land area under cultivation. The other 90% will have to occur by enhancing yields per unit area (yields ha^{-1}) (77%) and intensifying cropping intensity (yields $year^{-1}$) (13%) (FAO, 2018b).

Agriculture in the 21st century therefore faces a triple challenge: (1) outputs need to almost double to reach demands of a growing and wealthier population, (2) production needs to occur in changing and increasingly variable climatic conditions, whilst (3) environmental footprints need to be reduced (water, fertilizer consumption and emissions) (FAO, 2018b; Foley et al., 2011; Garnett et al., 2013; Hunter et al., 2017). Agriculture as a whole, stands before one of the biggest shifts of all time and techniques of the past are no longer sufficient for the challenges of the future (FAO, 2018b).

Banana and plantains are the 12th most important food crop in terms of production (fourth in Africa) and even the world's most important fruit (FAO, 2018a). Its global production was 153 million tons in 2017 (76% banana and 24% plantain) on 5.6 million hectares of land (worth 26.5 billion Euro) in over 135 countries. Only 15% of global production is traded internationally, with 85% of global banana production cultivated by small scale farmers, to be used as a staple food and sold at local and regional markets (De Buck & Swennen, 2016). Adapting the banana sector to the challenges of the 21st century (increasing production under a changing climate and reducing environmental footprints), is necessary, especially concerning water use as one of the biggest threats to banana production is water stress – both excess and deficit (Carr, 2009; Surendar et al., 2013; Van Asten et al., 2011). Bananas require constant supplies of water due to their perennial behavior, long cycle duration and phenological heterogeneity (i.e. multiple cycles in the field) (Carr, 2009; Surendar et al., 2013), and already show yield losses when 20-35% of total available soil moisture is depleted indicating drought sensitivity (Allen et al., 1998; Carr, 2009). Depending on the prevailing climate, annual rainfall requirements range from 1,100 to 2,690 mm $year^{-1}$ in rainfed systems (Van Asten et al., 2011). In addition, banana

production is increasingly being shifted to drier regions to reduce the impact of fungal infections as banana fungi thrive well under moist climates (Ploetz et al., 2015; Robinson & Galan-Sauco, 2010). Changing climatic conditions, surprisingly, might be beneficial in most African countries. An increase in temperature in most banana producing regions should extend suitable thermal land area, but should also result in areas with excessively high temperatures (>35°C) for more than 3 months (FAO, 2018a; German Calberto et al., 2015; Varma & Bebber, 2019). This increase in suitable land area is under the assumption that irrigation would supplement the necessary moisture, which is not always the case.

In regions where rainfall is not enough, irrigation is necessary to sustain production. At a global scale, 70% of freshwater is already used for agriculture. Soil degradation, climate change, population increases and a rising welfare will further put pressure on freshwater resources (FAO, 2014; Hamdy et al., 2003). By 2050, irrigation withdrawals are expected to increase by 11% (FAO, 2018b; Hunter et al., 2017). As water is a limited resource, more efficient use of both rainfall and irrigation water is needed. New innovative technologies should be embraced in the banana sector to expand production levels without depleting natural resources and the effect of technologies on crop production should be assessed under a changing climate (FAO, 2018b; Foley et al., 2011).

Solutions to address water footprints in banana plantations include crop centric approaches as breeding, discovering and/or genetically engineering drought tolerant high yielding varieties (Eyland et al., 2020; Kissel et al., 2015; Van Wesemael, 2019), and management centric approaches (Bodner et al., 2015; Peng et al., 2020). Management interventions reduce water footprints via guiding and storing more water in the root zone to be used for transpiration (Ali & Talukder, 2008; Bodner et al., 2015). Stresses are alleviated through techniques including (but not limited to) mulching, water harvesting, soil structural improvement, fertilization, and irrigation scheduling. In most cases, management is based on farmers' experience, which quite often does not correspond to water addition at the best moment (Boesveld et al., 2011; Mbonile, 2005). Since about 99% of all freshwater use in banana cultivation corresponds to the agricultural production phase (FAO, 2017), a proper understanding of plant-water relations, and correct irrigation scheduling and implementing management practices in line with crop water demands will have a big impact on banana water footprints.

The best strategy to increase production and limit water footprints, thus entails a better insight in plant-water relationships and in location specific yield responses to stress. The prediction of consequences by management practices on (1) agricultural performance and (2) environmental sustainability under future environments is challenging but vital to adapt agriculture to the 21st century (Peng et al., 2020).

Crop modelling offers an avenue because a well-calibrated model provides yield simulations over a range of genotypes, climates, soils, and management conditions, when field experiments would otherwise take years to provide the same information. Models can assist in designing management adaptation strategies by comparing their impacts on crop productivity and their environmental footprints. Yield modelling is a tool to understand production constraints, to project impacts of future climates and to pinpoint possible solutions (Bergez et al., 2012; Hoogenboom et al., 2004; Lehmann et al., 2013; Peng et al., 2020; Steduto et al., 2012). Dozens of models exist for modelling major annual crops as maize and wheat (Brisson et al., 2003; Van Ittersum et al., 2003), but annual crops differ in

growing behavior from the perennial, multi-cycle banana plant – so a different modelling approach is warranted. Thereby simulation models are needed that consider the growing behavior of a banana plant. Previous modelling efforts on banana and plantain (i.e. CENTURY (Woomer et al., 1998), STICS (Brisson & Dorel, 1998), SIMBA models (Damour et al., 2012; Dorel et al., 2008; Ripoche et al., 2012; Tixier et al., 2004, 2006, 2008, 2011), LINTUL (Nyombi, 2010; Taulya, 2015) and AAB plantain (Dépigny et al., 2017)) have led to a variety of different simulation models each with their own strengths, weaknesses and level of detail in incorporating the specific banana growth structure; and provide a necessary starting point to build upon (chapter 3). Largely due to their lack of physiological basis or complexity, most current (banana-)crop models remain unused by farmers, extension officers and irrigation experts (Wellens et al., 2017). Additionally, a model that correctly simulates soil moisture balances, looks foremost at the influence of water stress on production, and thereby allows users to simulate water-stressed banana production would be needed.

The Food and Agricultural Organization of the United Nations (FAO) has developed the AquaCrop growth model to simulate crop development in response to environmental and soil moisture conditions. It has been successfully used on over 15 crops including C3 (wheat, rice, soybean, barley, cotton, sugar beet, sunflower, potato, tomato, alfalfa, Bambara groundnut, quinoa) and C4 crops (maize, sorghum, sugarcane, teff) (Hsiao et al., 2009; Steduto et al., 2012; Vanuytrecht, Raes, Steduto, et al., 2014). Multiple studies highlight its good yield predictions in response to soil water content (Steduto et al., 2009; Todorovic et al., 2009b; Van Gaelen et al., 2015; Vanuytrecht et al., 2011; Zeleke et al., 2011).

The FAO AquaCrop project aims to calibrate the model for each important crop species (Hsiao et al., 2009). Banana, by its global production, remains the highest ranking crop for which AquaCrop has yet to be calibrated. Such a model can assist in calculating water requirements and irrigation guidelines for the banana plant.

1.2 Research objectives

Due to the importance of banana as a crop for both export and domestic use, its long cycle duration, perennial multi-cycle structure and sensitivity to water stress, a plantation wide study was carried out to study the effects of water stress on banana growth and phenology. These insights into plant-water relationships, together with the banana population structure, were then used to adapt and evaluate the current AquaCrop growth model for the first two growth cycles of a banana plantation**.** Following research objectives were defined. Each objective is addressed in a separate work package (WP), for which the different hypotheses are given in the corresponding chapters (Figure 1-1).

Objective 1: Study canopy cover (CC) and leaf area index (LAI) in banana plantations using two cultivars: the East African Highland banana cv. Mchare—Huti Green Bell (AA), a diploid, and the Cavendish—Grande Naine (AAA), a triploid under rainfed and irrigated conditions to determine the effects of cultivar and drought on plantation growth and assess if CC can be simulated using the generic AquaCrop canopy cover curve for both cultivars and treatments (WP1).

Objective 2: Assess the effect of irrigation on phenology, vegetative and generative growth parameters. Next, develop allometric models to estimate vegetative biomass over time and allow bunch yield forecasting based on easily observable characteristics, and assess whether these differ according to cultivar and irrigation regime (WP2).

Objective 3: Use information and insights from objective 1 and 2, and information on the banana growth structure from literature, to incorporate the banana growth structure in AquaCrop, calibrate model parameters and evaluate simulations for the first two growth cycles of a banana plant (WP3).

1.3 Dissertation outline

This dissertation consists of five parts (Figure 1-1). Firstly, an overview of the relevant theory concerning banana production, challenges and crop modelling will be given (chapter 1 to 3), followed by a detailed explanation of the current AquaCrop model (Chapter 4). Then research results from field trials are presented (Chapter 5 (WP1) and 6 (WP2)), that explain the influence of water stress on growth, phenology, and production under field conditions. These data were used for the calibration and evaluation of the AquaCrop growth model for the first two cycles of a banana plantation (Chapter 7 (WP3)). Finally, conclusions and recommendations are presented (Chapter 8).

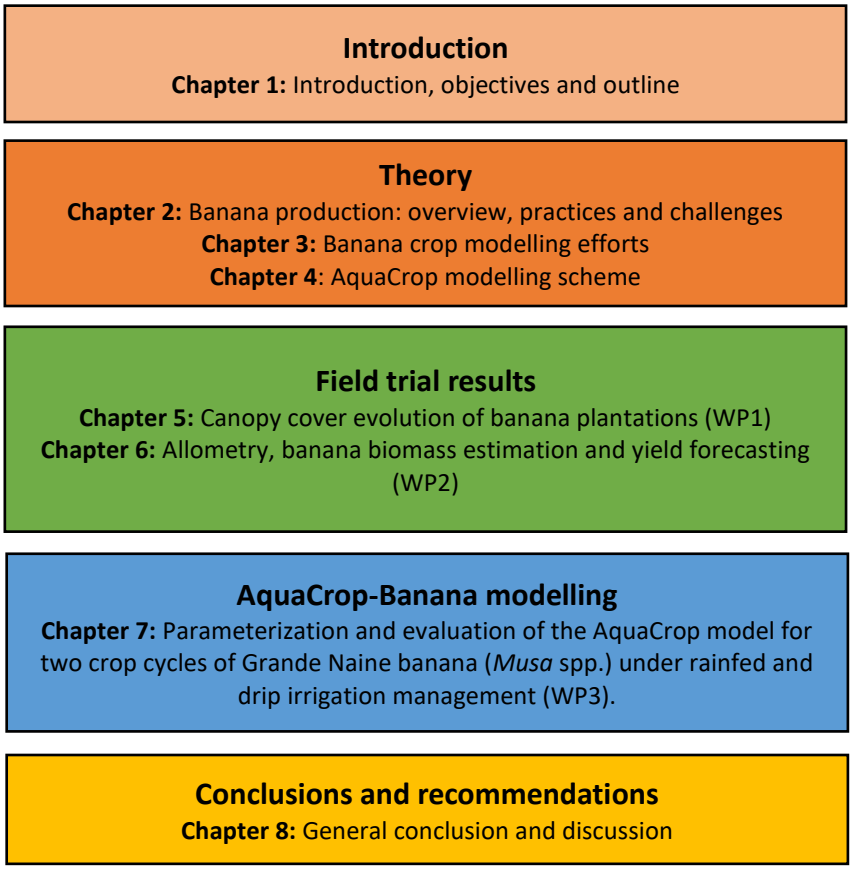


Figure 1-1: PhD Dissertation outline

2 Banana production: overview, practices, and challenges

2.1 Importance

More than 1,000 different banana cultivars exist worldwide (Christelová et al., 2017), but the most widely commercialized (and therefore well known) cultivar is Cavendish, a dessert type banana, constituting about 47% of the total global production (De Buck & Swennen, 2016). Almost all banana (99%) found in US and European supermarkets are of the Cavendish cultivar (De Buck & Swennen, 2016; FAO, 2018a). Only 15% of global production is traded internationally. The main exporters are Ecuador, the Philippines, Costa Rica, Colombia and Guatemala (FAO, 2018a). Ecuador, Belgium, Colombia and Costa Rica make up over 50% of the total value of banana exports (FAO, 2015) (Belgium, due to the strategic position of the port of Antwerp for further export to the European markets). 85% of global banana production is cultivated by small scale farmers and used as a staple food and sold at local and regional markets (De Buck & Swennen, 2016). The biggest producers are India (29.7 million ton), followed by Uganda (11.1 million ton) and China (10.7 million ton)(FAO, 2018a).

Africa alone constitutes 20% of total global banana and plantain production and the crop is estimated to act as a cornerstone to the livelihood for 90 million people in terms of food, income and employment (De Buck & Swennen, 2016; FAO, 2018a). In Sub Saharan Africa (SSA), and more particular East and Central Africa (ECA), banana has long held a champion role amongst food crops. Per capita consumption in this area is 15 times the global and 6 times the African average, corresponding to a daily intake of 3-11 bananas per person (300-400 kg ha^{-1} $year^{-1}$). Banana constitutes a significant portion of daily caloric intake ranging from 30-60% in these areas. In ECA, two and a half million hectares are currently under some kind of banana cultivation, reaching portions of about 50% of the total cultivated land under permanent crops with about 4.5 million people in the area earning about 20-80% of their total annual income from banana and plantain production (Abele et al., 2007; FAO, 2018a). Almost every rural household across the (sub)humid parts of SSA has banana plants growing in their backyards.

Banana cultivation is expected to increase in these developing regions, with production drivers being mostly an increased demand due to rising populations in developing countries and changing health awareness among US and European consumers (FAO, 2018a).

2.2 Classification

Banana belongs to the order Zingiberales, family Musaceae consisting of three genera (Musa, Musella and Ensete). The genus Musa is the most important for consumption and production. Most cultivated cultivars are diploid (2 sets of chromosomes: 2n=22) or triploid (three sets of chromosomes: 3n=33) and originated from intra- to interspecific hybridizations of the wild ancestors *Musa acuminata* (AA) and *Musa balbisiana* (BB). Genomes are noted using the letters A or B, referring to the origin of the chromosome set. Six major groups exist based on their genomic constitution: AA, AAA, AB, AAB, ABB and ABBB (Brown et al., 2017; E. De Langhe et al., 2010). There are indications that the relative contribution of the B genome might lead to increased drought stress resistance in banana plants (Carr, 2009; Kissel et al., 2015; Van Wesemael et al., 2019).

This dissertation will focus on two sets of genomes: the Musa AA-East African Highland Banana (EAHB) subgroup Mchare cv. Huti Green Bell (AA) and the commercial Musa AAA subgroup Cavendish cv.

Grande Naine (AAA). Mchare cv. Huti Green Bell was chosen due to its importance in the study area (Tanzanian Highlands) and Cavendish cv. Grande Naine due to its importance worldwide. Even though they are diploid and triploid respectively and phenotypically very different, genetically they are closely related (Christelová et al., 2017; Perrier et al., 2019). Mchare is consumed after cooking, while Cavendish is a dessert banana, eaten raw (Figure 2-1).



Mchare- Huti Green Bell bunch **Cavendish-Grande Naine bunch**

Figure 2-1: Bunches of Mchare Huti Green Bell (left) and Cavendish Grande Naine (right)

2.3 Morphology

The banana plant is a large monocotyledonous herbaceous plant (Figure 2-2). The *corm or "true stem"* is an underground rhizome from which the aerial shoot originates as well as the suckers. The apical meristem (apex) is located at the highest point of the corm, where it remains during vegetative growth. The apex initiates leaf primordia from which *leaves* arise sequentially, with the older leaves enclosing the newly formed leaves giving rise to the pseudostem which is thus composed of tightly compacted and enclosed leaf bases. Each new leaf is formed within the pseudostem and pushed out through the center of the pseudostem as a rolled cigar, after which it unfurls and reaches full photosynthetic capacity (Robinson & Galan-Sauco, 2010; Swennen & Rosales, 1994; Turner et al., 2007). Each leaf is composed of a sheath, petiole, lamina, midrib, and precursory appendage. The *petiole* is an extension of the leaf sheath and goes over into the midrib that supports the lamina. As each leaf develops within the pseudostem, the lamina increases in size until it begins to emerge from the top of the pseudostem. Once unrolled, the leaf area does not increase any further. Individual leaves can reach up to 2-3 m^2 (or more), but the leaf area is cultivar and environment dependent. In total, about 30-50 (or more) leaves can be produced, but only 10-14 leaves are present on a banana

plant at a time (cultivar, environment, and management dependent). On average, new leaves are formed every 7 – 14 days depending on climatic conditions, but under stress it might take longer (Carr, 2009; Robinson & Galan-Sauco, 2010; Turner et al., 2007). Under non-stressed conditions, each newly formed leaf is bigger than its predecessor until flower initiation. Aerial shoots are terminal. At *"flower initiation",* the apex rises above the leaf bases and will transition from the vegetative stage to the floral stage and develop the inflorescence (Robinson & Galan-Sauco, 2010; Turner et al., 2007). About 11-12 leaves are still inside the pseudostem at flower initiation, but these become increasingly smaller than the previously formed leaves as energy goes to the developing inflorescence inside the pseudostem. The last leaf, or spade leaf, emerging before the inflorescence is very small (Robinson & Galan-Sauco, 2010; Swennen & Rosales, 1994; Turner et al., 2007). The developing inflorescence is carried upwards by an aerial stem until it emerges at the top of the pseudostem *at "flower emergence or anthesis"* (Fortescue & Turner, 2005; Robinson & Galan-Sauco, 2010; Turner et al., 2007). The floral stage extends from floral initiation to inflorescence emergence at the top of the pseudostem, and is also called the vegetative apparent stage since the inflorescence develops inside the pseudostem (Robinson & Galan-Sauco, 2010). Therefore, "flowering" in banana is often used to describe the moment of "flower or bunch emergence" in the field. After flower/bunch emergence, the "*fruiting phase"* starts, which lasts until bunch maturity (Robinson & Galan-Sauco, 2010; Swennen & Rosales, 1994; Turner et al., 2007). The *bunch or inflorescence* is composed of a peduncle (or rachis) bearing flowers covered by bracts. Flowers are arranged in clusters (hands) connected to the peduncle. Each cluster is covered by a modified leaf or bract. These bracts are lifted at 1-3 bracts per day, exposing the flowers underneath to the environment (Robinson & Galan-Sauco, 2010; Swennen & Rosales, 1994). Generally, the first 10-11 hands are female flowers with non-functioning stamen which develop into fruits (fingers). The last terminal flower clusters, the male-bud, contain male flowers with a non-functioning stigma and produce pollen in some cultivars. Between female and male flowers are neutral flowers (Swennen & Rosales, 1994; Turner et al., 2007). Most edible and commercial banana cultivars produce fruits through parthenocarpy, the formation and filling of fruits without fertilization (pollination) resulting in seedless fruits (Carr, 2009; Fortescue & Turner, 2005; Robinson & Galan-Sauco, 2010; Turner et al., 2007).

Fruit growth occurs in two phases: before and after bunch emergence, with most fruit growth occurring after emergence. For example, in Poyo (Cavendish subgroup), 20% of the final finger length and 10% of final finger radius is reached before bunch emergence. After bunch emergence, rapid logistical increase in finger length, and linear increase in finger radius results in a logistical filling of the fingers until harvest (Robinson & Galan-Sauco, 2010). The number of hands per bunch, and the number of fingers per hand are determined at flower initiation and depend on genome, crop cycle, temperature, vegetative vigor and management (Robinson & Galan-Sauco, 2010; Turner et al., 2007). The bunch potential is proposed to be set around flower initiation, and thereby depends on conditions that affect general vegetative growth as large plants within a cultivar produce large bunches, although this has yet to be tested experimentally (Turner et al., 2007). The final size of each finger (fruit) is mostly determined after bunch emergence and depends on prevailing climatic conditions (temperature, soil moisture, fertility), photosynthetic capacity during bunch filling (leaf area index), presence of suckers, and grade at harvest (Dens, Romero, et al., 2008; Eckstein et al., 1995; Robinson & Galan-Sauco, 2010; Twyford & Walmsley, 1973). The final shape and size of banana fruits and hands are cultivar dependent (Ploetz et al., 2007; Robinson & Galan-Sauco, 2010). After harvest, the aerial

part of the mother shoot dies off and follower plants from suckers take over growth of the banana. That follower represents the next cycle (Robinson & Galan-Sauco, 2010; Turner et al., 2007).

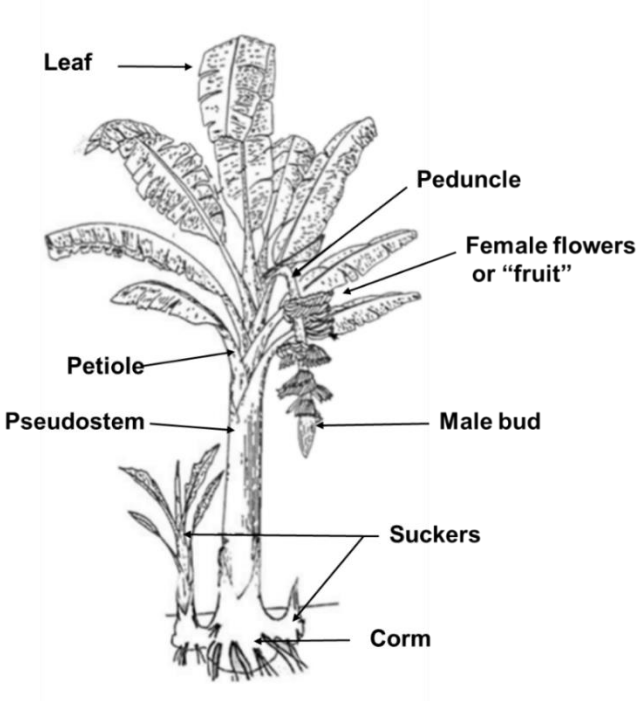


Figure 2-2: Banana plant morphology. Adapted from Champion (1963).

During the development of a single shoot, aerial shoots (suckers, followers, or daughters) arise from lateral buds on the rhizome. The *size of each sucker* increases with distance to the apical meristem. These suckers will constitute new cycles each producing their own sequence of leaves and inflorescence, and will take over from the mother plant after harvest resulting in the semi-perennial behavior (Lamour et al., 2020; Tixier et al., 2004). In commercial plantations, desuckering occurs and a single sucker is allowed to develop next to the mother plant (Robinson & Galan-Sauco, 2010).

The collection of all shoots and the corm is called a banana "mat" or "stool". Individual growing units in a banana plantation are therefore all shoots originating from the underground corm. When referring to a *banana "plant" or "cycle"***,** we refer to an individual shoot on a mat. When referring to a *banana "mat" or "stool",* we refer to the collection of shoot entities on a mat. In a well-managed plantation, each banana mat consists maximally of two to three generations of banana plants: the mother plant representing cycle 1 (C1), the daughter plant representing cycle 2 (C2) and the granddaughter plant representing cycle 3 (C3). The first cycle is often called the plant crop, whilst later cycles are referred to as ratoon crops. These shoots all grow on a single corm and influence each other during growth (Dens, Romero, et al., 2008; Robinson & Galan-Sauco, 2010; Turner et al., 2007; Turner & Hunt, 1987).

Roots of a banana plant originate from the corm and follow the same arrangement as other monocotyledons (Blomme et al., 2000; Draye et al., 1999; Turner et al., 2007). Banana has a shallow rooting system, with root production occurring continuously until flowering. Laterally, roots can spread 2-3m and even reach 5m, but most roots are found within 0.60 m from the base of the plant (Blomme et al., 2000; Draye et al., 1999). Effective rooting depths of banana are shallow and often

taken to be 0.40-0.60 m, but can even extend to 1.0-1.5 m provided there are no physical restrictions (Blomme et al., 2000; Carr, 2009; Draye et al., 1999; Robinson & Galan-Sauco, 2010; Turner et al., 2007).

Major phenotypical and cultivar variation exist in the growth and size of each banana component (Blomme et al., 1999; Carr, 2009; Draye et al., 1999; Ploetz et al., 2007; Robinson & Galan-Sauco, 2010; Turner et al., 2007).

2.4 Phenological development and plantation heterogeneity

Phenological development describes the timing of different growth stages in banana and plantain: juvenile phase, sucker emergence, vegetative growth stage, flower initiation, bunch/flower emergence and harvest (Table 2-1). Overall, vegetative growth lasts from planting/sucker selection until flower emergence, whilst reproductive growth lasts from flower initiation until harvest. The vegetative phase and the reproductive phase follow one another as the banana plant is terminal but coexist between flower initiation and flower emergence (intermediate phase). So far, banana phenology is poorly understood. Chronological time, expressed in days, is not suited to describe phenology as days to phenological events differ between environments with different growth potentials and even within a same environment depending on the season (Fortescue et al., 2011; Lamour et al., 2020; Robinson & Galan-Sauco, 2010; Taulya et al., 2014; Turner, 1987; Turner et al., 2007).

Table 2-1: Banana phenological growth stages in the Tropics in days after planting (DAP).

Phase	Name	Time-period (DAP)*	Definition
Vegetative phase	Juvenile phase	0 until 20-45	Dependent sucker phase
	Vegetative independent phase	20-45 until 100-140 DAP	When first fully developed leaf is formed. Suckers start emerging from 2-4 months after planting onward and constitute next cycles.
Intermediate phase	Vegetative apparent phase or floral phase	100 - 140 DAP until 172 - 224 DAP	Starts at flower initiation. About 11–12 leaves are inside the pseudostem at flower initiation (vegetative apparent = no indication of floral development). Transitioning stage between vegetative growth and reproductive growth.
Reproductive phase	Fruit phase	172 - 224 DAP until 270 - 341 DAP	Starts at emergence of the inflorescence/bunch from the pseudostem (anthesis). For practical phenological studies, the flower emergence is often used to note flowering.
	Harvest maturity	270 - 341 DAP	When bunch is mature (shows yellowing fingers)

* indicative timing values in the tropics expressed in days after planting (DAP) for banana ratoon plantations in the humid tropics (Honduras; cultivar 'Grande Naine') (Robinson and Galan-Sauco, 2010). Values vary significantly with environment and are to be used only as indicative values.

Based on physical plant parameters, phenology in banana cannot be accurately predicted. Cumulative leaf formation is often proposed as an indicator for flowering, but the number of cumulative leaves ranges significantly (30-50 leaves) between cultivars and environments (Robinson & Galan-Sauco, 2010; Turner et al., 2007; Van Asten et al., 2011). Taulya et al. (2014) proposed a minimal dry matter (DM) accumulation threshold of 1.5 kg DM plant^{-1} before flower emergence of the EAHB cultivar Kisansa. Actual DM accumulated before flower emergence ranged between 1.5-11 kg DM plant^{-1} in their experiments, showing that DM accumulation thresholds to reach flowering vary significantly.

Environmental cues play a role in the phenological development of banana (Fortescue et al., 2011; Lamour et al., 2020; Taulya, 2015; Turner et al., 2007). If phenology is only governed by temperature, plant development can be described by growing-degree-days (GDD, with units of °C days). GDDs or thermal units are measures of heat energy received above a certain critical temperature over a certain time. Phenological events in day-neutral plants (plants that do not require a photoperiodic effect to start flowering) are reached after the plant reaches a set GDD accumulation threshold (McMaster & Wilhem, 1997). Banana plants were often considered day-neutral plants, but it seems that other factors than temperature (photoperiod, soil moisture, stresses encountered) also drive development (Fortescue et al., 2011; Turner et al., 2007). GDD for sucker emergence, flower emergence and bunch maturity tend to follow log-normal distributions in a plantation (Figure 2-3), with increasing variation in each increasing cycle (Lamour et al., 2020; Robinson & Galan-Sauco, 2010; Tixier et al., 2004).

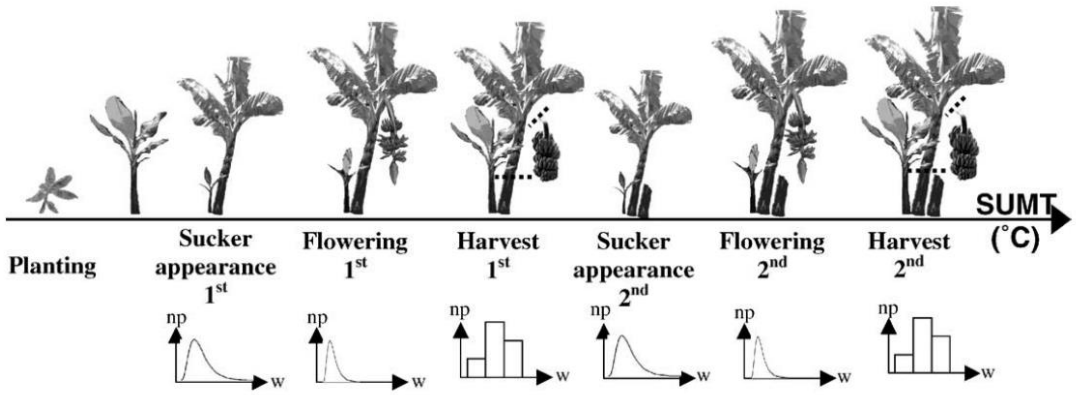


Figure 2-3: Heterogeneity between banana mats. Sucker appearance, flowering and harvest follow log-normal curves in a plantation level. np is number of plants, w is weeks after planting (varies significantly according to environment, cultivar and stresses encountered). The variation in w will increase in spread with increasing cycle. Source: Tixier et al. (2004).

Instead of a set GDD threshold, banana plants produce suckers, flowers, and harvest-ripe bunches over a (log-normal) range of GDDs. GDD thresholds are therefore not singular. Planting date experiments by Lassoudière (2007) in the tropics, and Turner & Hunt (1987) in the subtropics showed GDD between planting and harvest to also vary significantly between: (1) locations, (2) planting dates, (3) soils, (4) planting materials and (5) defoliation management. Analyses of planting date experiments by Fortescue et al. (2011) support the view that banana is a facultative long-day plant which hastens development and bunch appearance under long photoperiods, and delays it under soil moisture excess and deficit. In the tropics, governed by stable photoperiods of approx. 12 hrs., the photoperiod effect is expected to be small to negligible, giving rise to the day-neutral behavior of banana plants. In the subtropics however, the effect of photoperiod on phenology is bigger and plants behave as facultative long-day plants (Fortescue et al., 2011). Plantain cultivars also showed photoperiodic responses on phenological development. Under low photoperiods, plantain extended its flower initiation (Turner et al., 2016). Thereby both plantain and banana phenology can be influenced by temperature, photoperiod and/or soil water balance.

Most likely an interplay of physical plant attributes and/or environmental cues determines phenology in banana. Taulya et al. (2014) found banana plants exhibit phenotypic plasticity, i.e. plants do not flower at similar physiological times (GDD) and adjust phenology to the growing conditions (soil moisture and nutrients). Their study suggested GDD as such could not be used to pinpoint to flowering,

but a new factor regarding plant growth speed and DM accumulation needs to be considered to determine phenology. For flowering, banana plants seemed to balance their physiological age in GDD and total DM at flowering. Plants might delay physiological age to flower (increase GDD), under reduced DM accumulated at flowering, or plants might hasten their physiological age to flowering under fast DM growth rates.

2.5 Heterogeneity: structure of a banana plantation

The phenological phenomena (individual plant variation from planting to flowering duration, sucker emergence, plant death; and management strategies: type of sucker selected, selection moment, amount of selected suckers, and plant replacement strategy) lead to a heterogeneous plantation structure with time (Lamour et al., 2020; Tixier et al., 2004). Even plantations that start from homogenous in-vitro plant material, become heterogeneous with time. Heterogeneity in a plantation occurs at two scales: (1) within a banana mat and (2) between neighboring mats. Both within a single banana mat (first unit of heterogeneity) as between neighboring mats (second unit of heterogeneity), multiple shoots (cycles) develop at their own pace (Tixier et al., 2004; Turner et al., 2007). These shoots all grow on a single corm and influence one another during growth (Robinson & Galan-Sauco, 2010).

Resources are divided within the plant and mat through source – sink relationships, which change according to the phenological stage of the plants (Eckstein et al., 1995; Nyombi, 2010; Robinson & Galan-Sauco, 2010; Swennen, 1984a; Tenkouano et al., 2007; Twyford & Walmsley, 1973).

During sucker development, DM is allocated from the mother plant to the sucker. Increasingly, the sucker will start to grow, form leaves and start its own autotrophic growth process relying less and less on DM from the mother. Leaves then become the primary source through photosynthesis (Nyombi, 2010; Robinson & Galan-Sauco, 2010). Photosynthetic products (DM) created in the leaves during the vegetative stage are used primarily for the growth of new leaves, the corm and suckers (Eckstein et al., 1995). After flower initiation, DM starts to be allocated to the bunch, whereby DM allocation increases significantly after flower emergence (Eckstein et al., 1995; Nyombi et al., 2009; Twyford & Walmsley, 1973). DM from photosynthesis of the present leaves is preferably used for bunch filling, but when photosynthetic DM is not enough, DM stored in the leaves and corm is used. The leaves, pseudostem and corm can thus be considered a DM storage reservoir for bunch filling (Twyford & Walmsley, 1973). Suckers around the mother plant compete with the developing bunch (Dens, Romero, et al., 2008; Eckstein et al., 1995; Twyford & Walmsley, 1973), but also with each other (Tenkouano et al., 2007). Sink strengths of the bunch determine the percentage of DM allocated to the suckers and bunch, respectively. The bigger the sink strength of the bunch, the more sucker growth is limited (Dens, Romero, et al., 2008; Eckstein et al., 1995). Due to competing sinks, de-suckering practices in the field over the course of the growing season reduces the amount of competing sinks and thereby increases individual bunch yields in ratoon crops, and reduces time to flowering and harvest (Tenkouano et al., 2007). After harvest, the pseudostem, petioles, leaves and bunch of the harvested plant are removed, and the dominant sink disappears. Suckers (vegetative shoots) become the dominant sinks, and the growth cycle as stated above starts again leading to the perennial plantation structure of the banana plant (Dens, Romero, et al., 2008; Eckstein et al., 1995; Nyombi et al., 2009; Robinson & Galan-Sauco, 2010). In a single sucker management, only one sucker is selected to constitute the ratoon crop, resulting in lower inter-sucker and bunch competition (Tenkouano et al., 2007). Choosing vigorous early suckers also allows the next ratoon to be less

affected by competition as it can already produce own DM from leaves (Dens, Romero, et al., 2008; Eckstein et al., 1995; Robinson & Galan-Sauco, 2010).

2.6 Banana abiotic growth requirements and limitations

Banana originated in the tropics from South East Asia between 8,000 to 5,000 BCE, and are believed to be the world's first cultivated fruit (Turner et al., 2007). From there it spread outward to the pacific and westward, first to SSA (1st century AD) and later from west Africa to the Americas (17th century AD)(Robinson & Galan-Sauco, 2010), although plantain is believed to have reached Africa more than 2,500 – 3,000 years ago (Edmond De Langhe, 1995; Mindzie et al., 2001). It is currently grown throughout the tropics (between the Equator and 20°N and S) and subtropics (between 20° and 30° N and S of the Equator) (Carr, 2009). In the tropics, temperature and light fluctuations are small throughout the year. In the subtropics, temperature and light regime fluctuate highly between summer and winter months, and rainfall is less evenly spread throughout the year leading to a more pronounced seasonal growth and production (Robinson & Galan-Sauco, 2010). In this section, we provide a general overview of abiotic growth requirements for the banana plant. It has to be noted that bananas are composed of a diverse set of genotypes and phenotypes (Christelová et al., 2017), and in the end different cultivars have their own ecological niche for growth (Eyland et al., 2020).

Being of tropical origin*, temperature* foremost determines where bananas and plantains can be grown. Production can mostly occur between 13-38°C, but optimal production seems to be reached at temperatures between approx. 22-31°C. New leaf emergence and DM accumulation stops approx. below 13- 16°C. At approx. 38°C growth stops and heat stress starts to occur. At around 47°C the thermal danger point is reached and leaves start to die (German Calberto et al., 2015; Robinson & Galan-Sauco, 2010; Van Den Bergh et al., 2012).

Besides temperature, *rainfall amounts and frequency* determine where bananas and plantains can be grown. As a perennial, multi-cycle crop with shallow rooting system, banana needs ample and frequent amounts of evenly distributed water for optimal yields (Carr, 2009; Turner et al., 2007). Rainfall requirements range from 1,100-2,650 mm $year^{-1}$ depending on the prevailing climate (Robinson & Alberts, 1986; Van Asten et al., 2011; Varma & Bebber, 2019). In the humid tropics, water needs may be covered by rainfall amounts, but in the dry tropics and subtropics, irrigation becomes increasingly necessary (Robinson & Galan-Sauco, 2010).

Currently, potential global suitable climatic areas in the tropics and subtropics for banana cultivation (based on temperature) are 84 million km^2 (50% tropics, 50% subtropics), compared to 141 million km^2 unsuitable (German Calberto et al., 2015). The majority of suitable areas in the subtropics (90%) need irrigation to sustain production as they receive <900 mm annual rainfall (German Calberto et al., 2015). In the banana growing zones in the East African Highlands, where our study was conducted, rainfall varies both spatially and temporally (Figure 2-4). Rainfall is bimodal and averages between 900-1,400 mm $year^{-1}$. In Arusha, Tanzania, where our study was conducted monthly rainfall amounts do not cover evapotranspiration rates (Figure 2-5). Depending on the water holding capacity (WHC) of underlying soils, irrigation can be required to bridge dry spells.

Climate change on average will increase thermal suitability for banana worldwide (German Calberto et al., 2015; Van Den Bergh et al., 2012; Varma & Bebber, 2019). By 2070, global thermal suitable climatic areas will increase by approx. 8 million km^2, whilst only a small fraction (48,675 km^2) of previously suitable lands will shift to excessive temperature regimes (> 35°C). By 2070, 77% of suitable

areas in the subtropics and 20% in the tropics are expected to receive < 900mm annual rainfall (German Calberto et al., 2015). The increase in suitable thermal area will thereby need to be supplemented by irrigation practices to sustain production. This overall pattern has also been observed in SSA where an increase in suitable thermal area is coupled to an increased demand in irrigation to sustain production due to low or variable rainfall amounts (especially in the lowlands) (Adhikari et al., 2015; German Calberto et al., 2015; Van Den Bergh et al., 2012; Varma & Bebber, 2019). To reap benefits of the increasingly thermal suitable climate, a more efficient cultivation is necessary as yields are expected to drop without maintaining and improving cultivation efficiency (i.e. irrigation) (Adhikari et al., 2015; German Calberto et al., 2015; Van Den Bergh et al., 2012; Varma & Bebber, 2019).

Banana grows well on many different types of *soils*. Soils should have a high WHC, as roots utilize water at high water potential (pF should remain above 2.1-2.5 before stress starts occurring (Kissel et al., 2015)) but waterlogging should also be avoided due to the high sensitivity of roots to anaerobic conditions (roots already show to be affected when waterlogged for 1-2 days) (Turner et al., 2007). Soils should thereby be porous and well drained (Robinson & Galan-Sauco, 2010). In the humid tropics, extra drainage is the most important infrastructure necessity (Stover & Simmonds, 1987). A sandy to clay loam texture is best suited to banana cultivation (Robinson & Galan-Sauco, 2010).

Soil pH should preferably be between 5.5 and 6.5 (Haifa, 2020; Robinson & Galan-Sauco, 2010). Nutrient requirements of banana are higher than almost any other crop (Gagnard et al., 1984). Uptake of macronutrients in a Cavendish cultivar with a production of 50 ton ha^{-1} goes in the order of K (1,438 kg ha^{-1}), N (388 kg ha^{-1}), Ca (227 kg ha^{-1}), Mg (125 kg ha^{-1}) and P (52 kg ha^{-1}) (Haifa, 2020). In the East African Highlands (and many smallholder farming situations), nutrient levels are often suboptimal due to inherent soil fertility problems (N and K deficiency) and lack of cash and access to fertilizers (A. I. Meya et al., 2020; Nyombi et al., 2010; Lydia Wairegi & van Asten, 2011). Depending on the area, soil fertility (K deficiency) may limit production even more than drought stress (Taulya, 2013), although fertility and drought stress are often interlinked as dry soils also reduce fertilizer uptake in chemically suitable soils due to a reduced availability to the roots (Taiz & Zeiger, 2010).

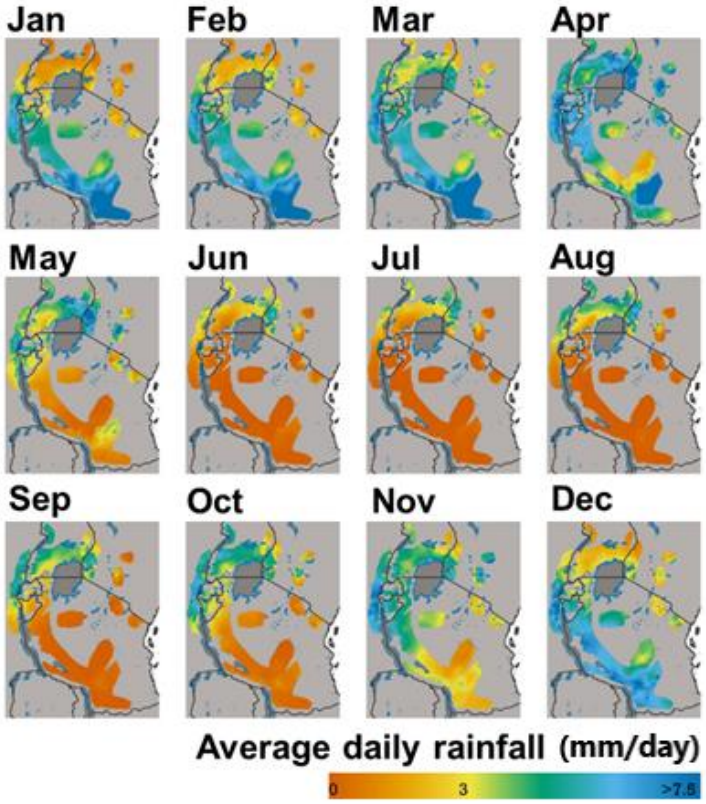


Figure 2-4: Average historical (1970-2000) daily rainfall (mm day^{-1}) for each month in the main banana growing regions in the East African Highlands (coordinates between 0-11°S and 29-37 °E). Banana growing regions according to Karamura et al. (1998). Source: Van Wesemael (2019).

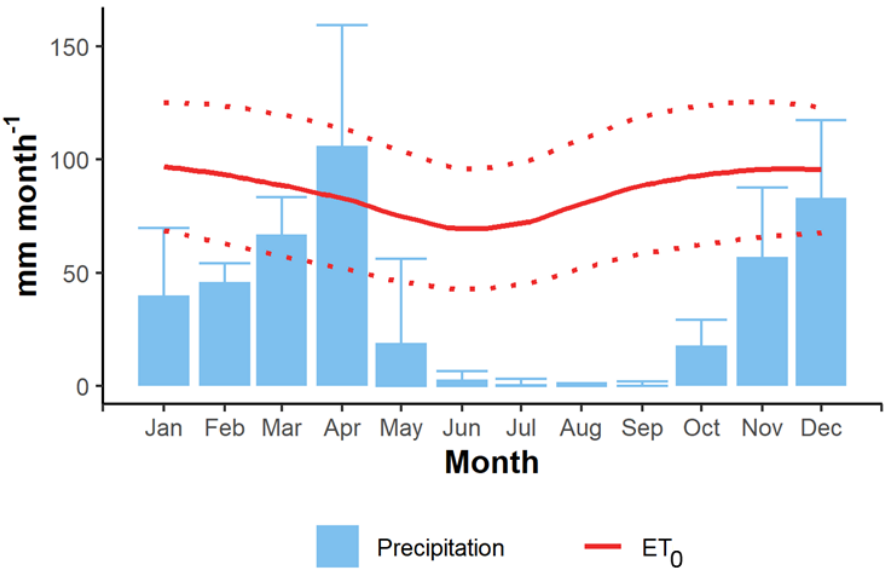


Figure 2-5: Growing season in Arusha, Tanzania (3°11'58" S and 36°40'22"E). Precipitation in mm month^{-1} (blue) with error bars showing ± 1sd. Reference evapotranspiration (ET_0) in mm per month. Solid line: average ET_0, dotted lines: ET_0 ± 1sd Data: NewLocClim (2020).

2.7 Banana response to moisture

Constraints to banana production can be biotic (i.e. pests and diseases) and abiotic (i.e. water stress, salinity, temperature, fertility) (Carr, 2009; Meya et al., 2020; Nyombi et al., 2010; Ploetz et al., 2015; Robinson & Galan-Sauco, 2010). Diseases caused by fungi, bacteria, viruses, and nematodes cause more losses than other biotic factors. The most threatening diseases are the Panama disease caused by the soil borne fungus *Fusarium oxysporum* f.sp. *cubense* and Black leaf streak disease (Black Sigatoka) caused by the fungi *Mycosphaerella fijiensis and Mycosphaerella musicola* (De Buck & Swennen, 2016; Ploetz et al., 2015). An overview of the most prevalent biotic stresses is given by Ploetz et al. (2015) Of the abiotic factors affecting production, water stress is considered the most threatening to production (Carr, 2009). The effect of climate change is regionally dependent (German Calberto et al., 2015; IPCC, 2019; Van Den Bergh et al., 2012; Varma & Bebber, 2019), but total global thermal suitable area for banana will increase by 8% by 2070. Of the entire thermal suitable area, 77% of the subtropics and 20% of the tropics cannot grow bananas without irrigation due to low rainfall amounts (<900 mm) (German Calberto et al., 2015). To combat disease pressure, bananas are more frequently being shifted to these dry areas (Ploetz et al., 2015). Furthermore, under the expected increasing temperatures worldwide, water demand is expected to further increase by 12-15% due to an increase in evaporative demand of the banana plant and speeding up of banana phenology leading to more production cycles per year (German Calberto et al., 2015). This leads to an increased importance in addressing water stress.

Water stress can come from excess of water, leading to oxygen stress in the plant and water deficits, leading to drought (Carr, 2009). Drought appears when the supply of water is less than the demand (Bodner et al., 2015). As banana is a long cycle crop, with heterogeneous plantation structure (Robinson & Galan-Sauco, 2010), a frequent and ample supply of water is needed as banana plants are very sensitive to soil moisture (Carr, 2009). Growth and production are already affected when 20-35% of total available water (TAW) is depleted (Allen et al., 1998; Carr, 2009; Robinson & Galan-Sauco, 2010) or when soil pF drops below 2.1-2.5 (Kissel et al., 2015). In banana, drought stress occurs well before plant physiological stress indicators are apparent such as wilting (leaf becomes limp through heat or loss of water due to turgor pressure drop) or increased leaf folding (leaf retains pressure, but actively folds halves to shed radiation) (Carr, 2009; Robinson & Galan-Sauco, 2010). Expanding tissues as emerging leaves and growing fruit are among the first to be affected visibly by drought (Carr, 2009; Kallarackal et al., 1990; Thomas & Turner, 1998). The most sensitive visible physiological indicator of plant water status is the leaf extension rate (Milburn et al., 1990; Turner et al., 2007), but this is not a reliable plant indicator when it is too hot (Turner & Thomas, 1998). Leaves are kept hydrated (0-0.35 MPa), even under severe water stress, most likely through root pressure (Carr, 2009; Kallarackal et al., 1990). Before the leaf water status is affected, under relatively mild soil drought conditions, banana plants already start to close their stomata, reducing gas exchange, transpiration, and photosynthesis. Leaf gas exchange (i.e. stomatal conductance) is more strongly linked to soil water status than leaf water status (Turner & Thomas, 1998). Based on physiological indicators drought can thereby only be spotted by farmers when yield losses already occur.

Drought during the vegetative stage induces stomata closure, reduces photosynthesis, reduces leaf area leading to lower DM accumulation in the banana mat (Carr, 2009; Thomas & Turner, 2001). Both leaf area and corm DM are built during the vegetative phase, and both sources determine the bunch potential which is set at approx. flower initiation (Eckstein & Robinson, 1995; Robinson & Galan-Sauco,

2010; Twyford & Walmsley, 1973). Drought may also delay time to flowering, time to harvest and sucker production (Fortescue et al., 2011; Taulya et al., 2014), reducing production ha^{-1} $year^{-1}$. Drought during vegetative growth and/or near flower initiation, may decrease the number of viable female flowers, thus reducing the number of hands and fingers on a bunch. Drought during bunch filling may reduce finger weight and thus bunch weight, and delay harvest compared to watered plants (Carr, 2009; Mahouachi, 2007; Robinson & Galan-Sauco, 2010; Turner et al., 2007).

Well performing commercial yields range between 40-50 ton ha^{-1} $year^{-1}$ for Cavendish type cultivars (FAO, 2018a). In contrast, actual banana production in the East African highlands is lower than 30 ton ha^{-1} $year^{-1}$ compared to attainable yields of 70 ton ha^{-1} $year^{-1}$ (Wairegi et al., 2010). Potential production is not reached due to diseases, soil fertility and drought (Taulya, 2013; Van Asten et al., 2011; Wairegi et al., 2009, 2010). Drought in the EAH is often cited as the main abiotic constraint for production (Van Asten et al., 2011; Wairegi et al., 2010), and improvements at the field scale are necessary.

2.8 Improving water use efficiencies in banana plantations through crop modelling

In crop production, Water Productivity (WP), or Water Use Efficiency (WUE), is the amount of crop produced per amount of water used (Ali & Talukder, 2008; Molden et al., 2010; Steduto et al., 2007a). It can be expressed at different scales: leaf scale (photosynthetic rate per transpired water), whole plant scale (DM production per plant per unit water use) and whole field scale (field DM production per unit area per unit water applied to the field), and for different outputs: total crop biomass (DM) produced, crop yield produced and/or crop economic value produced (Ali & Talukder, 2008; Steduto et al., 2007a). Further distinctions can be made on the nature of water used by the crop such as water transpired by the plant, total water in the soil and/or water applied by irrigation (Ali & Talukder, 2008; S. Geerts et al., 2010; Passioura, 2006; Pereira et al., 2002).

As many definitions exist, we define WP, or WUE, in this chapter as: "*the amount of aboveground DM (g or kg) produced per unit land area (m^2 or ha) per unit of water applied to the field by rainfall and irrigation"*.

WP is influenced by factors affecting crop production (numerator of WP) and factors affecting water in the field (denominator of WP). Factors include crop cultivar, nature of water applied and application systems (e.g. drip irrigation), soil type (e.g. water holding capacity) and agronomic management (e.g. mulching, planting time) (Ali & Talukder, 2008). Efforts to increase WP can be "crop focused" (affecting the WP numerator) and/or "management focused" (affecting the WP denominator), although a combination of both is necessary (Ali & Talukder, 2008; Bodner et al., 2015; Passioura, 2006; Peng et al., 2020).

Crop focus implies the use of improved cultivars (from within the existing biodiversity or genetically improved) that withstand drought stress better, by increasing the exchange of CO_2 per unit transpired water (Ali & Talukder, 2008; Bodner et al., 2015; Passioura, 2006). In banana, the occurrence of the B genome seems to be linked with an increased drought tolerance (Carr, 2009; Thomas et al., 1998), and research is being done into the genetic base of banana cultivars for drought tolerance (Ekanayake et al., 1994, 1998; Eyland et al., 2020; Van Wesemael, 2019). These insights are used to create a database of cultivars, to breed new drought tolerant cultivars, and to assess cultivar performance in different environments, improving WP at the plant level (plant biomass per mm water transpired). Improved cultivars may only improve WP when cultivated under good agronomic conditions, something not

always assured in farmer's fields. Crop focus strategies need to be supplemented by management focus strategies.

Management focus implies adjusting management practices in the field such that water flows through the soil-plant-atmosphere system are used optimally; where most water is used by transpiration and less water (both irrigation and rainfall) is lost through drainage, evaporation, and runoff. WP are improved at the field scale (field biomass per mm water added to the field) (Ali & Talukder, 2008; Bodner et al., 2015; Passioura, 2006; Pereira et al., 2002).

A wide cultivar of management interventions can be applied to banana fields ranging from low cost to capital intensive. Techniques include, but are not limited to: proper irrigation infrastructure (flood, basin, furrow, sprinkler, drip irrigation) and irrigation scheduling (full, supplemental and deficit) (S. Geerts et al., 2010; Lehmann et al., 2013; Molden et al., 2010; Passioura, 2006; Pereira et al., 2002); soil-water conservation practices through techniques as water harvesting, soil bunds, vegetative barriers, tillage management and sub-soiling (Ali & Talukder, 2008; Bodner et al., 2015; Molden et al., 2010; Wolka et al., 2018); increased soil fertility through nitrogen fertilization (Bodner et al., 2015; Lehmann et al., 2013); increased soil organic matter by application of organic matter, mulch, manure, bio-fertilizer, legumes (Ali & Talukder, 2008; Bodner et al., 2015; Meya et al., 2020); improved soil surface cover through mulching, soil and stubble management (Bodner et al., 2015; Passioura, 2006); adjustment of plant management through crop rotation, plant density, cover cropping, early and late sowing practices (Ali & Talukder, 2008; Bodner et al., 2015).

Success of management interventions depends on the biophysical nature of the location, spatial and temporal scale of proposed interventions and goals, capital and risk-taking behavior by multiple stake-holders affected by the management interventions (Bergez et al., 2012; Molden, 2007). Cost-benefit analyses need to occur before management strategies are implemented as more certainty regarding success by interventions is necessary. Market uncertainty and uncertainty in water and rain often characterizes a farmer's situation (Molden et al., 2010). Farmers often cannot spare resources (time, cash, and labor) to test water management strategies in the field. Indeed, the testing of management interventions is tedious, high cost and laborious. Better tools need to be developed for agricultural water management (Bergez et al., 2012; Molden et al., 2010; Peng et al., 2020). Alternatively, computerized simulations and growth simulations of fields should be developed and applied (Bergez et al., 2012; Hoogenboom et al., 2004; Lehmann et al., 2013; Peng et al., 2020; Steduto et al., 2012) as computer simulations allow to quickly assess management interventions, unlike with field experiments that take years. Good models however require good data, and models themselves are also characterized by uncertainties in simulation results. Models themselves are descriptions of a (simplified) reality and characterized by necessary trade-offs between accuracy, robustness and simplicity (Bouman et al., 1996; Van Ittersum et al., 2003). The overall usefulness of a model thereby depends strongly on the accuracy and robustness of simulation results, and the necessary simplification of the model structure compared to reality for adoption by end users. Smallholder farms, often characterized by a multitude of production defining factors, are most difficult to measure. Often simplified, idealized production scenarios are modelled which contrast to the physical smallholder reality in the field.

Well calibrated and performing model outputs can be used to facilitate management decisions at different spatial scales (field to catchment) and at different time scales: daily to weekly (e.g. timing

and duration of next irrigation), weekly to monthly decisions (e.g. planting density) and strategic yearly decisions (e.g. determine the duration before an irrigation investment pays back its costs) (Bergez et al., 2012; Steduto et al., 2012).

By running simulations, computer models have many potential uses such as:

- Predicting production under environmental changes such as impact by global warming, effect of rainfall variability and climate change on production (Hoogenboom et al., 2004; Lehmann et al., 2013; Peng et al., 2020; Steduto et al., 2012)
- Predicting consequence of different cultivars and cultivars on agricultural and ecosystem performance (Peng et al., 2020)
- Identifying optimal sowing dates and crop spacing in rainfed and irrigated fields (Hoogenboom et al., 2004; Steduto et al., 2012)
- Mapping water-limited yield potential of regions and estimating suitable areas for plantation expansion (Hoogenboom et al., 2004)
- Determining yield gaps in rainfed systems by comparing actual and potential yields (Hoogenboom et al., 2004; Steduto et al., 2012)
- Determining water requirement and development of seasonal irrigation schedules (full and deficit) for different crops and locations at field and farm scales (S. Geerts et al., 2010; S. Geerts & Raes, 2009; Steduto et al., 2012)
- Assessing the influence of multiple management options (mulching, soil water harvesting, date of planting, soil cover cropping) on production and water use in rainfed systems (Lehmann et al., 2013; Steduto et al., 2012; Tixier et al., 2008)
- Determining the economic viability of management interventions at the field scale (Steduto et al., 2012; Tixier et al., 2008)
- Quantifying risk and setting insurance prices for agricultural producers (Castañeda-Vera et al., 2015)

This is only a selection of potential uses, and many more can be conceived. Models are therefore useful tools to study banana plant growth in the field, and its response to external factors. As soil moisture quickly affects leaf gas exchange, unlike other visibly physiological indicators, the link between banana production and the soil moisture balance is crucial. Hence a computer simulation model for banana would be a handy tool to assess the impact of drought stress, production in the field and the testing of different management interventions. However, a widely known model simulating water-limited banana production in the field does not exist, largely due to the complexity of the banana growth structure (i.e. multiple cycles on a mat, perennial growth, long cycle duration) and the difficulty in obtaining complete banana growth data for model calibration spanning multiple cycles (i.e. large plants, frequently rainfed so no optimal production, long experimental trials).

Following chapter will detail the previous banana modelling efforts and highlight the model of choice used in this thesis.

3 Banana crop modelling efforts

3.1 Crop modelling introduction

Since the 1960s simulation models have been used in various agricultural disciplines to study crop growth in relation to biochemical and physical components as radiation, soil moisture and nutrients (Hoogenboom et al., 2004; Van Ittersum et al., 2003; Zotz & Bader, 2009). Models are characterized by (1) an incomplete system description through mathematical equations, (2) assumptions and (3) a trade-off between accuracy and simplicity (Van Ittersum et al., 2003). Based on the objectives and details, many different models can describe a same system. Models are either empirical/functional (descriptive) or mechanistic (explanatory), or combine the aforementioned models (Bouman et al., 1996; Van Ittersum et al., 2003). *Empirical, functional or descriptive models* describe relationships between variables of interest (e.g. transpiration and biomass) without explaining underlying biological or physical features that exist between variables (Van Ittersum et al., 2003). Allometric biomass models are rather functional and empirical (Niklas, 2004). *Mechanistic or explanatory models* are "process based". They aim to simulate variables (e.g. biomass production) in terms of the underlying processes of a plant (e.g. photosynthesis). In contrast to functional models, mechanistic models are developed from an understanding of the behavior of the system's components (Bouman et al., 1996; Van Ittersum et al., 2003). These models are more detailed and computationally intensive.

Most of the current crop growth models are empirical, mechanistic or combine components of both. In the beginning of crop modelling, the focus was most on scientific insight and understanding of the system (Bouman et al., 1996). Models designed for understanding systems, are mostly mechanistic and very accurate, but require intense parameterization and comprehensive input data (often unavailable) limiting their use to researchers (Bouman et al., 1996).

Later, through the development of personal computing, the focus in modelling shifted from understanding systems towards practical decision support (Bouman et al., 1996). Models designed for decision support are intended for widespread adoption, being more descriptive, robust and simpler to use (Bouman et al., 1996; Van Ittersum et al., 2003). Balancing simplicity, robustness and accuracy is at the outset of any crop model and determines the model type and intended use.

Three groups of growth factors determine the crop production situation: growth defining factors, growth limiting factors and growth reducing factors (Figure 3-1). Potential production is the level of production that can be optimally reached in a given region for a given crop and can be modelled based on growth defining factors related to the environment: CO_2, radiation, temperature, and crop characteristics: physiology, phenology, and canopy structure. Attainable production considers growth limiting factors: water and nutrient stresses. The difference between potential and attainable production is practical: growth defining factors cannot be influenced by a farmer, whilst growth limiting factors can be alleviated with agronomical practices e.g. irrigation and fertilization. To model attainable production, information on moisture and nutrient fluxes need to be embedded in crop models. Actual production includes growth reducing factors: weeds, pests, diseases and pollutants (Bouman et al., 1996; Nyombi, 2010; Van Ittersum et al., 2003).

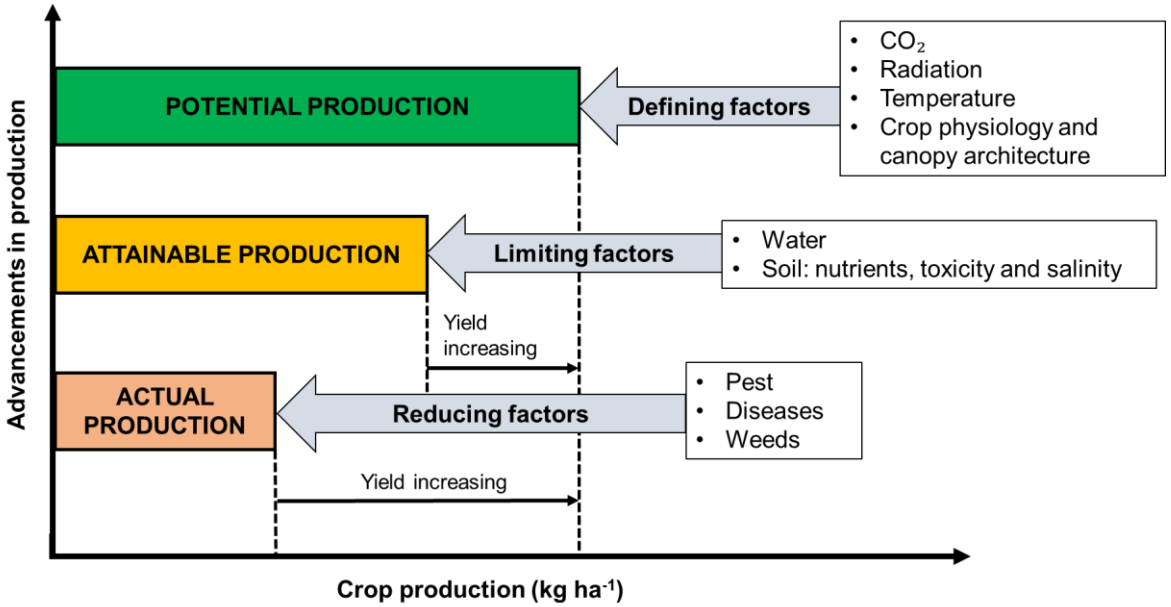


Figure 3-1: Crop production model building: Potential, attainable and actual production. Adapted from Bouman et al. (1996); Van Ittersum et al. (2003) and Nyombi (2010).

Due to the difficulty of incorporating growth reducing factors, most crop models focus on potential and attainable production (Nyombi, 2010; Steduto, 2006; Van Ittersum et al., 2003; Zotz & Bader, 2009). Some crop models started by modelling potential production based on defining factors, and later adjusted these models for modelling attainable production (e.g. LINTUL, WOFOST, STICS), whilst others started at the outset for modelling attainable production by focusing on different simulation processes and growth engines (e.g. AquaCrop, see further).

3.2 Simulated processes in crop models

Crop models mostly simulate three things: (1) crop phenology (timing of events in a crop's lifetime), (2) total dry biomass (DM) production and (3) allocation of DM to various plant organs (Bouman et al., 1996; de Wit et al., 1970; Tixier et al., 2008; Van Ittersum et al., 2003; Zotz & Bader, 2009).

3.2.1 Modelling crop phenology

Crop phenology describes timing of crop development stages as e.g. flowering and harvest in banana. Timing between events can be expressed in days, but this will differ substantially between environments with different growth potentials as phenology of plants can be influenced by temperature, photoperiod and occurrence of stress (Carr, 2009; Fortescue et al., 2011; Taiz & Zeiger, 2010).

A more robust way of measuring crop phenology consists in the accumulation of heat units or growing degree days (GDD in °C day^{-1}) (Fortescue et al., 2011; McMaster & Wilhem, 1997; Taiz & Zeiger, 2010). GDD are measures of heat energy received by the plant over a certain time and calculated daily:

$$GDD = [(T_{max} + T_{min})/2] - T_{base}; \quad (3\text{-}1)$$

where T_{max} and T_{min} are daily maximal and minimal air (or plant) temperatures (°C) and T_{base} is a crop-specific base temperature (°C) below which growth ceases (McMaster & Wilhem, 1997).

Summing of daily GDD accumulated by the plant leads to GDD accumulation over time (GDD in °C days or °Cd).

In day-neutral plants, development between stages is driven by temperature only, and phenological events are reached upon accumulating a specified GDD sum threshold (°C days). In environments differing in climatic (temperature) conditions, plants can flower at different days after planting, but accumulated GDD will be similar between environments (McMaster et al., 2008; McMaster & Wilhem, 1997; Taiz & Zeiger, 2010). Some plants require an additional period of low temperatures (vernalization) before flowering. In photoperiod-sensitive plants, flowering is co-determined by day length. Some plants further delay phenology under stress (Fortescue et al., 2011; McMaster et al., 2008; Taiz & Zeiger, 2010; Van Ittersum et al., 2003).

Phenology in crop simulation models is mostly expressed in terms of singular critical thresholds, expressed in days or GDD. Upon reaching these thresholds, all plants shift between phenological stages. Most crop models use GDD to drive development (AquaCrop (Steduto et al., 2009); LINTUL (Nyombi, 2010; Taulya, 2015; Van Ittersum et al., 2003)), possibly modified by a vernalization, photoperiodic or stress limiting factor (STICS (Brisson et al., 2003; McMaster et al., 2008)).

3.2.2 Modelling biomass production through growth engines

Photosynthetic organisms use solar energy to synthesize carbon compounds from water and CO_2 creating oxygen in the process. The most photosynthetic active tissue in higher plants is the mesophyll of the leaves containing most of the chloroplasts. The amount of solar energy intercepted and utilized by the leaves largely determines the amount of carbon accumulated. Photosynthesis assimilates CO_2, whilst cellular respiration releases CO_2 to keep the metabolism of the organism running. The balance between photosynthesis and maintenance respiration determines plant growth and DM production (Taiz & Zeiger, 2010).

Growth models explain biomass production through an underlying growth engine, which formalizes how carbon compounds are assimilated. Generally, there are three main types of growth engines: (1) carbon-driven growth engine, (2) radiation-driven growth engine, and (3) water-driven growth engine (Steduto, 2006; Zotz & Bader, 2009).

In *carbon-driven* models, growth is based on carbon assimilation by the leaves through photosynthesis. The leaf area of a plant is separated in discrete layers based on canopy height, and carbon is assimilated in these discrete layers by knowing the light response curve in these layers, and the diurnally variable light interception (photosynthetic active radiation) in these layers. Integration over the entire canopy height over a day, results in simulation of daily carbon accumulation, which is reduced by daily maintenance and growth respiration of the various organs (Steduto, 2006; Van Ittersum et al., 2003). The mechanistic description of photosynthesis in equations is very detailed, but loses robustness as uncertainties in light response curves, photosynthesis and respiratory processes, can lead to large growth error rates (Steduto, 2006).

Radiation driven models work like carbon-driven models but bypass the extensive equations (light response curves, photosynthesis and respiration) by using a single Light Use Efficiency (LUE), or Radiation Use Efficiency (RUE) parameter (Bouman et al., 1996; de Wit et al., 1970; Steduto, 2006; Van Ittersum et al., 2003; Zotz & Bader, 2009). These models make use of the linear relationship between accumulated intercepted solar radiation (R_{Sint}) and the accumulated aboveground biomass (B) for crops. Its core can be formalized as:

$$B = LUE \times \sum R_{Sint}; \quad (3\text{-}2)$$

with B being the accumulated aboveground dry biomass (DM per unit area), LUE being light (radiation) use efficiency (DM per unit area per unit intercepted solar radiation), and R_{Sint} being the intercepted solar radiation by the plant canopy (unit intercepted solar radiation). Radiation can be expressed as total solar radiation or the photosynthetic active radiation (PAR) (MJ m^{-2}).

LUE factors have shown to vary with plant species, age, water deficit, leaf nitrogen content, temperature and other stresses (Sinclair & Muchow, 1999; Steduto, 2006; Van Ittersum et al., 2003). This creates a significant difficulty in using radiation driven models under stress conditions or extrapolating their use to other environments.

Models using light interception (carbon driven and radiation driven growth engines) comprise most well-known crop models e.g. BACROS, SUCROS, WOFOST, CROPGRO, SOYGRO, TOMGRO, CERES, EPIC, STICS, CROPSYST, LINTUL, SIMBA (Bouman et al., 1996; Steduto, 2006; Tixier et al., 2008; Van Ittersum et al., 2003).

In contrast, *Water driven* growth models rely on the link between transpiration (Tr) and biomass production (Steduto et al., 2007a; Taiz & Zeiger, 2010). The core of water driven growth models, can be formalized as:

$$B = WP_b \sum T_r; \quad (3\text{-}3)$$

with B being the accumulated aboveground dry biomass (DM per unit area), WP_b being the biomass water productivity (DM per unit area per unit water transpired) and T_r being transpiration (unit water transpired). This relationship has proven to hold at the leaf, plant and field scale (Steduto et al., 2007b), but is dependent on the environment. WP at the leaf scale (WP_p) is determined by gradients in water vapour and CO_2 between the intercellular spaces and the atmosphere (Steduto et al., 2007a; Taiz & Zeiger, 2010). WP_p, and by extension WP_b, thereby depends on environmental conditions governing water vapor removal (VPD and ET_0) and CO_2 concentrations. At a stable VPD and ET_0, an increase in atmospheric CO_2, will increase WP_p. At a stable atmospheric CO_2, an increase in VPD and ET_0 will lead to larger water gradients between the atmosphere and the intercellular space in the leaf, and thereby reduce WP_p through faster transpiration.

In order to use a stable WP_b across different environments, normalizing WP_b for evaporative demand (ET_0 or VPD) and CO_2 content is necessary. WP_b^* is the normalized WP_b for ET_0, and describes the slope between the sum of T_r/ET_0 and accumulated biomass (eq. 3-4) (Steduto et al., 2007b).

$$WP_b^* = \frac{B}{\sum_{i=1}^{n} t_i \left(\frac{T_r}{ET_0}\right)_i} \quad (3\text{-}4)$$

with B being the total accumulated aboveground dry biomass (DM per unit area), WP_b^* being the normalized biomass water productivity for ET_0 (DM per unit area per time interval), T_r being transpiration (unit water transpired per time interval) and ET_0 being the reference evapotranspiration (unit water evapotranspired per time interval). n is the number of time intervals, t is the length of each time interval (in days), i is the number of discrete time intervals over which T_r is normalized. Often, the time interval is taken as 1 day for daily normalization.

WP_b^* can be used across climates and similar crop cultivars. This makes it highly useful for use in water-limited environments (Steduto et al., 2007a). WP_b can similarly be normalized for VPD, but normalizing for ET_0 has shown to be more robust across environments. The only drawback is the difficulty in determining actual T_r at field scales for comparison against modelled values (Steduto et al., 2007a; Steduto, 2006). AquaCrop uses a water driven growth model (Vanuytrecht, Raes, Steduto, et al., 2014).

3.2.3 Modelling dry matter partitioning

Total biomass produced by the leaves is partitioned to different plant organs depending on sink strength of the organs (Taiz & Zeiger, 2010). Depending on a model's detail, allocation to many different plant organs can be modelled. Most agricultural crop models, however, minimally use a harvest index factor (HI), that sets the percentage of DM that is allocated to yield (Lacointe, 2000; Le Roux et al., 2001; Raes et al., 2018c; Van Ittersum et al., 2003; Zotz & Bader, 2009).

There are four main concepts of assimilates partitioning used in crop modelling: (1) empirically determined allocation coefficients, (2) growth rules models, (3) source/sink relationship models and (4) transport resistance models (Lacointe, 2000; Le Roux et al., 2001; Zotz & Bader, 2009).

In *empirical* models, daily allocation coefficients are determined experimentally, and no underlying mechanism is assumed. The shortcoming is that allocation coefficients vary according to plant species, plant organ, environment, phenology and stress, and may not be valid under conditions that vary from the experimental conditions (Lacointe, 2000; Zotz & Bader, 2009). When the same conditions occur, these models can be very efficient and most simulation models use empirically derived partitioning coefficients as this simplifies calculations (Le Roux et al., 2001; Van Ittersum et al., 2003).

In *growth rules models*, carbon is partitioned with an intrinsic goal in mind. These goals can be based on empirical rules, architectural rules and/or functional rules. *Empirical allometry* includes a relationship between dimensional variables that are put under internal constraints or balances, without an underlying mechanism explaining the relationship. For example, a relationship between height and girth of a plant. *Architectural rules*, in contrast, involve partitioning of resources to maintain architectural structures (e.g. needle architecture in pine trees). *Functional allometry* is similar to empirical allometry, but here the underlying mechanism between variables of interest is known. An example is plants that maintain a constant root-shoot ratio, or partition resources to load bearing structures to prevent plant collapse (Lacointe, 2000; Zotz & Bader, 2009).

Assimilate movements based on *source-sink* relationships are based on the capacity of different sinks to subtract assimilates from different sources. Sink strength, a flux that can be imported in a sink under non-limiting conditions is used in these models (Lacointe, 2000; Zotz & Bader, 2009). In *proportional models*, the flux allocated to each sink is proportional to its demand. Factors decreasing the proportion of assimilates with distance between source and sink can be added. In *hierarchical models*, sinks are ranked according to a priority level. Higher ranked sinks receive assimilates first, and lower ranked sinks receive assimilates only if demand of higher sinks are met. Hierarchical models are flexible in use by changing the priority in view of crop phenology, environmental and stress influences (Lacointe, 2000).

Transport-resistance models describe assimilate movements as driven by concentration gradients across resistive pathways. These models are the most mechanistic as they are based on the

mechanism of mass flow, from high to low concentration. This approach remains largely theoretical and has not been used widely (Lacointe, 2000; Zotz & Bader, 2009).

In most agricultural crop models an empirical approach is used with fixed partitioning coefficients that depend on development stages, as other approaches are more computationally intensive and mostly used in single tree growth models (Zotz & Bader, 2009).

3.2.4 Modelling attainable production: soil moisture balance and stress

When simulating attainable production (limited by water and/or nutrients) crop models need to incorporate the effect of these stresses (Bouman et al., 1996; Van Ittersum et al., 2003). Water stress (deficit and excess) is often based on soil water contents (SWC), whilst nutrient stress is linked to nutrient levels in the soil. In this thesis, water-stressed simulation is of interest. Since soil moisture affects production, proper simulation models need to incorporate water balances in the root zone as an indicator for stress. Crop models use mainly two approaches for modelling the soil water balance: (1) the tipping bucket mechanism, or (2) the Richards approach (Van Ittersum et al., 2003).

In the tipping bucket mechanism, the soil underlying the crop is specified into one or multiple soil layers, characterized by their own physical and chemical characteristics. The soil is assumed horizontally homogenous, as is the root proliferation in the soil. Characteristics can be moisture content at saturation (θ_{SAT}), at field capacity (θ_{FC}), at permanent wilting point (θ_{PWP}), air dry moisture content (θ_{AD}), anaerobic stress moisture content (θ_{aer}), together with porosity (%), hydraulic conductivity (K_{SAT}) and drainage rate (τ in $m^3\ m^{-3}$). Each layer is minimally characterized by its θ_{FC}, the volumetric water content below which water no longer drains from the soil layer. Inflow occurs through rainfall, irrigation, and capillary rise. Outflow occurs through evaporation, transpiration, and deep percolation. The water infiltrating the soil fills the specific horizons to field capacity from the surface downwards (Emerman, 1996; Van Ittersum et al., 2003). Using this simple approach, soil water fluxes in and out of the rooting zone are specified, and water is redistributed according to the root proliferation and tipping bucket mechanism (Emerman, 1996). Depending on the used model, the tipping bucket approach can be adjusted minimally or extensively to better describe soil water fluxes in the soil horizons.

The Richards approach describes soil moisture transport in the soil through water potential gradients created by gravity, root water extraction and water suction profiles due to entering of soil water. Being a mechanistic model it is more computationally intensive and rarely used in crop modelling exercises (Van Ittersum et al., 2003).

Based on daily SWC in the root zone, soil moisture stress can be calculated. In most crop models, effect of stress is simulated using stress coefficients (K_S), which are multiplied by certain target parameters underlying modelling processes. They range from 1 (no stress) to 0 (full stress). Stress factors are defined by specifying upper and lower thresholds for the stress indicators (e.g. moisture content) and by selecting a stress curve shape. Shapes can be linear, logistic or convex between these upper and lower thresholds of K_S (Hsiao et al., 2009; Raes et al., 2009; Vanuytrecht, Raes, Steduto, et al., 2014). This allows easy adjustment to stressed production, without a complete overhaul of modelling structures and schemes.

3.3 Banana crop production models

Modelling efforts on banana or plantain plants have been performed, of which the most important are and ranked chronologically: Leaf production model by Mekwatanakarn and Turner (1989), CENTURY (Woomer et al., 1998), STICS (Brisson & Dorel, 1998), SIMBA (Damour et al., 2012; Dorel et al., 2008; Ripoche et al., 2012; Tixier et al., 2004, 2006, 2008, 2011) LINTUL (Chaves et al., 2009; Nyombi, 2010; Taulya, 2015) and ABB plantain model (Dépigny et al., 2017). These models differ substantially in their degree of complexity, adjustment to the banana cropping structure, growth engine and intended use. Models presented here simulate at least one component of banana production. Other models that only consider climatic suitability's (e.g. ECOCROP (Van Den Bergh et al., 2012)) are not presented.

3.3.1 Leaf production model

Mekwatanakarn and Turner (1989) developed a simple empirical model using daily temperature to simulate weekly leaf production and flowering onset for a "Williams" Cavendish variety based on data from New South Wales, Australia. They adapted an apex model, that assumed new leaf formation to occur whenever a specific apex weight was obtained based on temperature. After a preset number of leaves formed, plants were assumed to flower. This model was intended to gain an understanding in leaf formation and flowering of banana plants in relation to the environment. An increase in temperature would lead to a faster leaf development, and hence, flowering in banana. However, the model was created empirically and was only suitable in the environment and cultivar of the study. As leaves emerging before flowering vary substantially between cultivars, environments, planting dates and even among individual plants planted at the same date (Fortescue et al., 2011; Robinson & Galan-Sauco, 2010; Tixier et al., 2008), this model cannot to be generalized to different environments and cultivars.

3.3.2 CENTURY

CENTURY is a modular plant-soil environmental simulation model originally developed by Parton et al. (1987) to simulate dynamics of carbon (C), nitrogen (N), phosphorus (P) and sulfur (S) under grasslands. CENTURY runs on a monthly time-step, with main inputs being monthly maximum and minimum temperature, monthly precipitation, lignin content of plant material, plant N, P, and S content, soil texture, atmospheric and soil N inputs and initial soil C, N, P and S levels. Inputs are already quite technical as nutrient contents need to be specified. Its main focus is the soil organic matter flow (C, N, P and S flows through plant litter and the soil system) for ecosystem analysis (Metherell et al., 1993; Parton et al., 1987). Plant production is modelled using sub models. Potential production is defined by an empirically derived maximum for each crop, adjusted by scalars depending on soil temperature, moisture, shading, and seedling growth. A simplified water budget model calculates monthly water contents, evaporation, transpiration and soil water loss through a tipping bucket mechanism (Metherell et al., 1993).

Woomer et al. (1998) used the CENTURY model for simulating steady state highland banana plantations. Calibration was done by iteration and trial and error without extensive field observations. CENTURY remains hence more suited to explore nutrient flows, than to simulate crop production.

3.3.3 STICS

STICS (Simulateur mulTIdisciplinaire pour les Culture Standards) is a daily time-step model simulating crop growth together with nitrogen and water balances in the soil. In contrast to CENTURY, crop production is central to the STICS model (Brisson et al., 2003).

STICS is a radiation-driven model, whereby growth depends on the amount of light intercepted and utilized by foliage. STICS is a modular growth model. A first set of modules describes the aboveground ecophysiology, as determined by the modules phenology, shoot growth and yield formation. A second set describes soil-plant interactions, as determined by the root growth, water and nitrogen balance and soil transfers. Crop management models describe how applied management influences the soil-plant system (Brisson et al., 2003).

Crop phenology is driven by GDD possibly adjusted for photoperiod and vernalization. The aboveground plant parts are characterized by LAI, and the number and biomass of harvested organs. LAI determines potential light interception which determines potential biomass accumulation. Stress indices in terms of water, nitrogen or trophic stress may influence phenology and potential daily biomass accumulation through multiplication by stress coefficients. Yields are determined through partitioning the accumulated biomass to harvested organs, determined by harvest indices, and sink strengths varying over the developmental stages. Plant roots, which determine the contact between soil and plant, are characterized by their root length and density distribution, and given their position in the soil, determine nitrogen and water stress by assessing moisture contents and nitrogen levels in their root zones. Water balances in the soil are calculated through a simple tipping bucket mechanism (Brisson et al., 2003).

Brisson and Dorel (1998) adapted the generic crop model STICS to tropical banana plantations in terms of phenological development, leaf and root growth and number of fingers in a bunch based on data from different tillage and irrigation experiments. Parameters where adjusted based on literature values or experimental data in a way that experimental data and simulations achieved an as good as possible overlap. However, only generic parameters were adjusted and extensive adjustment for the banana structure (perennial multi-cycle behavior) was not embedded. The STICS model did not incorporate any information on heterogeneity of banana plantations. In addition, it did not account for the banana ratooning behavior and cycling.

Results indicated a poor agreement of experimental and simulated rooting patterns (RLD) and soil water contents (SWC). LAI was satisfactorily simulated. Simulated finger number was close to actual observed finger number in all irrigation treatments (within 2% of observed values), but authors did not specify how fingers were modelled, nor at what stage fingers were at harvest. Future studies on banana modelling building upon the STICS software were not presented.

3.3.4 SIMBA models

The *SIMBA* models were built specifically for assessing agronomic, environmental and economic characteristics of multiple banana cropping systems (Tixier et al., 2008). These models run in a weekly time step (Damour et al., 2012; Tixier et al., 2008). SIMBA has a modular structure. It is composed of many sub-models or modules describing the different subsets of a banana plantation system. Plant growth modules include SIMBA-GROW, an individual plant growth module (Tixier et al., 2008) and SIMBA-POP a module describing population structure (Tixier et al., 2004). Soil modules include SIMBA-SOIL describing the physical soil properties, and SIMBA-COV describing the soil cover dynamics by

weeds and mulch. SIMBA-CC describes growth (LAI and biomass) of 11 cover crop species in terms of radiation under banana plants. Water and nutrient modules are the SIMBA-WAT module, describing the soil water balance and the SIMBA-N module, describing the soil mineral N content (Dorel et al., 2008; Tixier et al., 2008). SIMBA-NEM describes population dynamics of two major nematode species affecting banana (Tixier et al., 2006). The SIMBA-ECO module calculates the gross margin in Euro of a plantation by comparing weekly fruit production with selling price, manpower and input costs (Tixier et al., 2008).

These modules are interlinked tightly, and outputs of specific sub-models are used as inputs of other sub-models. Inputs to start the overall SIMBA model are climate variables (e.g. temperature) and management practices which can be tactical (short term e.g. frequency and amount of N fertilization) or strategic (long term e.g. planting in monoculture) (Tixier et al., 2008). Of the given sub-modules, SIMBA-POP and SIMBA-GROW simulate banana production. Linking these modules to SIMBA-N and SIMBA-WAT, allows simulation under abiotic limited conditions (Dorel et al., 2008; Tixier et al., 2008). The extensive composition of many sub-models however makes the SIMBA model difficult to use. The authors themselves state "due to the high number of inputs (parameters and data) and outputs … numerical validation of the whole model is complex and almost impossible" (Tixier et al., 2008). Validation of the SIMBA model can only be carried out by validating single SIMBA sub-modules on various datasets, but validation of individual modules, does not ensure validation of interaction between the modules (Tixier et al., 2008). Yet these models were the first to incorporate banana generation cycling into a growth simulation model and as such have great scientific value even if validation cannot be ensured.

The *SIMBA-POP* model was the first modelling effort to incorporate the heterogeneous population structure of banana plantations (Tixier et al., 2004). SIMBA-POP aimed at describing population over time by simulating the number of suckers emerged, plants flowered, and bunches harvested per week on a plot level based on daily temperature. Its main purpose is to describe phenological distributions and harvest dynamics within a plantation. Heterogeneous plantations are divided into homogenous cohorts, i.e. groups consisting of banana plants characterized by the same phenological age. Cohorts are linked end-to-end in cohort chains, allowing plants from one cohort to move to another cohort upon reaching a specified amount of heat units (GDD). The model is composed of two cohort chains: a pre-flowering cohort chain, and a post-flowering cohort chain. Stochastic curves for sucker emergence, flowering and harvest underlie the model, following observations of Ganry (1976), Lassoudière (1979; 1980) who noticed that flowering, sucker emergence and harvest patterns follow log-normal distributions over time. These probability distributions determine the number of emerged suckers, flowered and harvested plants at each time step under optimal conditions. Newly formed suckers (which can occur in each cohort) move to the first cohort, whilst flowering plants from the pre-flowering cohort move to the first cohort of the post flowering cohort-chain. At each time step plants move through the cohorts. Calibration and validation of the model used non-stressed data from banana fields in Guadeloupe and Martinique, French West Indies. The model showed predicted 29 harvest peak dates within 3 weeks of actual peak harvest dates for the first 3 cropping cycles (R^2 = 0.99). A shortcoming of the model is that it only simulates phenology under optimal conditions. Banana shows a slower growth under water and nutrient stress, and temperature alone therefore does not govern phenology alone (Fortescue et al., 2011; Lamour et al., 2020).

The *SIMBA-GROW* module is a radiation-driven model. Leaf growth (LAI), total DM production (B) and DM allocation (leaves, pseudostem, roots and bunch) is simulated in each cohort (defined by

SIMBA-POP) (Damour et al., 2012; Tixier et al., 2008). Biomass production is based on intercepted radiation by the leaves. DM is partitioned to the different plant organs (leaves, pseudostem, sucker, bunch) depending on plant phenology (Tixier et al., 2008) and sink strength (priority rules) (Damour et al., 2012). Four growth stages are present: (1) planting to sucker appearance, (2) sucker appearance to flower initiation, (3) flower initiation to flower emergence and (4) flower emergence to harvest (Damour et al., 2012; Tixier et al., 2008). Floral initiation is simulated when LAI production exceeds a threshold; intervals after floral initiation are driven by GDD (Ripoche et al., 2012). During the vegetative phase, DM is partitioned to vegetative organs depending on phenology dependent allocation coefficients. LAI growth is based on specific leaf surface produced per DM unit accumulated ($cm^2\ g^{-1}$). During the generative phase, biomass is allocated first to the bunch, and remaining assimilates are partitioned to other structures depending on fixed partitioning coefficients (Damour et al., 2012). LAI at generative phase decreases by senescence. Stress factors were calculated from outputs of other modules and include nematode stress (SIMBA-NEM), fertility stress (SIMBA-N) and drought (SIMBA-WAT). These stress factors reduce the LUE, potential LAI and biomass depending on severity of stress and range from 1 (no stress) to 0 (full stress) (Tixier et al., 2008).

Calibration of the SIMBA-GROW module by Tixier et al. (2008) was based on data from Dorel (2001) and Jannoyer (1995) in Guadeloupe. Additional validation of the calibrated model on field survey data in 2000 in Guadeloupe lead to moderate good to poor model fits (R^2 = 0.55-0.72 and RRMSE= 26.3%) between observed and simulated yield per year. Other validation outputs of the SIMBA-GROW module (LAI, total DM) were not published in their research. Damour et al. (2012) linked a simple water and nitrogen availability module to SIMBA-GROW to validate water and nutrient limited growth. They focused on parameters LAI at flowering and thermal time to flowering (GDD) using data from cover-crop experiments in Guadeloupe. Treatments were rainfed (2,000 mm) and differed only by soil cover: bare soil versus cover crops, leading to moisture stress and N differences between treatments. Flowering date was simulated satisfactorily for both (-3 to -11%), whilst LAI at flowering was simulated satisfactorily for bare soil (+3%) but not for cover crops (+20%). No observations were present for LAI evolution over time, biomass, and yield, so simulations over time could not be compared to plantation growth over time.

The *SIMBA-WAT* model simulates soil water content in the crop root zone through a simple tipping bucket mechanism (Tixier et al., 2008). Water is distributed throughout the horizon from top to bottom when a horizon reaches VWC values above FC. Based on critical SWC, stress factors are computed and range from 1 (optimal moisture) to 0 (permanent wilting point) to be used in other sub-models as SIMBA-GROW and SIMBA-POP. Previous validation of the SIMBA-WAT module on data from Guadeloupe plantations showed a moderately good fit between simulated and actual water potential per week (RRMSE: 20.6%) (Tixier et al., 2008). This indicates this module to perform fair in field conditions.

Dorel et al. (2008) designed the *SIMBA-N* model to simulate the soil nitrogen balance in banana plantations. Weekly N balances are computed considering N flows as leaching, N uptake by banana and soil organic matter mineralization. N nutrition stress indices were defined based on critical soil mineral N values (40 kg ha^{-1}) and range from 1 (no stress) to 0 (no N in soil) and are to be linked to SIMBA-GROW and SIMBA-POP for fertility stressed production. Fertilizer experiments in Guadeloupe were used for model validation. Parameters used for comparison were monthly soil mineral N dynamics. Soil mineral N dynamics were simulated accurately to moderately fair by SIMBA-N (RRMSE:

15-26%), indicating N levels in the soil and potential nutrient stress can be simulated underneath banana plantations.

Ripoche et al. (2012) created *SIMBA-IC*, an intercropping model that simulated banana (SIMBA-GROW) and cover crop growth (SIMBA-CC) combined with soil N dynamics (SIMBA-N) at a weekly time step for different zones in a banana plantation soil: banana rows and inter row areas. Evaluated outputs were banana vegetative biomass at flowering from SIMBA-GROW and banana cover crop vegetative biomass from SIMBA-CC for three banana crop cycles of data collected in Martinique from fertilizer response – intercropping experiments. The model simulated date of flowering and banana aboveground dry biomass at flowering satisfactorily for four fertilization levels (range from 30-440 kg N ha^{-1}) for three crop cycles, indicating nutrient stressed banana production was accurately captured in the models.

Overall, the *SIMBA* model shows a lot of promise due to its extensive modular structure, and extensive adaptation to the banana plantation structure. Some sub-models perform well (SIMBA-POP, SIMBA-N, SIMBA-WAT), whilst others perform poorly (SIMBA-GROW). Linking all sub-models creates great complexity and may lead to massive errors due to small errors in the sub-models which are used as inputs in other models. SIMBA remains highly theoretical and is very suitable for researchers interested in gaining understanding of the agronomic, environmental and economic dimensions of a banana plantation (Tixier et al., 2008).

3.3.5 Individual plant growth model

Dens, Swennen, et al. (2008) created an empirical growth model to simulate weekly banana plant height and leaf number for the Cavendish cultivars Williams and Grande Naine in response to time and average weekly temperature (°C) from individual plant growth data collected in Honduras. Given its empirical nature and lack of underlying physiological theory, the model cannot be extrapolated to other environments with other cultivars.

3.3.6 LINTUL models

The LINTUL (Light INTerception and UtiLisation) models are radiation driven models developed by the Wageningen group (Van Ittersum et al., 2003). The first version (LINTUL 1) simulates potential DM production from intercepted photosynthetic active radiation (PAR) by the leaf area (in LAI) and a light use efficiency (LUE) (Monteith & Moss, 1977; Spitters, 1990). LAI development can be simulated using two methods: 1) driven by temperature (GDD) only and/or 2) as a result of DM increase in the leaf (g $leaf^{-1}$) and a specific leaf area (cm^2 g^{-1}) (Spitters, 1990). DM partitioning to plant organs is modelled using empirically derived allocation factors that vary with phenology of the crop (Spitters, 1990). The second version (LINTUL 2) combines LINTUL 1 with a tipping bucket mechanism describing soil moisture to simulate water-limited production (Spitters & Schapendonk, 1990). The model was adapted for banana by Chaves et al. (2009), Nyombi (2010) and Taulya (2015).

3.3.6.1 LINTUL 1

Chaves et al. (2009) calibrated LINTUL 1 based on data of a plantain cultivar Dominico-Harton in Colombia. Details on climate, soil moisture, irrigation and fertilization were not presented in their study, indicating water and/or nutrient stresses could not be excluded. The unit of modelling was an individual plant, and not a mat. LAI growth curves were developed in function of GDD, and curves followed LAI observations closely (R^2 0.98). LAI values of 10-15 m^2 m^{-2} were reached in their fields which are well out of the normal LAI range of 2-5 m^2 m^{-2} in fully mature banana plantations (Turner et

al., 2007). The LAI curve, which lies at the basis of LINTUL, is questionable. Light interception by the canopy was simulated by the Lambert-Beer equation. LUE and extinction coefficients were estimated to minimize differences between observed and simulated total DM. DM allocation coefficients were determined empirically for two phases: the vegetative phase (before flowering), and the reproductive phase (after flowering). Chaves et al. (2009) did not provide evaluations for simulated total DM, DM partitioning and yield. Their modelling efforts remain of limited practical value and offer only limited theoretical value.

3.3.6.2 LINTUL 1 East African Highland Banana

Nyombi (2010) aimed to include the ratooning behavior of EAHB banana plants in crop modelling efforts in LINTUL1, as opposed to Chaves et al. (2009) who focused on individual plants. Their LINTUL1-banana model was thereby more ambitious in its scope and simulated potential production and assumed three generations were present on each mat: cycle 1 (mother), cycle 2 (daughter) and cycle 3 (grand-daughter). It is assumed all mats are homogenous. LINTUL 1 simulated (1) phenological development, (2) light interception and use, (3) leaf area development and death, (4) DM production, (5) DM allocation between cycles and (6) root:shoot DM partitioning.

Phenology was expressed using GDD. Phenological stages described by the model were: sucker emergence, start of growth of functional leaves, end of exponential increase of LAI, flower initiation, flowering, and harvest. Phenology thresholds were determined based on the mean plant concept, whereby thresholds were determined based on average GDD accumulation. Singular GDD thresholds were obtained. By moving through the phenological stages, cycles take over one another as happens in grown banana plantations.

Light interception and use were modelled considering different cycle canopies. LAI was separated into three layers corresponding to the individual cycles. Each LAI layer intercepts PAR based on the Lambert beer Law. PAR levels leaving the above leaf layer, were used as input of the next leaf layer. Each canopy layer was characterized by its LUE and a light extinction coefficient. LAI was simulated in two stages. In the juvenile stage, LAI was driven by GDD only. In the maturation stage, LAI production was resource limited and calculated as the product of leaf DM increase and the specific leaf area ($m^2\ g^{-1}$). *DM production* was calculated for each cycle separately based on the LAI, intercepted PAR and LUE of each cycle. Total DM was allocated to different regions within a mat. Firstly, DM was *partitioned across cycles* based on phenological stages. Generally, cycle 1 provides DM to cycle 2 which in turn provides DM to cycle 3. The percentages and amounts of allocation across the different generations are all phenological dependent and determined empirically. Secondly, DM was *allocated between root and shoots* in individual cycles, with partitioning coefficients being phenological dependent. Thirdly, shoot DM was *allocated amongst the leaves, pseudostem, petioles, corm and bunch* depending on the phenological stage of the plant. *Allocation coefficients* were empirically determined for each plant organ depending on the growth stage at destructive sampling

The model was calibrated based on data from fertilizer response trials in Kawanda and Ntungamo, Uganda. The best performing fields (characterized with fertilizer treatment: 400N-50P-600K kg ha^{-1} $year^{-1}$) were chosen for calibration. Irrigation was applied in the first four months after planting, but no information was given on the duration and amount of irrigation. Given the reference evapotranspiration well exceeded the amount of rainfall for both Ntungamo and Kawanda, it can be assumed plants experienced drought stress in the fields. Actual fresh bunch yields for C1 and C2 in Kawanda were respectively 7.9 kg $bunch^{-1}$ (5.7 ton FM ha^{-1} $year^{-1}$) and 11.7 kg $bunch^{-1}$ (22.1 ton FM

ha^{-1} year^{-1}) whilst in Ntungamo C1 and C2 reached 16.3 kg bunch^{-1} (9.1 ton FM ha^{-1} year^{-1}) and 22.7 kg bunch^{-1} (43.2 ton FM ha^{-1} year^{-1}). These yields are low compared to fresh yields in commercial banana plantations using Cavendish (40-50 ton FM ha^{-1} year^{-1}) (FAO, 2018a) and compared to fresh attainable banana yields of EAHB cultivars in Uganda (31-37 ton FM ha^{-1}) (L. Wairegi et al., 2010). LINTUL1 simulations led to potential LAI, leaf DM and bunch DM values that were evaluated against literature values, not against actual observations in the region. Potential LAI values at flowering reached 4.5-5.3 m² m^{-2}, which are within the range of LAI values of banana plantations (Turner et al., 2007). Potential leaf DM at flowering reached 3.8-4.4 ton ha^{-1}, which are above actual leaf DM values of 1.28-2.56 ton ha^{-1} (Nyombi et al., 2009). Calculated bunch potentials of 18-20 ton ha^{-1} DM (100-113 ton FM ha^{-1}) were obtained, which are far above fresh yields in Uganda for EAHB (31-37 ton FM ha^{-1}) (L. Wairegi et al., 2009).

Nyombi (2010) created the potential model in a theoretical manner, and calibrated the model based on experimental plots, but stresses were expected to confound potential production. Inclusion of the ratooning behavior in LINTUL is especially interesting from a physiological standpoint, but this also increases difficulty in usage. The calibrated model has not been validated, so care must be taken for extrapolation to different environments and different cultivars.

3.3.6.3 LINTUL 2

LINTUL 2, an extension of LINTUL 1 with a functional soil water balance, was adapted for the perennial highland cropping system by Taulya (2015). LINTUL 2 follows the same growth equations as LINTUL 1, only the effects of water stress on the system were incorporated by the introduction of water stress reduction factors based on daily soil moisture values. The soil water balance in LINTUL 2 was simulated through a tipping bucket mechanism in a single soil layer bounded by the soil surface (upper boundary) and the rooting depth (lower boundary).

Key components of the water-limited model were the introduction of fluxes evaporation (E) and transpiration (T_r). The reference E and T_r were calculated through the Penman-Equation (Penman, 1948), based on incoming solar radiation. As the banana cropping structure is characterized by a three layer canopy structure and mulch layer, the energy moving between these layers was taken into account. Potential E and T_r were calculated by adjusting the reference E and T_r rates using sequential extinction functions to the energy term applied to the different canopy and mulch layers. Energy received at a soil surface is the difference between incident and transmitted energy for each layer. Intercepted energy by the canopy layers was a function of the LAI of the different canopy layers. Actual E and T_r were determined by adjusting the potential values in view of the soil moisture balance. When the daily soil moisture balance dropped below a critical soil moisture threshold or raises above a wet critical moisture content, T_r and E were reduced through multiplication of potential values with a stress coefficient. Below the critical water content, the plant was assumed to experience drought stress, while above the wet moisture content soil aeration was so limited that plants also experience stress. This reduction factor ranges between 0 (permanent wilting point) and 1 (moisture contents above a critical moisture value) (Taulya, 2015).

The ratio of actual to potential T_r was defined as the moisture stress index, which influenced three steps in LINTUL2: (1) the moisture stress index reduced LUE linearly as limited soil moisture supply induces stomatal closure (Turner & Thomas, 1998), (2) it also reduced growth rates of the LAI, as newly emerging leaves will be among the first tissues to be reduced by moisture stress, (3) the

moisture stress index delayed phenological development due to drought stress by affecting GDD accumulation.

The model was calibrated and tested against empirical growth and yield data collected from individual plants from fertilizer response trials in Kawanda and Ntungamo, Uganda. Validation of the water-limited model was focused on physiological timing of growth stages, SWC, total DM production and total DM partitioning between organs. The LINTUL 2 model was validated fully on individual mat basis (n=4) receiving 400-600 kg K ha^{-1} $year^{-1}$, for both Kawanda and Ntungamo. Further yield validation was done on yield data of plants (n=20 for Ntungamo, and n= 23 for Kawanda), randomly selected across fertilizer treatments 150-400 kg N ha^{-1} $year^{-1}$ and 250-600 kg K ha^{-1} $year^{-1}$ (Taulya, 2015).

Simulated SWC diverged from observed soil moisture contents. While trends in soil moisture were accurately predicted, absolute values of volumetric water content were not matched. SWC were continuously underestimated in Kawanda (R^2 -0.05), even dropping below the PWP at multiple times, whilst for Ntungamo the opposite was true and soil moisture contents were overestimated (R^2 0.15). Total DM, leaf DM, pseudostem DM and bunch DM all differed significantly (p<0.0001) between simulated and observed values. Simulated fresh bunch yields were 2 to 3 times the observed values. The model correctly simulated phenology: vegetative cycle duration (425 days, 14.8 SE, p=0.517), and total cycle duration (561.40 days, 11.7SE, p=0.392), but failed to correctly simulate the bunch-filling duration, even though differences were small. Simulated bunch filling duration was 137.60 days ±3.1SE, whilst observed bunch filling duration was 130.60 days ±1.9SE (Taulya, 2015).

While theoretically interesting, LINTUL 2 failed to correctly simulate water limited growth in banana plantations and needs to be further calibrated and tested against independent datasets.

3.3.7 AAB plantain model

Dépigny et al. (2017) built a model specifically for plantain (AAB model) describing growth, phenological development and yield of plantain. The model is a radiation-driven model running at a weekly time interval (like the SIMBA-GROW model (Tixier et al., 2008)) and simulates (1) radiation (PAR) interception based on LAI development, (2) DM production based on radiation interception and (3) DM allocation to different organs dependent on phenology (roots, vegetative organs, bunch and suckers) in a homogenous plantation. Phenological stages (first sucker appearance, sucker selection, flower initiation, flower emergence, harvest) are based on the mean plant concept, and reached upon accumulating a set GDD thresholds (with base temperature 0°C).

Their objective was to parameterize a growth model for nine plantain cultivars, and as such better understand cultivar specific growth and yield responses. For calibration of the cultivar dependent model, 5 plantain cultivars and 4 plantain-like hybrids were used (differing in agronomic potential and growth) for which cultivar specific model parameters were created based on field observations or literature. Model accuracy was estimated by comparing observed vs. simulated bunch weights for each of the cultivars. Model accuracy for bunch DM weights ranged from 3.1% to 50.6% RRMSE between the cultivars, thereby pointing to cultivar-specific model accuracy. The model was accurate to predict the bunch DM for 5 cultivars, whilst 4 cultivars were continually underestimated. Photosynthetic efficiency was higher in real plantain cultivars, indicating a genotypical effect on growth parameters underlying the plantain growth model. Three cultivar groups were identified in their potential for accurate AAB bunch biomass prediction. Different genotypes in plantain thereby have shown a different production potential, influencing parameterization of models significantly.

3.4 Modelling the banana plant: towards an AquaCrop growth model

Previous modelling efforts of banana plantations differ widely in their intended use and complexity. Models as CENTURY (Woomer et al., 1998) are more focused on soil nutrient fluxes than actual banana production, and should thus be used by researchers interested in ecosystem functioning. Models from the SIMBA categories (Ripoche et al., 2012; Tixier et al., 2004, 2006, 2008, 2011) are useful for studying banana systems as a whole due to the very specific submodules. These models are useful for researchers interested in studying details of the entire agronomic, environmental, and economic dimensions of a banana plantation. When the production estimation of a plantation is the goal, the radiation-driven LINTUL models seem more useful. LINTUL 1 and 2 aimed to thoroughly describe DM buildup and allocation patterns across different plant cycles and organs in a banana mat. These modelling efforts have value from a crop model building and physiological point of view. The perennial banana cropping structure became embedded in LINTUL by Nyombi (2010) and Taulya (2015) further included a simple water balance model to simulate water limited production. The AAB model of Dépigny et al. (2017) furthermore highlighted the effect of cultivar specific parameterization and model performance.

This thesis however focusses on a crop simulation model that differs in its intended use from the previously created crop models. AquaCrop (developed in 2009) shows a lot of promise for modelling water-limited production as it contains a more detailed soil water balance and irrigation scheduling component and the various ways in which water stress affects crop development. In contrast to other previously mentioned models on banana, it has a water-driven growth engine (Steduto et al., 2007b) and puts its emphasis at the outset on water-limited production (Abdalhi & Jia, 2018). Other features distinguishing AquaCrop from other models are its use of CC as opposed to LAI, the low number of parameters that are moreover intuitive and easy to calibrate, a well-developed user interface and the possibility of describing a multitude of existing field management and irrigation practices (e.g. drip, furrow, flood irrigation infrastructures) within the model (Abdalhi & Jia, 2018; Raes et al., 2018c).

Since AquaCrop has shown to model water-limited production of a multitude of crops and varieties within a crop with good accuracy in different environments under different management scenarios, it seems a good candidate for modelling water-limited banana plantations (Steduto et al., 2012). This PhD research used the AquaCrop model and proposes adjustments for usage in banana plantations.

The next chapter will focus on AquaCrop as a model and focus on its current modelling scheme.

4 AquaCrop modelling scheme

4.1 Introduction

AquaCrop, the crop water productivity model developed by the Food and Agricultural Organization of the United Nations (FAO) is a simplified yet robust computer crop model specifically targeted to extension personnel, farm and water managers, economists and irrigation designers (Steduto et al., 2008; Vanuytrecht, Raes, Steduto, et al., 2014). Its approach consists of balancing simplicity, accuracy, and robustness.

AquaCrop is structured along a soil-plant-atmosphere continuum. It includes (1) the soil, with its water balance, (2) the plant, with its growth and yield and (3) the atmosphere with its thermal regime, rainfall, evaporative demand and CO_2 content. AquaCrop simulates daily crop canopy cover (CC), rooting depth (Zr), transpiration (Tr), aboveground dry biomass (B), yield (Y) and the soil water balance under user specified environment and management inputs (Hsiao et al., 2009; Raes et al., 2009; Steduto et al., 2008, 2012; Vanuytrecht, Raes, Steduto, et al., 2014). At its core, AquaCrop is a water driven crop simulation model, as opposed to other carbon and radiation driven models (Steduto et al., 2007b, 2012; Steduto, 2006).

This chapter highlights the most relevant AquaCrop calculation procedures as implemented in AquaCrop v6.0 and v7.0. It provides the necessary input requirements, followed by the calculations governing crop development. Then the soil water balance as part of the AquaCrop model is discussed, followed by the effects of stress on crop development and production.

For a more detailed explanation, we refer to the articles by Hsiao et al. (2009), Raes et al. (2009) and Steduto et al. (2009) which were released when AquaCrop was first developed. AquaCrop v7.0 was used in our study, which was similar to v6, but contained modules for simulating perennial crops (regrowth) and for simulating multiple harvests which are necessary in banana plantations. Newly released versions of the AquaCrop model, and corresponding changes to the modelling scheme can be found at the FAO site: http://www.fao.org/aquacrop/en/ (FAO, 2020) and in the corresponding updated AquaCrop reference manuals (Raes et al., 2018a, 2018b, 2018c).

4.2 Input requirements

AquaCrop is a mechanistic model based on actual biophysical processes (Hsiao et al., 2009; Steduto et al., 2009), yet uses a relative small number of mostly intuitive input parameters (Table S1 in Annex I). Input parameters are specified in climate, crop, soil and management files to be used in the model (Raes et al., 2009, 2018b, 2018a).

Minimal needed *climate input variables* include minimum and maximum air temperature, rainfall, and reference evapotranspiration (ET_0). ET_0 data can be used directly as input or can be calculated by AquaCrop using the FAO 56 Penman-Monteith method (Allen et al., 1998). Weather input data are preferably daily, but 10-day or monthly data can also be used for temperature and ET_0. Mean annual atmospheric CO_2 concentration measured at Mauna Loa Observatory in Hawaii are provided as a default in AquaCrop for the past. The user can specify CO_2 concentrations per year, or enter future year CO_2 levels derived from prospective climate change scenarios (Raes et al., 2009).

The *soil profile* needs to be parameterized and can be composed of up to five soil horizons, which the model can further subdivide into soil compartments for calculation purposes. For each horizon, the required soil physical characteristic parameterization includes the saturated hydraulic conductivity

(K_{SAT}) and the volumetric water content at saturation (θ_{SAT}), at field capacity (θ_{FC}) and at permanent wilting point (θ_{PWP}). When such data are missing, estimates can be obtained as AquaCrop comes with indicative values for various soil textural classes. Based on the soil inputs, the Curve Number (CN) and readily evaporable water (REW) are automatically estimated for the topsoil horizon. The depth (and salinity) of the groundwater table also need to be specified, as this will influence the amount (and quality) of water that can be transported upward through capillary rise (CR) (Raes et al., 2009, 2012b, 2018b, 2018a; Vanuytrecht, Raes, Steduto, et al., 2014).

Crop parameters constitute the core parameter set of AquaCrop (Raes et al., 2009; Steduto et al., 2008). Crop parameters can be conservative (C) or non-conservative (NC) parameters. Conservative parameters do not change with cultivar, time, management, or environment. These parameters are stable, can be calibrated once and used across a wide range of scenarios without further adjustment. Conservative parameters include e.g. temperature and soil water stress thresholds for crop development, growth, and other physiological processes. Non-conservative parameters change with the used cultivar, time, environment, or management conditions, and need to be adjusted to local conditions or used cultivars. Non-conservative crop parameters include e.g. maximum canopy cover, length of phenological stages and effect of soil fertility on the crop development (Raes et al., 2009, 2012b, 2012a; Steduto et al., 2008; Vanuytrecht, Raes, Steduto, et al., 2014). AquaCrop has been successfully applied to 15 annual herbaceous crops including wheat, rice, soybean, barley, cotton, sugar beet, sunflower, potato, tomato, alfalfa, Bambara groundnut, quinoa (C3 crops) and maize, sorghum, sugarcane, teff (C4 crops) (Steduto et al., 2009, 2012). The AquaCrop database provides crop parameter values for 15 previously calibrated crops. Only non-conservative parameters need to be fine-tuned to local conditions when using these database values. AquaCrop specifies default crop parameter value sets that can be used as a starting point in the calibration process (Vanuytrecht, Raes, Steduto, et al., 2014).

Management input is separated into field management and irrigation management (Raes et al., 2012a, 2018a, 2018b).

Field management specifies the level of soil fertility, the application of mulches, field surface practices, weed management and in case of multiple harvests the time and duration of harvest events in a growing season. Soil fertility is not modelled in AquaCrop, but instead an overall soil fertility level is specified semi quantitatively as an input variable (Van Gaelen et al., 2015). Soil fertility stress levels specify the relative biomass production that can be expected in a field assuming there would be no other stresses compared to non-limiting soil fertility. For example, a very poor soil fertility level can specify a relative biomass production of 25% indicating that only 25% of potential biomass can be produced compared to non-limiting conditions (Raes et al., 2018b; Van Gaelen et al., 2016). The effect of weeds can also be modelled through its effect on CC. Weed infestation is expressed as the relative weed cover in the season (RC, the percentage of CC due to weeds). The total CC of a crop in a weed infested field (CCw) is then calculated by subtracting the RC from the total CC in the field (Van Gaelen et al., 2016). AquaCrop v7.0 further contains the option of multiple harvests that allows to specify the frequency of harvest over the course of a growing season or assists in calculating when crops need to be harvested.

Irrigation management inputs specify the irrigation system characteristics. If irrigated, AquaCrop can be run to (1) calculate the net irrigation requirement based on maximum allowable soil moisture depletion, (2) set up an irrigation schedule by specifying each application date and depth, or (3)

generate a potential irrigation schedule based on specified time and depth criteria. The irrigation method (sprinkler, basin, border, furrow, and drip irrigation) is specified, together with the percentage surface wetted during irrigation. Time criteria specify when irrigation is applied to the field, whilst depth criteria specify the amount of water added during irrigation (Raes et al., 2018b).

Finally, the model requires a specification of the simulation period and initial field conditions in terms of soil water content, salinity and previously acquired canopy cover, rooting depth and biomass (Raes et al., 2012a, 2018b). After setting all input values, the model will run at a daily time step and simulate crop development and production, as well as the underlying soil water balance.

4.3 Crop development

Crop phenology can be expressed in calendar days (d) or in accumulated heat units (GDD in °Cd). GDD in AquaCrop are calculated following procedures by McMaster and Wilhem (1997) (eq. 4-1). Only temperature effects are incorporated in the calculation of heat units. The heat units required to reach various phenological stages are specified for a given crop cultivar (Raes et al., 2009, 2018c; Vanuytrecht, Raes, Steduto, et al., 2014).

$$GDD = T_{avg} - T_{base} \quad (4\text{-}1)$$

with T_{avg}, being the average daily temperature (°C) and T_{base} being the base temperature below which crop development does not progress (°C).

Calibration of crop parameters originally occurs in days, after which the model calculates automatically the associated GDD using the specified climate data inputs (Raes et al., 2012b, 2012a, 2018c, 2018b). Crop files in GDD are more robust for extrapolation to different environments.

As AquaCrop is a water driven model, crop production is based on the amount of water transpired following a four step process (Figure 4-1).

(1) Green CC is simulated instead of LAI. Canopy development and senescence under optimal conditions are described by four parameters: CC_0, the initial canopy cover (%), cgc or the canopy growth coefficient (% day^{-1} or % GDD^{-1}), CC_x or the maximum canopy cover (%) and cdc or the canopy decline coefficient (% day^{-1} or % GDD^{-1}). Canopy development is simulated by two equations depending on the size of the simulated CC (eq. 4-2). In the late season stage, the decline in CC is described through a cdc coefficient.

(2) Crop transpiration (Tr) is simulated based on governing environmental conditions (ET_0) and a crop transpiration coefficient (Kc_{Tr}) related to the CC (eq 4-3). Also stress factors affecting CC are thereby considered.

(3) The amount of water transpired is linked to aboveground dry biomass (B) production through a normalized crop water productivity factor (WP^*), forming the core of the AquaCrop model (eq 4-4). WP^* is a conservative parameter for each crop.

(4) In a final step, the developed crop biomass is converted to dry yield (Y) through a harvest index (HI), which can also be affected by stresses (f_{HI}) (eq. 4-5) (Raes et al., 2018c).

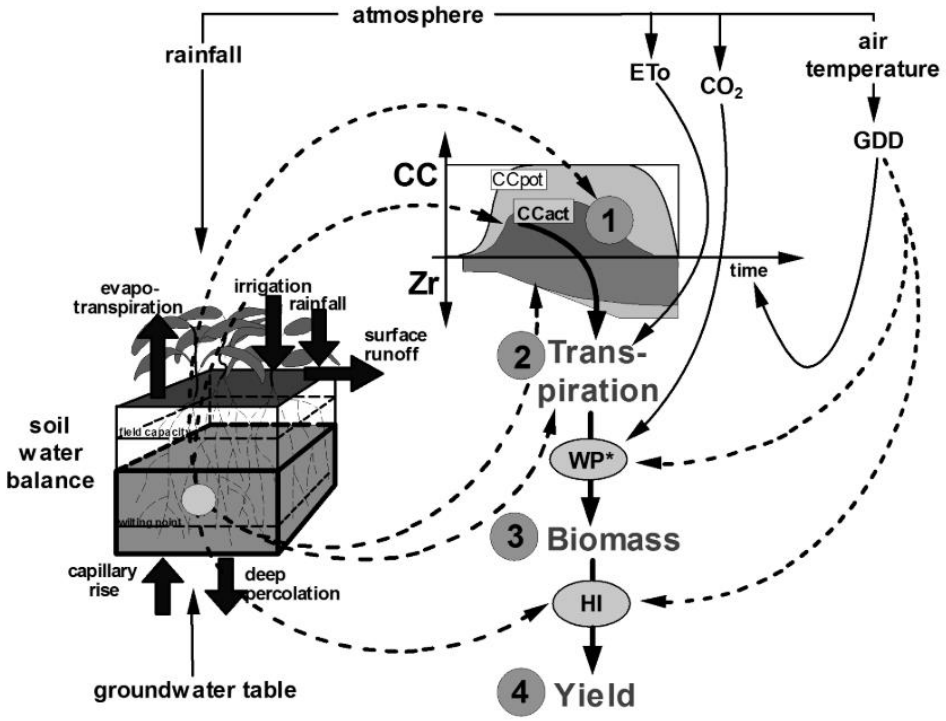


Figure 4-1: AquaCrop modelling scheme indicating the four steps (1) Canopy cover (CC), (2) Transpiration, (3) Dry aboveground biomass and (4) Yield. The effects of water and temperature stress affecting the different steps are indicated by dotted arrows. Source: Vanuytrecht et al. (2014). Abbreviations are as follows. ET_0: reference evapotranspiration, CO_2: carbon dioxide, GDD: growing degree days, CC: Canopy Cover, Zr, rooting depth, WP*: normalized crop water productivity, HI: harvest index.

$$CC_t = \begin{cases} CC_0 \times e^{t \times cgc} & when\ \left(CC_t < \frac{CC_x}{2}\right) \\ CC_x - 0.25 \times \frac{(CC_x)^2}{CC_0} \times e^{-t \times cgc} & when\ \left(CC_t > \frac{CC_x}{2}\right) \end{cases}; \quad (4\text{-}2)$$

$$Tr = Ks \times Ks_{Tr} \times (Kc_{Trx} \times CC^*) \times ET_0; \quad (4\text{-}3)$$

$$B = Ks_b \times WP^* \times \sum \frac{Tr}{ET_0}; \quad (4\text{-}4)$$

$$Y = f_{HI} \times HI_0 \times B; \quad (4\text{-}5)$$

where CC_t is canopy cover (%) at time t (d or GDD), CC_0 is the initial canopy cover (%), cgc is the canopy growth coefficient (% day^{-1} or % GDD^{-1}), CC_x is the maximum canopy cover (%), Tr is transpiration (mm), Ks is a water stress coefficient (0-1) being either Ks_{sto} (stomatal stress coefficient) or Ks_{aer} (aeration stress coefficient), Ks_{Tr} is the cold stress coefficient for crop transpiration (0-1), Kc_{Trx} is the maximum crop coefficient (-), CC^* is the adjusted green canopy cover (%), ET_0 is the reference evapotranspiration as calculated by the FAO 56 method (mm), B is the aboveground dry biomass (ton DM ha^{-1}), Ks_b is the cold temperature stress coefficient (0-1), WP^* is

the normalized water productivity factor (for ET_0 and CO_2 content) (ton DM ha^{-1}), $\sum \frac{Tr}{ET_0}$ is the sum of daily normalized transpiration over the duration (t) of simulations (-), Y is the dry yield (ton DM ha^{-1}), f_{HI} is the adjustment factor under water, heat and/or cold stress (0-1.6), and HI_0 is the reference harvest index (-) (Raes et al., 2018c; Vanuytrecht, Raes, Steduto, et al., 2014).

4.4 Soil water balance

The daily soil water balance in AquaCrop is calculated from incoming and outgoing water fluxes, and redistribution through the soil horizons. In and out fluxes are assumed one dimensional (vertical) between the upper boundary (soil horizon) and the lower boundary (root zone depth). Ingoing fluxes constitute precipitation (P), irrigation (I) and capillary rise (CR), whilst outgoing fluxes comprise evaporation (E), transpiration (Tr), deep percolation (DP) and runoff (RO) (Raes et al., 2012b, 2018c).

Daily soil water contents (SWC) are calculated as:

$$SWC_t = SWC_{t-1} - DP + P + I - RO + CR - E - Tr \quad (4\text{-}6)$$

where SWC_t is the soil water content (mm) on day t, SWC_{t-1} is the soil water content on the previous day (t-1), P is the precipitation (mm), I is the amount of irrigation (mm), CR is the capillary rise (mm), E is the evaporation from the field surface (mm), Tr is the transpired water (mm), DP is the deep percolation (mm) and RO is the runoff (mm). SWC are updated based on the position of parameters in eq. 4-6. First the SWC of the previous day is specified, next DP is calculated from this zone, then P and I are added that define the water that infiltrates the soil after subtracting RO. Next CR fluxes are accounted for based on the position of the groundwater table, and finally E and Tr are subtracted from the profile (Raes et al., 2018c).

P and I are direct user specified inputs. CR, E, Tr, DP and RO are calculated based on weather data, crop growth, soil profile characteristics, presence of a groundwater table and field management characteristics (Raes et al., 2012b, 2018c). For a more detailed explanation of underlying calculations the reader is referred to Raes et al. (2018c).

The soil water balance is intricately linked to the saltwater balance in AquaCrop, as salts enter the soil as solutes in I and CR. The extent of salt stress depends largely on the quality (salt content) of irrigation and groundwater. EC values less than 1.50 mS cm^{-1} are considered good values in AquaCrop. A detailed explanation of salt budgeting is beyond the scope of this thesis. The reader is referred to Raes et al. (2018a, 2018b, 2018c) for further details.

4.5 Crop response to abiotic factors

Crop growth might be affected by soil water stress, soil salinity stress, temperature stress and/or soil fertility stress. The effect of stress is simulated using crop stress coefficients (Ks)(Table 4-1). Ks affect different parameters in the AquaCrop process (Figure 4-1 and Table 4-1) and can range from 1 (no stress) to 0 (full stress). Ks are defined by specifying upper and lower thresholds for the stress indicators (e.g. moisture content) and by selecting a stress curve shape (f_{shape}). Shapes can be linear, logistic or convex between these upper and lower thresholds of Ks (Hsiao et al., 2009; Raes et al., 2009, 2012b, 2018c; Vanuytrecht, Raes, Steduto, et al., 2014).

Soil water stress affects canopy cover development, root zone expansion, stomatal closure, crop transpiration rate and the harvest index depending on the severity of soil moisture depletion (Table 4-1). Under increasingly depleted soil moisture levels, canopy cover is affected first, followed by root zone expansion and transpiration rate. Under severe water depletions, failure of pollination and early canopy senescence can occur. In contrast, excess of water (waterlogging) can result in anaerobic stress (Raes et al., 2012b, 2012a, 2018c; Vanuytrecht, Raes, Steduto, et al., 2014).

Salt stress (Ks_{salt}) affects multiple processes as canopy cover expansion, maximum canopy cover and reduces crop transpiration (Raes et al., 2012b, 2018c). Indicators for soil salinity stress are the average electrical conductivity of the saturation soil paste extract (ECe) from the root zone (Raes et al., 2012b, 2018c).

Table 4-1: Stress coefficients in AquaCrop. Source: Raes et al. (2018a)

Stress coefficient	Target model parameters	Effect
Water: soil moisture depletion		
$Ks_{exp,w}$	cgc and HI	Reduces canopy expansion and/or might positively affect harvest index
Ks_{sto}	Tr_x, dZ and HI	Reduces transpiration, root zone expansion and/or might negatively affect harvest index
Ks_{sen}	CC	Reduces canopy cover
$Ks_{pol,w}$	HI_0	Negatively affects degree of pollination, which determines the reference harvest index
Ks_{aer}	Tr_x	Reduces transpiration
Temperature: temperature and GDD		
Ks_{Tr}	$Kc_{Tr,x}$	Reduces crop transpiration
Ks_b	B	Reduces biomass production
$Ks_{pol,c}$	HI_0	Negatively affects degree of pollination, which determines the reference harvest index
$Ks_{pol,h}$	HI_0	Negatively affects degree of pollination, which determines the reference harvest index
Soil fertility: soil fertility levels		
Ks_{CCx}	CC_x	Reduces canopy cover
$Ks_{exp,f}$	cgc	Reduces canopy expansion
$f_{CCdecline}$	CC	Decline of the CC once CCx is reached
Ks_{wp}	WP^*	Reduces biomass production
Soil salinity: ECe values		
Ks_{salt}	CC and $Kc_{Tr,x}$	Reduces canopy cover and biomass production

Note: stress coefficients and target model parameters are specified in the abbreviations and in Table S1 in Annex I

Crop development occurs within a range of temperatures specified by T_{base} and T_{up}, respectively below and above which crop development stops. Temperatures can result in both *heat and cold stress.*

Cold stress affects transpiration, whilst pollination is affected by both cold and heat stress. Indicators for temperature stress can be GDD (Ks_{Tr} and Ks_B) affecting crop transpiration and biomass, or actual air temperature (Ks_{pol}) affecting pollination of flowers (Raes et al., 2012b, 2018c). Temperature stress also acts indirectly via water stress. Higher temperatures are often linked to higher ET_0. Under high temperature regimes, ET_0 is more pronounced leading to faster moisture depletion and faster stress responses. The stress response curves for canopy expansion, transpiration and senescence can be adjusted to prevailing daily ET_0, such that effects of water stress are more pronounced on days with high ET_0 at similar depletion levels (Raes et al., 2012b, 2015a, 2018c).

Stress indicators for *soil fertility* follow the degree of soil fertility stress as specified in the input parameters. Soil fertility stresses affects canopy cover development (Ks_{CCx}, $Ks_{exp,f}$, $f_{CCdecline}$) and reduces the biomass production (Ks_{wp}). The shape of these stress coefficients (f_{shape}), the degree to which a crop is affected, is fixed when calibrating a crop response to soil fertility stress (Raes et al., 2012b, 2015b, 2018c; Van Gaelen et al., 2015).

4.6 Evaluation of model outputs

AquaCrop simulates among others CC, SWC, B and Y on a daily timescale. To assess the accuracy of modelling, simulations are compared against observed values using multiple goodness-of-fit characteristics.

AquaCrop, and this research, makes use of the following statistical indicators: squared value of the Pearson's correlation coefficient (R^2) (Krause et al., 2005), Root mean square error (RMSE) (Jacovides & Kontoyiannis, 1995), Relative root mean square error (RRMSE) (Jamieson, 1991), Nash and Sutcliffe model efficiency (NSE) (Nash & Sutcliffe, 1970) and Wilmot's index of agreement (d) (Willmott, 1981) (Raes et al., 2018b).

$$R^2 = \left(\frac{\sum_{i=1}^{n}(O_i-\bar{O})(P_i-\bar{P})}{\sqrt{\sum_{i=1}^{n}(O_i-\bar{O})^2}\sqrt{\sum_{i=1}^{n}(P_i-\bar{P})^2}} \right); \quad (4\text{-}7)$$

$$RRMSE = RMSE \times \frac{100}{\bar{O}} = \sqrt{\frac{\sum_{i=1}^{n}(O_i-\bar{O})^2}{n}} \times \frac{100}{\bar{O}}; \quad (4\text{-}8)$$

$$NSE = 1 - \frac{\sum_{i=1}^{n}(O_i-P_i)^2}{\sum_{i=1}^{n}(O_i-\bar{O})^2}; \quad (4\text{-}9)$$

$$d = 1 - \frac{\sum_{i=1}^{n}(P_i-O_i)^2}{\sum_{i=1}^{n}(|P_i-\bar{O}|+|O_i-\bar{O}|)^2}; \quad (4\text{-}10)$$

where O_i and P_i are the observed and simulated values; $\bar{O}$ and $\bar{P}$ are the mean of the observed and simulated values, and n is the number of observations.

Model performance is evaluated according to Table 4-2.

Table 4-2*:* Goodness-of-fit interpretation table. R^2 (Pearson's correlation coefficient), RRMSE (relative root mean square error), NSE (Nash and Sutcliffe model efficiency) and d (Wilmot's index of agreement). R^2, NSE and d are based on Raes et al. (2018b), RRMSE is based on Jamieson (1991).

Model performance	R^2 range	RRMSE range	NSE range	d range
Very good	≥ 0.90	≤ 10%	≥ 0.80	≥ 0.90
Good	0.8 - 0.89	10 – 20%	0.60 - 0.79	0.8-0.89
Moderately good	0.70 - 0.79	20 – 30%	0.40 - 0.59	0.65-0.79
Moderately poor	0.5 - 0.69	30 – 40%	0 - 0.39	0.50-0.64
Poor	0 - 0.49	40 – 50%	(-10) - 0	0.25-0.49
Very poor	<0	>50%	< (-10)	<0.25

4.7 Model performance assessment and uncertainty

New crops are continually added to the AquaCrop model, but before new crop parameter sets can be included their validity and performance needs to be assessed by multiyear and multi-location trials (Hsiao et al., 2009; Vanuytrecht, Raes, Steduto, et al., 2014).

Proper calibration and validation guidelines for AquaCrop are provided by Steduto et al. (2012). A database for calibration and parameterization with AquaCrop should collect observations on CC, SWC, B and Y as these components are simulated (Figure 4-1). Calibration requires minimal data on climate and ET_0 (daily maximum and minimum temperature, solar radiation and ET_0) , crop (periodic measurement on CC, B, Y, rooting depth Zr and signs of water stress and dates), soil and fertility (hydraulic conductivity K_{SAT} and volumetric water contents θ_{SAT}, θ_{FC} θ_{PWP} of soil horizons) and irrigation and water in soil (periodic measurements of SWC, frequency and amount of irrigation applications) from experiments growing modern high-yielding cultivars with optimal soil fertility when water is not limiting (Steduto et al., 2012). Using this collected data, conservative parameters (which remain constant under different growing conditions and water regimes) are calibrated until simulated results agree closely with experimental data. Next a validation of this parameter set needs to be carried out collecting similar data but obtained at (1) several locations and climates, (2) for different soil types and (3) in experiments with treatments experiencing water stress at different times and different severities.

Validation studies for crops in the AquaCrop database were previously carried out under a diverse set of environments and irrigation systems for e.g. wheat (Andarzian et al., 2011; Iqbal et al., 2014; Stricevic et al., 2011), rice (Maniruzzaman et al., 2015), soybean (Adeboye et al., 2019), barley (Araya, Habtu, et al., 2010), cotton (Farahani et al., 2009), sugar beet (Stricevic et al., 2011), sunflower (Todorovic et al., 2009a), tomato (Darko et al., 2016), bambara groundnut (Karunaratne et al., 2011; Mabhaudhi et al., 2014b), quinoa (Sam Geerts et al., 2009), maize (Abedinpour et al., 2012; Heng et al., 2009; P. Paredes et al., 2014), sorghum (Hadebe et al., 2017), sugarcane (Bahmani & Eghbalian, 2018), tef (Araya, Keesstra, et al., 2010; Tsegay et al., 2012). Many more studies exist, and new ones are published every year. Steduto et al. (2011) provide a brief overview of several validation studies for the AquaCrop model performance for different crops: Maize, Cotton, Quinoa, Bambara Groundnut, Barley and Teff. Their review compared AquaCrop model outputs against observed data in environments where (1) climate, (2) management, (3) irrigation systems and (4) water treatments were different from the ones used for crop parameter calibration. Model performance of AquaCrop varied for the different crops and production scenarios. Simulations often performed satisfactorily, but suboptimal performance could be achieved under quite different environments than the ones of

original calibration. This warrants the need for local calibration and validation of model outputs under different environments.

Multiple sensitivity analyses were carried out for the AquaCrop model in different production scenarios to identify parameters that have highest influence on model outputs (Guo et al., 2020; Jin et al., 2018; Silvestro et al., 2017; Steduto et al., 2011; Vanuytrecht, Raes, & Willems, 2014). Influential parameters were found to depend on environmental conditions (crop, soil, climate) in which the model was used, indicating the significance of calibration conditions on parameter values and model outputs. Even though non-influential parameters often overlapped (Silvestro et al., 2017; Vanuytrecht, Raes, & Willems, 2014), parameters that were influential under tested environments in one study (Vanuytrecht, Raes, & Willems, 2014), could be non-influential for different environmental conditions and irrigation systems in other studies (Silvestro et al., 2017). These validation studies and sensitivity analyses highlight the necessity to validate crop model parameters in a wide variety of environments to arrive at a robust set of crop parameter values to be used in different production scenarios and determine parameters that need local calibration.

Before validation can occur, an initial calibration should occur. Every crop parameter set needs a start and a first calibration for the banana plant would lay the groundwork for further validation studies in different environments. Hence, this thesis provides the foundation of banana calibration for the AquaCrop model.

5 Canopy cover evolution, diurnal patterns, and leaf area index relationships in a Mchare and Cavendish banana cultivar under different soil moisture regimes

Bert Stevens[a,*], Jan Diels[b], Eline Vanuytrecht[b,e], Allan Brown[c], Stanley Bayo[c], Alvin Rujweka[d], Emmanuel Richard[c], Patrick Alois Ndakidemi[d] and Rony Swennen[a,c,f]

[a]KU Leuven, Department of Biosystems, Willem De Croylaan 42 - box 2455, 3001 Heverlee, Belgium

[b]KU Leuven, Division of Soil and Water Management Celestijnenlaan 200e - box 2411, 3001 Leuven, Belgium

[c]International Institution of Tropical Agriculture, IITA, PO Box 447, Arusha, Tanzania

[d]Nelson Mandela African Institution of Science and Technology, NMAIST, P.O.BOX 447, Arusha, Tanzania

[e]Flemish Institute for Technological Research (VITO), Environmental Modelling Unit, Boeretang 200, 2400 Mol, Belgium

[f]Bioversity International, Willem De Croylaan 42, 3001 Heverlee, Belgium

[*]Lead author

This chapter is based on its published form:

Stevens, B., Diels, J., Vanuytrecht, E., Brown, A., Bayo, S., Rujweka, A., Richard, E., Ndakidemi, P., & Swennen, R. (2020). Canopy cover evolution , diurnal patterns and leaf area index relationships in a Mchare and Cavendish banana cultivar under different soil moisture regimes. *Scientia Horticulturae*, *272*, 109328. https://doi.org/10.1016/j.scienta.2020.109328

5.1 Introduction

By 2050, global population levels are expected to reach 9.7 billion (+32% from 2015), with over two thirds of this expansion happening in developing countries, and sub-Saharan Africa (SSA) accounting for half the total growth (United Nations, 2019). To feed this growing population, food production needs to increase by 25-70% (FAO et al., 2018; Hunter et al., 2017). One of the most important crops in terms of consumption, land area and production is banana (*Musa* spp.). Global production of banana and plantains was 153 million ton in 2017 covering 5.6 million ha in over 135 countries. They are the 12th most important food crop in terms of production (fourth in Africa) and the world's most important fruits (FAOSTAT, 2019).

In East and Central Africa (ECA), daily per capita consumption is 15 times the global average, and constitutes a very significant portion of daily energy intake ranging from 30-60% (Abele et al., 2007; FAOSTAT, 2019). Actual production in the area is low (<30 ton ha^{-1} year^{-1}) compared with attainable yields (>70 ton ha^{-1} year^{-1}) (Van Asten et al., 2011; L. Wairegi et al., 2010). Water is the primary limiting factor for agriculture in SSA, where only 18% of the total irrigable land is currently irrigated (Adhikari et al., 2015). Water (both excess and deficit) is considered to be the largest limiting abiotic factor

affecting banana production worldwide (Carr, 2009). Depending on the prevailing climate, water needs for banana range from 1,100 to 2,650 mm evenly distributed per year (Carr, 2009; Robinson & Alberts, 1986; Van Asten et al., 2011; Varma & Bebber, 2019). Even distribution is essential, as plants are already affected after two to three days of soil moisture deficit (Carr, 2009).

By 2050, climate change in ECA is expected to increase the thermal suitable area for banana production by 1-11%, but extension of land area under beneficial temperatures is expected to be offset by an increase in rainfall variability (Adhikari et al., 2015; German Calberto et al., 2015; Varma & Bebber, 2019). Moreover, as temperature drives development rates of banana (Fortescue et al., 2011), the increase in temperature is coupled with faster crop cycles, an increase in evapotranspiration, thereby increasing transpiration rates and putting more pressure on water resources (Adhikari et al., 2015; Varma & Bebber, 2019).

In view of the above, agriculture needs to be intensified by a more efficient use of both rainfall and irrigation water, and the enhancement of water use efficiency. In most cases, management of irrigation systems is based on farmers' intuition and experience, which is suboptimal (Boesveld et al., 2011), rather than allocating water when plants are in need. This is because easy physiological indicators for water deficit are lacking in banana, and most farmers find current irrigation scheduling tools overwhelming and lack the means and skills to install and operate them (Boesveld et al., 2011; Carr, 2009). Under relatively mild soil drought conditions, banana plants close their stomata, reduce transpiration and photosynthesis. This keeps leaves hydrated, most likely through root pressure, but masks that banana are under water deficit (Carr, 2009; Turner et al., 2007).

Expanding tissues, as emerging leaves and growing fruit, are among the first to be affected by soil drought (Carr, 2009; Kallarackal et al., 1990; Robinson & Galan-Sauco, 2010; Turner & Thomas, 1998). Following this, the canopy of a plantation might offer insights to spot drought stress. At the field (plantation) level, canopy development can be measured by the leaf area index (LAI) or green canopy cover (CC).

LAI is defined as the total one-sided leaf area of all leaves per unit ground area ($m^2\ m^{-2}$). LAI values in banana plantations range from zero at planting to five at maturity in well-managed plantations, even reaching values more than six in ratoon crops (Turner, 1998; Turner et al., 2007). It is measured directly or indirectly. When leaves and plant parameters are measured directly, the most accurate LAI is obtained, but given the spatial heterogeneity of the canopy, many sampling points are needed which is time consuming, tedious, and sometimes destructive (Weiss et al., 2004). Indirect measurements are based on the estimation of "contact frequency" or the "gap fraction" with various optical devices (e.g. LAI2000, TRAC, Demon and cameras for hemispherical photography). Contact frequency methods are based on the likelihood that a beam penetrating the canopy will reach a vegetative structure. Gap frequency methods are inverse, as the beam has no contact with the vegetative structure until reaching a reference level and consequently the gaps in the canopy are measured. These techniques therefore use light transmittance through the canopy. Indirect methods need to be calibrated to the specific architecture of banana plants, as they are based on canopy characteristics such as leaf angle distribution, leaf inclination function and planting density (Weiss et al., 2004). When not yet parameterized, indirect LAI methods are difficult to use and given the widespread heterogeneity of banana plants in the field, parameterization of LAI measurements for one cultivar at a specific location might not be useful in other plantations or fields with another cultivar.

A simpler indicator is the CC, defined as the proportion (%) of ground area covered by the vertical projection of the canopy (Jennings et al., 1999). In contrast to LAI, CC is easier to estimate given current drone technology. CC can easily and reliably be determined from image analysis. Unlike LAI, remote sensing and drone imagery allows a dynamic view of the CC averaged over much larger areas, as repeated images can be gathered at multiple times during the day of a complete plantation. This dynamic view of plantations is needed as individual banana plants unfold their lamina differently in response to variable environmental stimuli and soil conditions, typically following a diurnal rhythm with leaf halves forming a single plane aligned with the midrib during the night and early morning, and folding down to become more vertical during the day under periods of high radiation (Kallarackal et al., 1990; Thomas et al., 1998; Turner, 1998; Turner et al., 2007). Lamina folding occurs in drought stressed plants (Milburn et al., 1990; Thomas & Turner, 1998; Turner & Thomas, 1998), but this is questioned (Lu et al., 2002). While the effect of drought on leaf emission and growth has been described (Turner and Thomas, 1998; Turner et al., 2007; Carr, 2009), the overall effect on CC, and therefore at the plantation level, is not known. Furthermore, the diurnal effect of leaf folding measured by CC cannot be reflected at the plantation scale by LAI as leaf size remains quite similar on a daily scale.

Given the lack of knowledge on CC in banana plantations, the overall objective was to investigate to what extent plot-scale observations of CC provide insights into water deficit. Firstly, we hypothesize that soil moisture readily affects CC development as emerging leaves are among the first organs to be affected by drought. Secondly, we hypothesize diurnal changes in CC which are correlated with changes in daily evaporative demand, and that these changes are larger in plants experiencing water deficits. Thirdly, we hypothesized that CC - LAI relationships can be obtained per cultivar, allowing to calculate CC values from LAI values. An additional objective was to calibrate the AquaCrop canopy growth curve for first cycle plants based on optimally irrigated plants and assess the performance of this AquaCrop growth curve.

5.2 Material and methods

5.2.1 Experimental site and conditions

Experiments (Annex II with details on the field trial experimental design) were conducted at the joint research farm of the Nelson Mandela African Institution of Science and Technology (NM-AIST) and the International Institute of Tropical Agriculture (IITA) in Arusha, Tanzania (3° 23’ 58” S, 36° 47’ 48” E). Soils were Endocalcic Phaeozems (Geoabruptic, Clayic, Humic) (IUSS Working Group WRB, 2014) or Udertic to Vertic Haplustols (USDA, 1999) on gently sloping land (3%) located at the foothill of Mt. Meru at an altitude of 1,188 m asl. Soils were moderately shallow to deep (90-120 cm), well structured, well drained with a silty clay loam to silty clay texture (Annex II, Table S1). Soil water holding capacity was determined based on a pF curve analysis of the soil (Annex II, Figure S6).

The climate is a tropical highland climate with a moderately cool thermal zone (FAO, 2012). Rainfall follows a bimodal yearly pattern with a long rainy season extending from late March to early June and a shorter rainy season from October to December (Grieser et al., 2006). An automated weather station (TAHMO weather station: Decagon DS-2 sonic anemometer with pyranometer, REC-1 rain gauge, and VP-4 thermometer and humidity sensor with a solar-powered and GPRS-enabled EM50G), located at the edge of the field, measured air temperature (°C), wind speed at 2 m height (m s^{-1}), relative humidity (%), precipitation (mm) and solar radiation (MJ m^{-2} min^{-1}) at a 5 minute interval. Daily reference evapotranspiration (ET_0) was computed using the FAO Penman-Monteith approach (Allen

et al., 1998). Daily weather variables of the entire experimental run can be found in supplementary data (Annex II, Figure S1).

5.2.2 Plant material

Banana plantations are composed of individual plants often of different reproductive cycles each growing on individual mats. When referring to a "plant" we refer to an individual reproductive cycle. When referring to a "mat", we refer to the total composition of different reproductive cycles present in one location. Generally, there are maximally three cycles present on a mat: a mother plant or cycle 1 (C1), a daughter plant or cycle 2 (C2) and a granddaughter plant or cycle 3 (C3). Our research focused on C1 and C2.

Two experiments were carried out differing only in cultivar and date of planting.

In experiment 1, the East African Highland banana Huti Green Bell (HG, Musa AA Mchare subgroup; ((Perrier et al., 2019)) was planted on 2017-05-03. In experiment 2, Grande Naine (GN, Musa AAA Cavendish subgroup) was planted on 2017-11-13. Planting material for both experiments consisted of in vitro plants, hardened in growth chambers and screenhouses. Plant height of HG at planting was 6.6 (±2.5) cm, with 4.19 (±1.3) leaves, whilst plant height of GN was 25.5 (±4.3) cm with 4.75 (±0.74) leaves. Plant holes were 0.6 m × 0.6 m × 0.6 m deep at a spacing 2 m (row) × 3 m (line) (1,666 plants ha^{-1}). Time is noted in weeks after planting (WAP). In following sections, the different experiments are noted by the planted cultivar (HG vs. GN). Experimental design, management and plant measurements were similar in both experiments unless stated otherwise.

5.2.3 Experimental design

The experiments were conducted on fields with no recent history of banana cultivation. The design was a blocked design with drip irrigation as treatment but given the infrastructure the irrigation treatments could not be randomized (Annex II, Figure S2).

In experiment 1, two blocks were planted with HG. Each block contained five rows of 15 mats, subdivided in three plots of 25 mats (5×5), of which the central nine mats (3×3) were used for data collection. Each block consisted of a different irrigation treatment, as valves to shut off irrigation were installed at the front of each block. For HG, there were three plots for each treatment. Border mats were used for periodic destructive sampling.

In experiment 2, four blocks were planted with GN. Each block contained five rows of 14 mats, subdivided in two plots of 35 mats (7×5), receiving two different irrigation treatments. Valves were installed in the middle of a plant row (between mat 7 and 8); therefore, two irrigation treatments were present in a block. The central nine mats (3×3) were used for growth data collection, leading to four replications (plots) per treatment. The first and last two mats of each row (2×5 mats) together with the border rows were used for destructive sampling. Each treatment was replicated four times across the blocks.

5.2.4 Management

Mats received a mixture of mineral fertilizers and manure. Mineral fertilizers were split applied: 153 kg N ha^{-1} $year^{-1}$ (urea), 206 kg K ha^{-1} $year^{-1}$ (Muriate of potash), 19.26 kg Mg ha^{-1} $year^{-1}$ and 25.6 kg S ha^{-1} $year^{-1}$ ($MgSO_4$) were applied monthly in the rainy season and every two months in the dry season, while 40.2 kg P ha^{-1} $year^{-1}$ (triple super phosphate) was applied every five months. Twenty L of fresh farmyard cow manure was applied per mat twice yearly before the start of the rainy season. All suckers

were allowed to grow until four months after planting (MAP), at which time one sucker of approx. 30 cm height was selected and the others pruned. Each banana mat thereafter was composed of C1 and C2, and de-suckering was carried out afterwards monthly. Weeds and dead leaves were cut monthly and removed from the field.

Three additional leaf pruning events (P) occurred due to the development of Black Sigatoka (*Pseudocercospora fijiensis*) in the long wet season of 2018 at 2018-05-21 (P1), 2018-06-05 (P2), and 2018-07-30 (P3). At P1 and P2, only the oldest leaves with symptoms of the fungus (yellowing and petiole collapse) were cut. At P3 the oldest six leaves of each plant were cut away to retain the spread of the fungus affecting the older leaves.

5.2.4.1 Soil moisture and irrigation

Each banana row was fitted with two driplines, at each side of a banana mat (Annex II, Figure S3). Originally each mat's position was fitted with two drippers (one at each side of the mat). Each dripper supplied approx. 4L hr^{-1}. Two extra drippers were installed on 6 June 2018. For the HG experiment, this was at 57 WAP and for the GN experiment at 29 WAP.

Uniformity of the driplines was assessed, and regardless of the position (front vs. end) of a dripline, drippers supplied approx. 4 L hr^{-1} (Annex II, Figure S4). Hence the pressure did not drop significantly over an irrigation line so that no differences in discharge rate were found. Similarly irrigation discharge also showed no systematic pattern across the different blocks. Blocks closer to the irrigation pump (block 1) received similar amounts than those further away (block 4) (Annex II, Figure S5). Differences in discharge between the blocks were possibly due to small leaks in the driplines, and not due to a systematic pressure drop along the dripline.

Soil moisture was monitored daily by Time Domain Reflectometry (TDR). Within each plot, the central mat was fitted with two TDR probes installed vertically at different depths: 0-30 cm (horizon 1) and 30-60 cm (horizon 2). TDR probes were installed in the area wetted by the drippers, at 50 cm from the central mat and read out each morning before irrigation by a TDR-200 (Campbell scientific, Inc.). Daily moisture depletion, Dr (mm), was calculated at the plot level as:

$$Dr, i = 1000(\theta_{FC} - \theta_i) \times Z_r \quad (5\text{-}1)$$

with Dr, i being depletion on day i, θ_{FC} being the volumetric water content (VWC) at field capacity (FC, [m^3 m^{-3}]), θ_i being the actual VWC at day i (m^3 m^{-3}) and Z_r being the rooting depth (m). The rooting depth was estimated as a logistical interpolation between the depth at 10 days after planting (0.1 m) and at flowering (0.6 m). Rooting depths were checked every three months over the course of the growing season through root trenching methods. Banana reaches a maximum rooting depth at flowering (Turner et al., 2007), and trenches revealed that roots were continually present until depths of 1 m after flowering in both HG and GN mats, as the soil profile was bounded by a saprolite hardpan layer at 1m. Roots were present up to 1 m depth from flowering onwards, but number of roots declined substantially below 60 cm depth. The effective maximum rooting depth (Zr_x) was taken as 0.6 m (Carr, 2009).

Depletion values are negative when water contents are below FC and positive when values are above FC.

Daily depletion values were compared against the readily available water (RAW [mm]), as an indicator of moisture deficit. RAW was calculated as:

$$RAW = 1000\left(\theta_{FC} - \theta_{pwp}\right) \times Z_r \times p = TAW \times p_{adj} \quad (5\text{-}2)$$

with θ_{pwp} being the VWC at Permanent wilting point ($m^3\ m^{-3}$), p_{adj} being a depletion factor (-) and TAW being the total available water (mm). The value of p_{adj} was chosen to be the generic factor *p* of 0.35 for banana as given by Allen et al. (1998), adjusted for the reference evapotranspiration (ET_0) according to Raes et al. (2018c). When the $D_{r,i} < RAW$, plants are assumed to experience moisture deficit.

All mats received irrigation until 4 MAP (establishment period). Thereafter, two irrigation treatments were installed: optimal "full" irrigation (FI) and rainfed (RF). In the FI treatment, mats received water whenever more than 25% TAW was depleted in the first or second soil horizon. Water in the RF treatment was shut off after 4 MAP.

5.2.5 Banana growth measurements

Non-destructive plant growth data were measured monthly at the plot level (3×3 mats), on individual plants (C1 and C2) present on the mat until harvest of C1 as this corresponds to a CC growth cycle. Every three months, mats (n=3) were selected in each treatment in both experiments for destructive sampling. Measured variables and variables calculated from growth measurements are listed in Annex II, Table S2. The phenological flowering event denotes the point of flower emergence from the pseudostem as flower initiation (which happens inside the plant at soil level) cannot be observed from the outside of a plant in the field. Harvest denotes the time when bunches are harvest ready (fingers on a bunch start to yellow). As measurements continued on the same plants over time, the data required a repeated measures analysis of variance.

5.2.5.1 Canopy cover

CC was determined monthly for each plot, to assess the CC evolution over time. Before November 2017, when plants were small, images were taken at the individual mat level and CC was determined as an average of the CC of mats present in a plot. From November 2017 onwards, digital photographs of every plot were taken with a DJI-phantom 4 Pro drone (JPEG, image format, 20MP, 4000 × 2250 pixels, and 72 dpi) at a height of 35 m above the ground with the center of the plot aligning to the center of the image. Before images were taken, the soil surface was weeded, and residues removed.

To assess the influence of timing on diurnal CC patterns, CC pictures were taken at an hourly interval between 8 h and 16 h at nine different dates in both experiments: 2018-01-09, 2018-03-08, 2018-04-05, 2018-05-15, 2018-06-14, 2018-08-06, 2018-08-28, 2018-11-28 and 2018-12-17. CC values from the same plots taken at the same day were compared across different time points to assess the effect of timing on CC values. To compare CC values across measurement dates, the earliest CC pictures were used to exclude possible diurnal effects.

Canopy cover image analysis

ImageJ software (Abràmoff et al., 2004) was used to process images (Figure 5-1). First, images of individual mats were cropped to a ground area of 6 m^2 to only retain the mat of interest, whilst plot images were cropped to retain the central nine mats of each plot (ground area of approx. 54 m^2). Each

image was cropped four times. Second, CC was calculated based on color segmentation according to HSB thresholding (Hue, Saturation, Brightness), where threshold ranges for H, S and B were determined for the green CC pixels. All pixels within these thresholds were set to 1 and the remaining pixels were set to 0. A noise reduction was applied so only pixel areas above a certain minimal pixel size were counted as green CC pixels. HSB threshold ranges and minimal pixel size were determined subjectively for each individual picture as lighting conditions in the field were not uniform and did not allow single HSB ranges to be applied to all pictures. The CC was then calculated as:

$$CC = 100 \times Green\ CC\ pixels/Total\ pixels \quad (5\text{-}3)$$

with CC being Canopy cover (%), Green CC pixels being the absolute number of pixels that are selected and total pixels being the absolute number of pixels of the cropped photograph.

To examine CC diurnal variation, a relative CC was calculated for each hour of image taking. The relative CC was calculated as

$$CC_{rel,i} = 100 \times CC_i/CC_{i=0} \quad (5\text{-}4)$$

with $CC_{rel,i}$ being the relative CC (0 to 1) at time point i,CC_i being the absolute CC (%) at time point i and $CC_{i=0}$ being the absolute CC (%) of the first drone measurements of the day.

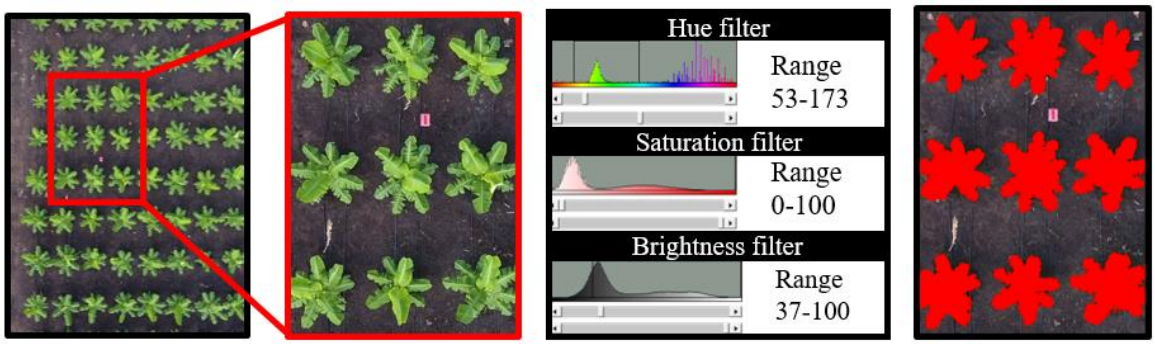


Figure 5-1: Drone image analysis procedure. a) Original picture at 35 m above the ground of a GN plantation at approx. 3 MAP, b) image cropped to retain nine central mats from a plot, c) HSB threshold selection for green pixels and d) filtered image with only green pixels selected shown in red.

Correction for plant death

In experiment 1, weak plants due to disease and other unknown factors, were replaced by sucker derived plants on 2017-09-21. The area of the diseased or replanted mats was excluded in further image analysis. The total area of the central plot was divided into nine squares corresponding to the ground area of the single mats. Empty and diseased mat positions were then blocked out, after which the CC was determined on the other plant positions (Annex III, Figure S1).

5.2.5.2 Leaf area index

The LAI was calculated from monthly collected growth parameters. The leaf area of individual leaves ($LA_{leaf,i}$) was calculated as follows:

$$LA_{leaf,i} = LL \times LW \times laf \quad (5\text{-}5)$$

with LL and LW being the length and width of the leaf i, and laf being a leaf area factor (-). The laf was calculated following Nyombi et al. (2009), from leaves measured during destructive sampling (Annex III, Figure S2a). During development, leaves were numbered cumulatively and the LL and LW of each leaf was either measured during monthly growth measurement, at harvest or interpolated between LL and LW of measured leaves leading to a database with LL and LW for each developed leaf (Annex III, Figure S3), showing the exponential nature of leaf area over time.

The total leaf area of a plant ($LA_{plant,\ calc}$) was calculated by summing the area of all the present leaves as:

$$LA_{plant,\ calc} = \sum_{i=cumO}^{cumY} LA_{leaf,i} \quad (5\text{-}6)$$

with $LA_{leaf,i}$ is the leaf area of the i[th] leaf, $cumO$ is the oldest cumulative leaf present and $cumY$ is the youngest cumulative leaf present on a plant. Comparison of $LA_{plant,\ calc}$ with LA_{plant} measured for destructively sampled plants is shown in supplementary material (Annex III, Figure S2b). The total leaf area of an individual mat (LA_{mat}) was then calculated as the sum of the leaf area of C1 plants ($LA_{plant,C1}$) and its successor C2 ($LA_{plant,C2}$):

$$LA_{mat} = LA_{plant,C1} + LA_{plant,C2} \quad (5\text{-}7)$$

whilst summing the leaf mat areas of all the nine plants within a plot led to the leaf area plot (LA_{plot}):

$$LA_{plot} = \sum_{i=1}^{n=9\ mats} LA_{mat} \quad (5\text{-}8)$$

LAI_{plot} was then calculated by dividing LA_{plot} with its ground area (m²).

5.2.6 Statistical analysis

5.2.6.1 Linear mixed models for irrigation effects

Field plots were the experimental units for the statistical analysis. As data were collected from the same plots over time, they constitute longitudinal repeated measures data. We used linear mixed models to analyze the effect of irrigation treatment on soil moisture, CC and LAI observations and diurnal canopy cover variation. Differences in soil moisture, LAI and CC used WAP and treatment as fixed factors, and block and plot as random factors. Differences in diurnal CC variation between FI and RF plots used time (h) and treatment as fixed factors, whilst using block and plot as random factors. Using block and plot as random factors ensured that potential differences in discharge rate between plots and blocks were taken into account in the statistical analysis.

5.2.6.2 Growth curve analysis

CC growth curves were obtained through nonlinear least squares (nls) regression (Ritz & Streibig, 2008) on CC values obtained during drone flights early in the day, to exclude a potential diurnal CC effect. Observations were average CC per plot level until C1 harvest.

Curve fitting through the observations was done by (1) the standard logistical equation, and (2) the AquaCrop canopy cover growth equation.

The standard logistical equation is as follows:

$$CC_t = \frac{CC_x}{1+\left(\frac{CC_x - CC_0}{CC_0}\right)e^{-rt}} \quad (5\text{-}9)$$

with CC_t being CC (%) at time t (days), CC_x being the max. CC (%), CC_0 being the initial CC at planting (%) and r being the CC growth rate (days^{-1}). During regression, days were treated as numeric variables. Residual plots and ANOVA comparison of fitted models were used to determine model selection. Curve fitting with this model was called **standard logistical curve fitting.**

AquaCrop uses a different growth curve to describe green canopy cover throughout the crop cycle. Canopy development in AquaCrop was simulated by two equations (Part 1 and Part 2):

$$CC_t = \begin{cases} CC_0 \times e^{t \times cgc} & when\ \left(CC_t < \frac{CC_x}{2}\right);\ Part\ 1 \\ CC_x - 0.25 \times \frac{(CC_x)^2}{CC_0} \times e^{-t \times cgc} & when\ \left(CC_t > \frac{CC_x}{2}\right);\ Part\ 2 \end{cases} \quad (5\text{-}10)$$

with CC_t being CC (%) at time t (WAP, days or GDD) , CC_x being the max. CC (%), CC_0 being the initial CC at planting (%) and cgc being the canopy growth coefficient (% day^{-1} day or % GDD^{-1}). Curve fitting using the AquaCrop growth equations was called **AquaCrop curve fitting.**

For both curve fitting procedures, initially only FI data points were used to obtain curve parameters under optimal conditions. Each curve has three parameters to be estimated: CC_0, CC_x and a growth coefficient r or cgc. Firstly, CC_0 and CC_x were set based on actual field data of CC at planting (WAP = 0) and CC at approximate flower emergence respectively, after which cgc and r were regressed to obtain best estimates according to Ritz and Streibig (2008). Secondly, all parameters (CC_0, CC_x and growth coefficients r and cgc) were estimated without prior value setting. Goodness-of-fit characteristics (Chapter 4) between observed CC and simulated CC were used to compare simulations.

In a second step, treatment specific regressions were carried out to assess whether model coefficients differed between FI and RF data.

5.2.6.3 Treatment specific regressions

Regressions were compared across treatments to assess the influence of treatment on regression coefficients. In the first method, RF and FI specific regression models were created and 95%CI of the specific model coefficients were compared. The second method used an analysis of covariance (ANCOVA) by adding categorical variables ‘treatment’ and ‘cultivar’ as dummy variables in the regression models. It was assessed whether the parameter coefficients in the models were

significantly different between the treatment/cultivar groups, or whether they could be estimated by a common coefficient (Picard et al., 2012).

5.2.7 CC-LAI curve

CC-LAI curves were created for HG and GN. Monthly LAI_{mat} values were compared with monthly CC estimates from the obtained logistic growth functions. A functional equation of the Lambert-Beer Law was fitted as:

$$CC = 100 \times \left[1 - exp^{(-b \times LAI)}\right]; \quad (5\text{-}11)$$

with b being the extinction coefficient and LAI being the leaf area index (m^2 m^{-2}). To exclude a potential diurnal CC effect, CC values used were obtained during the first drone flights of the day. Observations were average CC per plot level.

5.2.8 Goodness of Fit characteristics

Observed and simulated values for the obtained regression curves were compared, and goodness-of-fit characteristics used were R^2 (Pearson's correlation coefficient), Root mean square error (RMSE), Relative Root mean square error (RRMSE), the Nash and Sutcliffe model efficiency (NSE) and the Wilmot's index of Agreement (d) (Chapter 4, Table 4-2).

5.2.9 Software and used packages

Statistical analyses were performed in R version 3.4.3 (R Core Team, 2017). Linear mixed models were fitted using REML with the function lmer from the package nlme (Pinheiro et al., 2019). Plots were made using the package ggplot2 (Wickham, 2016). Nls regressions were performed using the package nls (R Core Team, 2017).

5.3 Results

5.3.1 Soil moisture depletion

During the establishment periods (0-20 WAP), soil moisture depletions did not differ significantly (p> 0.05) between FI and RF in both experiments except for GN at WAP 15 when FI plots were less depleted than RF plots (diff=18.27 mm ±8.69 mm, p=0.039) (Figure 5-2). After the establishment period, differences in soil moisture closely followed the dry season.

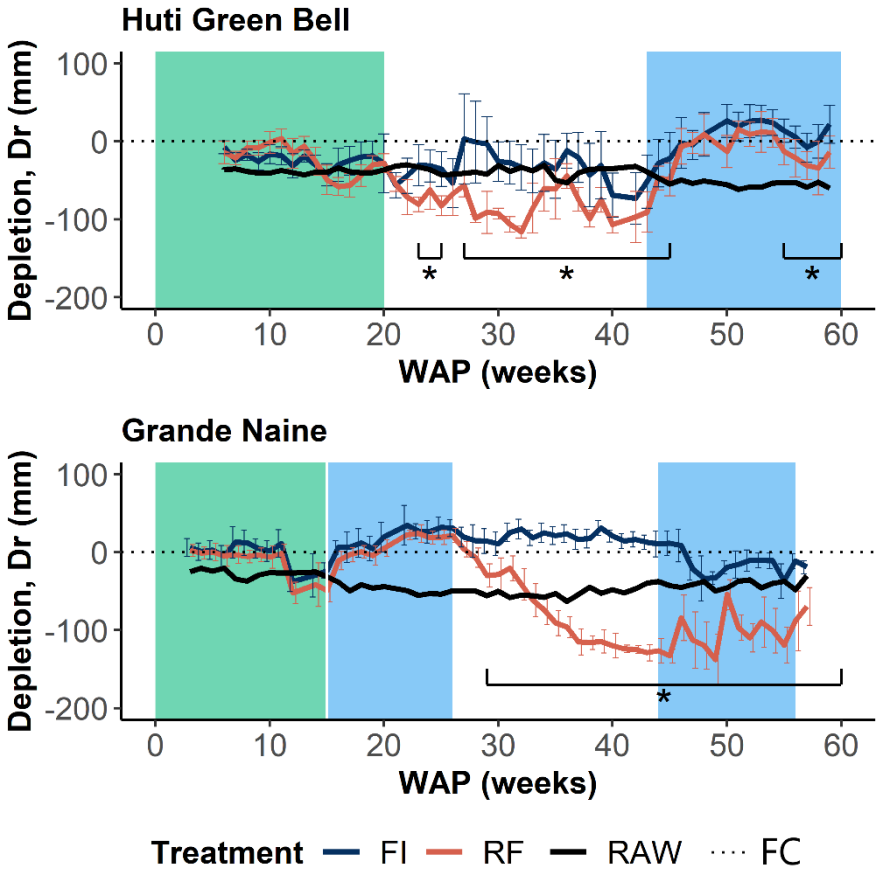


Figure 5-2: Average soil moisture depletion (mm) versus time (WAP: weeks after planting) for two experiments. a) HG: Mchare - Huti Green Bell. b) GN: Cavendish - Grande Naine. Under two irrigation regimes (FI: full irrigation and RF: rainfed). Green period: establishment period. Blue period: rainy season. Error bars denote mean ±standard deviation. '*' indicates a statistically significant (p<0.05) difference between FI and RF. Black line indicates the Readily Available Water (RAW, 35% of the Total Available Water). Dotted line indicates Field Capacity (FC).

In HG, soil moisture depletion in the RF plots first became significantly larger at 23 WAP (diff= 54.29 mm ±19.25 mm, p=4.22e^{-3}) until 45 WAP (diff= 67.62 mm ±17.50 mm, p=8.81e^{-3}). From 45 until 55 WAP soil moisture depletions were similar (p>0.05). At 55 WAP, one week after rains ended, RF plots became significantly more depleted than FI plots (diff= 45.80 mm ±19.06 mm, p=0.015) until the end of the growth trial (60 WAP [diff=88.94 mm ±19.064 mm, p=1.7e^{-4}]). Soil moisture in FI plots exceeded the RAW multiple times during the growing season, so moisture deficit could not fully be excluded in these plots.

In GN, RF plots became significantly more depleted from 27 WAP (diff= 17.89 mm ±8.69 mm, p=0.04) until the end of the growth trial (57 WAP [diff = 100.07 mm ±11.95 mm, p<2e^{-16}]). In GN, soil moisture of the FI plots remained mostly below the RAW (except at 12 WAP), so plants were considered non-stressed.

5.3.2 Canopy growth over time

CC at planting (WAP 0) was similar for FI and RF and was 0.29% (±0.21) for HG, and 0.79% (±0.12) for GN based on initial canopy cover estimates. Maximum canopy cover values (CC_x) for C1 were 87.86% (±3.25) for HG and 90.34% (±2.28) for GN FI plots and were reached close to onset of flower emergence.

Irrigation treatment had a significant effect on actual CC in both experiments (p<0.05) (Figure 5-3). For HG, CC was reduced significantly in the RF plots from 31 WAP (diff= 7.66% ±3.77%, p=0.05) (8 weeks after moisture divergence) to 48 WAP (diff= 8.50% ±3.77%, p=0.04). For GN, CC was affected significantly from 38 WAP (diff= 3.54% ±1.14%, p=0.008) onwards (9 weeks after moisture divergence).

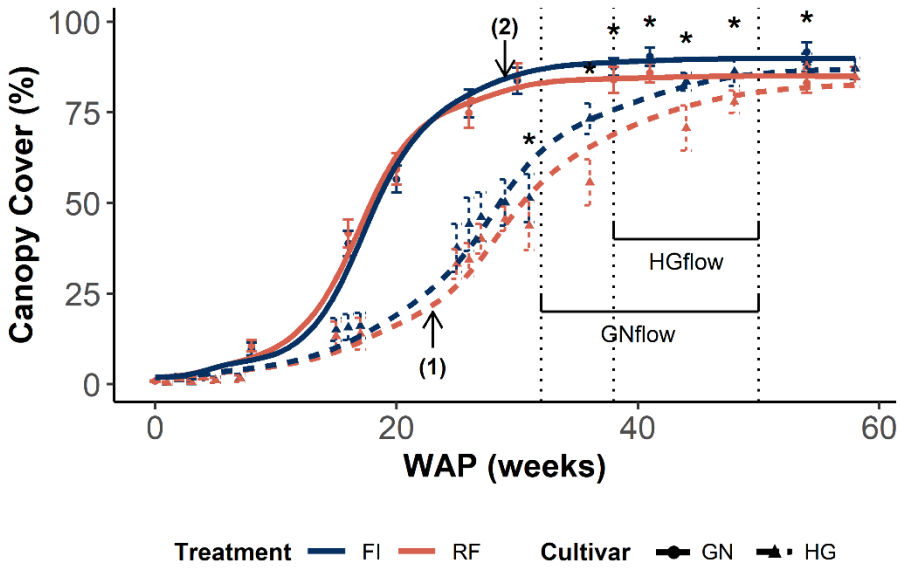


Figure 5-3: Nonlinear least squares (nls) regression curves of canopy cover (CC: %) over time (WAP: weeks after planting) for two experiments (HG: Mchare - Huti Green Bell, GN: Cavendish - Grande Naine) under two irrigation regimes (FI: full irrigation and RF: rainfed) Points denote actual average CC, error bars denote mean ±standard deviation as determined at plot level (n=3 for HG and n=4 for GN). HGflow indicates period of flower emergence of C1 in HG experiment. GNflow indicates period of flower emergence of cycle 1 (C1) in GN experiment; (1) denotes the onset of moisture divergence in HG experiment, whilst (2) indicates the onset of moisture divergence in GN experiment. '*' indicates a statistically significant (p<0.05) difference between FI and RF.

5.3.3 Standard logistical regression

Growth curves were created using the obtained CC observations per plot level. All nls parameters were significant (p<0.05) in the regression analyses (Table 5-1 and Table 5-2).

Using CC_0 and CC_x as estimated from field observations at planting and around flower emergence respectively, the growth coefficient (r) became 0.03 (±3.82e^{-4}) for HG and 0.037 (±3.85e^{-4}) for GN. The curves for logistical regression performed well for HG (RRMSE= 19%) and very well for GN (RRMSE= 6%) (Table 5-1). Setting no initial CC_0 and CC_x, but estimating all parameters in the growth curves led to parameters as seen in Table 5-1. The curves for logistical regression performed excellent for HG (RRMSE= 7%) and excellent for GN (RRMSE= 3%). Estimating all parameters showed better goodness-of-fit than setting parameters as observed in the field, although improvement of goodness-of-fit values is slightly marginal. For comparing the regressions across treatments, the regressions estimating all parameters were used.

5.3.3.1 Treatment specific regressions

In HG, all treatment specific regressions parameters overlapped as shown by 95%CI intervals (Table 5-2). Also in GN, all parameters overlapped, although intervals for CC_x and r were only slightly overlapping (Table 5-2). ANCOVA analysis revealed treatment to have an effect on regression coefficients. All ANCOVA model comparisons are shown in Annex III.

For HG, logistical regressions differed only in r, reducing r in the RF plots (r=0.018 ±8.94e^{-4}) versus the FI plots (r=0.02 ±9.79e^{-4}). CC_x remained similar (89.34% ±1.49%, p=0.25), leading to a significant CC divergence between 25 and 54 WAP which corresponds with the dry season (Figure 5-3 and Table 5-2). HG plots entered the dry season at 20 WAP (Figure 5-2) when CC values were approx. 25% and rapid canopy development was expected to start. CC divergence between treatments reached a maximum divergence at 36 WAP (diff=17.59% ±3.77%, p=2.89e^{-3}), at the middle of the dry season. From 36 WAP onwards, the divergence between curves declined again and became negligible at 54 WAP (p=0.746). For both RF and FI, CC growth continued significantly from 38 WAP to 50 WAP, the period of flower emergence of C1 plants.

In GN, r and the CC_x were both affected by treatment (p=8.04e^{-8}). RF reduced the CC_x in RF (85.85% ±8.44e^{-1}) versus FI (89.29% ±8.96e^{-1}), whilst slightly increased the r in RF (0.034 ±1.08e^{-3}) versus FI (0.032 ±1.03e^{-3})(Table 5-2). Differences in r were statistically significant but lie very close to each other as shown by the overlapping 95% CI: [0.031, 0.037] for RF and [0.029, 0.034] for FI. CC_x differences were more pronounced: 95% CI [84.03, 87.52] for RF and [87.50, 91.29] for FI (Table 5-2). GN entered the dry season at 29 WAP (Figure 5-2), when CC values were approx. 85% for both RF and FI, hence close to reaching CC_x (Figure 5-3). CC_x, or the stationary phase of the CC curve, was reached near flower emergence for C1 (32 WAP to 50 WAP).

5.3.4 AquaCrop logistical regression

AquaCrop growth curves were created using the obtained CC observations per plot level. All nls parameters were significant (p<0.05) in the regression analyses (Table 5-3 and Table 5-4). Using CC_0 and CC_x as observed in the field, the cgc in AquaCrop nls regression became 0.026 (±4.4e^{-4}) for HG and 0.032 (±3.02e^{-4}) for GN (Table 5-3). Canopy development of GN was faster than of HG (Figure 5-3). AquaCrop regressions performed moderately well for HG (RRMSE= 25%) and well for GN (RRMSE= 13%). Setting no initial CC_0 and CC_x, but estimating all parameters in the growth curves led to parameters as seen in Table 5-3. The curves for AquaCrop regression performed well for HG

(RRMSE= 15%) and very well for Grande Naine (RRMSE= 8%). Estimating all parameters for the growth curves showed better goodness-of-fit than setting parameters as observed in the field, and lead to significant improvement of goodness-of-fit values (Table 5-3). When comparing the regressions across treatments, the regressions estimating all parameters were used.

5.3.4.1 Treatment specific regressions

For each part of the AquaCrop growth curve (Part 1 and Part 2) specific ANCOVA regressions were created, and all ANCOVA model comparisons are shown in Annex III.

HG AquaCrop equation part 1 did not show differences in cgc between treatments as coefficients overlapped and following ANCOVA (p=0.748). HG AquaCrop equation part 2 showed non overlapping 95% CI for cgc, and slightly overlapping 95%CI for CC_x. Differences were significant in both cgc and CC_x following ANCOVA (p=2.04e^{-6}). Soil moisture affected the cgc and CC_x significantly in the overall AquaCrop growth equation. Cgc did not overlap in 95%CI between RF [1.52e^{-2}, 1.62e^{-2}] and FI [1.64e^{-2}, 1.73e^{-2}], and was reduced significantly under RF conditions (Table 5-4). CC_x showed overlap in 95%CI between RF [80.7, 88.3] and FI [85.1, 91.7], but differences were significant following ANCOVA (p=0.039) (Annex III). CC_x was reduced (although slightly) under RF conditions (Table 5-4). The specific regression models showed good goodness-of-fit for both RF (RRMSE= 13%) and FI (RRMSE= 12%) (Table 5-4 and Figure 5-3).

GN AquaCrop equation part 1 did not show differences between treatments in cgc as coefficients overlapped and following ANCOVA (p=0.90) (Annex III). HG AquaCrop equation part 2 showed slight overlapping 95% CI for cgc, and slightly overlapping 95% CI for CC_x. Differences were significant in both cgc and CC_x following ANCOVA (p=1.21e^{-3}) (Annex III). Overall, soil moisture affected the cgc and CC_x significantly in the AquaCrop growth equation (p=1.21e^{-3}). Cgc showed slight overlap in 95%CI between RF [2.68e^{-2}, 2.83e^{-2}] and FI [2.58e^{-2}, 2.70e^{-2}]. Cgc in FI was significantly reduced, but slightly. CC_x showed no overlap in 95%CI between RF [82.87, 87.23] and FI [87.6, 92.41] (Table 5-4), and differences were significant following ANCOVA (p=0.039) (Annex III). The treatment specific regression models showed excellent goodness-of-fit for both RF (RRMSE= 5%) and FI (RRMSE= 6%) (Table 5-4 and Figure 5-3).

Table 5-1: Standard logistical canopy cover growth curve regression of growth data of Mchare Huti Green Bell and Cavendish Grand Naine under irrigation (FI) until harvest of cycle 1. CC_0 denotes initial canopy cover, CC_x denotes maximum canopy cover and cgc denotes the canopy growth coefficient.

		Parameter estimation							Goodness-of-fit				
Cultivar	**Parameters estimated**	**Parameter**	**value**	**SD**	**t value**	**P-value**	**sign. level**	**95%CI**	**R^2**	**RMSE**	**RRMSE(%)**	**NSE**	**d**
Huti Green Bell	r	CC_0[a]	0.290	2.11e^{-01}					0.98	6.87	19	0.94	0.99
		CC_x[a]	87.865	3.25e^{+00}									
		r	0.030	3.82e^{-04}	78.73	<2e^{-16}	***	[0.029; 0.031]					
	CC_0, CC_x and r	CC_0	1.780	4.32e^{-01}	4.116	1.55e^{-4}	***	[1.087; 2.71]	1	2.59	7	0.99	1
		CC_x	90.537	1.90e^{+00}	47.714	<2e^{-16}	***	[86.947; 94.452]					
		r	0.020	1.39e^{-03}	14.693	<2e^{-16}	***	[0.018; 0.023]					
Grande Naine	r	CC_0[a]	0.788	1.22e^{-01}					1	2.39	6	1	1
		CC_x[a]	90.341	2.28e^{+00}									
		r	0.037	3.85e^{-04}	96.79	<2e^{-16}	***	[0.036; 0.038]					
	CC_0, CC_x and r	CC_0	1.661	2.62e^{-01}	6.347	1.71e^{-07}	***	[1.193; 2.207]	1	1.14	3	1	1
		CC_x	89.363	8.88e^{-01}	100.584	< 2e^{-16}	***	[87.591; 91.199]					
		r	0.032	1.3e^{-03}	24.629	< 2e^{-16}	***	[0.03; 0.035]					

[a]: set as observed values in the field. Sign. level *** = 0.05

Table 5-2: Treatment specific standard regression parameters of Mchare Huti Green Bell and Cavendish Grand Naine under two irrigation regimes (FI: full irrigation and RF: rainfed). Growth curves parameters were obtained through nonlinear least squares regression. If no specification occurs, parameters were similar between drought and irrigated plots (p<0.05). cgc-RF and cgc-FI denote canopy growth coefficients in RF and FI plots, whilst CC_x-RF and CC_x-FI denote CC_x coefficients in RF and FI plots (p<0.05). CC_0 is similar in both treatments.

	Standard logistic regression parameters							Goodness-of-fit					
Cultivar	**Parameters**	**Value**	**SD**	**95%CI**	**t value**	**P-value**	**sign. level**	**Treatment**	**R^2**	**RMSE**	**RRMSE(%)**	**NSE**	**d**
Huti Green Bell	CC_0	2.181	3.50e^{-01}	[1.59; 2.89]	6.225	1.33e^{-08}	***	RF	0.99	3.15	8	0.98	1
	CC_x	89.340	1.49e^{+00}	[86.49; 92.44]	59.963	< 2e^{-16}	***	FI	1	2.71	7	0.99	1
	r-RF	0.018	8.94e^{-04}	[0.016; 0.019]	19.65	< 2e^{-16}	***						
	r-FI	0.020	9.79e^{-04}	[0.018; 0.022]	20.151	< 2e^{-16}	***						
Grande Naine	CC_0	1.609	1.96e^{-01}	[1.12; 2.18]	8.22	3.24e^{-12}	***	RF	1	2.23	5	1	1
	CC_x-RF	85.820	8.44e^{-01}	[84.03; 87.53]	101.71	<2e^{-16}	***	FI	1	1.14	3	1	1
	CC_x-FI	89.286	8.96e^{-01}	[87.51; 91.29]	99.61	<2e^{-17}	***						
	r-RF	0.034	1.08e^{-03}	[0.031; 0.037]	31.28	<2e^{-18}	***						
	r-FI	0.032	1.03e^{-03}	[0.029; 0.035]	31.23	<2e^{-19}	***						

Table 5-3: AquaCrop logistical canopy cover growth curve regression of growth data of Mchare Huti Green Bell and Cavendish Grand Naine under irrigation (FI) until harvest of cycle 1. CC_0 denotes initial canopy cover, CC_x denotes maximum canopy cover and cgc denotes the canopy growth coefficient.

		Parameter estimation							Goodness-of-fit				
Cultivar	**Parameters estimated**	**Parameter**	**Value**	**SD**	**t value**	**P-value**	**sign. level**	**95%CI**	**R^2**	**RMSE**	**RRMSE(%)**	**NSE**	**d**
Huti Green Bell	cgc	CC_0[a]	0.290	2.11e^{-01}					0.97	9.46	25	0.89	0.97
		CC_x[a]	87.865	3.25e^{+00}									
		cgc	0.026	4.46e^{-04}	62.305	<2e^{-16}	***	[0.025; 0.027]					
	CC_0, CC_x and cgc	CC_0	1.780	4.32e^{-01}	4.116	1.55e^{-4}	***	[1.087; 2.71]	0.99	5.77	15	0.96	0.99
		CC_x	90.537	1.90e^{+00}	47.714	<2e^{-16}	***	[86.947; 94.452]					
		cgc	0.017	2.57e^{-04}	70.57	<2e^{-16}	***	[0.016; 0.017]					
Grande Naine	cgc	CC_0[a]	0.788	1.22e^{-01}					0.99	5.47	13	0.98	0.99
		CC_x[a]	90.341	2.28e^{+00}									
		cgc	0.032	3.02e^{-04}	106.81	<2e^{-16}	***	[0.031; 0.033]					
	CC_0, CC_x and cgc	CC_0	1.661	2.62e^{-01}	6.347	1.71e^{-07}	***	[1.193; 2.207]	1	2.66	6	0.99	1
		CC_x	89.363	8.88e^{-01}	100.584	< 2e^{-16}	***	[87.591; 91.199]					
		cgc	0.027	2.51e^{-04}	106.065	<2e^{-16}	***	[0.026; 0.027]					

[a]: set as observed in the field. Sign. level *** = 0.05

Table 5-4: Treatment specific AquaCrop regression parameters of Mchare Huti Green Bell and Cavendish Grand Naine under two irrigation regimes (FI: full irrigation and RF: rainfed). Growth curves parameters were obtained through nonlinear least squares regression. If no specification occurs, parameters were similar between rainfed and irrigated plots (p<0.05). cgc-RF and cgc-FI denote canopy growth coefficients in RF and FI plots, whilst CC_x-RF and CC_x-FI denotes CC_x coefficients in RF and FI plots (p<0.05). CC_0 is similar in both treatments.

	AquaCrop regression parameters							Goodness-of-fit					
Cultivar	**Parameters**	**Value**	**SD**	**95%CI**	**t value**	**P-value**	**sign.level**	**Treatment**	**R^2**	**RMSE**	**RRMSE(%)**	**NSE**	**d**
Huti Green Bell	CC_0	1.780	4.32e^{-01}	[1.08; 2.71]	4.116	1.55e^{-04}	***	RF	0.98	5.14	13	0.95	0.99
	CC_x-RF	84.470	1.89e^{+00}	[80.66; 88.29]	44.81	<2e^{-16}	***	FI	0.99	4.42	12	0.98	0.99
	CC_x-FI	88.390	1.62e^{+00}	[85.12; 91.66]	54.75	<2e^{-16}	***						
	cgc-RF	0.016	2.51e^{-04}	[0.015; 0.016]	68.225	<2e^{-16}	***						
	cgc-FI	0.017	2.27e^{-04}	[0.016; 0.017]	76.525	<2e^{-16}	***						
Grande Naine	CC_0	1.661	2.62e^{-01}	[1.19; 2.21]	6.347	1.71e^{-07}	***	RF	1	2.2	5	1	1
	CC_x-RF	85.050	1.07e^{+00}	[82.88; 87.23]	79.25	<2e^{-16}	***	FI	1	2.66	6	0.99	1
	CC_x-FI	90.010	1.19e^{+00}	[87.60; 92.42]	75.81	<2e^{-16}	***						
	cgc-RF	0.028	3.63e^{-04}	[0.025; 0.031]	83.79	<2e^{-16}	***						
	cgc-FI	0.027	3.04e^{-04}	[0.023; 0.030]	95.065	<2e^{-16}	***						

5.3.5 Diurnal CC variation

Due to practical reasons (weather conditions, drone regulations and flight scheduling) pictures of CC could not always be taken at an hourly interval at each day, yet CC was always determined at minimally three time points (Figure 5-4).

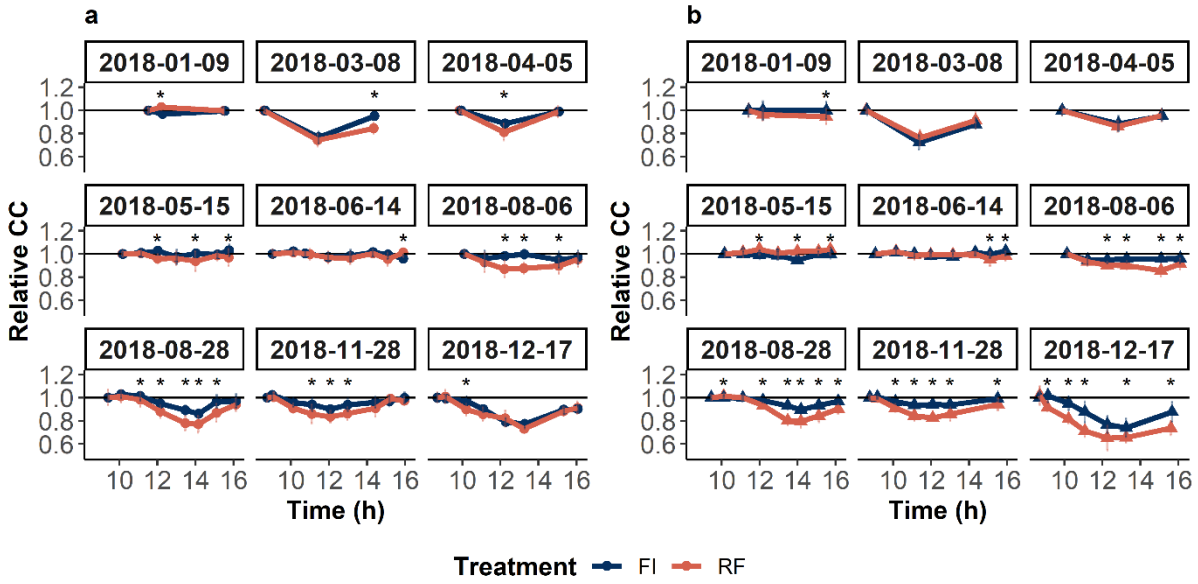


Figure 5-4: Relative canopy cover (CC_{rel}) evolution during the day for different dates of drone flights. a) Experiment 1, HG: Mchare - Huti Green Bell and b) Experiment 2, GN: Cavendish - Grande Naine, under two irrigation regimes (FI: full irrigation and RF: rainfed). Points denote average CC_{rel}, error bars denote ± standard deviation as determined on plot level (n=3 for HG and n=4 for GN). "*" notes when CC_{rel} of RF is significantly lower than CC_{rel} of FI (p<0.05 and 95% CI do not overlap).

Hour of measurement influenced relative CC (CC_{rel}) values significantly at all measurement dates in both cultivars (all p<0.05), but the effect of time on CC_{rel} varied by date. Although significant, time point had a weak effect on CC_{rel} in January, May, and June for both HG and GN as CC_{rel} during the day remained close to 1 (Figure 5-4)**.** Time effects were more pronounced in March, April, August, November, and December 2018 as curves show a more pronounced deviation from the 1 line.

CC_{rel} was compared against weather parameters, as similar patterns emerged at the same date in both HG and GN experiments (Figure 5-4 and Figure 5-5). Daily ET_0 was highly correlated (R^2>0.86) with solar radiation, relative humidity, and vapor pressure deficits (other indicators of evaporative demand). Dates with more pronounced CC_{rel} reduction (in both RF and FI) (Figure 5-4 and Figure 5-5) were characterized by a higher ET_0 (Figure 5-5 and Figure 5-6a). Overall a clear pattern emerges. Under high ET_0 (>3 mm day^{-1}), CC reduces from morning values and reaches minimal values around noon, after which it increases again in the afternoon (Figure 5-4 and Figure 5-5).

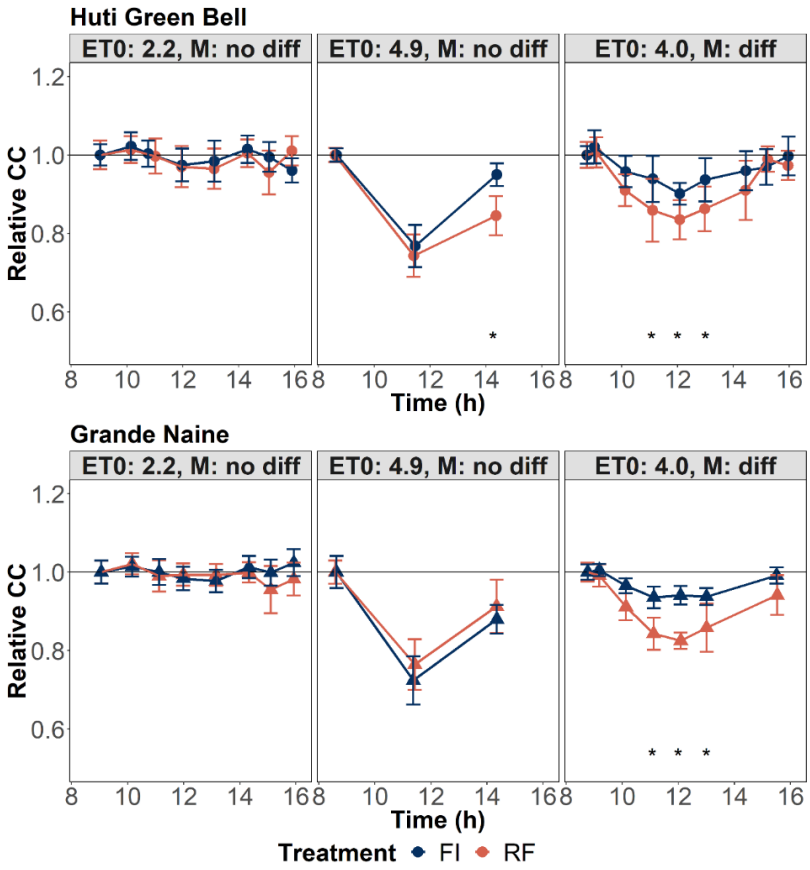


Figure 5-5: Diurnal CC variation for three different scenarios in the field. ET_0 notes the ET_0 in mm day^{-1}, whilst M notes whether moisture values in the field differed significantly (diff) between treatments or did not differ significantly (no diff) between treatments. '*' notes significant difference in relative CC between FI and RF plots (p<0.05)

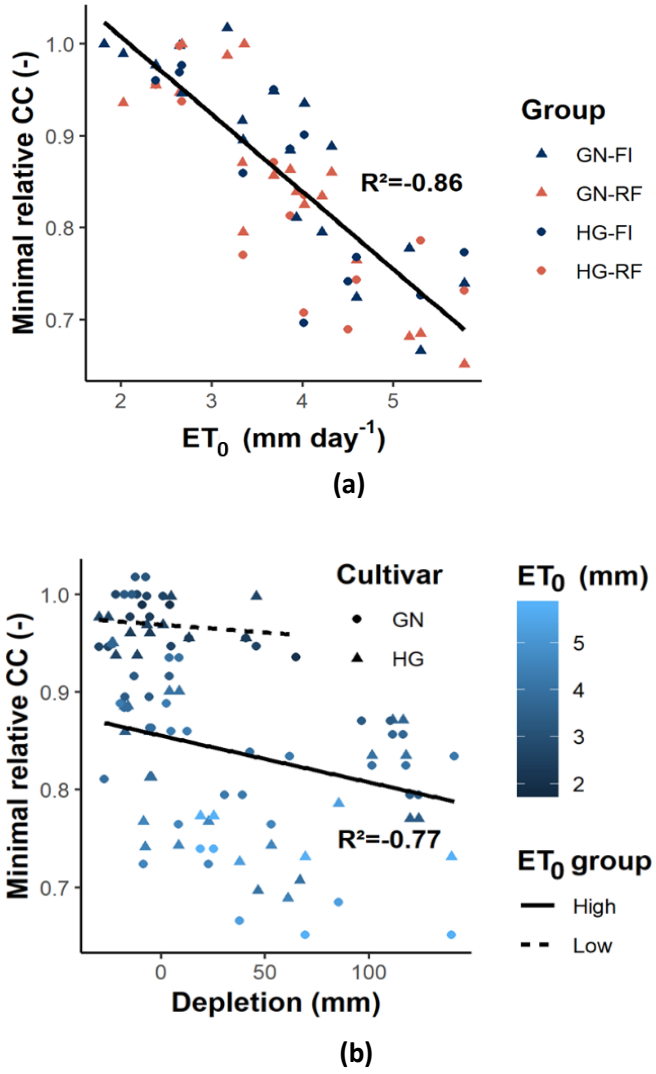


Figure 5-6: Minimal daily relative canopy cover (CC_{rel}) for different drone flying dates compared against (a) daily reference evapotranspiration: ET_0 (mm day^{-1}) and (b) daily soil moisture depletion on plot level (mm) for two experiments (HG: Mchare - Huti Green Bell, GN: Cavendish - Grande Naine) under two irrigation regimes (FI: full irrigation and RF: rainfed)

Soil moisture deficits had an additional effect on CC_{rel} patterns, depending on the prevailing ET_0 (Figure 5-5 and Figure 5-6). When ET_0 is low (<3 mm day^{-1}), there is no additional folding with increasing depletion (p=0.79). Only when ET_0 increases (> 3 mm day^{-1}), do increasing depletion values exacerbate the folding (p=8.72e^{-3})(Figure 5-5 and Figure 5-6). At low ET_0 (<3 mm day^{-1}), the CC_{rel} is therefore similar in RF and FI, whilst under high ET_0 (>3 mm day^{-1}), increasing depletion leads to a lower CC_{rel}.

5.3.6 CC-LAI relationship

5.3.6.1 Leaf area factor

Destructively sampling plants allowed to establish a laf of 0.66 (±0.018, p<2e^{-16}) for HG, while laf of GN was determined to be 0.75 (±0.012, p<2e^{-16}). Single laf values were used for calculating LA values, as no pattern emerged with increasing leaf size (Annex III, Figure S2a).

5.3.6.2 LAI evolution

Irrigation treatment had a significant effect on LAI_{plant} and LAI_{mat} in both experiments (Figure 5-7).

In HG, LAI_{plant} and LAI_{mat} were significantly reduced by drought from 31 WAP onwards (p<0.05). Fungus pruning started at 55 WAP, after which LAI could no longer be calculated due to the big size of the plants.

In GN, LAI_{plant} of C1 increased steadily until the first onset of flower emergence (32 WAP), after which there was a big drop in LAI_{plant} of C1 due to leaf pruning at 37 WAP (P3), whereby the lowest six leaves were cut from all plants in both FI and RF (Figure 5-7). LAI_{plant} of C1 was significantly reduced in the RF plots from 42 WAP onwards (p=0.009), whilst LAI_{plant} of C2 was affected from 46 WAP (p=1.65e^{-5}). LAI_{mat} behaved similarly and started diverging from 42 WAP onwards (p=5e^{-4}).

As such, LAI in both experiments reacted to moisture deficit at about 8 to 9 weeks after soil moisture divergence, similarly as CC values.

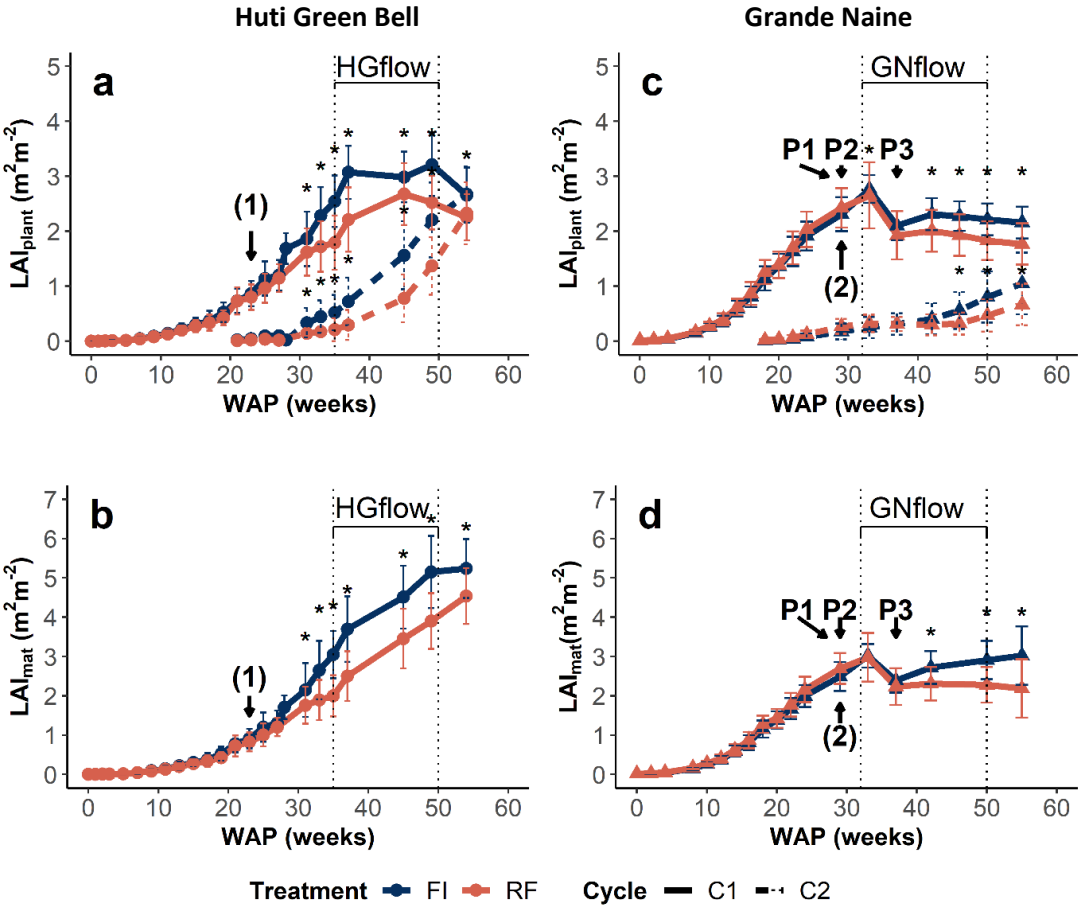


Figure 5-7: LAI evolution for two experiments (HG: Mchare - Huti Green Bell, GN: Cavendish - Grande Naine) under two irrigation regimes (FI: full irrigation and RF: rainfed). a) LAI_{plant} values for HG cycle 1 (C1) and cycle 2 (C2), b) LAI_{plant} values for GN cycle 1 (C1) and cycle 2 (C2), c) LAI_{mat} values for HG, composed of both cycles, d) LAI_{mat} values for GN, composed of both cycles. Points denote average LAI, error bars denote ±standard deviation as determined on plot level (n=3 for HG and n=4 for GN). P1, P2 and P3 indicate the different leaf pruning events. GNflow indicates the period of flower emergence of C1 in GN; HGflow indicates the period of flower emergence of C1 in HG. (1) indicates the onset of moisture divergence in experiment 1, whilst (2) indicates the onset of moisture divergence in experiment 2. '*' indicates a statistically significant (p< 0.05) difference between LAI in FI and RF plots.

5.3.6.3 CC-LAI curves

LAI_{mat} values were used to create CC- LAI curves for both cultivars, which follow an exponential function (Figure 5-8).

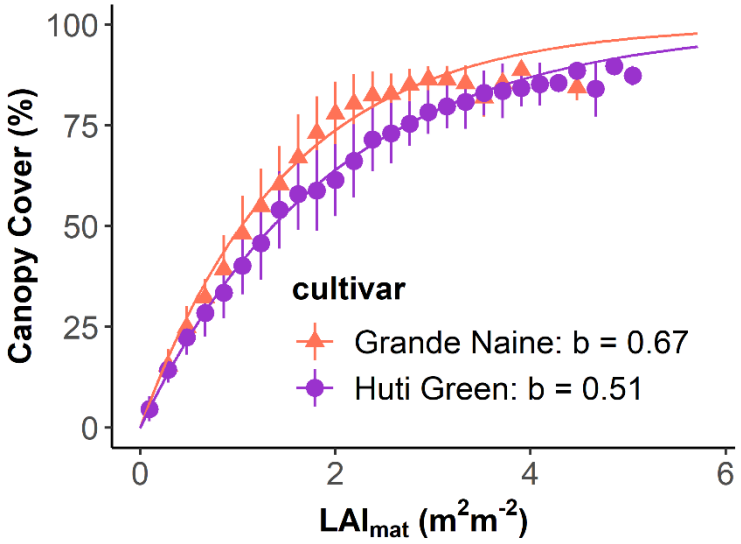


Figure 5-8: Relationship between leaf area index (LAI_{mat}) and canopy cover (CC) for two banana cultivars (HG: Huti Green Bell, GN: Grande Naine). Fitted lines are regressed on plot data (points) until flower emergence of Cycle 1 in HG (n=3) and GN (n=4). Extinction coefficients are significantly different (p<0.05).

CC and LAI were accurately fitted by the Lambert-Beer equation for both cultivars. HG had significantly lower extinction coefficient (b=0.51 ±3.8e^{-3}, p<2e^{-16}) than GN (b= 0.67 ±4.6e^{-3}, p<2e^{-16}) showing that at a similar LAI, a lower CC is reached in HG.

5.4 Discussion

5.4.1 Canopy growth over time

Irrigation and precipitation combined, FI plots received approx. 3,100 mm (HG) and 4,003 mm (GN), compared to RF plots which received 1,916 mm (HG) and 2,549 mm (GN) over the entire growing season (until harvest of C2). FI plots received approx. 1,522 mm year^{-1} (HG) and 2,000 mm year^{-1} (GN). RF plots received approx. 935 mm year^{-1} (HG) and 1,297 mm year^{-1} (GN**).** Total amounts of added moisture in RF plots were less than optimal values for banana production (1,100 to 2,650 mm year^{-1}) and not evenly spread as there were distinct rainy seasons interrupted by dry spells of more than two months implying the need for irrigation (Robinson & Alberts, 1986; Van Asten et al., 2011; Varma & Bebber, 2019). As growth was significantly reduced in RF plots, irrigation proved necessary in Arusha for both experiments.

CC in both experiments was significantly affected by soil moisture deficit (Figure 5-3), but timing and severity occurred at different developmental stages in the experiments (Figure 5-2). Divergence of soil moisture in HG started at the start of the exponential growth phase (23 WAP) when CC values were approx. 25%. As drought coincided with the beginning of the exponential growth phase absolute CC differences were more pronounced and became first significant (diff=7.66% ±3.77, p=0.05) at around 8 weeks after the onset of soil moisture differences (31 WAP). At 36 WAP, in the middle of the dry season, CC in FI plots was 17% (±3.77) larger than the RF plots (p=1.65e^{-4}).

For GN, the absolute effect of drought on CC was less, as CC reached about 85 % at moisture divergence (29 WAP onwards), and most of the leaves of C1 had already formed so close to flower emergence. CC differences between RF and FI plots became significantly different from 38 WAP onwards (diff=3.54% ±1.15), about 9 weeks after soil moisture values started diverging indicating moisture deficit to influence the CC even close to flower emergence.

CC as such reacted quickly to moisture deficit in both experiments. Drought induces stomatal closure, reducing transpiration, photosynthesis, thereby reducing leaf area and leaf emission rate (Carr, 2009; Kallarackal et al., 1990; Taiz & Zeiger, 2010; Thomas & Turner, 1998) both playing a role in CC formation. As new leaves emerge at the top of the pseudostem, and newly formed leaves cover older ones, a reduction in leaf appearance rate and a corresponding decrease in leaf area of new leaves due to moisture deficit, will have a significant effect on the CC, depending on the severity and timing of drought. Indeed, CC and LAI (Figure 5-3 and Figure 5-7) were both significantly reduced by moisture deficits in both experiments.

5.4.2 Standard logistical growth curve

Logistic growth curves accurately captured CC growth for both HG and GN (RRMSE< 19%) when setting CC_0 and CC_x as measured in the field. The estimation of parameters CC_0, CC_x and r led to an improved model fit (RRMSE< 8%) for both cultivars and treatments. CC values were slightly overestimated (1-2%) at the beginning of the growing season when using the estimated CC_0 (Figure 5-3, Table 5-1 and Table 5-3), making sense considering the growth behavior of suckers and seedlings. At plantation establishment, plants grow on reserves for the first few weeks and later become autotrophic in their growth behavior (Robinson & Galan-Sauco, 2010; Twyford & Walmsley, 1973). As such, more reserves are present in the plant, than based solely on the photosynthetic capacity from CC during the initial weeks. Hence plants develop faster due to these reserves. The overestimation of the initial CC takes this into account.

For HG, CC growth curves for RF and FI differed in their growth coefficient r (Table 5-2), leading to diverging CC curves (Figure 5-3). CC divergence from optimal values during the vegetative growth stage can therefore be an indicator of moisture deficit. Similar CC_x values were reached due to the occurrence of the rainy season between 43 and 54 WAP, allowing mats in RF plots to reach LAI_{mat} values leading to near maximum CC (Figure 5-7). So even though LAI_{mat} differed significantly (Figure 5-7), CC did not differ significantly (Figure 5-3). For GN, the growth rate r slightly increased under moisture deficit, but this statistically significant difference led to very small CC growth curve differences (Figure 5-3). CC_x differed significantly being lower in RF plots (Table 5-2).

5.4.3 AquaCrop logistical growth curve

The AquaCrop growth curve accurately captured CC growth for both HG (RRMSE= 25%) and GN (RRMSE= 13%) when setting CC_0 and CC_x as determined in the field (Table 5-3). Running a regression by estimating all parameters of the AquaCrop growth curve (CC_0, CC_x and cgc) led to significantly increased model fit for HG (RRMSE= 15%) and GN (RRMSE = 6%) (Table 5-3). Estimation of CC_0 led to higher initial CC_0 (1.78% in HG, 1.61% in GN) compared to observed values (0.29% in HG, 0.79 % in GN). This initial overestimation of 1-2% was again due to the transitioning from a reserve dependent seedling/sucker to an autotrophic plant. With reserves plant develops faster than with photosynthesis only. The initial overestimation of the CC_0 takes these reserves into account and leads to a more correct CC_0 after regressing all parameters. Hence the model estimating all parameters was used for

treatment specific regressions. Calibration of the curve based on parameters as seen in the field (a feature of AquaCrop) can lead to discrepancies between observed and simulated values. It is therefore better to have a range of possible CC_0, CC_x and cgc values, which are based on nls regressions for all the parameters as shown here.

Similar patterns were found for standard and AquaCrop logistical regressions. For HG, CC growth curves for RF and FI differed in their growth coefficient cgc and CC_x (Table 5-4), leading to diverging CC curves (Figure 5-3). For GN, the growth rate cgc slightly increased under moisture deficit, but this statistically significant difference led to very small CC growth curve differences (Figure 5-3). CC_x differed significantly (Table 5-4) which is due to differential leaf formation in C1 and C2 after soil moisture divergence (Figure 5-7). Even the last developed leaves before flower emergence of C1 and leaves of C2 therefore influence overall CC, albeit a small absolute effect given the exponential nature of the CC- LAI curve (Figure 5-8).

The effect of moisture on the AquaCrop growth curve as seen in this experiment follows the effect of the stress coefficients in the AquaCrop growth model. A stress coefficient on canopy expansion, K_{exp}, runs from 1 (zero stress) to 0 (full stress) in the AquaCrop model. When soil moisture drops below a certain critical threshold (p_{exp-up}), K_{exp} which acts as a multiplier on the cgc drops below 1 reducing the actual cgc. When stress is significant, the reduced cgc may even lead stressed plants not to reach CC_x values (Raes et al., 2018c). Deviation from the AquaCrop growth curve, as parameterized on non-stressed plants, may therefore point to soil moisture stress in the field.

Similar CC_x values of approx. 90% were reached in both experiments under FI, being close to values in other crops under optimal spacing: peach 93% (McClymont et al., 2011), apple 93% (McClymont et al., 2011), Amaranthus 95% (Bello & Walker, 2017), cabbage 95% (Wellens et al., 2013), vining pea 95% (Paula Paredes & Torres, 2017), cotton 90% (Farahani et al., 2009), maize 90-95 % (Hsiao et al., 2009). CC_x values of 100%, while theoretically possible, are rarely reached even with dense planting. Increasing plant densities in the field, leads to larger CC values, as it increases LAI (Figure 5-8). An increasing LAI leads to an increasing CC until beyond LAI 4.5 m^2m^{-2}, when an increase in LAI does not correspond to a significant increase in CC in banana plantations and CC_x is approx. reached (Turner et al., 2007). Wellens et al. (2013) found a significant relationship between CC_x, and used planting density (R^2=0.94) for irrigated cabbage, thereby CC_x can perhaps increase under increased planting density. Commonly used densities of HG are 2 × 2 m (2,500 plants ha^{-1}) and of GN is 3 × 2.5 m (1,333 plants ha^{-1}) respectively and differed from the used planting density (1,667 plants ha^{-1}). Using optimal densities for HG, might then increase cgc (and possibly CC_x), whilst using optimal densities for GN might reduce cgc (and possibly CC_x). Different CC curves would be obtained with these spacing, where CC curves (Figure 5-3) would shift upward for HG (faster CC growth), and downward for GN (slower CC growth). Under optimal density, differences between cultivar CC curves might not be as pronounced as now. Additional research should look at the CC evolution in plantations under different densities planted at the same time to see the density effect on CC growth curves.

5.4.4 Diurnal CC variation

CC showed a significant diurnal pattern on days characterized by high evaporative demands (ET_0>3 mm day^{-1}) in both experiments (Figure 5-4 and Figure 5-5). CC_{rel} over the course of the experiment ranged from 1 (no folding) at ET_0 2 mm day^{-1}, to approx. 0.7 (severe folding) at ET_0 6 mm day^{-1} (Figure 5-6), indicating CC values can be significantly affected by folding in the field. As both experiments showed similar diurnal CC patterns at similar dates (Figure 5-4 and Figure 5-5), diurnal CC adjustment

is expected to occur in both varieties regardless of age of the plantation as on the same date cultivars were in a different growth stage due to differences in planting.

Overall a clear pattern emerged. Under high ET_0 (>3 mm day^{-1}), CC reduces from morning values and reaches minimal values around noon, after which it increases again in the afternoon (Figure 5-4 and Figure 5-5). The larger the daily ET_0, the larger this CC reduction at noon (Figure 5-5 and Figure 5-6a). On days of high ET_0, soil moisture depletion in RF plots significantly increased the CC reduction at midday (p<0.05) compared to FI plots (Figure 5-5 and Figure 5-6b). Hence, both environmental stimuli and the soil moisture deficit status play a role in diurnal CC patterns. We hypothesize this CC pattern to occur due to leaf folding of banana plants.

Leaf folding occurs in well-watered (non-stressed) banana plants and typically follows a diurnal rhythm with leaf halves bounding a single plane aligning the midrib during the night and early morning, becoming more vertical (fold downward) during periods of high evaporative demand and returning to their original position (fold upward) in the late afternoon (Carr, 2009; Milburn et al., 1990; Thomas & Turner, 1998; Turner et al., 2007; Turner & Thomas, 1998).

Leaf folding in response to drought is still debated, but some research suggests diurnal leaf folding to be more pronounced under drought (Milburn et al., 1990; Thomas & Turner, 1998; Turner & Thomas, 1998), whilst others refute this claim (Lu et al., 2002). Our results indicate leaf folding indeed is increased under drought, given ET_0 is high enough.

Other plants also exhibit leaf folding at field scale under drought. Maize, rice, wheat, and sorghum (amongst other grasses) roll their lamina upward transversally to the mid rib under stress conditions due to a drop in water potential (turgor) in the leaf. Leaf “rolling” results from varying degrees of dehydration in different cross sections of the rolled leaf (Kadioglu et al., 2012). Rolling in maize leaves follows a diurnal pattern whereby maximum closure is reached at solar noon during days of high evaporative demand, but not present in well-watered plants. Leaf rolling in grasses is therefore a visible indication of moisture deficit and also present at the canopy level (Baret et al., 2018).

In banana, leaf folding results from differential turgor of cells in the leaf pulvinar bands, following a similar process as changes in stomatal aperture which are being controlled by the turgor of the guard cells (Satter & Galston, 1981; Turner et al., 2007). Diurnal leaf folding in banana may therefore be due to changes in leaf turgor pressure on a diurnal scale. Zimmermann et al. (2010), studied the effects of environment and irrigation on leaf turgor pressure using a leaf patch clamp pressure probe on diurnal timescales. They showed leaf turgor varied diurnally in both irrigated and non-irrigated plants. Generally, leaf turgor pressure declined from morning values, reached a minimal value around noon after which turgor increased again in the late afternoon and during the night. On days with high evaporative demands, turgor pressure drops were more pronounced, indicating leaf turgor pressure reacted directly to the environment. Under optimal irrigation, turgor pressure dropped less and recovered during the night, whilst under sub-optimal irrigation turgor pressure drops were more pronounced and did not recover. They concluded turgor pressure amplitudes and stabilization time might therefore be indicators of moisture deficit on a diurnal scale (Zimmermann et al., 2010).

Given our findings and the fact leaf turgor plays a role in leaf folding, we hypothesize the diurnal CC pattern to reflect these diurnal turgor pressure pattern in a leaf. At high evaporative demands (possibly exacerbated by soil drought), leaf turgor drops, resulting in folding of the leaves and closing of the stomata. We hypothesize the bigger the evaporative demand, and the more soils are moisture

depleted, the more leaf turgor is affected leading to a more pronounced leaf folding and a more pronounced diurnal CC pattern. Further research is needed to prove this hypothesis.

CC diurnal patterns by themselves are not good indicators of moisture deficit, as they do not occur when ET_0 is low and occur even in well irrigated plots when ET_0 is high. However, comparison of irrigated with non-irrigated plots on days of high ET_0 could indicate moisture deficit due to an increased and prolonged CC drop at midday.

This diurnal CC pattern needs to be considered when creating CC curves for crop growth modelling as the effect on actual CC values can be significant. A hypothetical mature plantation with CC values of approx. 90% would reduce its CC to 63% under ET_0 of 6 mm day^{-1}, indicating diurnal adjustments can be profound. CC pictures need to be taken early in the morning (<8 h) or in the evening (>18 h) to reduce the CC variation and make use of optimal light conditions.

5.4.5 CC-LAI relationship

As banana cultivars are phenotypically diverse (Ploetz et al., 2007), it is necessary to determine a laf to correctly determine the LA_{leaf} for each cultivar. laf was 0.66 (±0.004, p<2.2e^{-16}) for HG, and 0.75 (±0.004, p<2.2e^{-16}) for GN. These values are in the range of published laf values (Blomme & Tenkouano, 1998; Nyombi et al., 2009; Obiefuna & Ndubizu, 1979). Using the laf for HG and GN, LAI_{mat} values for HG and GN ranged between 0-5 m² m^{-2} (Figure 5-7 and Figure 5-8) corresponding with the LAI range noted in commercial plantations (Turner, 1972, 1998; Turner et al., 2007).

CC- LAI relationships were obtained for both cultivars with LAI_{mat} being composed of both C1 and C2 (Figure 5-8). The CC- LAI relationship was exponential as in wheat, triticale (Nielsen et al. 2012) and maize (Hsiao et al., 2009; Nielsen et al., 2012). Turner et al. (2007) state that a plantation of LAI 4.5 m²m^{-2} will have a CC of approx. 90%, and that increasing beyond this LAI will lead to a negligible increase of intercepted solar radiation. This is reflected in our CC-LAI curves where LAI can increase, but CC does not increase beyond LAI 4.5-5 m²m^{-2}. At a similar spacing, CC- LAI curves differed significantly (p=4.73e^{-10}) between the two cultivars. HG had a significantly lower extinction coefficient (b=0.51 ±0.006) than GN (b=0.67 ±0.004), indicating that at similar LAI values a lower CC will be obtained for HG. This can be due to the ploidy of the cultivars as diploids (HG) exhibit more erect leaves than triploids (GN). At similar LAI values, erect leaves cover less ground than more horizontal leaves. This remains speculation, as to test whether it is a ploidy effect, rather than a cultivar effect, more cultivars need to be tested.

Overall, CC, LAI and corresponding CC- LAI curves are influenced by cultivar, plant spacing, mother-daughter relationships, management and environments (Turner, 1998; Turner et al., 2007; Wellens et al., 2013). Hence a single CC- LAI curve cannot be proposed for banana (*Musa* spp.), but these can be used for the specific cultivars.

5.5 Conclusion

CC growth, and growth curves where significantly affected by moisture deficit, indicating CC growth over time can be used as an indicator of moisture deficit in plantations. Over a growing season, both CC and LAI were significantly reduced 8-9 weeks after moisture divergence between the RF and FI plots in both experiments. Solely using CC as an indicator of growth, however, does not allow to separate the effect of drought between the different cycles, and therefore CC curves over time can only be used as indicators of the total plantation reaction to drought. When separating growth of the

different cycles, LAI is of better use as this could more easily be separated between mother and daughter plants.

The AquaCrop growth curve was able to correctly simulate CC over the first growth cycle for both HG and GN. Setting CC_0 and CC_x values as observed in the field, already led to moderately good to good model fits. Fits were significantly improved by estimated CC_0 values through regression than estimating from field observations. Drought affected the growth rates and CC_x values of the growth curve, as built in the AquaCrop model through the crop stress coefficient acting on canopy expansion. The next step is to investigate the evolution of biomass and yield in the field for further development of the AquaCrop database. This will be done in the following chapter 6.

On a daily timescale LAI remains stable, whereas CC varies according to evaporative demands and moisture depletion. At low evaporative demands, CC did not vary significantly. At high evaporative demands CC was reduced at midday, with reductions being increased by increasing soil moisture depletion. In view of this diurnal CC pattern, we hypothesize CC drops to reflect the leaf turgor pressure, which has proven to vary similarly on a diurnal timescale and plays a role in leaf folding. More research is however needed to prove this hypothesis. Daily monitoring of CC at morning compared to midday might be an indicator of soil moisture deficit if a reference plot that is fully irrigated is present.

CC- LAI curves for both cultivars followed the Lambert-Beer law, with both cultivars having significantly different extinction coefficients. CC- LAI curves are expected to depend on the plant spacing and used cultivar, as the difference in extinction coefficient might be due to the different leaf physiology of the used cultivars.

In summary, CC as an indicator of growth offers potential in monitoring soil moisture deficit in banana plantations.

6 Banana biomass estimation and yield forecasting from non-destructive measurements for two contrasting cultivars and water regimes

Bert Stevens[a,*], Jan Diels[b], Allan Brown[c], Stanley Bayo[c], Patrick Alois Ndakidemi[d] and Rony Swennen[a,c,e]

[a]KU Leuven, Department of Biosystems, Willem De Croylaan 42 - box 2455, 3001 Heverlee, Belgium

[b]KU Leuven, Division of Soil and Water Management Celestijnenlaan 200e - box 2411, 3001 Leuven, Belgium

[c]International Institution of Tropical Agriculture, IITA, PO Box 447, Arusha, Tanzania

[d]Nelson Mandela African Institution of Science and Technology, NMAIST, P.O.BOX 447, Arusha, Tanzania

[e]Bioversity International, Willem De Croylaan 42, 3001 Heverlee, Belgium

[*]Lead author

This chapter is based on its published form:

Stevens, B., Diels, J., Brown, A., Stanley, B., Ndakidemi, P. A., & Swennen, R. (2020). Banana biomass estimation and yield forecasting from non-destructive measurements for two contrasting cultivars and irrigation treatments. *Agronomy*, *10*(9), 1435. https://doi.org/10.3390/agronomy10091435

6.1 Introduction

Banana (*Musa* spp.), the most important fruit worldwide (FAOSTAT, 2019), is a long cycle crop with a vegetative phase between 7-13 months depending on environmental conditions, such as water and nutrients (Robinson & Galan-Sauco, 2010). For most of the plant's life, it develops without a bunch. Bunch biomass is linked to biomass buildup during the vegetative phase (aboveground: pseudostem, petioles and leaves, and belowground: corm), since (1) formed leaves determine the photosynthetic capacity and (2) previously stored assimilates can be translocated from within the banana mat to the developing bunch (Eckstein et al., 1995; Mukasa et al., 2005; Nyombi et al., 2009; Robinson & Galan-Sauco, 2010; Swennen & De Langhe, 1985; Twyford & Walmsley, 1973). Monitoring vegetative biomass enables the following of growth over time and, due to its link with yields, can provide an indicator of future yields.

Monitoring biomass over time can be done by destructive whole-plant sampling, but it is more practical to quantify the biomass during the growth cycle or to forecast the yield from non-

destructive observations using allometric relationships. Destructive sampling is very labor intensive, time consuming, and provides only one sampling point for one plant. To capture biomass over time, plants need to be sampled periodically, requiring lots of plants and space. Sampling plants before they are harvest ready also stands in the way of quantifying bunch weights.

Allometric relationships specify how growth and size in plants or plant components is related to their allocated biomass (Henry et al., 2011; Niklas, 2004; Picard et al., 2012). Parameters can be vegetative characteristics (e.g., pseudostem girth at base) (Negash et al., 2013; Nyombi, 2010; Swennen, 1984b; Swennen & De Langhe, 1985; Wairegi et al., 2009; Yamaguchi & Araki, 2004), bunch components (e.g., number of hands, fingers, finger volume) (Soares et al., 2014; Wairegi et al., 2009; Woomer et al., 1999) or phenological observations (e.g., days to flowering, days to harvest). Vegetative parameters that are well connected to biomass, and/or parameters that are connected to future yields and allow bunch weight 'forecasting', are of significant interest. Measuring such parameters in the field is much faster than destructive sampling and keeps fields intact. Allometric equations are useful for periodic biomass monitoring in the field (Wairegi et al., 2009), which is needed to calibrate and further improve computer crop simulation models (Nyombi et al., 2009; Taulya, 2015; Tixier et al., 2004). Crop models can be used (among others) to analyze management interventions under different environments, to mitigate and adapt crop production to climate change (Nyine et al., 2019; Peng et al., 2020; Soares et al., 2014) and for economic analysis to manage financial decisions (e.g., manpower and cost of agricultural inputs as irrigation) (Tixier et al., 2008). As allometric relationships are the foundation of such models, correct relationships are of crucial importance.

Allometric relationships were previously developed for a limited number of banana cultivars for both vegetative and bunch biomass estimation. Nyombi et al. (2009) developed allometric relationships for both biomass and bunch weight estimation for two East African highland banana (EAHB) cultivars (Mbwazirume and Kisansa) with data from two locations under various nutrient regimes. Their models followed a power function using girth and height of pseudostem as predictors, whereby covariates included banana phenological stages (vegetative growth stage, flower emergence and harvest ready stage). Plants were irrigated, but with unspecified amounts of water, and fresh bunch weights ranged from 20-40 kg plant^{-1}. Stress can therefore not be excluded in their fields. Pooling data across cultivars and growth stages lead to a high R^2 (>0.7) but increased the variance in biomass estimations. Model performance increased when data were partitioned between growth stages, indicating that allometric relationships vary with the growth stage. Yamaguchi and Araki (2004) estimated biomass components using linear regression models based on pseudostem volume (V_{pseudo}) for EAHB cultivars from farmers' fields. Models had good fits (R^2=0.93) but the plant sample was small (*n*=4) and stress could not be excluded as plants were rainfed. Negash et al. (2013) estimated biomass based on pseudostem diameter and height in Enset

(*Ensete ventricosum*), another genus of the *Musaceae*. Models performed well for total biomass estimation (R^2>0.89), but plants came from rainfed farmers' fields without information on potential stresses.

Allometric models for bunch weight estimation were previously created, but these include parameters that change until harvest so cannot be used in forecasting bunch weights. Soares et al. (2014) estimated bunch weights using multiple linear regression and neural networks for an AAAB tetraploid hybrid. Models were accurate (R^2>0.71), but predictors included variables that can only be measured in a destructive manner at harvest (e.g., average fruit weight at harvest). Woomer et al. (1999) estimated bunch weights for a rainfed EAHB cv. Mbwazirume based on estimated bunch volume through linear regression (R^2=0.85-0.94), but as bunch volume changes until harvest (Robinson & Galan-Sauco, 2010), yields were not forecasted and no information on potential stress was given. Wairegi et al. (2009) quantified bunch weights of 39 triploid EAHB cultivars from 179 farms in Uganda, whereby multiple linear regression models used pseudostem girth at base and height at 1 m, number of hands, and number of fingers in the lower row of the second hand as predictors. Data partitioning along cultivars, developmental stages, and regions improved model accuracy but differences were not significantly different compared to the pooled dataset. Plants were rainfed and given the wide range of fresh bunch weights in this study (2-60 kg plant^{-1}) stress from multiple sources was presumed, but its effect on allometry was not analyzed.

The major constraint in all previously developed allometric models is that fields were not growing under optimal conditions as they were stressed by inadequate amounts of water and/or nutrients. Water (excess and deficit) is the most limiting abiotic constraint to banana production (Carr, 2009; Van Asten et al., 2011; Wairegi et al., 2010). Suboptimal rainfall may lead to significant reduction in vegetative parameters (e.g., pseudostem height, girth), bunch components (number of hands, number of fingers, individual finger weight, fruit filling) (Carr, 2009; Mahouachi, 2007; Van Asten et al., 2011), and may delay phenological events as flowering or harvest (Carr, 2009; Fortescue et al., 2011; Holder & Gumbs, 1982; Turner et al., 2007). Parameters underlying allometric models are often impacted by moisture, but the overall effect on the relationship between a parameter and allocated biomass due to soil moisture is not specified in earlier allometric models. Their general use and applicability can be questioned. Similar genotypes may lead to different biomass allocation patterns and phenotypes under different biotic and abiotic environments (Weiner, 2004), and banana has shown dry matter allocation plasticity due to drought and soil nutrients (Taulya, 2013) and plant density (Robinson & Nel, 1989). Furthermore, due to the large phenotypic and or genetic differences between banana cultivars, allometric models can differ between cultivars (Nyombi et al., 2009; Wairegi et al., 2009).

So far, no research has compared allometric models between differently irrigated plants in the same field. As allometric models relate growth and size, which are affected by soil moisture, to

accumulated biomass, we are interested to check whether allometric relationships remain similar under different soil moisture regimes.

The objective of this research was three-fold:

Firstly, to assess the effect of soil moisture on growth parameters, phenology and growth rates using two distinctly different cultivars: the EAHB cv. Mchare—Huti Green Bell (AA), a diploid, and the Cavendish—Grande Naine (AAA), a triploid of immense commercial appeal.

Secondly, to use easily observable plant growth parameters to establish allometric relationships in both cultivars for (1) vegetative biomass estimation (aboveground: pseudostem, petioles, and leaves and belowground: corm) to allow monitoring vegetative biomass production over time, and (2) bunch weight forecasting to allow quantifying bunch weights before harvest.

Thirdly, to compare these allometric relationships across water regimes for both cultivars to assess whether banana plasticity under drought results in significant different relationships. As drought readily affects vegetative parameters, yield, and phenology (Carr, 2009; Fortescue et al., 2011; Robinson & Galan-Sauco, 2010; Turner et al., 2007; Weiner, 2004), we hypothesize drought to significantly influence allometric relationships of both vegetative biomass estimation and bunch weight forecasting.

6.2 Material and methods

6.2.1 Experimental design

Experiments (Annex II with details on the field trial experimental design) were established in fields of the International Institute of Tropical Agriculture (IITA) and the Nelson Mandela African Institution of Science and Technology (NM-AIST) in Arusha, Tanzania (3°23’58” S, 36°47’48” E) at an altitude of 1,188 m asl as described in Chapter 5. Soils were Endocalcic Phaeozems (Geoabruptic, Clayic, Humic) (Annex II, Table S1). The climate is a tropical highland climate with a moderately cool thermal zone. Rainfall follows a bimodal yearly pattern with a long rainy season extending from late March to early June and a shorter rainy season from October to December, although rainfall is variable from year to year (FAO, 1996) (Annex II, Figure S1).

Total precipitation received during the experiment was about 903 mm $year^{-1}$ for HG, and 913 mm $year^{-1}$ for GN, lower than those for optimal banana production (1,100–2,650 mm $year^{-1}$) and not evenly spread (dry spells of more than two months) (Figure 6-1a) implying the need for irrigation (Robinson & Alberts, 1986; Van Asten et al., 2011; Varma & Bebber, 2019).

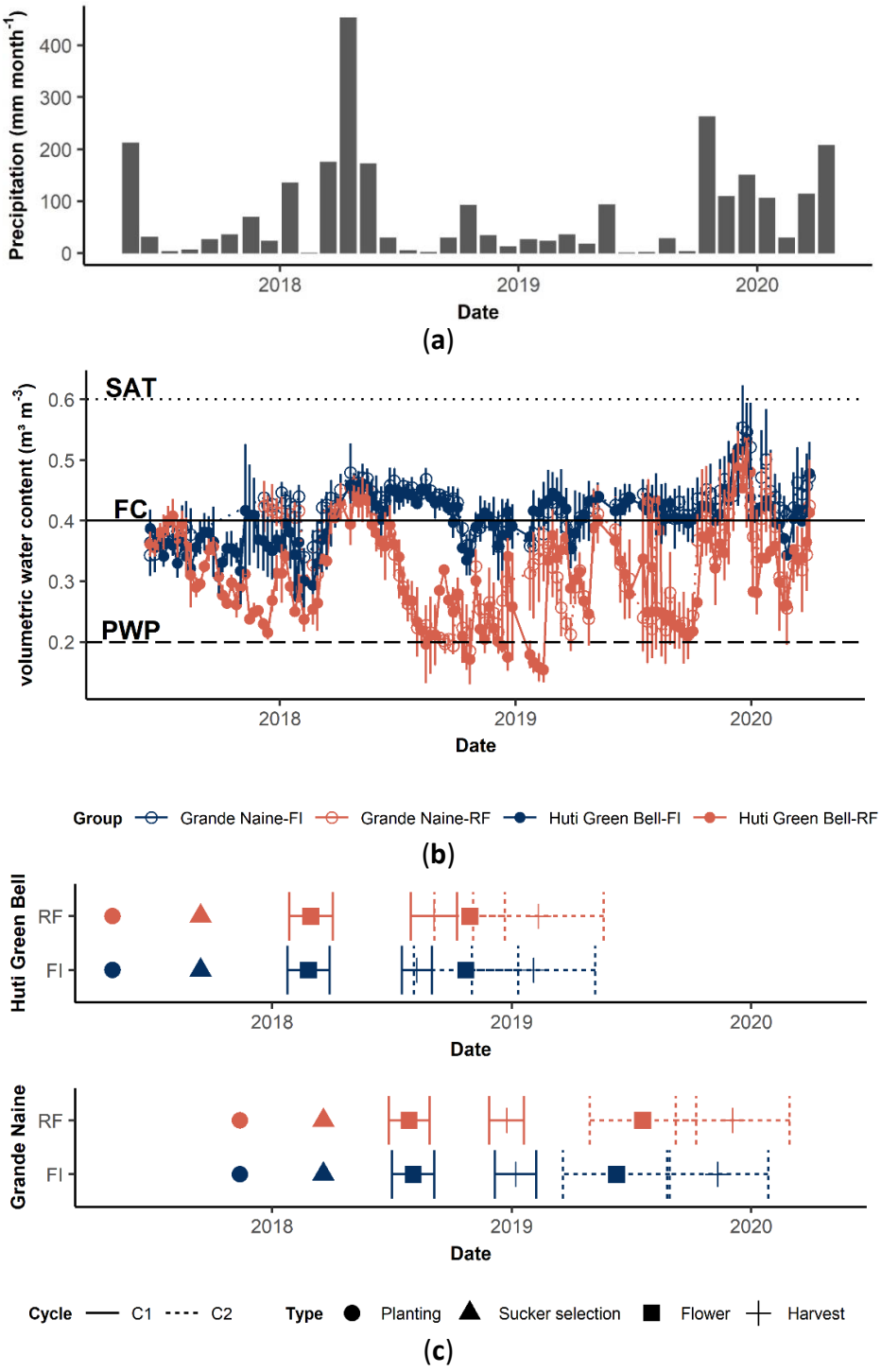


Figure 6-1: Water regimes in Huti Green and Grande Naine Experiments (a) Precipitation (mm month^{-1}) in Arusha, Tanzania over the course of the experiments; (b) Average weekly volumetric water content, vwc (m^3 m^{-3}) in the upper 60 cm of the soil under two irrigation regimes (FI: full irrigation noted in blue, and RF: rainfed noted in orange). Error bars note mean ± standard deviation. SAT notes the vwc at saturation, FC notes the vwc at field capacity and PWP notes the vwc at permanent wilting point; (c) Phenological events for Huti Green Bell and Grande Naine (planting, sucker selection, flower emergence and harvest readiness) for cycle 1 (C1) and cycle 2 (C2). Error bars note mean date ±standard deviation. Planting and sucker selection occurred on a single day; hence no standard deviations are present.

Two experiments were carried out differing in cultivar and date of planting over the course of two full crop cycles (until harvest of C2). Planting material was provided by IITA and Crop Bioscience

Solutions Ltd, Arusha, Tanzania. In experiment 1, the EAHB Huti Green Bell (HG, Musa AA Mchare subgroup) was planted on 2017-05-03. In experiment 2, Grande Naine (GN, Musa AAA Cavendish subgroup) was planted on 2017-11-13. The diploid HG is characterized by a slender tall pseudostem, with erect foliage and a bunch that bears fruits with marked ridges (Perrier et al., 2019). The triploid GN is characterized by a short, thick pseudostem, with semi-drooping foliage and producing almost round fingers (Ploetz et al., 2007). Both cultivars are of significantly different phenotypical constitution. Planting material for both experiments consisted of in vitro plants, hardened in growth chambers and screen houses. Plant spacing was 2 m (row) × 3 m (line) leading to 1,666 plants ha^{-1}.

The design was a blocked design with drip irrigation as treatment but given the infrastructure the irrigation treatments could not be randomized (Annex II, Figure S2). In experiment 1, two blocks were planted with HG. Each block contained five rows of 15 mats, subdivided in three plots of 25 mats (5 × 5), of which the central nine mats (3 × 3) were used for continuous data collection. Each block consisted of a different irrigation treatment. For HG, there were three plots for each treatment. Border mats were used for periodic destructive sampling. In experiment 2, four blocks were planted with GN. Each block contained five rows of 14 mats, subdivided in two plots of 35 mats (7 × 5), receiving two different irrigation treatments. The central nine mats (3 × 3) in each plot were used for continuous growth data collection, leading to four replications (plots) per treatment. The first and last two mats of each row (2 × 5 mats) together with the border rows were used for periodic destructive sampling. Each treatment was replicated four times across the blocks.

All mats received irrigation for the first four months post-transplant (establishment period, four MAP). Thereafter, two irrigation treatments were applied: optimal 'full' irrigation (FI) and rainfed (RF), based on volumetric water contents in the root zone (as determined by Time Domain Reflectometry) (Figure 6-1b). In the FI treatment, mats received water whenever more than 25% of total available water in the root zone was depleted. No supplemental irrigation was provided in RF treatments after the initial four month establishment period (except between December 2018 to February 2019 when irrigation was applied to limit plant death by drought in the field as plants were stressed for a long time and started showing severe physiological stress indicators as petioles that collapsed). These differential irrigation regimes lead to divergence of soil moisture between RF and FI in HG and GN, which closely followed the dry seasons (Figure 6-1a,b). In HG, soil moisture first became significantly different at 23 weeks after planting (WAP) (October 2017) until 45 WAP (March 2018) during the vegetative growth stage of C1, followed by a rainy season after which they diverged again from 55 WAP (May 2018). In GN, RF plots became significantly more depleted from 27 WAP onwards (May 2018), close to the onset of flower emergence of C1, therefore in GN most of the vegetative growth of C1 occurred under similar soil moisture in RF and FI plots (Chapter 5).

Irrigation and precipitation combined, FI plots received approx. 3,100 mm (HG) and 4,003 mm (GN) over the entire growing season (until harvest of C2), compared to RF plots which received 1,916 mm

(HG) and 2,549 mm (GN). FI plots received approx. 1,522 mm year^{-1} (HG) and 2,000 mm year^{-1} (GN). RF plots received approx. 935 mm year^{-1} (HG) and 1,297 mm year^{-1} (GN). For a more detailed explanation on the onset of moisture stress and its effect on leaf formation and canopy cover in these fields, the reader is referred to Chapter 5.

Mats received an optimal mixture of mineral fertilizers and manure, to exclude nutrient stresses (Meya et al., 2020). Mineral fertilizers were split applied: 153 kg N ha^{-1} year^{-1} (urea), 206 kg K ha^{-1} year^{-1} (muriate of potash), 19.26 kg Mg ha^{-1} year^{-1}, and 25.6 kg S ha^{-1} year^{-1} ($MgSO_4$) were applied monthly in the rainy season and every two months in the dry season, while 40.2 kg P ha^{-1} year^{-1} (triple super phosphate) was applied every five months. Twenty L of fresh farmyard cow manure was applied per mat twice yearly before the start of the rainy season.

All suckers were allowed to grow until four MAP after which suckers were selected for C2 (Annex II, Figure S7). Afterwards, suckers were pruned monthly until bunch filling of C1, when a sucker for C3 was chosen. Maximally, three generations were allowed to grow at any time. Weeds and dead leaves were cut monthly and removed from the field. No pests were present in the field. No disease control was applied, except for Black Sigatoka (*Pseudocercospora fijiensis*) in the wet season, when moderately infected leaves were pruned to avoid further spread of this fungus (Chapter 5).

6.2.2 Plant data collection

Growth data included periodic non-destructive growth data and destructive data (Table 6-1). Additional collected growth data is presented in Annex II, Table S2.

'Non-destructive growth data' were measured monthly at the plot level (3 × 3 mats), on all individual plant cycles (cycle 1, C1; cycle 2, C2 and cycle 3, C3) present on the mat until harvest of C2 (Table 6-1). The main plant is the oldest plant on a mat, whereby ratoon plants (sucker) are new selected shoots springing from the base of the plant. To address multicollinearity, measured parameters were recombined into new parameters as pseudostem volume (V_{pseudo}), leaf area index (LAI), V_{finger}, and $Ratio_{finger}$ (Table 6-1).

Leaf areas were estimated by measuring leaf length, leaf width, and using an experimentally determined leaf area factor (laf) as explained in Chapter 5. LAI was determined by summing the area of all the leaves on a banana plant and dividing it by the ground area for each mat.

Table 6-1: Growth data measured. Non-destructive data includes phenological data collected for the individual plants on a mat, vegetative growth data measured monthly at the plot level on all plants on a mat and at harvest/destructive sampling of a plant, and bunch data measured on harvest ready plants. Destructive data includes biomass data that was determined destructively at harvest or during periodic destructive sampling.

Parameter	Description
Non-Destructive	
Phenology	
Days to flower emergence, DTF (days)	From planting/selection to flower emergence
Days to flower initiation, $DTFI$ (days)	Approx. 11-12 weeks (80.2 days) before flower emergence
Days to harvest, DTH (days)	From planting/selection to harvest
GDD to flower emergence, $GDDF$ (°C d)	Growing degree days from planting/selection to flower emergence
GDD to flower initiation, $GDDFI$ (°C d)	Growing degree days from planting/selection to flower initiation
GDD to harvest, GDDH (°C d)	Growing degree days from planting/selection to harvest
Flower cycle duration days, FCD_D (days)	Days from flower emergence C1 to flower emergence C2
Harvest cycle duration days, HCD_D(days)	Days from harvest C1 to harvest C2
Flower cycle duration GDD, FCD_{GDD} (°C d)	Growing degree days from flower emergence C1 to flower emergence C2
Harvest cycle duration GDD, HCD_{GDD} (°C d)	Growing degree days from harvest C1 to harvest C2
Vegetative growth data, periodic	
Height of pseudostem, H (cm)	Measured until petiole divergence on the top
Girth of pseudostem at base, G_{base} (cm); Girth of pseudostem at mid, G_{mid} (cm)	Measured at base; measured at middle
Radius of pseudostem at base, R_{base} (cm); Radius of pseudostem at top, R_{up} (cm)	Measured at base; measured at petiole divergence
Functional leaves, $functL$ (no.)	Leaves with less than 3/4 necrotic area
Dead leaves, $deadL$ (no.)	Leaves with more than 3/4 necrotic area
Leaf length of third functional leaf, $LL3$ (cm)	Leaf length of third leaf along midrib
Leaf width of third functional leaf, $LW3$ (cm)	Leaf length of third leaf perpendicular to midrib
Pseudostem volume, V_{pseudo} (L)	$V_{pseudo} = \frac{1}{3}\pi H \times \left({r_{base}}^2 + {r_{up}}^2 + r_{base} \times r_{up}\right)/1000$
Pseudostem growth rate, V_{rate} (L day^{-1})	$V_{rate} = V_{pseudo,flower}/DTF$
Leaf area of ith leaf, $LA_{leaf,i}$ (m²)	$LA_{leaf,i} = LL_i \times LW_i \times laf$ (laf from Chapter 5)
Leaf area of plant, LA_{plant} (m²)	$LA_{plant} = \sum_i^{i=n} LA_{leaf,i}$ (from ith to nth leaf)
Leaf area index, LAI (m² m^{-2})	$LAI_{plant} = LA_{plant}/6m^2$

Table 6-1 (cont.). Growth data measured. Non-destructive data includes phenological data collected for the individual plants on a mat, vegetative growth data measured monthly at the plot level on all plants on a mat and at harvest/destructive sampling of a plant, and bunch data measured on harvest ready plants. Destructive data includes biomass data that was determined destructively at harvest or during periodic destructive sampling.

Parameter	Description
Non-Destructive	
Bunch growth data	
Bunch maturity grade, Grade (1–5)	Bunch maturity grade as specified in (NARO, 2001)
Number of hands on bunch, N_{hand} (no.)	Counted hands on a bunch
Number of fingers on bunch, N_{finger} (no.)	Counted fingers on a bunch
Finger length, L_{finger} (cm); Finger radius, r_{finger} (cm)	Average length/radius of individual finger
Volume of a finger, V_{finger} (cm³)	$V_{finger} = \pi \times {r_{finger}}^2 \times L_{finger}$
Ratio r_{finger} to L_{finger}, $Ratio_{finger}$ (-)	$Ratio_{finger} = r_{finger}/L_{finger}$
Destructive	
Leaf dry weight, $leafD$ (kg plant^{-1}); petiole dry weight, $petioleD$ (kg plant^{-1}); pseudostem dry weight, $pseudostemD$ (kg plant-^{1})	Calculated from fresh weight and dry matter %
Aboveground vegetative dry weight, $ABGVD$ (kg plant-^{1})	Sum of $leafD$, $petioleD$ and $pseudostemD$
Corm dry weight, $cormD$ (kg plant^{-1})	Calculated from fresh weight and dry matter %
Bunch fresh weight, $bunchF$ (kg plant^{1})	Measured bunch weight of plants in the field
Bunch growth rate, B_{rate} (kg day^{-1})	$B_{rate} = bunchF/DTH$
Individual finger weight, $fingerF$ (g plant^{1})	Average weight of individual finger on second hand

Phenological events as days to flower emergence (DTF) and days to harvest (DTH) were noted for each plant on a mat. Flower initiation is not visible from the outside of a banana plant as the flower develops at ground level within the pseudostem. Days to flower initiation ($DTFI$) were calculated by assuming flower initiation occurs approximately 11-12 weeks before flower emergence (Robinson & Galan-Sauco, 2010). Phenological events were presented for C1 and C2 (Table 6-2). For C1, the $DTF, DTFI$ and DTH were determined from planting. For C2, the $DTF, DTFI$ and DTH were determined from the moment of sucker selection. Flower cycle duration (FCD) notes the duration in days between flower emergence of C1 and C2 (successive cycles) on the same mat, and harvest cycle duration (HCD) notes the duration in days between successive harvest of C1 and C2 on the same mat. Phenological events were also expressed in GDD (°C d), calculated using a base temperature of 14°C (eq. 3-1, chapter 3) (Table 6-1 and Table 6-2). The vegetative growth stage was defined as the period from planting/selecting until flower emergence as this is the period of potential vegetative growth, whilst the bunch filling stage was defined as the period from flower emergence until bunch harvest as during this period the largest part of the bunch is filled and fruit weights are determined (Mahouachi, 2007; Robinson & Galan-Sauco, 2010).

The pseudostem volume at flower emergence ($V_{pseudo,flower}$) and the LAI at flower emergence (LAI_{flower}) were interpolated for flower emergence dates through local non-parametric regression (loess) on the V_{pseudo} and LAI data collected over the growing season (Annex IV, Figure S1). Similarly, the V_{pseudo} and LAI of the follower (S for sucker) of the flowering main plant was determined ($V_{pseudo,flowerS}$ and $LAI_{flowerS}$).

Biomass component weights (pseudostem, leaf, petiole, bunch, and corm) were measured destructively during 'harvest' and 'periodic destructive sampling'.

At *'harvest'*, harvest-ready plants of C1 and C2 showing ripe bunches were cut down at the base of the pseudostem, but succeeding cycles were left on the mat. Non-destructive vegetative and bunch characteristics (Table 6-1) were determined on the harvested plant together with destructive biomass. Fresh weight of vegetative components (pseudostem, leaf, petioles) and bunch ($bunchF$) was measured using a field balance (±0.05 kg), and subsamples were taken, chopped, and dried at 80 °C for 48 h in a hot-air oven (to not destroy plant tissue) until subsample weights did not vary anymore to determine the dry matter (DM) percentage (Annex IV, Table S1). Aboveground vegetative DM ($ABGVD$) included the pseudostem, petioles, and leaves. Hereafter, when using the term 'harvest', plants that are harvest ready for their bunches were noted.

At *'periodic destructive sampling'*, entire mats were randomly sampled every three months from planting onwards to obtain a database of plants spanning different sizes and growth stages including C1, C2, and C3 plants. Mats (*n*=3) were chosen from border rows or from destructive sampling areas in each treatment in both experiments. Whole mats were excavated and for each individual cycle, growth data were measured (Table 6-1) and biomass components (corm, pseudostem, petioles, leaves, bunch) were separated and weighted. Non-differentiated suckers (not protruding above ground level) were counted as part of the corm. All cycles present on a mat (C1, C2, and C3) were used for data collection. $ABGVD$ was calculated similarly as at harvest. Corms were separated per cycle, weighted and corm DM ($cormD$) was calculated based on fresh corm weight and subsample DM percentages (Annex IV, Table S1).

6.2.3 Moisture effect on plant growth

Kruskal–Wallis non-parametric tests (α=0.05) for multiple comparison of growth parameters between irrigation treatments, cultivar, and growth cycle were applied on collected growth data at flower emergence and harvest of C1 and C2 (Table 6-2). Linear mixed effect models using treatment, cultivar and growth cycle as fixed effects and plot as random effect were also used to assess differences between treatment, cultivar, and growth cycle. Using the plot as random effect allowed to consider potential differences in irrigation between the different plots (Annex II, Figure S2). Kruskal-Wallis and linear mixed effect models generally showed similar differences. Whenever Kruskal-Wallis and linear mixed effect models differed, the linear mixed effect models were presented.

As the effect of added water (precipitation and irrigation) is very dependent on the environment in which a plant develops the ratio (R) of cumulative water added (W) and cumulative ET_0 was determined for each plant between: planting and flower emergence (R_{PF}), flower emergence and harvest (R_{FH}), and planting and harvest (R_{PH}) (Table 6-2). The estimated ratio of W to ET_0 between flower initiation and emergence (R_{FIF}) was assessed by counting 11-12 weeks backwards from the moment of flower emergence to note the flower initiation time point, and using this time point for calculating R_{FIF}.

The average pseudostem growth rate ($V_{rate,}$ Table 6-1), an indicator of vegetative growth was analyzed in terms of R_{PF}, an indicator of moisture between planting and flower emergence. Linear models were created with V_{rate} as a dependent variable and R_{PF} as the independent variable for each cultivar and cycle (Table 6-3). The average bunch growth rate (B_{rate}, Table 6-1) of plants in the field was analyzed in terms of V_{rate} (the earlier vegetative growth rate) and R_{FH}, an indicator of moisture between flower emergence and harvest (when the largest portion of bunch filling will occur). Linear models were created with B_{rate} as a dependent variable and V_{rate} and R_{FH} as the independent variable for each cultivar and cycle. Effects of the parameters were significant if coefficients in the linear models were significant (Table 6-3).

6.2.4 Allometric regression

Two types of allometric relationships were created corresponding to the different objectives: (1) models for estimating vegetative biomass ($ABGVD$ and $cormD$), and (2) models for forecasting fresh bunch weights ($bunchF$) based on data from flower emergence onward. Since allometry specifies how growth and size in plants or plant components is related to their allocated biomass, only parameters measured on a plant were put into the allometric equations.

6.2.4.1 Non-destructive vegetative biomass estimation

Plants sampled during harvest and periodic destructive sampling were used for $ABGVD$ allometry. Data spanned multiple cycles (C1, C2, and C3) with plants of different sizes. Vegetative parameters at the moment of destructive sampling (V_{pseudo}, LAI) and bunch parameters (N_{finger}, N_{hand}, V_{finger}, $Ratio_{finger}$) for plants sampled when bearing bunches were used for regression (Table 6-1 and Table 6-4).

Plants sampled during periodic destructive sampling were used for $cormD$ allometry. $CormD$ was regressed on vegetative parameters at the moment of sampling (V_{pseudo}, LAI), but given the lack of replications of bunch bearing plants at destructive sampling, other parameters were not included (Table 6-4).

6.2.4.2 Bunch fresh weight forecast

Plants with bunches ready for harvest (sampled at harvest) were used for $bunchF$ regression. Only C1 and C2 were used, as C3 was not yet ready for harvest. As early estimation is of interest, the $bunchF$ was regressed sequentially on predictors that can be grouped according to the period when first measurement is possible. Predictors were organized in three groups: Early predictors, relating to parameters at flower emergence: days to flower emergence (DTF), $V_{pseudo,flower}$, LAI_{Flower}; Middle predictors, describing bunch characteristics that do not change during fruit filling: N_{hand} and N_{finger}; and late predictors, describing bunch parameters that change up until the moment of harvest: $Ratio_{finger}$ and V_{finger} (Table 6-4). In addition to parameters measured on the main plant, the size of the sucker at flower emergence of the main plant ($V_{pseudo,flower}$) on the same mat was also used as a predictor in regressions (Table 6-4).

6.2.4.3 Regression approach

Observations used in the regression analyses for $ABGVD$, $cormD$ and $bunchF$ were subjected to a principal component analysis to identify multivariate outliers, and assess underlying correlations of the parameters (Annex IV, Figure S3). Scatterplots in the first four PCs were made, and observations where PCA scores lay outside the 95% confidence interval (95%CI) ellipse for treatment × cultivar group were removed.

First, multiple linear regression models were created for FI plants to determine the best model form for each cultivar (Table 6-4). Estimation of biomass and yield, as a rule rather than an exception, is heteroscedastic. As transforming variables leads to non-intuitive relations, heteroscedasticity was dealt with through weighted least squares regression (WLS) (Picard et al., 2012). After WLS regression, residual plots were checked to confirm whether WLS models became homoscedastic. The regression models were compared to assess the most suitable linear regression form. Criteria used in model selection were the adjusted correlation coefficient (R^2), relative root mean square error (RRMSE), and the Akaike information criterion (AIC). AIC can only be compared on models with similar number of observations. Whenever multiple predictors needed to be retained in the model, variance inflation factors (VIF) were checked as correlated predictors might lead to collinearity. Model performance was classified on RRMSE values as excellent (≤10%), good (10% < RRMSE≤ 20%), fair (20% < RRMSE≤ 30%), and poor (>30%) (Jamieson, 1991) (Chapter 4). Next to goodness-of-fit criteria, the practicality of predictors in the field was also considered in choosing the final model form.

After determining the best model forms for FI plants, pooled (combining data from cultivars and treatments) and specific regression models (separating data across cultivars and treatments) were created (Table 6-5). Specific regression models were compared between irrigation treatments and cultivars. Comparison of specific regression models were done using three methods. In the first method, the 95%CI for parameter coefficients in the regressions were compared across groups to evaluate overlap. If 95%CI overlapped, models were not different. The second method used an analysis of covariance (ANCOVA) by adding categorical variables treatment and cultivar as dummy variables in the linear regression models. It was assessed whether the parameter coefficients in the models were significantly different between the groups, or whether they could be estimated by a common coefficient (Picard et al., 2012). The third method used FI models for predicting both FI and RF data. These predicted values (x_i) were plotted against observed values (y_i), whereby the regression line was evaluated for bias. The bias% for each group (treatment x cultivar) was calculated as

$$bias\% = \left(\sum_{i=1}^{n} \frac{x_i - y_i}{x_i}\right) \times \frac{100}{n}; \quad (6\text{-}1)$$

with x_i and y_i being the observed and predicted values for the i[th] observation and n is the number of observations (Wairegi et al., 2009). If the bias% is positive, the models underestimate reality and if the bias% is negative, models overestimate reality.

6.2.5 Software and used packages

Statistical analyses were performed in R version 3.4.3 (R Core Team, 2017). Linear mixed models were fitted using REML with the function lmer from the package nlme (Pinheiro et al., 2019). Plots were made using the package ggplot2 (Wickham, 2016). Nls regressions were performed using the package nls (R Core Team, 2017).

6.3 Results

Due to a storm in the field on 2019-01-01, a large portion of the plants in the HG-C2 plots toppled leading to a significant reduction of the data. Data presented for HG-C2 is data from the remaining standing plants after the storm, or plants harvested before 2019-01-01. Thereby, care must be taken when drawing conclusions based on HG-C2 data.

6.3.1 Moisture effect on phenology, vegetative growth, and bunch parameters

6.3.1.1 Difference in moisture

The onset of soil moisture differences differed between experiments, due to differences in planting time resulting in rainfall periods affecting plants at a different growth stages (Figure 6-1a-c). In HG, moisture differences became significant during the vegetative growth stage of C1 onwards, whilst for GN, moisture differences occurred from the approximate onset of flower emergence in C1 (Figure 6-1b,c and Chapter 5).This is reflected in the ratio between water and ET_0 between planting and flower emergence (R_{PF}) (Table 6-2).

R_{PF} differed significantly between treatments in both cycles and cultivars (p<0.05). R_{PF} during HG-C1 differed between treatments but remained suboptimal for both FI (0.74 ±0.03) and RF (0.64 ±0.04), indicating stressed vegetative growth. R_{PF} during GN-C1 was optimal in both FI (1.44 ±0.02) and RF (1.26 ±0.04), indicating non stressed vegetative growth until flower emergence. At the approximate time between flower initiation and flower emergence HG-C1 received slightly suboptimal moisture in both treatments (R_{FIF}≤0.6) whilst in HG-C2 only RF received suboptimal moisture (R_{FIF}= 0.348±0.138). For GN-C1, both treatments received optimal moisture between flower initiation and emergence (R_{FIF} ≥1.1), whilst in GN-C2 the RF plants were severely stressed (R_{FIF}=0.463±0.280). After flower emergence, R_{FH} differed significantly between treatments in all cycles and cultivars (p<0.05). R_{FH} was always close or higher than 1.1 in FI, but not in RF except in HG-C1 where RF plants developed bunches during the rainy season (R_{FH}=1.47 ±0.18). Contrastingly, GN-C1 plants developed bunches during the dry season (R_{FH} = 0.33±0.02) for C1.

6.3.1.2 Effect on phenology

Under soil moisture stress a delay in banana phenology occurred, but severity of delay differed according to cultivar, cycle and the banana growth stage during which moisture stress occurred. In HG, differences in flower emergence were small (4 days or 60 GDD)(p>0.05) in C1 and C2, although

the non-significance in C2 could very well be due to a significant loss of plants. In GN, RF plants flowered slightly earlier in C1 (6 days or 45 GDD) (p>0.05) whilst in C2 FI plants flowered earlier (40 days or 428 GDD) (p<0.05).

Differences in harvest were similarly affected and delays started to occur due to RF treatments. In HG, FI plants were harvested 37 days (248 GDD) earlier in C1 (p<0.05) and 76 days (764 GDD) earlier in C2 (p<0.05). In GN, there was no difference in harvest in C1 (p>0.05), and a slight difference in C2 (34 days or 186 GDD)(p<0.05) (Table 6-2). It thereby seems RF treatments started to delay banana phenology in both calendar days and GDD.

6.3.1.3 Effect on vegetative components

Vegetative growth until flower emergence was affected significantly by irrigation (Table 6-2). FI increased parameters H, G_{base}, and thereby V_{pseudo} significantly, except for GN-C1 (p=0.24 for H, p=0.55 for G_{base}) since both FI and RF plants developed under R_{PF} >1.1 (Table 6-2). Correspondingly, FI increased vegetative biomass $ABGVD$ at harvest for both cultivars and cycles (p<0.05) (Table 6-2).

6.3.1.4 Effect on bunch components

Bunch growth was also significantly affected by irrigation and corresponding moisture stress in different banana growth stages. $BunchF$ differences under irrigation were reflected in measured bunch parameters (Table 6-2). N_{finger} and N_{hand} depend mostly on vegetative growth and moisture between flower initiation and flowering (R_{FIF}), whilst V_{finger} and $fingerF$ (finger filling) depend mostly on the vegetative growth of a plant (indicating finger filling potential) and the moisture between flower emergence and harvest (R_{FH}).

In HG, N_{hand} was increased slightly in FI in C1 (p=2.7e^{-4}), but similar in C2 (p=0.83). N_{finger} increased in both cycles, and fingers were also bigger (V_{finger}) under irrigation (p<0.05). This is related to the R_{FIF}, R_{FH} and overall R_{PH} which were bigger in FI treatments in both cycles. This resulted in significant increased $bunchF$ under irrigation in C1 and C2 (p<0.05).

In GN, N_{hand} and N_{finger} were similar in C1 between FI and RF (p>0.05) (Table 6-2), but N_{hand} and N_{finger} increased under FI in C2 (p=4.4e10^{-4}) (Table 6-2), which can be due to an optimal R_{FIF} for both treatments in C1 and a suboptimal R_{FIF} for RF C2. Large differences were obtained during bunch filling, as $FingerF$ and V_{finger} increased under FI in both cycles (p<0.05), due to differential soil moisture during bunch filling (R_{FH}=0.33 in RF C1 and R_{FH}= 0.463 in RF C2).

Table 6-2: Descriptive plant growth parameters at flowering or harvest for plant growth cycles (Cycle 1, C1 and Cycle 2, C2) and irrigation treatments (full irrigation, FI and rainfed, RF) noted as mean (±SD) of cultivars Huti Green Bell (HG) and Grande Naine (GN)

	Huti Green Bell				**Grande Naine**			
	C1		**C2**		**C1**		**C2**	
	FI	**RF**	**FI**	**RF**	**FI**	**RF**	**FI**	**RF**
				Moisture and ET_0 Ratios				
R_{PF} (-)	0.743(±0.0343)^{TC}	0.638(±0.0404)^{TC}	1.29 (±0.0408)^{TC}	0.807(±0.0791)^{TC}	1.44 (±0.0213)^{TC}	1.26 (±0.0448)^{TC}	1.33 (±0.0334)^{TC}	0.687(±0.0373)^{TC}
R_{FH} (-)	2.17 (±0.210)^{TC}	1.47 (±0.182)^{TC}	0.920 (±0.107)^{TC}	0.333 (±0.194)^{TC}	1.08 (±0.106)^{TC}	0.329 (±0.0239)^{TC}	1.54 (±0.154)^{TC}	0.950 (±0.222)^{TC}
R_{FIF} (-)	0.621(±0.100)^{T}	0.583(±0.129)^{T}	1.48(±0.373)^{TC}	0.348(±0.138)^{TC}	1.72(±0.166)^{TC}	1.31± (0.772)^{TC}	1.10(±0.291)^{TC}	0.463(±0.280)^{TC}
R_{PH} (-)	1.19 (±0.0172)^{T}	0.902(±0.0372)^{TC}	1.17 (±0.0396)^{T}	0.661(±0.0436)^{TC}	1.30 (± 0.0404)^{TC}	0.873 (±0.0323)^{TC}	1.38 (±0.0211)^{TC}	0.742(±0.0247)^{TC}
				Growth Data				
Height† (cm)	304.5 (±18.1)^{TC}	272.6 (±14.4)^{TC}	476.3 (±22.6) ^{TC}	451.4 (±22.5) ^{TC}	264.1 (±12.1) ^{C}	265.1 (±18.0) ^{C}	277.6 (±19.1) ^{TC}	234.2 (±20.3) ^{TC}
$G_{base}{}^{\dagger}$ (cm)	77.3 (±3.57) ^{TC}	66.7 (±3.46) ^{TC}	100.9 (±5.05) ^{TC}	97.0 (±6.09) ^{TC}	91.7 (±4.43) ^{C}	93.2 (±6.07) ^{C}	82.3 (±5.36) ^{TC}	72.5 (±5.06) ^{TC}
Height‡ (cm)	305.3 (±20.8) ^{TC}	272.0 (±23.3) ^{TC}	457.5 (±39.1) ^{TC}	424.2 (±32.7) ^{TC}	258.5 (±18.2) ^{C}	255.4 (±17.2) ^{C}	277.6 (±28.7) ^{TC}	236.7 (±37.3) ^{TC}
$G_{base}{}^{\ddagger}$ (cm)	68.0 (±5.42) ^{TC}	55.7 (±5.56) ^{TC}	87.0 (±11.6) ^{TC}	75.2 (±12.9) ^{TC}	82.0 (±7.25) ^{C}	78.4 (±8.21) ^{C}	82.5 (±7.42) ^{TC}	72.4 (±7.16) ^{TC}
ABGVD‡(kg plant^{-1})	3.49 (±0.374) ^{TC}	2.41 (±0.46) ^{TC}	7.49 (±1.43) ^{TC}	5.18 (±0.897) ^{TC}	4.65 (±0.884) ^{TC}	4.04 (±0.845) ^{T}	6.16 (±1.78) ^{TC}	3.73 (±1.22) ^{T}
BunchF‡ (kg plant^{-1})	25.4 (±3.87) ^{TC}	19.6 (±3.96) ^{T}	40.8 (±8.02) ^{TC}	24.4 (±0.636) ^{T}	49.6 (±7.61) ^{T}	33.2 (±9.1) ^{T}	52.4 (±15.2) ^{T}	33.3 (±9.9) ^{T}
$N_{hand}{}^{\ddagger}$ (no.)	9.69 (±0.535) ^{TC}	8.94 (±0.583) ^{TC}	11 (±1.49) ^{C}	10.8 (±2.5) ^{C}	10.8 (±1.01)	10.5 (±0.987)	11 (±1.56) ^{T}	10.2 (±1.67) ^{T}
$N_{finger}{}^{\ddagger}$ (no.)	151 (±12.0) ^{TC}	128 (±13.7) ^{TC}	195 (±50.1) ^{TC}	163 (±42.3) ^{TC}	202 (±21.5)	202 (±18.3) ^{C}	204 (±57.7) ^{T}	174 (±43.3) ^{TC}
fingerF‡ (g finger^{-1})	180 (±27.7)^{TC}	160 (±30.7)^{T}	227 (±41.3)^{TC}	139 (±50.5)^{T}	253 (±3.53)^{TC}	166 (±4.75)^{TC}	222 (±5.84)^{TC}	149 (±4.63)^{TC}
$V_{finger}{}^{\ddagger}$ (cm^3)	354 (±54.7)^{TC}	325 (±76.8)^{TC}	434 (±91.6)^{TC}	305 (±116.00)^{TC}	417 (± 48.90) ^{TC}	280 (±74.9) ^{TC}	467 (±67.3) ^{TC}	359 (±81.9) ^{TC}
$Ratio_{finger}{}^{\ddagger}$ (-)	0.073 (±0.004)^{TC}	0.078 (±0.01)^{TC}	0.068 (±0.005)^{C}	0.072 (±0.007)^{C}	0.078 (±0.015)^{T}	0.081 (±0.005)^{T}	0.078 (±0.005)^{T}	0.082 (±0.007)^{T}
				Phenology (days)				
DTF (days)	293 (±14.8)^{C}	297 (±17.8)^{C}	405 (±87.1)^{C}	406 (±57.6)^{C}	264 (±32)^{C}	258 (±31)^{C}	447 (±81)^{TC}	487 (±80)^{TC}
DTFI (days)	211(±15.0)^{C}	215(±18.0)^{C}	324(±87.1)^{C}	325(±57.6)^{C}	183 (±32)^{C}	187(±31)^{C}	366(±31)^{TC}	406(±80)^{TC}
DTH (days)	468 (±18.8)^{TC}	487 (±23.6)^{TC}	546 (±113)^{TC}	662 (±164)^{TC}	420 (±31.2)^{C}	410 (±31.8)^{C}	612 (±54)^{TC}	636 (±56)^{TC}
DFH(days)	175(±17.7)^{T}	188(±13.7)^{T}	153(±96.7)^{T}	180(±34.6)^{T}	152(±16.3)	151(±28.2)	169(±35.4)	155(±28.7)
				Phenology (GDD)				
GDDF (°Cd)	3162(±202)	3222(±235)	4350(±983)	4355(±670)	2811(±317)	2766(±292)	4561(±799)^{T}	4989(±645)^{T}
GDDFI (°Cd)	2094(±196)	2160(±237)	3599(±878)	3552(±508)	2174(±262)	2125(±249)	3777(±928)^{T}	4232(853)^{T}
GDDH (°Cd)	4698(±182)^{T}	4948(±384)^{T}	5516(±1043)^{T}	6280(±1794)^{T}	4555(±413)	4344(±333)	6081(±720)^{T}	6267(±874)^{T}
GDDFH (°Cd)	1587(±157)	1677(±142)	1530(±188)	1491(±133)	1703(±194)	1630(326)	1569(327)	1442(239)

$ABGVD$, aboveground vegetative dry matter includes pseudostem, petiole and leaf dry matter. $BunchF$, fresh bunch weight; N_{hand}, number of hands on a bunch; N_{finger}, number of fingers on a bunch. Phenology data: DTF, days to flower emergence; DTH, days to harvest; Moisture (precipitation and irrigation) and ET_0 ratios: between planting and flower emergence (R_{PF}), flower emergence and harvest (R_{FH}), flower initiation and flower emergence (R_{FIF}), planting and harvest (R_{PH}); Cycle duration: FCD, flower cycle duration, the time (in days) between flower emergence of C1 and flower emergence of C2 (on matlevel), HCD is the duration (in days) between harvest of C1 and harvest of C2 (on matlevel). Treatments: full irrigation (FI), rainfed (RF). Cultivars: Huti Green Bell (HG), Grande Naine (GN). †flowering, ‡harvest. T: notes difference between treatment FI and RF (within a cycle and cultivar) (p= 0.05), C: notes difference between cycles (within a moisture treatment and cultivar) (p = 0.05).

Table 6-2 (cont.): Descriptive plant growth parameters at flowering or harvest for plant growth cycles (Cycle 1, C1 and Cycle 2, C2) and irrigation treatments (full irrigation, FI and rainfed, RF) noted as mean (±SD) of cultivars Huti Green Bell (HG) and Grande Naine (GN)

	Huti Green Bell				**Grande Naine**			
	C1		**C2**		**C1**		**C2**	
	FI	**RF**	**FI**	**RF**	**FI**	**RF**	**FI**	**RF**
	Growth Rates							
V_{rate} (L day^{-1})	0.203(±0.0331)^{TC}	0.156(±0.0251)^{TC}	0.398(±0.0874) ^{TC}	0.297(±0.0698) ^{TC}	0.308(±0.0418) ^{TC}	0.320(±0.0520) ^{TC}	0.183(±0.0491) ^{TC}	0.111(±0.0307) ^{TC}
B_{rate} (kg day^{-1})	0.144(±0.0271)^{T}	0.103(±0.0201)^{T}	0.266 (±0.0856)^{TC}	0.167 (±0.141)	0.333 (±0.0419) ^{TC}	0.193(±0.0460) ^{TC}	0.315(±0.0462)^{TC}	0.205 (±0.0369) ^{TC}
	Huti Green Bell				*Grande Naine*			
	Cycle Duration (C1 to C2)							
	HG-FI		HG-RF		GN-FI		GN-RF	
FCD_D(C2 –C1) (days)	243 (±82.8)^{C}		237 (±55.2)^{C}		307 (±69)^{TC}		360 (±78)^{TC}	
FCD_{GDD} (C2-C1)(°C d)	2029(±603)		2120(610)		3354(±643)^{TC}		3960(±727)^{TC}	
HCD_D (C2-C1) (days)	222 (126)^{TC}		282 (53.7)^{TC}		315 (±43.1)^{TC}		332 (±59.0)^{TC}	
HCD_{GDD} (C2-C1) (°C d)	2494(±1167)		2250(±1450)		3241(±508)^{TC}		3703(±610)^{TC}	

$ABGVD$, aboveground vegetative dry matter includes pseudostem, petiole and leaf dry matter. $BunchF$, fresh bunch weight; N_{hand}, number of hands on a bunch; N_{finger}, number of fingers on a bunch. Phenology data: DTF, days to flower emergence; DTH, days to harvest Moisture (precipitation and irrigation) and ET_0 ratios: between planting and flower emergence (R_{PF}), flower emergence and harvest (R_{FH}), flower initiation and flower emergence (R_{FIF}), planting and harvest (R_{PH}); Cycle duration: FCD, flower cycle duration, the time (in days) between flower emergence of C1 and flower emergence of C2 (on matlevel), HCD is the duration (in days) between harvest of C1 and harvest of C2 (on matlevel). Treatments: full irrigation (FI), rainfed (RF). Cultivars: Huti Green Bell (HG), Grande Naine (GN). †flowering, ‡harvest. T: notes difference between treatment FI and RF (within a cycle and cultivar) (p= 0.05), C: notes difference between cycles (within a moisture treatment and cultivar) (p = 0.05).

6.3.1.5 Effect on growth rates

Combining phenology and growth parameters shows growth speeds (V_{rate} and B_{rate}) of plants differed significantly between the treatments (Figure 6-2 and Table 6-3). Moisture (R_{PF}) had a significant effect on growth rates of the pseudostem (V_{rate}), except in GN-C1 as these plants all developed under optimal conditions (R_{PF}>1.1). In all other groups, R_{PF} had a significant (p<0.05) positive effect on V_{rate} in HG and GN. Both V_{rate} and moisture after flower emergence (R_{FH}) had a significant effect on bunch growth rates (B_{rate}) (Figure 6-2 and Table 6-3).

Generally, an increase in V_{rate} led to an increase in B_{rate}, except for HG-C2. V_{rate} on its own does not fully explain B_{rate} as coefficients for R_{FH} were significant in several models (Table 6-2). This is shown clearly in GN–C1, as V_{rate} in FI plants was smaller, but B_{rate} was significantly larger (p<0.05) (Table 6-2 and Figure 6-2). Inclusion of R_{FH} proves necessary for correctly assessing B_{rate}(Table 6-3).

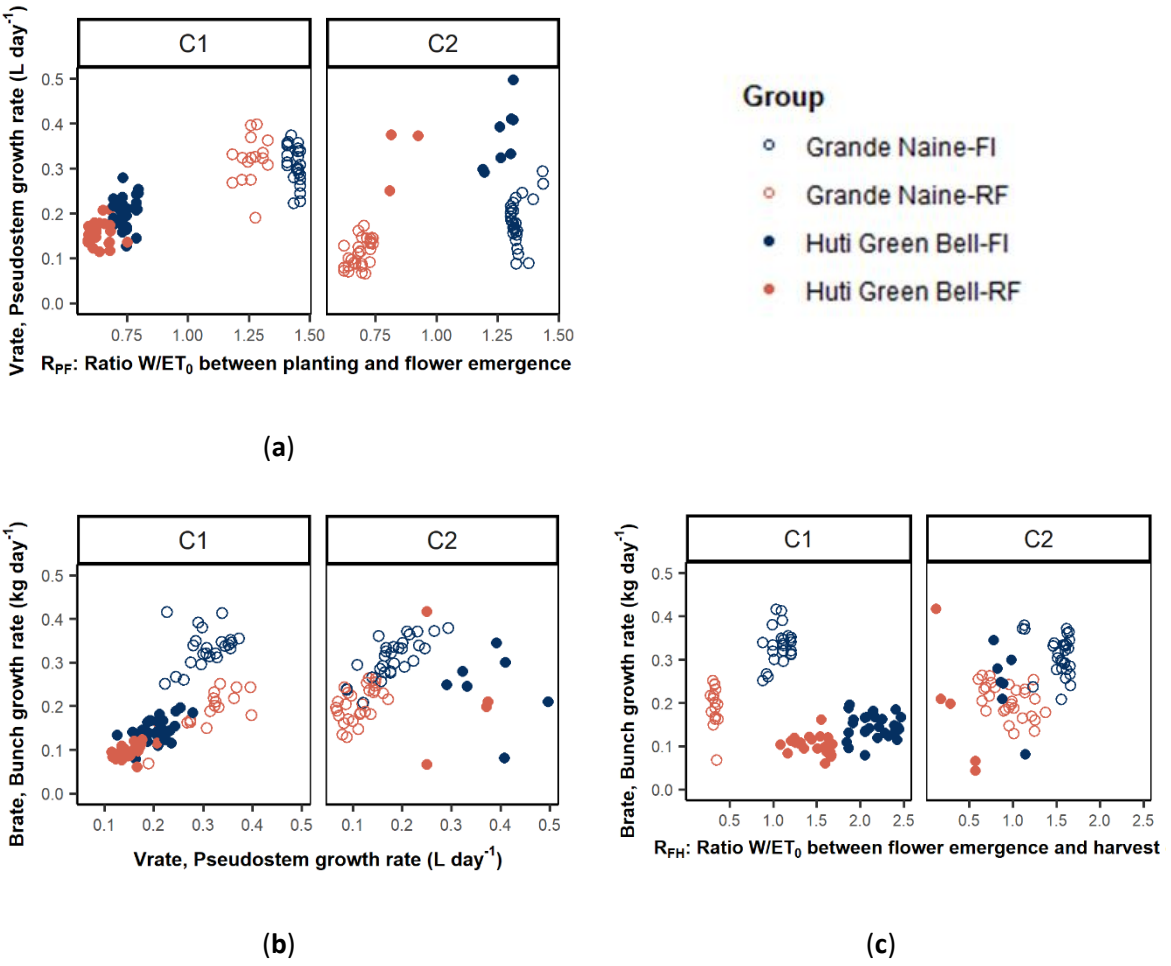


Figure 6-2: Effect of moisture and ET_0 on growth rates. (a) V_{rate}, pseudostem growth rate (L day^{-1}) vs. R_{PF}, Ratio of cumulative water added (W) and cumulative ET_0 between planting and flowering; (b) B_{rate}, bunch growth rate (kg day^{-1}) vs. V_{rate} (L day^{-1}) specifying the effect of earlier vegetative growth on bunch rates; and (c) B_{rate} vs. R_{FH}, Ratio of cumulative water added (W) and cumulative ET_0between flowering and harvest. Dots note observations for individual plants. Lines note regression lines for each cultivar-cycle group. C1 and C2 note C1 and C2, respectively. FI notes full irrigation, RF notes rainfed

Table 6-3: Linear regression model output for average pseudostem growth rate until flowering (V_{rate}, L day^{-1}), and average bunch growth rate between flower emergence and harvest (B_{rate}, kg day^{-1}) in terms of added moisture and reference evapotranspiration. Models are characterized by parameter x, intercept 'a' and slope 'b' and 'c' as y = a+b*x+c*y. V_{rate} and B_{rate} models note models with y being V_{rate} and B_{rate} respectively. P indicates pooled model; S indicates specific model. Both indicates pooling of data across cultivars and/or cycles. FI notes full irrigation and RF notes Rainfed. R_{PF} and R_{FH} note ratio of cumulative added moisture (rainfall and precipitation) to cumulative ET_0 between planting and flowering, and flowering and harvest, respectively.

				Model Coefficients								Goodness-of-fit Characteristics				
	V_{rate} **Models**															
Data	**Cultivar**	**Cycle**	**Parameters**	**Intercept (a)**	**95%CI**	**Coefficient (b)**	**95%CI**	**Coefficient (c)**	**95%CI**	**n**	**df**	**R^2**	**AIC**	**RMSE**	**RRMSE(%)**	***p*-Value**
P	Huti Green	Both	R_{PF}	−0.06	(−0.11; −0.01)	0.36	(0.28; 0.43)			66	2	0.59	−238.86	0.041	20	3.09×10^{-14}
S		C1	R_{PF}	ns		0.26	(0.25; 0.27)			54	1	0.97	−220.75	0.031	17	2.57×10^{-43}
S		C2	R_{PF}	ns		0.30	(0.27; 0.34)			12	1	0.97	−27.72	0.065	19	1.41×10^{-9}
P	Grande Naine	Both	R_{PF}	−0.04	(−0.07; −0.01)	0.22	(0.19; 0.25)			99	2	0.65	−273.66	0.067	31	4.88×10^{-24}
S		C1	R_{PF}	0.41	(0.19; 0.64)	ns				40	2	−0.00	−129.28	0.045	14	3.65×10^{-1}
S		C2	R_{PF}	0.03	(0; 0.06)	0.11	(0.08; 0.14)			59	2	0.49	−219.96	0.038	26	4.45×10^{-10}
	B_{rate} **Models**															
	Cultivar	**Cycle**	**Parameters**	**Intercept (a)**	**95%CI**	**Coefficient (b)**	**95%CI**	**Coefficient (c)**	**95%CI**	**n**	**df**	**R^2**	**AIC**	**RMSE**	**RRMSE(%)**	***p*-Value**
P	Huti Green	Both	V_{rate}, R_{FH}	ns		0.73	(0.70; 0.77)	ns		65	1	0.96	−233.43	0.053	38	4.34×10^{-48}
S		C1	V_{rate}, R_{FH}	ns		0.53	(0.37; 0.69)	0.01	(0; 0.03]	54	2	0.97	−264.12	0.020	16	2.91×10^{-42}
S		C2	V_{rate}, R_{FH}	ns		0.58	(0.39; 0.77)	ns		11	1	0.80	−13.63	0.120	60	4.91×10^{-05}
P	Grande Naine	Both	V_{rate}, R_{FH}	ns		0.56	(0.50; 0.65)	0.14	(0.12; 0.15)	99	2	0.98	−340.63	0.043	17	2.32×10^{-85}
S		C1	V_{rate}, R_{FH}	ns		0.42	(0.34; 0.50)	0.19	(0.16; 0.22)	40	2	0.98	−139.73	0.004	14	3.92×10^{-33}
S		C2	V_{rate}, R_{FH}	0.05	(0.02; 0.09)	0.91	(0.76; 1.06)	0.06	(0.03; 0.08)	59	3	0.78	−232.16	0.323	13	9.58×10^{-20}

6.3.2 Aboveground vegetative dry matter estimation

V_{pseudo} was linearly related to $ABGVD$ in both HG and GN (Figure 6-3), and to all its components ($leafD$, $petioleD$, and $pseudostemD$) (Annex IV, Figure S2). PCA also revealed the factor loadings to be similar for the variables $ABGVD$ and V_{pseudo} (and other vegetative components e.g. LAI, $Height$, $Girth$) indicating correlations (Annex IV, Figure S3). VIFs higher than 5 (indicating collinearity) were not found in our models (Table 6-4).

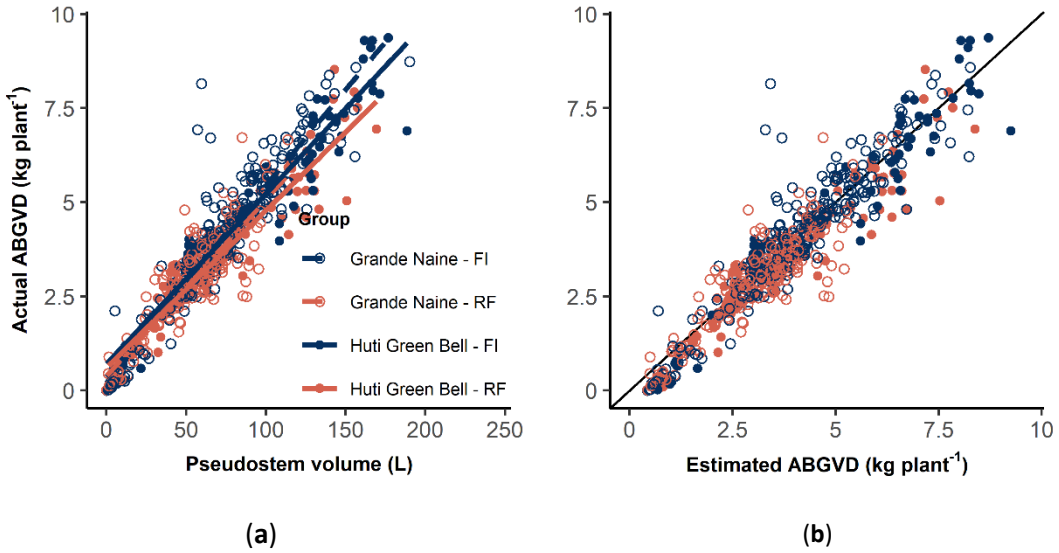


Figure 6-3: Aboveground vegetative dry matter (ABGVD, kg plant^{-1}) models. (a) actual ABGVD vs. pseudostem volume (V_{pseudo}) at sampling (L) for Huti Green Bell (HG) and Grande Naine (GN). Regression models were specific models for treatment and cultivar as shown in Table 6-5; (b) Comparison of actual ABGVD (kg plant^{-1}) with estimated ABGVD (kg plant^{-1}) as obtained using the specific regression models for treatment and cultivar as shown in Table 5. FI notes full irrigation, RF notes rainfed.

Models using only V_{pseudo} as a predictor already had a good model fit in HG and GN (RRMSE= 14%) (Table 6-4). Lm.1 was the best model in terms of goodness-of-fit, and practicality, and was used for creating pooled and specific regression models (Table 6-5).

Table 6-4: Allometric regression models for fully irrigated plants of Huti Green Bell and Grande Naine, with goodness-of-fit characteristics. Models are multiple linear regression models with each parameter 'x' characterized by intercept 'a' and slope 'b': y = a+b*x. ABGVD notes the aboveground vegetative dry biomass (leaves, petioles, and pseudostem), $cormD$ notes the corm dry biomass, and $bunchF$ notes the fresh bunch weight. Additional parameters are explained in Table 6-1 and given underneath the table.

		Huti Green Bell						Grande Naine					
							$\boldsymbol{ABGVD}$						
Model	**Parameters**	**n**	**df**	**R²**	**AIC**	**RRMSE(%)**	***p*-Value**	**n**	**df**	**R²**	**AIC**	**RRMSE(%)**	***p*-Value**
Lm.1[x]	V_{pseudo}	91	2	0.92	221.22	14	5.62×10^{-52}	221	2	0.88	480.4	14	7.30×10^{-102}
Lm.2	LAI	88	2	0.79	297.89	22	5.16×10^{-31}	214	2	0.92	573.2	19	1.20×10^{-116}
Lm.3	V_{pseudo}, LAI	88	3	0.93	192.41	13	1.70×10^{-51}	213	3	0.93	379.0	11	1.30×10^{-124}
Lm.4	N_{finger}, N_{hand}	62	3	0.68	209.93	22	1.32×10^{-15}	138	3	0.19	475.5	27	3.13×10^{-07}
Lm.5	$V_{pseudo}, N_{finger}, N_{hand}$	62	3	0.99	111.47	12	1.16×10^{-60}	138	3	0.99	308.1	14	4.81×10^{-124}
Lm.6	$V_{finger}, Ratio_{finger}$	58	3	0.29	236.14	31	2.81×10^{-05}	144	3	0.07	521.2	29	3.22×10^{-3}
Lm.7	$V_{pseudo}, Ratio_{finger}, N_{finger}, N_{hand}$	56	4	0.90	116.74	12	3.59×10^{-27}	137	4	0.90	116.7	17	3.59×10^{-27}
							$\boldsymbol{CormD}$						
Model	**Parameters**	**n**	**df**	**R²**	**AIC**	**RRMSE**	***p* Value**	**n**	**df**	**R²**	**AIC**	**RRMSE**	***p*-Value**
Lm.1[x]	V_{pseudo}	21	2	0.94	72.73	24	1.80×10^{-13}	36	2	0.54	210.38	33	2.19×10^{-07}
Lm.2	LAI	14	2	0.71	83.14	75	9.95×10^{-05}	35	2	0.36	214.67	39	7.35×10^{-05}
Lm.3	V_{pseudo}, LAI	14	3	0.97	59.62	22	2.20×10^{-09}	34	3	0.53	199.99	34	2.87×10^{-06}
							$\boldsymbol{BunchF}$						
Model	**Parameters**	**n**	**df**	**R²**	**AIC**	**RRMSE**	***p*-Value**	**n**	**df**	**R²**	**AIC**	**RRMSE**	***p*-Value**
Lm.1[x]	$V_{pseudo,flower}$	40	2	0.70	228.08	12	1.42×10^{-11}	54	2	0.43	372.01	15	4.50×10^{-08}
Lm.2	LAI_{flower}	41	2	0.62	258.56	17	6.17×10^{-10}	54	2	0.22	383.2	17	1.96×10^{-04}
Lm.3	DTF	41	2	0.32	268.02	22	7.71×10^{-05}	55	2	−0.01	406.85	20	4.83×10^{-01}
Lm.4	$V_{pseudo,flower}, DTF$	40	3	0.69	229.76	12	1.20×10^{-10}	54	3	0.42	373.99	15	3.48×10^{-07}
Lm.5	$V_{pseudo,flower}, DTF, LAI_{flower}$	38	4	0.60	220.54	13	1.93×10^{-07}	54	4	0.57	360.48	13	5.90×10^{-10}
Lm.6	$V_{pseudo,flowerS}$	38	2	−0.01	257.52	25	4.97×10^{-01}	52	2	−0.02	381.38	20	6.66×10^{-01}
Lm.7	$V_{pseudo,flower}, V_{pseudo,flowerS}$	38	3	0.63	218.83	14	1.24×10^{-08}	52	3	0.48	361.57	14	4.22×10^{-08}
Lm.8	$V_{pseudo,flower}, DTF, N_{finger}, N_{hand}$	35	5	0.64	204.24	12	3.31×10^{-07}	37	5	0.65	248.92	13	8.38×10^{-08}
Lm.9	$V_{pseudo,flower}, V_{finger}$	36	3	0.80	191.12	11	1.05×10^{-12}	40	3	0.56	277.63	14	8.44×10^{-08}
Lm.10	$V_{pseudo,flower}, V_{finger}, Ratio_{finger}$	36	4	0.80	192.48	11	6.59×10^{-12}	40	4	0.60	276.25	14	7.81×10^{-08}
Lm.11	$V_{pseudo,flower}, DTF, N_{finger}, N_{hand}, V_{finger}$	34	6	0.81	183.17	10	3.92×10^{-10}	37	6	0.78	234.28	10	1.88×10^{-10}

DTF: days to flowering, LAI: leaf area index at sampling, LAI_{flower}: leaf area index at flower emergence, N_{finger}: number of fingers per hand, N_{hand}: number of hands per bunch, $Ratio_{finger}$: ratio between finger radius to finger length, V_{pseudo}: pseudostem volume at sampling, $V_{pseudo,flower}$: pseudostem volume at flower emergence, $V_{pseudo,flowerS}$: pseudostem volume of sucker at flower emergence. Vegetative predictors: $V_{pseudo,flower}$, LAI_{flower}; Predictors measured on bunch after emergence: N_{finger}, N_{hand}; Predictors measured at bunch maturity: V_{finger}, $Ratio_{finger}$; Predictors measured on sucker at flowering of main plant: $V_{pseudo,flowerS}$. [x]Selected model.

Table 6-5: Allometric linear regression model comparison. $ABGVD$ notes aboveground vegetative dry biomass, $cormD$ notes corm dry biomass and $bunchF$ notes bunch fresh biomass. Models are characterized by parameter x, intercept 'a' and slope 'b' as y = a+b*x. P indicates pooled model, S indicates specific model. Both indicates pooling of data across cultivars and/or treatments. FI notes full irrigation and RF notes Rainfed. V_{pseudo} notes pseudostem volume, V_{pseudo},flowering, notes V_{pseudo} at flowering.

				Model coefficients							Goodness-of-fit Characteristics				Chosen Model
	***ABGVD* models**														
Data	**Cultivar**	**Treatment**	**Parameters**	**Intercept (a)**	**95%CI**	**Coefficient (b)**	**95%CI**	**n**	**df**	**R^2**	**AIC**	**RMSE**	**RRMSE(%)**	***p*-Value**	
P	Both	Both	V_{pseudo}	0.33	(0.24; 0.43)	6.02×10^{-02}	(0.06; 0.06)	700	2	0.90	1571.50	0.78	18	1.18×10^{-203}	x
P	Huti Green	Both	V_{pseudo}	0.54	(0.38; 0.71)	5.56×10^{-02}	(0.05; 0.06)	187	2	0.92	407.46	0.77	16	1.80×10^{-105}	
S		FI	V_{pseudo}	0.75	(0.47; 1.04)	5.54×10^{-02}	(0.05; 0.06)	89	2	0.93	205.82	0.77	14	1.32×10^{-53}	
S		RF	V_{pseudo}	0.43	(0.25; 0.6)	5.51×10^{-02}	(0.05; 0.06)	98	2	0.92	193.43	0.72	17	1.54×10^{-53}	
P	Grande Naine	Both	V_{pseudo}	0.22	(0.11; 0.34)	6.27×10^{-02}	(0.06; 0.06)	513	2	0.89	1149.31	0.76	18	1.17×10^{-245}	
S		FI	V_{pseudo}	0.26	(0.06; 0.47)	6.34×10^{-02}	(0.06; 0.07)	266	2	0.89	656.39	0.82	17	2.28×10^{-126}	
S		RF	V_{pseudo}	0.32	(0.18; 0.45)	5.91×10^{-02}	(0.06; 0.06)	247	2	0.88	468.21	0.66	19	7.13×10^{-113}	
	***CormD* models**														
Data	**Cultivar**	**Treatment**	**Parameters**	**Intercept (a)**	**95%CI**	**Coefficient (b)**	**95%CI**	**n**	**df**	**R^2**	**AIC**	**RMSE**	**RRMSE(%)**	***p*-Value**	
P	Both	Both	V_{pseudo}	0.39	(0.29; 0.49)	1.74×10^{-02}	(0.02; 0.02)	180	2	0.64	271.47	0.52	40	2.46×10^{-41}	
P	Huti Green	Both	V_{pseudo}	0.16	(0.1; 0.23)	1.94×10^{-02}	(0.02; 0.02)	45	2	0.89	6.50	0.32	26	7.89×10^{-23}	x
S		FI	V_{pseudo}	0.13	(0.05; 0.22)	2.24×10^{-02}	(0.02; 0.03)	23	2	0.92	−2.59	0.26	24	4.00×10^{-13}	
S		RF	V_{pseudo}	0.26	(0.18; 0.34)	1.67×10^{-02}	(0.01; 0.02)	22	2	0.90	9.25	0.31	21	1.44×10^{-11}	
P	Grande Naine	Both	V_{pseudo}	0.51	(0.37; 0.65)	1.57×10^{-02}	(0.01; 0.02)	135	2	0.50	224.77	0.55	43	6.00×10^{-22}	x
S		FI	V_{pseudo}	0.62	(0.37; 0.86)	1.62×10^{-02}	(0.01; 0.02)	69	2	0.57	140.02	0.64	41	4.62×10^{-14}	
S		RF	V_{pseudo}	0.56	(0.39; 0.72)	1.08×10^{-02}	(0.01; 0.01)	66	2	0.34	61.48	0.37	38	1.53×10^{-07}	
	***BunchF* models**														
Data	**Cultivar**	**Treatment**	**Parameters**	**Intercept (a)**	**95%CI**	**Coefficient (b)**	**95%CI**	**n**	**df**	**R^2**	**AIC**	**RMSE**	**RRMSE(%)**	***p*-Value**	
P	Both	Both	$V_{pseudo,flower}$	−0.42	(−4.84; 4)	5.21×10^{-01}	(0.45; 0.6)	167	2	0.53	1235.75	13.27	35	7.27×10^{-29}	
P	Huti Green	Both	$V_{pseudo,flower}$	11.69	(9.17; 14.22)	1.99×10^{-01}	(0.16; 0.24)	68	2	0.57	389.73	4.34	17	5.30×10^{-14}	
S		FI	$V_{pseudo,flower}$	15.20	(11.88; 18.52)	1.73×10^{-01}	(0.13; 0.22)	38	2	0.60	217.29	4.06	13	7.55×10^{-09}	x
S		RF	$V_{pseudo,flower}$	13.29	(10.36; 16.23)	1.30×10^{-01}	(0.08; 0.18)	30	2	0.47	158.86	3.09	15	1.92×10^{-05}	x
P	Grande Naine	Both	$V_{pseudo,flower}$	−0.17	(−6.97; 6.62)	5.91×10^{-01}	(0.49; 0.69)	99	2	0.56	726.68	9.79	23	2.02×10^{-19}	
S		FI	$V_{pseudo,flower}$	−7.28	(−17.3; 2.74)	7.37×10^{-01}	(0.6; 0.87)	54	2	0.69	363.80	6.89	14	3.54×10^{-15}	x
S		RF	$V_{pseudo,flower}$	20.12	(10.39; 29.85)	5.21×10^{-01}	(0.04; 0.34)	45	2	0.11	315.94	7.57	23	7.27×10^{-29}	x

Specific FI and RF models for $ABGVD$ showed overlapping 95%CI model coefficients for intercept and slope in both HG and GN (Table 6-5), but coefficients were slightly different between treatments using the ANCOVA method. For HG, the intercept was reduced in the RF model by 0.32 (p=8.25e^{-14}), and the slope was very slightly reduced by 3×10^{-4} (p=0.014). For GN, there was no effect on the intercept (p=0.13) and the slope was reduced by 4.3 × 10^{-3} (p =4.46e^{-3}) in RF (Figure 6-3 and Table 6-5).

Comparing predictions of the FI models with RF models, led to bias% of −92.1% (HG) and −81.9% (GN) for FI plants and bias% of −44.6% (HG) and −41.4% (GN) for RF plants. Both FI and RF plants were overestimated. Small plants (<25L) were overestimated in small absolute terms (<1 kg DM plant^{-1}), but as bias% calculates the relative deviation, these had a large effect on the overall bias%. Recalculating bias% after removal of the smaller plant (<25L) led to bias% of 2.07% (HG) and −1.48% (GN) in FI, and bias% of −7.26% (HG) and −10.1% (GN) in RF. Plants <25L were overestimated in both FI and RF (in small absolute terms), but plants >25L were only overestimated in RF.

Comparison of cultivar FI models showed 95%CI model coefficients overlapped for intercept and slope (Table 6-5) but models were distinctly different in intercept (p=0.01) and slope (p=8.89e^{-4}) following ANCOVA.

As 95%CI for coefficients overlapped between treatments and cultivars, the differences although significant, may be small in practice. Pooling data from both cultivars and treatments (n=700) and performing the regression on this pooled data led to a good model fit (R^2=0.90, RRMSE= 18%), using V_{pseudo} as predictor (Table 6-5). Combining goodness-of-fit and practicality a single $ABGVD$ model is considered the best.

The model for estimating ABGVD in HG and GN becomes:

$$ABGVD = 0.33 + 6.02 \times 10^{-2} \times V_{pseudo}; \text{ HG and GN combined} \qquad (6\text{-}2)$$

with $ABGVD$, aboveground vegetative DM (kg DM plant^{-1}) and V_{pseudo}, pseudostem volume (L).

6.3.3 Corm dry matter estimation

V_{pseudo} was linearly related to $cormD$ in both HG and GN (Figure 6-4). PCA also revealed the factor loadings to be similar for the variables $cormD$ and V_{pseudo} indicating correlations (Annex IV, Figure S3). VIFs higher than 5 were not found in the $cormD$ models.

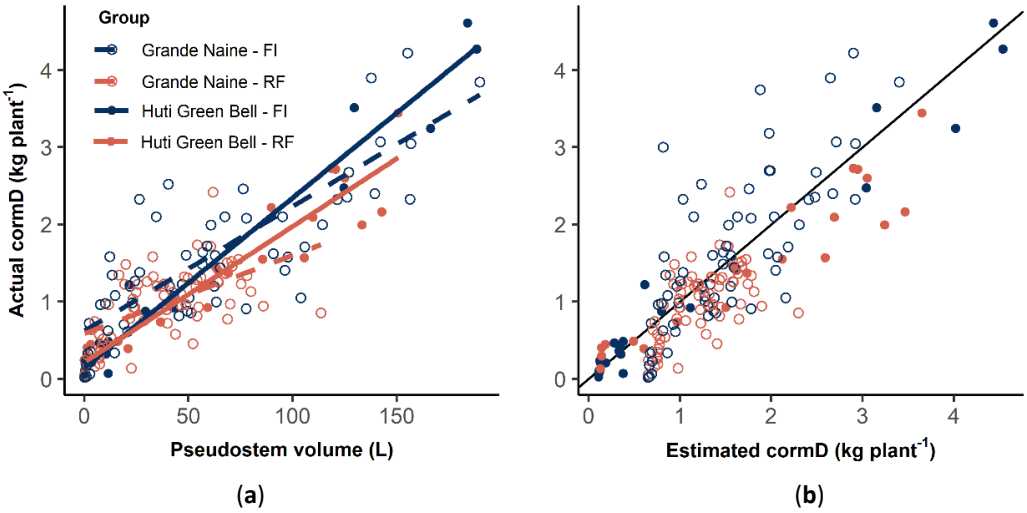


Figure 6-4: Corm dry matter ($cormD$, kg plant−1) models. (a). Actual $cormD$ vs. pseudostem volume (V_{pseudo}) at destructive sampling (L) for Huti Green Bell (HG) and Grande Naine (GN). Regression models were specific models for treatment and cultivar as shown in Table 6-5; (b) Comparison of actual $cormD$ vs. estimated $cormD$ as obtained using the specific regression models for treatment and cultivar as shown in Table 6-5. FI notes full irrigation, RF notes rainfed.

Models with only V_{pseudo} and LAI as predictors for $cormD$ led to a fair model performance for HG (RRMSE = 22%) but moderately poor model performance for GN (RRMSE= 34%) (Table 6-4). Lm.1 was the best model in terms of goodness-of-fit and used for creating pooled and specific regression models (Table 6-5).

Specific FI and RF models revealed 95%CI of coefficients overlapped for both HG and GN (Table 6-4), but coefficients were different between treatments in both HG and GN using the ANCOVA method. For HG, RF reduced the slope by 5.7×10^{-3} (p=5.18e^{-3} and had no effect on the intercept (p = 0.09) (Figure 6-4, Table 6-5). For GN, RF reduced the intercept by 0.06 (p=2.22e^{-5}) and the slope by 5.4×10^{-3} (p=7.59e^{-4}) (Figure 6-3). Due to overlap of 95%CI, and very small coefficient differences using ANCOVA, actual differences between models were not so pronounced, indicating a single treatment model could be used for the cultivars. However, all models for $cormD$ (Table 6-4 and Table 6-5) were suboptimal given the fair to poor RRMSE values, and the large variation around the 1/1 line (Figure 6-4). Therefore, specific model differences may not be correct, and care should be taken.

Using the specific FI regression models led to a bias% of −54.5% (HG) and −156% (GN) for FI plants, and bias% of −13.2% (HG) and −73.2% (GN) for RF plants. Models overestimated the $cormD$ in both treatments and cultivars. Overestimation occurred again through the influence of smaller plants. Recounting bias% after removal of smaller plants led to a bias% of −3.78% (HG) and −11.0% (GN) for FI compared to −23.6% (HG) and −39.2% (GN) for RF. Thereby, the RF plants were overestimated more strongly compared to the FI plants. In general, models overestimated small plants (<25L), whereas bigger plants show no overestimation in HG FI, show a slight overestimation in GN FI plants, and show a large overestimation in RF plants of both cultivars.

Cultivar FI models were also different as 95%CI coefficients did not overlap, and following ANCOVA, HG model intercepts were reduced (p=1.77e^{-4}) and slopes increased (p=0.05) compared to GN. The best models for estimating $cormD$ for HG and GN thus became:

$$cormD = 0.16 + 1.94 \times 10^{-2} \times V_{pseudo};\ HG \quad (6\text{-}3)$$

$$cormD = 0.51 + 1.57 \times 10^{-2} \times V_{pseudo};\ GN \quad (6\text{-}4)$$

with $cormD$, corm DM (kg DM plant^{-1}), and $V_{pseudo,}$ the pseudostem volume (L).

6.3.4 Bunch weight forecast

$ABGVD$ was significantly positively correlated to $bunchF$ (p<0.05) with R² of 0.73 (FI) and 0.65 (RF) for HG, and R² of 0.61 (FI) and 0.54 (RF) for GN (as also shown by the similar factor loadings in the first two PC in Annex IV, Figure S3). Similarly, $V_{pseudo,flower}$ was linearly related to $bunchF$ at harvest (Figure 6-5). VIFs higher than 5 were not identified in the bunch models.

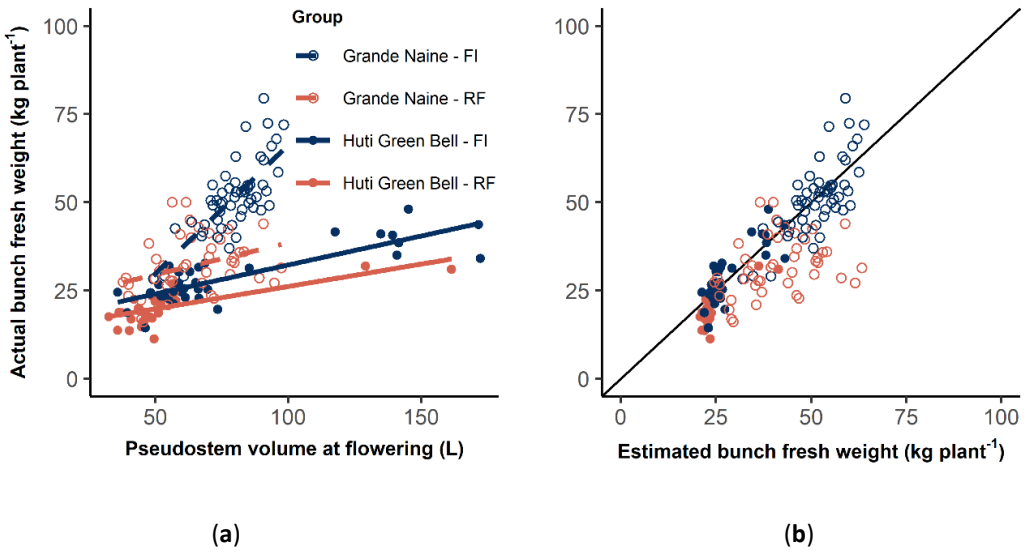


Figure 6-5: Bunch fresh weight ($bunchF$, kg plant^{-1}) models. (a) Actual $bunchF$ vs. pseudostem volume at flowering ($V_{pseudo,\ Flower}$, L) for Huti Green Bell (HG) and Grande Naine (GN). Regression models were specific models for treatment and cultivar as shown in Table 6-4; (b) Comparison of actual $bunchF$ (kg plant^{-1}) with estimated $bunchF$ (kg plant^{-1}) as obtained using the specific regression models for treatment and cultivar as shown in Table 6-4. FI notes full irrigation, RF notes rainfed.

Models containing only early bunch data (lm.1 to lm.7) had RRMSE values ranging from 12-25% (HG) and 13-20% (GN) indicating good model fit (Table 6-4). Inclusion of data on sucker size ($V_{pseudo,flowerS}$) did not improve the RRMSE of the models (lm.6 to lm.7) compared to models with only $V_{pseudo,flower}$ (lm.1). Inclusion of data collected at later stages (lm.8 to lm.11) improved model fits as RRMSE values reduced and R² increased. To allow for earliest bunch estimation, model containing $V_{pseudo,flower}$ (lm.1) were retained for both HG (R²=0.70, RRMSE= 12%) and GN (R²=0.43, RRMSE= 15%).

Pooled and specific regression models proved different between treatments in both HG and GN (p<0.01) (Table 6-5). Model coefficients did not show overlap in the 95%CI. For HG, RF led to a

significantly lower intercept (ANCOVA, p=7.18e^{-12}), whilst slopes remained similar (ANCOVA, p=0.38). For GN, the intercept and slope were both different between treatments (p<0.05) leading to widely different relationships with $V_{pseudo,flower}$ (Figure 6-5, Table 6-5).

Using the specific FI regression models to estimate $bunchF$ for both FI and RF plants, led to a significant overestimation of RF bunches in both HG and GN (Figure 6-5). The bias% for FI plants was −2.31% (HG) and −1.74% (GN) and the bias% of the RF plants was −28.0% (HG) and −24.1% (GN). Therefore, using FI models significantly overestimated the RF plants.

The specific models were also different between the cultivars (p<0.01, Figure 6-5 and Table 6-5). Models for optimal bunch weights (FI conditions) became:

$$bunchF = 15.20 + 1.73 \times 10^{-1} \times V_{pseudo,flower};\ HG\text{-FI} \quad (6\text{-}5)$$

$$bunchF = -7.28 + 7.37 \times 10^{-1} \times V_{pseudo,flower};\ GN\text{-FI} \quad (6\text{-}6)$$

with $bunchF$ being fresh bunch weight (kg plant^{-1}), and $V_{pseudo,flower}$ being the pseudostem volume (L) at flowering.

Since $bunchF$ models were significantly different between the treatments and R_{FH} proved significant in the development of the bunch (B_{rate}, Table 6-3), linear models were created using both $V_{pseudo,flower}$ and R_{FH} as independent variables (Table 6-6).

A similar pattern appeared as observed in Table 6-3. An increase in $V_{pseudo,flower}$ led to an increase in $BunchF$, except for HG-C2. $V_{pseudo,flower}$ on its own does not fully explain $BunchF$ as coefficients for R_{FH} were significant in several models (**Table 6-6**). This is shown clearly in GN–C1, as $V_{pseudo,flower}$ in FI plants was similar, but $BunchF$ was significantly larger (p<0.05), due to differing moisture regimes during bunch filling (R_{FH}, Table 6-2).

Overall, models for HG and GN seem to perform well when cycles were pooled (RRMSE 16% for HG, RRMSE 19% for GN). As such, models for estimating $bunchF$ based on $V_{pseudo,flower}$ and R_{FH} became:

$$bunchF = 5.9 + 2.2 \times 10^{-1} \times V_{pseudo,flower} + 2.75 \times R_{FH};\ HG \quad (6\text{-}7)$$

$$bunchF = -11.21 + 5.7 \times 10^{-1} \times V_{pseudo,flower} + 11.89 \times R_{FH};\ GN \quad (6\text{-}8)$$

with $bunchF$ being fresh bunch weight (kg plant^{-1}), and $V_{pseudo,flower}$ being the pseudostem volume (L) at flowering and R_{FH} being the ratio of moisture received to ET_0 between flower emergence and harvest.

Table 6-6: Linear regression model output for bunch fresh mass ($bunchF$ in kg) in terms of pseudostem volume at flower emergence ($V_{pseudo,flower}\ in\ L$) and ratio of cumulative added moisture (rainfall and precipitation) to cumulative ET_0 between flower emergence and harvest (R_{FH}). Models are characterized by parameter x, intercept 'a' and slope 'b' and 'c' as y = a+b*x+c*y. P indicates pooled model, S indicates specific model. Both indicates pooling of data across cycles.

				Model Coefficients												
	$\boldsymbol{BunchF}$ **Model**															
Data	**Cultivar**	**Cycle**	**Parameters**	**Intercept (a)**	**95%CI**	**Coefficient (b)**	**95%CI**	**Coefficient (c)**	**95%CI**	**n**	**df**	**R^2**	**AIC**	**RMSE**	**RRMSE (%)**	***p*-Value**
P	Huti Green	Both	$V_{pseudo,flower}, R_{FH}$	5.90	(0.87; 10.92)	0.22	(0.17; 0.26)	2.75	(0.67; 4.84)	66	3	0.64	376	4.15	16	$4.87x10^{-15}$
S		C1	$V_{pseudo,flower}, R_{FH}$	6.06	(0.76; 11.34)	0.31	(0.21; 0.41)	ns		54	2	0.43	299	3.66	16	$4.60x10^{-8}$
S		C2	$V_{pseudo,flower}, R_{FH}$	29.79	(27.12; 32.46)	ns		10.81	(5.18; 6.46)	12	2	0.61	68	5.29	16	$1.6x10^{-3}$
P	Grande Naine	Both	$V_{pseudo,flower}, R_{FH}$	-11.21	(-19.98; -2.43)	0.57	(0.46; 0.68)	11.89	(7.88; 5.90)	99	3	0.61	709	8.39	19	$1.6x10^{-20}$
S		C1	$V_{pseudo,flower}, R_{FH}$	ns		0.31	(0.25; 0.37)	22.56	(17.69; 7.42)	40	2	0.98	253	5.48	13	$8.29x10^{-37}$
S		C2	$V_{pseudo,flower}, R_{FH}$	ns		0.63	(0.60; 0.66)	ns		59	1	0.97	414	8.08	19	$2.55x10^{-44}$

6.4 Discussion

6.4.1 Moisture effect on phenology, vegetative growth, and bunch parameters

Irrigation resulted in significant soil moisture differences (Figure 6-1b) affecting phenology, vegetative, and bunch characteristics (Table 6-2). Drought in banana induces stomatal closure, reducing transpiration and photosynthesis which reduces leaf area, leaf emission rate, and vegetative growth in general (Kallarackal et al., 1990; Thomas and Turner, 1998; Carr, 2009; Taiz and Zeiger, 2010) Drought during the vegetative stage and flower initiation may reduce N_{hand} per bunch and N_{finger} per hand (Robinson & Alberts, 1986) whereas drought after flower emergence results in suboptimal fruit filling (Mahouachi, 2007; Twyford & Walmsley, 1973). For optimal banana production, average R_{PF} for the vegetative growth stage (until flower emergence) should remain approx. above 0.6-0.8, whilst average R_{FH} during bunch filling should remain above 1.1-1.2 (Allen et al., 1998; Carr, 2009).

HG plants experienced different moisture regimes during C1 vegetative growth and thereby differed between FI and RF in both vegetative and bunch parameters (Table 6-2). HG experienced large R_{FH} (>1.5) in C1 which could have led to water excess, but no waterlogging was observed based on TDR measurements (Figure 6-1b). GN plants in contrast developed under optimal conditions (R_{PF} and R_{FIF} >0.6-1.1) until flower emergence of C1, thereby FI and RF plants of C1 did not differ in V_{pseudo}, N_{hand}, and N_{finger} (Table 6-2). Differences in R_{FH} from C1 flower emergence onward led to differences in $ABGVD$, $fingerF$, V_{finger}, $Ratio_{finger}$, and $bunchF$ at harvest of C1 and C2 (Table 6-2).

Phenology started to be delayed slightly under drought. Differences in flower emergence (DTF and $GDDF$) remained small and only became significant in GN-C2 (Table 6-2). In GN-C1, R_{PF} and R_{FIF} in both treatments was bigger than 1.1, so RF plants developed under optimal moisture until flower emergence of C1. After flower emergence of C1, drought stress was frequently encountered which could have resulted in a delayed flowering in C2. Differences in harvest (DTH and $GDDH$) also became pronounced. In HG, plants were harvested earlier in FI treatments in both cycles. For GN, average harvest also started to be delayed in C2 in RF plants in contrast to FI plants, but differences remained small (Table 6-2). After flower emergence of C1, R_{PF}, R_{FH} and R_{PH} of GN-RF plants was significantly lower than 1.1, which could have resulted in a harvest delay under stress which became significant in C2 (Table 6-2).

Environmental stress due to suboptimal soil moisture has been shown to delay floral development and increase bunch filling duration in banana plants in both days and GDD (Carr, 2009; Fortescue et al., 2011; Lamour et al., 2020; Robinson & Galan-Sauco, 2010; Taulya et al., 2014; Turner et al., 2007). Fortescue et al. (2011) showed the effect of stress on phenology can be very pronounced in banana as moisture and/or photoperiod stresses could delay GDD to flower emergence by 1,000-2,000 °Cd. Our GDD ranges until flower emergence fit within observed GDD ranges for flower emergence in literature. Fortescue et al. (2011) found GDD to vary between 3,000-4,200 °Cd between different planting dates and environments. Taulya (2013) showed GDD to flower emergence to vary between 3,000-4,500 °Cd (in Kawanda, Uganda) and 2,000-3,800 °Cd (in Ntungamo, Uganda) for the EAHB Kisansa. Lassoudière (1979) and Turner (1987) found GDD to flower emergence to vary between 2,500-3,500 °Cd depending on date of planting. Our observed GDD to flower emergence in C2 seems large compared to literature values, which might be due to the nature of the selected sucker. Suckers were chosen at a similar side around the mother plant, and suckers of a similar height were selected to keep the plantation lines intact in the following cycles. This could entail that not always the most

vigorous and well-connected sucker was chosen to constitute the following cycle and resulting in longer development. Choosing the most vigorous sucker could speed up phenology in the following cycle leading to a reduction in days and GDD to harvest.

Combining absolute growth and phenology, showed effects of moisture on V_{rate} and B_{rate} (Table 6-3, Figure 6-2). V_{rate} was influenced by R_{PF} (p<0.05, Table 6-3), although effects differ due to the size of R_{PF}. If R_{PF}>0.8-1.1, moisture covers the evaporative demand as shown in GN-C1. Here, R_{PF} did not influence V_{rate} as it was optimal for both RF and FI (Table 6-3). Only when R_{PF}<0.8, as in GN-C2, V_{rate} seemed to be negatively affected (Figure 6-2 and Table 6-3). In order to achieve fast vegetative growth rates, average R_{PF} should thus preferably remain above 0.8. The effect of V_{rate} on B_{rate} was also significant as a faster V_{rate} resulted in an increased B_{rate} (Figure 6-2b and Table 6-3). Moisture after flower emergence (R_{FH}) also influenced B_{rate} significantly. Within cycles and cultivars, we see that an increased R_{FH} has a bigger B_{rate} for GN and HG (except HG-C2). R_{FH} needs to be bigger or close to 1.1-1.2 to ensure optimal bunch filling (Figure 6-2c, Table 6-2 and Table 6-3).

Moisture deficit thereby has a double effect on bunch growth. Firstly, moisture deficits during the vegetative stage reduces the vegetative growth of the plant. The earlier vegetative growth determines the leaf area (which determines the photosynthetic assimilates that can be produced) and is an indication of previously stored nutrients which can be translocated to fill the bunch (Eckstein et al., 1995; Eckstein & Robinson, 1995; Mukasa et al., 2005; Nyombi et al., 2009; Robinson & Galan-Sauco, 2010; Swennen & De Langhe, 1985; Twyford & Walmsley, 1973). Less vegetative biomass thereby indicates less photosynthetic and translocation potential. Secondly, moisture deficits during the bunch filling stage affect photosynthesis (closing of the stomata) resulting in less DM production such that increasingly bunches are filled more due to translocation which on its own can be suboptimal (Carr, 2009; Robinson & Galan-Sauco, 2010; Turner et al., 2007; Twyford & Walmsley, 1973). Both the vegetative stage and the bunch filling stage are thus important in the eventual outcome of the bunch weight. In order to achieve optimal growth for the pseudostem and the bunch, added moisture amounts could be compared to evaporative demands of the atmosphere. This gives an indication of moisture requirements of the banana plant, yet does not provide an indication of water stored in the soil which (depending on the soil) can be significant.

6.4.2 ABGVD estimation from non-destructive observations

V_{pseudo} was significantly linearly correlated to the $ABGVD$ (Figure 6-3), and a good predictor for $ABGVD$ in both HG and GN (RRMSE 14%) (Table 6-4). Height, girth, and diameters (components for volume estimation) are often used in biomass regression (Picard et al., 2012). In trees, height and diameter at breast height are significantly correlated to biomass of a stand (Henry et al., 2011; Kebede & Soromessa, 2018; Picard et al., 2012). Negash et al. (2013) found girth at base to be the best predictor for aboveground biomass estimation (R^2=0.77–0.98) in Enset. Nyombi et al. (2009) found girth at base to be the best predictor in development-stage specific regressions (R^2=0.79–0.99), but height to be the best predictor of $ABGVD$ when pooling the data across development stages (R^2=0.98). Combining height and girth leads to a parameter describing the pseudostem (volume) in three dimensions, without leading to high co-linearity when keeping both parameters in the model (Picard et al., 2012). V_{pseudo} is linked to all components of aboveground biomass (pseudostem, leaves, and petioles) in our field (Annex IV, Figure S2). The pseudostem is composed of tightly compacted leaf sheaths, which result from previous cumulative leaf formation (Turner et al., 2007). V_{pseudo} was therefore also correlated to the petiole and leaf mass in our field. However, the number of leaves and

petioles at a given time are also affected by management practices (e.g., pruning) and stress conditions, indicating correlations can differ in other plantations.

Even though V_{pseudo} was affected by soil moisture deficit, the relationship between V_{pseudo} and $ABGVD$ was not influenced strongly. Specific regression models for ABGVD between treatment and cultivar differed according to ANCOVA (p<0.05) (Table 6-5), reducing the slope and/or intercept in RF treatments compared to FI treatments. This indicates plants with similar V_{pseudo} may reach lower $ABGVD$ in RF than FI plants. However differences were small as 95%CI for model coefficients overlapped. Pooling cultivar and treatment data led to a good model fit (R^2=0.90 and RRMSE= 18%, Table 6-5) indicating a single $ABGVD$ model based on V_{pseudo} can be used in our fields (Equation 6-2). We conclude that allometry on $ABGVD$ under drought was thus not significant.

Perhaps stress was not marked enough for pronounced $ABGVD$ plasticity under drought as average bunches in RF plots ranged from 19.6-24.4 kg plant^{-1} in HG, and from 33.2-33.3 kg plant^{-1} for GN, which are considered good yields. Nyombi et al. (2009) had irrigated yields for EAHB cv. Mbwazirume ranging from 20-40 kg plant^{-1}, whilst Wairegi et al. (2009) showed yields for different rainfed EAHB cultivars from on farm visits ranging from 2–60 kg plant^{-1}. Our yields are therefore higher compared to their lower range; hence less stress was present. Increasing drought stress over the full course of the growing season might lead to a more pronounced allometric difference in $ABGVD$ estimation based on V_{pseudo}. Thereby, our obtained relationships are expected to remain valid under non-stressed to moderate stressed plants, but to assess the usefulness of our $ABGVD$ model under increased stress (both in terms of duration as other potential stresses) additional research needs to be carried out.

Models did overestimate small plants (<25L). This overestimation might be a characteristic of the model, as the intercept was not forced through zero during modelling as this may lead to poorer goodness-of-fit characteristics (Eisenhauer, 2003). At V_{pseudo} zero, there is an overestimation of 0.54 kg DM plant^{-1} (HG) and 0.22 kg DM plant^{-1} (GN), which are small absolute DM values, but with a large influence on the total bias%. Removing smaller plants reduced bias%. Overestimation of small plants could also be due to the growing behavior of suckers. Small suckers have scale and lanceolate leaves but produce foliage leaves at approx. 1.5 m height (Lassoudière, 2007; Swennen & De Langhe, 1985). Shading results in improved partitioning to aboveground structures (Rodrigo et al., 1997) and leads to an increase in pseudostem growth to faster reach sunlight. Therefore, small plants might have a lower pseudostem density (kg DM volume^{-1}), leading to an overestimation when presuming their density to be similar to bigger plants. Another possibility is that all smaller plants are in the vegetative stage. Nyombi et al. (2009) found that vegetative aboveground biomass models differ according to plant growth stage (vegetative, flowering, or harvest). Plants in the vegetative stage had a lower ABGVD compared to plants at flowering and harvest with similar girths and heights. Pooling the data across these plant growth stages might have led to this overestimation caused by small plants, but the overestimation is small in absolute terms (<1 kg DM plant^{-1}), still warranting the use of a general regression model as this is more practical. The general regression model to use for $ABGVD$ estimation to be used is given in Equation 6-2.

6.4.3 $CormD$ estimation from non-destructive observations

V_{pseudo} was linearly correlated to the belowground $cormD$ (Figure 6-4). $CormD$ models based on V_{pseudo} ranged from fair in HG (RRMSE=24%) to moderately poor in GN (RRMSE= 33%) (Table 6-4),

making V_{pseudo} less suitable for $cormD$ estimation. Nyombi et al. (2009) found good exponential relationships between pseudostem girth at base and $cormD$ (R^2=0.59–0.98) but $cormD$ in their field ranged between 0–0.40 kg plant^{-1}, which seems low compared to our $cormD$ values ranging from 0.09–4.27 kg plant^{-1}. Negash et al. (2013) found good correlations between belowground biomass (corm and adventitious roots) and diameter at base for Enset (R^2=0.75) but found no such correlation with height (R^2=0.23–0.27). Creating power models with radius at base instead of V_{pseudo} did not improve model fits for cormD in both HG (RRMSE= 38%) and GN (RRMSE= 41%) (data not shown).

Using aboveground characteristics to describe a belowground structure has shortcomings. Parameters relating to corm dimensions (e.g., corm height and girth) are expected to considerably improve the $cormD$ estimation, but in order to estimate these the corm needs to be excavated. Corm dimensions also vary in diameter and height with plant growth phase (vegetative, flower development, bunch filling, harvest) and whether the plant is in the first or second cycle (Eckstein & Robinson, 1995; Robinson & Galan-Sauco, 2010; Twyford & Walmsley, 1973). The corm is a storage organ whose reserves can be used for fruit growth and sucker development, whereby bunch development stage, size, stresses encountered and the amount of produced suckers also play a role in corm biomass (Robinson & Galan-Sauco, 2010; Twyford & Walmsley, 1973). In our field, the variation of $cormD$ with V_{pseudo} increased with cycle, thereby partitioning models in terms of cycle or plant growth phase (vegetative, flowering, harvest) might significantly improve the model. Nyombi et al. (2009) found growth stage specific allometric relationships for $cormD$, whereby R^2 reduced from the vegetative (0.98) to the harvest phase (0.57), signifying increased variation with increasing growth stage.

The comparison of specific models across treatments revealed irrigation to slightly increase intercept and slope in FI treatments (ANCOVA, p<0.05). At a given V_{pseudo} the $cormD$ seems slightly larger in FI than in RF plants indicating the onset of allometric plasticity under drought. As 95%CI intervals overlapped between specific treatment models, differences were not very pronounced (Table 6-5). Pooled treatment data per cultivar also did not reduce RRMSE much, leading to the conclusion that $cormD$ models were similar among RF and FI in our fields. This can be due to the fact that plants were irrigated during establishment (and during prolonged dry field conditions to limit plant death in the field). Plants experiencing a higher degree of stress might experience a more pronounced allometric plasticity than observed in our field. Allocation to underground structures (roots) has shown to increase relative to aboveground structures under increasing nutrient and water stress (Poorter & Nagel, 2000). Taulya (2013) studied DM allocation plasticity between above (pseudostem and leaves) and belowground (corm) biomass in banana fields in response to drought stress, K and N deficiencies. Drought during the vegetative growth (cumulative rainfall < 1,100 mm year^{-1}) and N deficiency had no effect on DM allocation to the corm. Allometric plasticity only became apparent under K deficiency, where more DM was sent to the corm relative to aboveground structures. Under K deficient conditions allometric plasticity was the opposite than observed in our field: more DM was sent to the corm. Allometric plasticity under more severe drought stress or under different stress than drought alone (nutrients, salt, pests, diseases) might thus be different and more pronounced than observed in our study. However, stress during bunch formation could result in more DM translocated from the corm to fill the bunch leading to lower $cormD$ than under non-stressed conditions (Twyford & Walmsley, 1973). This would result in opposite plasticity than what Taulya (2013) observed due to stress during vegetative development. This has to be considered when extrapolating our relationships to other environments. Furthermore, the biomass of the underground corm structure is too variable to be accurately predicted based on aboveground vegetative characteristics alone.

Future research should incorporate corm based parameters in their predictions (e.g. corm height and girth) and/or include a large number of plants in different phenological stages (vegetative stage, flower emergence stage, bunch filling stage and harvest stage) to assess a phenology effect on $cormD$ estimations.

6.4.4 Bunch yield forecast

Vegetative growth (V_{rate}) was linked to bunch growth in our field (B_{rate}) (Figure 6-2 and Table 6-3). Others have also shown pseudostem size significantly correlates with bunch weights: R^2=0.63–0.85 (Mukasa et al., 2005), R^2=0.66 (Wairegi et al., 2009), R^2=0.57–0.7 (Nyombi et al., 2009), R^2=0.97- 0.98 (Yamaguchi & Araki, 2004). The pseudostem size relates to bunch filling potential as it is linked with the previously formed leaf area supplying photosynthetic DM to the bunch (Dens, Romero, et al., 2008; Eckstein et al., 1995; Twyford & Walmsley, 1973) and with previously stored assimilates that can be translocated to the bunch during the bunch filling stage (Mukasa et al., 2005; Nyombi et al., 2009; Robinson & Galan-Sauco, 2010; Stover & Simmonds, 1987; Twyford & Walmsley, 1973) even across ratoon plants (Dens, Romero, et al., 2008). High yields are also linked to vigorous early plant growth in plantain (Swennen & De Langhe, 1985).

As such, stepwise regression revealed $V_{pseudo,flower}$ to be the most important predictor of $bunchF$ compared to other regression models (R^2=0.7 for HG and 0.43 for GN; RRMSE= 12% for HG and 0.15 for GN) (Table 6-4). Inclusion of bunch related predictors (N_{finger}, N_{hand}, V_{finger}) improved model fits as R^2 increased (0.81 for HG and 0.78 for GN) and RRMSE decreased (10% for both HG and GN lm.11) (Table 6-4). The more parameters were included closer to bunch harvest, the better the prediction. Practically, using $V_{pseudo,flower}$ as a predictor for $bunchF$ already led to good model performance in both HG and GN FI models (RRMSE=13–14%).

Bunch models based on $V_{pseudo,flower}$ were very different between FI and RF, as 95%CI did not overlap and following ANCOVA(p<0.05)(Table 6-5). FI models performed better (RRMSE= 13% for HG, 14% for GN) than RF models (RRMSE=15% for HG, 23% for GN).

These different relationships between $bunchF$ and $V_{pseudo,flower}$ under drought follow differences in bunch characteristics under RF vs. FI conditions (Table 6-2). Drought during the vegetative stage and near flower initiation may reduce N_{hand} and N_{finger} whereas drought during bunch filling results in suboptimal fruit filling (V_{finger}) (Carr, 2009; Mahouachi, 2007; Robinson & Galan-Sauco, 2010; Twyford & Walmsley, 1973). Moisture regimes after flower emergence are thereby crucial in determining actual bunch weights in the field, but these are not reflected in $V_{pseudo,flower}$. Up until flower emergence, GN plants of C1 developed optimally in both treatments (R_{PF}>1.1, Table 6-2 and Chapter 5). Height and girth (V_{pseudo}), N_{finger} and N_{hand} did not differ at flower emergence (p>0.05), whilst $bunchF$, $fingerF$, and V_{finger} did differ between FI and RF at harvest (p<0.05) (Table 6-2). Weight and size of the fingers determined the bunch weights. Plants of similar $V_{pseudo,flower}$ subjected to different environments (R_{FH}) after flower emergence (e.g., GN C1) will thereby have different $bunchF$ at harvest, changing relationships between these parameters. This was observed further in the regression models taking into account R_{FH} as an independent variable. R_{FH} was significant in the cycles where R_{FH} for RF plants was <1.1, whilst R_{FH} was not significant when both RF and FI plants developed under optimal conditions (R_{FH} >1.1). An increase in R_{FH} from suboptimal to optimal conditions thereby increases $bunchF$ significantly.

For accurate bunch weight estimation, bunch characteristics need to be included (Soares et al., 2014; Wairegi et al., 2009). Our models improved when bunch parameters were included (RRMSE became lower), but this no longer allows the forecasting of bunch weights as bunch characteristics (e.g., V_{finger}) change until harvest. We propose our FI models to be used to forecast bunch weights based on $V_{pseudo,flower}$ if plants developed without drought stress from flower emergence onwards. Forecasting of $bunchF$ based on $V_{pseudo,flower}$ allows to estimate bunch 'potential' weights as in Equations 6-4 and 6-5. To estimate 'actual' bunch weights, the environmental effects during bunch filling need to be incorporated either directly (e.g., as R_{FH}) or indirectly (incorporating bunch characteristics as e.g. V_{finger}). Using bunch characteristics that keep changing until the moment of bunch harvest (e.g. V_{finger}) is no longer forecasting, so estimating bunch weights ahead of time is better done using an expected R_{FH}. To assess the overall usefulness of our equations incorporating R_{FH} (Equations 6-6 and 6-7), and the degree to which they can be extrapolated to other environments, future research should preferably include a wider range of R_{FH} and a larger number of plants spanning multiple cycles. Our equations provide an indicative effect of R_{FH}, but additional validation still needs to occur.

The large phenotypical differences between HG and GN plants, also led to significantly different bunch weight regression curves for cultivars (p<0.05). However, as cultivars were planted at a different time, differences in planting might confound differences in cultivars and we should not compare these cultivars with each other. Nyombi et al. (2009) found different allometric relationships for bunch weight for two EAHB cv Mbwazirume and Kisansa. Wairegi et al. (2009) proposed the use of a general banana regression curve for estimation of EAHB bunch yields, but their results showed cultivar specific curves were characterized by lower overall variances and increased model fits. Their cultivar specific curves were similar but were significantly different in model parameters. Our results support the statement that even genetically close cultivars have different phenotypical characteristics (Perrier et al., 2019; Ploetz et al., 2007).

6.5 Conclusion

Irrigation and corresponding soil moisture differences had a significant effect in both HG and GN, reducing vegetative and bunch growth, and starting to delay phenology under RF conditions depending on the onset of moisture stress. Of the affected parameters, V_{pseudo} seems a promising indicator for allometry as it is linked to both vegetative growth and bunch growth rates. The universal nature of V_{pseudo} as a regression parameter between the two cultivars is more valuable for future allometric studies than girth or height alone.

Allometric relationships for vegetative biomass ($ABGVD$ and $cormD$) were not strongly affected by irrigation as 95% CI overlapped between FI and RF models indicating a single allometric model can be used across RF and FI plants for vegetative biomass estimation. However, increasing moisture stress severity and subjecting plants to other types of stress (nutrient, pests, and diseases) might still lead to pronounced allometric plasticity between RF and FI models. Models did also not differ much between our phenotypically very different cultivars for $ABGVD$, hinting V_{pseudo} models can be used across a range of cultivars. V_{pseudo} did not prove sufficient to estimate $cormD$ reliably, as a lot of variation remained in the underground biomass. Aboveground characteristics are therefore lacking to estimate belowground structures. For better estimation of belowground vegetative biomass, components relating to the corm dimensions can be added although these are more difficult to measure. This research shows the potential for non-destructive vegetative biomass monitoring at the field scale. As

biomass over time often underlies crop simulation models, this is especially useful for researchers wanting to calculate biomass in the field for calibrating such models without destroying plants.

Bunch weight ($bunchF$) forecasting models based on V_{pseudo} at flower emergence were significantly different between FI and RF, showing bunch weights cannot be estimated on vegetative parameters only, without including information on stress during bunch filling or bunch components. Both vegetative growth (V_{rate}) and moisture during bunch filling (R_{FH}) determine bunch growth rates. Our FI models allow prediction of bunch weights under optimal conditions after flower emergence (R_{FH}≥1.1) and can be used to forecast bunch weight potentials based on V_{pseudo} at flower emergence. Dropping below R_{FH} of 1.1 reduced the intercept and slope of created models significantly and leads to lower $bunchF$ at similar V_{pseudo}.

7 Parameterization and evaluation of the AquaCrop model for two crop cycles of a Grande Naine banana (Musa spp.) cultivar under irrigated and rainfed conditions

Bert Stevens[a,*], Jan Diels[b], Dirk Raes[b], Allan Brown[c], Stanley Bayo[c], Patrick Alois Ndakidemi[d], Eline Vanuytrecht[b,e] and Rony Swennen[a,c,f]

[a]KU Leuven, Department of Biosystems, Willem De Croylaan 42 - box 2455, 3001 Heverlee, Belgium

[b]KU Leuven, Division of Soil and Water Management Celestijnenlaan 200e - box 2411, 3001 Leuven, Belgium

[c]International Institution of Tropical Agriculture, IITA, PO Box 447, Arusha, Tanzania

[d]Nelson Mandela African Institution of Science and Technology, NMAIST, P.O.BOX 447, Arusha, Tanzania

[e]Flemish Institute for Technological Research (VITO), Environmental Modelling Unit, Boeretang 200, 2400 Mol, Belgium

[f]Bioversity International, Willem De Croylaan 42, 3001 Heverlee, Belgium

*Lead author

This chapter is based on its article currently under review:

Stevens, B., Diels, J., Raes, D., Brown, A. Bayo, S., Ndakidemi, P.A., Vanuytrecht, E., Swennen R. Parameterization and evaluation of the AquaCrop model for two crop cycles of a Grande Naine banana (Musa spp.) cultivar under irrigated and rainfed conditions. *Agricultural Water Management*. (under review).

7.1 Introduction

Agriculture in the 21st century faces a triple challenge: (1) outputs need to double to reach demands of a growing and richer population, (2) under increasingly changing variable climatic conditions, whilst (3) reducing agricultural inputs and polluting outputs. Current agriculture covers 38% of global land area, uses 70% of all global freshwater and emits 30-35% of global greenhouse gasses. Previous improvements in agriculture focused on increasing inputs, which was often detrimental to the environment. Future production needs to be enhanced in an environmentally sustainable manner using less resources (Foley et al., 2011).

Water is the most limiting factor to banana (*Musa* spp.) production (Carr, 2009). Water needs range from 1,100 to 2,650 mm evenly distributed throughout the year depending on the prevailing climate (Robinson & Alberts, 1986; Van Asten et al., 2011; Varma & Bebber, 2019). Where rainfall is not sufficient, irrigation is necessary to sustain production (German Calberto et al., 2015; Robinson & Galan-Sauco, 2010; Van Den Bergh et al., 2012). Future water consumption in the banana sector will increase, due to increasing production demands (FAO, 2018a), rising temperatures resulting in 15–

20% increase in water use (German Calberto et al., 2015) and shifting of production areas to drier regions due to climate change and as a strategy to reduce fungal infections (Ploetz et al., 2015; Robinson & Galan-Sauco, 2010). About 99 % of all fresh water use in export banana cultivation is already used for irrigation (FAO, 2017), often based on farmer's intuition rather than allocating water when plants are in need (Boesveld et al., 2011). Proper irrigation scheduling and management will have a very big impact on banana production and water footprints (FAO, 2017).

Crop simulation models can aid farmers with the assessment of irrigation practices. These models provide a low-cost support to field trials to evaluate the impact of a wide range of management options under different climatic scenarios on crop yields and water footprints. Models have a multitude of applications and can, amongst others, be used to: (1) study a crop's response to environmental changes, (2) compare actual and optimal yields for specific locations (determine yield gap in rainfed systems), (3) determine seasonal water requirement and irrigation schedules for different crops and locations and (4) compare the effect of management options (mulching, soil water harvesting, type of irrigation infrastructure) on production and water use (Steduto et al., 2012; Vanuytrecht, Raes, Steduto, et al., 2014).

Most models often require many input variables, making them more useful for researchers than for practical decision support. To handle this discrepancy, the FAO developed the AquaCrop model that balances simplicity, accuracy and robustness to enhance adoption by end users (Steduto et al., 2008, 2012). AquaCrop simulates crop development in terms of canopy cover, biomass and yield in relation to the environment, soil moisture, soil fertility and other agronomic management practices (Steduto et al., 2008; Vanuytrecht, Raes, Steduto, et al., 2014). The model is underlain by actual crop physiological processes, and only uses a small number of easily understandable input parameters that can be adjusted to crop and environment as needed, often intuitively (Raes et al., 2009). In contrast to other crop simulation models, using a radiation or light use efficiency methodology to simulate production (e.g., STICS, SIMBA, LINTUL), AquaCrop is a water driven growth model relying on the tight link between transpiration and biomass production (Steduto et al., 2007a, 2012). AquaCrop has been successfully used on over 15 annual crops including wheat, rice, soybean, barley, cotton, sugar beet, sunflower, potato, tomato, alfalfa, Bambara groundnut, quinoa (C3 crops) and maize, sorghum, sugarcane, teff (C4 crops) (Hsiao et al., 2009; Steduto et al., 2012; Steduto et al., 2009; Vanuytrecht, Raes, Steduto, et al., 2014). At this moment, perennial crops are lacking (Steduto et al., 2012). For an overview of model performance for multiple crops, the reader is referred to Steduto et al. (2011). AquaCrop comparison with more elaborate input models like CropSyst and WOFOST (for sunflower and barley) shows its value because it requires less inputs but still shows similar prediction accuracy of biomass and yield under deficit and rainfed irrigation conditions (Abi Saab et al., 2015; Todorovic et al., 2009a).

The FAO AquaCrop project aims to calibrate the model for each important crop species (Raes et al., 2009; Steduto et al., 2008). Banana, by its global production, remains the highest-ranking crop for which no widely applicable crop model exists to simulate both production and soil moisture. Previous banana modelling efforts were not based on physiological crop processes (Dens, Swennen, et al., 2008; Mekwatanakarn & Turner, 1989; Woomer et al., 1998) or all used a light use efficiency growth model (Brisson & Dorel, 1998; Nyombi, 2010; Taulya, 2015; Tixier et al., 2008). These light use efficiency models are cumbersome and require extensive knowledge on input parameters and crop modelling, making these models difficult to use for practical decision support (Bouman et al., 1996; Tixier et al., 2008; Van Ittersum et al., 2003).

Given banana's worldwide importance and the success of AquaCrop as a management tool to improve water productivity in annual crops, this research aims at calibrating the AquaCrop growth model for the first and second cycle of banana plantations. In contrast to the 16 crops presently in the AquaCrop database which are all annual crops, banana is a perennial crop that exists of multiple cycles growing on the same mat (Turner et al., 2007). We calibrated it for the Cavendish cultivar as it constitutes 47% of global production (FAO, 2018a).

7.2 Material and methods

7.2.1 Field experiments

Experiments (Annex II with details on the field trial experimental design) were conducted at the research farm of the Nelson Mandela African Institution of Science and Technology (NM-AIST) and the International Institute of Tropical Agriculture (IITA) in Arusha, Tanzania (3° 23′ 58″ S, 36° 47′ 48″ E). A detailed description of the experimental design is given in Chapter 5 and 6, and shown in Annex II, Figure S2.

Grande Naine (GN, *Musa* AAA Cavendish subgroup) in vitro plants were hardened in growth chambers and screenhouses and transplanted in the field on 2017-11-13. Plant spacing was 2×3 m leading to 1,666 plants ha^{-1}, each mat having a ground area of 6 m^2.

The design was a blocked design with drip irrigation as treatment. Four blocks were planted, each block containing five rows of 14 mats, subdivided in two plots of 35 mats (7×5), receiving two different irrigation treatments. The central nine mats (3×3) in each plot were used for monthly growth data collection, leading to four replications (plots) per treatment (Annex II, Figure S2). All mats received drip irrigation in the first four months post-transplant (establishment period). Thereafter, two irrigation treatments were applied: optimal "full" irrigation (FI) and rainfed (RF). In the FI treatment, mats received water whenever more than 25% of total available water (TAW) in the root zone (as determined by Time Domain Reflectometry) was depleted. In the RF treatment, irrigation was shut off after the establishment period and only switched on from December 2018 to February 2019 to limit plant death in the field as plants were stressed for a long time. No fertility stress was assumed as mats received locally recommended doses of nutrients (Meya et al., 2020). Mineral fertilizers were split applied: 153 kg N ha^{-1} $year^{-1}$ (urea), 206 kg K ha^{-1} $year^{-1}$ (muriate of potash), 19.26 kg Mg ha^{-1} $year^{-1}$ and 25.6 kg S ha^{-1} $year^{-1}$ ($MgSO_4$) were applied monthly in the rainy season and every two months in the dry season, while 40.2 kg P ha^{-1} $year^{-1}$ (triple super phosphate) was applied every five months. Twenty L of fresh farmyard cow manure was applied per mat twice yearly before the start of the rainy season. Plots were weeded and non-selected suckers were cut away monthly.

7.2.2 Weather and soil data

A weather station located at the edge of the field measured air temperature (°C), wind speed at 2 m height (m s^{-1}), relative humidity (%), precipitation (mm) and solar radiation (MJ m^{-2} min^{-1}) at a 5 min interval. Daily reference evapotranspiration (ET_0) was computed using the FAO Penman-Monteith method using temperature, wind speed, humidity and radiation data (Allen et al., 1998). The climate is a tropical highland climate with a moderately cool thermal zone (FAO, 2012). Rainfall generally follows a bimodal yearly pattern with a long rainy season extending from late March to early June and a shorter rainy season from October to December (Grieser et al., 2006). We defined rainy seasons in our field based on the FAO (1978) growing season concept, which assumes the rainy season to be the period during a year when precipitation exceeds half the potential evapotranspiration, extended with

a lag period required to evapotranspire 100 mm of water stored in the soil profile. For a fully grown banana plantation, the length of the growing season can be slightly reduced compared to the FAO (1978) growing season concept as the growing season starts when precipitation exceeds 0.7*ET_0 and is extended with a shorter lag period required to evapotranspire 40 mm (RAW). The TAW in our banana field in the rooting zone (0.6m) is 115.5 mm (Annex V, Table S1). With a p value of 0.35 the RAW (water to deplete before stresses occur) becomes 40mm. However, our plantations started from in vitro material and hence were not fully grown. Since we were working on a beginning plantation with lower water requirements than fully mature plantations, the FAO (1978) rainy season concept was used. If a dry season between two rainy seasons was short (< 1 month), we concluded the rainy season to be uninterrupted by a dry season. Consequently this approach led to a pattern of succession of dry and rainy seasons (Figure 7-1).

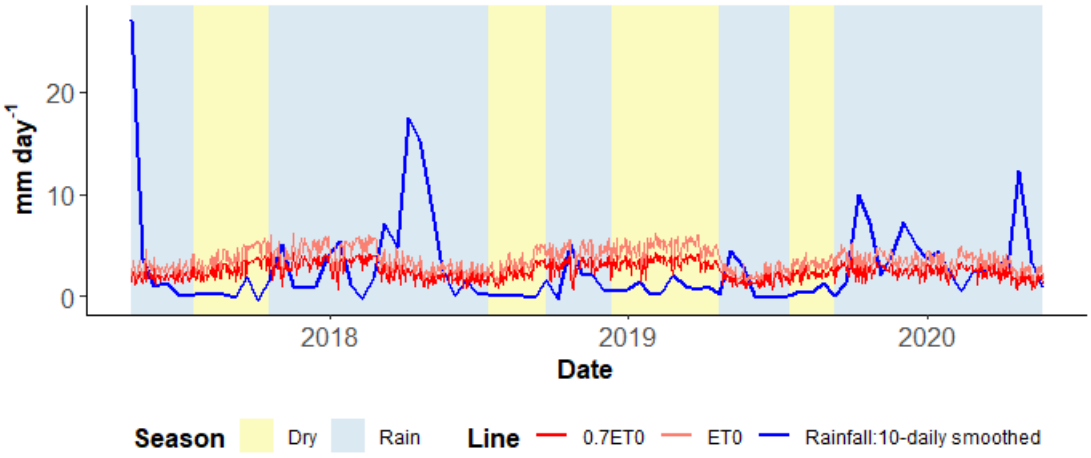


Figure 7-1: Growing seasons based on rainfall, reference evapotranspiration (ET_0) and a lag period to evapotranspire 100 mm. Rainfall data shown are smoothed on individual rainfall events with a span of 10 days.

The soil at the site is an Endocalcic Phaeozem (Geoabruptic, Clayic, Humic) (IUSS Working Group WRB, 2014) on gently sloping land (3%) located at the foothill of Mt. Meru at an altitude of 1188 m asl. Soil physico-chemical description for the different horizons is given in annex (Annex II, Table S1) and further explained by Meya et al. (2020) and in Chapter 5 and 6. A soil pF curve was derived from this soil (Annex II, Figure S5). The AquaCrop soil input file based on the physico-chemical properties and pF curve is presented in supplementary data (Annex V, Table S1 and Annex II, Figure S6).

7.2.3 Irrigation infrastructure and soil moisture measurements

Water was applied using drip irrigation. Until 7 MAP, two drippers were present per mat. Afterwards, four drippers were fitted around each mat. Drippers were located at a distance of 0.3-0.5 m from the center of a mat. Four drippers wetted an area of approx. 0.7 m radius around a banana mat, corresponding to an area of 25% (f_{drip}) of the total field (Annex II, Figure S3).

Soil water content (SWC) was monitored daily by Time Domain Reflectometry (TDR). In each plot, the central mat was fitted with two 30 cm long 3-pin sensors installed vertically at different depths: 0-30 cm (horizon 1) and 30-60 cm (horizon 2), within the horizontal area wetted by the drippers. TDR probes were read out each morning before irrigation by a TDR-200 (Campbell Scientific, Inc.). As four plots were present per treatment, soil moisture measurements were replicated four times.

7.2.4 Crop data

For each banana mat maximally three different cycles (C1, C2 and C3) were monitored. For each plant, phenological events were noted: planting (for C1), sucker selection (for C2 and C3), flower emergence and harvest dates (for C1-C3). Monthly growth measurements (Chapter 5 and 6) were taken from individual plants on a mat from planting until harvest and were used to calculate Leaf area indices (LAI), canopy cover (CC), aboveground dry biomass (B) and dry yields (Y). These include LL and LW of the third functional leaf, pseudostem height, pseudostem girth at base, girth at mid, girth at 1 m, number of functional leaves and number of dead leaves.

7.2.4.1 Canopy cover

The leaf area of individual leaves ($LA_{leaf,i}$), the leaf area of individual plants (LA_{plant}) and the leaf area and LAI of mats (LA_{mat}, LAI_{mat}) were calculated using eq. 7-1 to 7-4.

$$LA_{leaf,i} = LL \times LW \times laf \tag{7-1}$$

$$LA_{plant} = \sum_{i=cumO}^{cumY} LA_{leafi} \tag{7-2}$$

$$LA_{mat} = LA_{plant,C1} + LA_{plant,C2} + LA_{plant,C3} \tag{7-3}$$

$$LAI_{mat} = LA_{mat} \div ground\ area\ (m^2) \tag{7-4}$$

where LL and LW are the length and width (cm) of the ith leaf, laf is an experimentally determined leaf area factor (-) (Chapter 5), $LA_{leaf,i}$ is the leaf area (m²) of the ith leaf, $cumO$ is the oldest leaf present (-) and $cumY$ is the youngest leaf present on a plant (-), $LA_{plant,C1}$, $LA_{plant,C2}$, $LA_{plant,C3}$ are the leaf area (m²) of C1, C2 and C3 respectively, LA_{mat} is the leaf area of a mat and LAI_{mat} is the leaf area index of the mat.

LAI_{mat} values were averaged per plot (LAI_{plot}) and CC values computed following Chapter 5 (eq. 7-5).

$$CC = 100 \times \left[1 - exp^{(-0.67 \times LAI_{plot})}\right] \tag{7-5}$$

where CC is canopy cover (%) and LAI_{plot} is the average LAI_{mat} in a plot (m² m^{-2}).

7.2.4.2 Biomass and yield

The dry aboveground biomass (B) of a mat, is a sum of the individual plants (B_{plant}) present on a mat. B_{plant} is composed of the pseudostem, petiole and leaves (aboveground vegetative components), corm (belowground components) and male bud and bunch (generative components) (Chapter 6). The corm is the actual true stem of the banana plant, and as such needs to be incorporated in computing the B in AquaCrop.

The aboveground vegetative dry matter ($ABGVD$) and corm dry matter ($cormD$) were calculated for individual plants based on the pseudostem volume (eq. 7-6 to 7-7) (Chapter 6).

$$ABGVD = 0.22 + 6.27 \times 10^{-2} \times V_{pseudo} \quad (7\text{-}6)$$

$$cormD = 0.51 + 1.57 \times 10^{-2} \times V_{pseudo} \quad (7\text{-}7)$$

where $ABGVD$ is the aboveground vegetative dry matter (kg plant^{-1}), V_{pseudo} is the pseudostem volume (L plant^{-1}) and $cormD$ is the corm dry matter (kg plant^{-1}).

Male buds were removed when hermaphrodite hands became visible, and fresh weight was determined using a balance (±0.05kg). The male bud dry matter ($malebudD$) was calculated from the fresh weight and the percentage DM in the male bud (Annex IV, Table S3). Suckers were pruned monthly, fresh weights determined and dry weights ($suckerD$) computed per mat using percentage DM of suckers (Annex IV, Table S3). Ripe bunches were cut down when fingers on the second hand started to yellow indicating bunch maturity. The maximum bunch DM ($bunchD_{max}$) was taken as the actual bunch fresh weight at harvest multiplied by the percentage of bunch DM at harvest (15%). The bunch is the parameter of interest and taken as Yield (Y). Before flower emergence, the bunch was assumed zero. Between flower emergence and bunch maturity, the bunch develops logistically (Mahouachi, 2007; Robinson & Galan-Sauco, 2010). A logistical model (eq. 7-8) was specified to estimate the logistical development of the yield between flower emergence and harvest, following similar logistical models underlying root growth in AquaCrop.

$$Y = bunchD_{max} \quad \sqrt[n]{\frac{(t)}{(t_x)}} \quad (7\text{-}8)$$

where t is time after flower emergence (days), t_x is time from flower emergence to harvest (days), $bunchD_{max}$ is bunch DM at harvest (kg plant^{-1}); Y is yield (bunch DM) at time t (kg plant^{-1}) and n is a shape factor (-). The shape factor n is crop specific and was assumed 1.5 (slightly logistically).

The B of individual plants (C1, C2 and C3) (B_{plant}) and the total mat (B) were calculated using eq. 7-9 to 7-10.

$$B_{Plant} = ABGVD + cormD + malebudD + suckerD \ + Y \quad (7\text{-}9)$$

$$B = \ B_{mat} = B_{C1} + B_{C2} + B_{C3} \quad (7\text{-}10)$$

where B_{plant} is the total DM of a plant, B_{C1}, B_{C2} and B_{C3} are the total DM of cycle 1, 2 and 3, and B is the DM of a mat.

Root depths were checked every three months from planting onwards through root trenching methods. Roots were present up to 1 m depth from flowering onwards, but the number of roots declined substantially below 60 cm depth. The effective maximum rooting depth ($Z_{r,x}$) was taken as 0.6 m following our observations and summarized observations by Carr (2009).

7.2.5 AquaCrop model

7.2.5.1 Model description

AquaCrop is a water driven model that simulates daily crop development in response to SWC (Steduto et al., 2008, 2012). For a detailed explanation of the AquaCrop process the reader is referred to Chapter 4. Crop development is modelled in four steps: (1) green CC is simulated instead of LAI, (2)

crop transpiration (Tr) and root water uptake are simulated based on ET_0 and a crop coefficient (Kc_{Tr}) which is directly related to the CC (eq. 7-11), (3) aboveground biomass (B) is simulated based on Tr and a normalized crop-specific water productivity factor (WP^*) (eq. 7-12), and (4) yields (Y) are simulated by means of a harvest index (HI) (eq. 7-13) (Raes et al., 2009, 2018c; Vanuytrecht, Raes, Steduto, et al., 2014). Simultaneously, SWC in the root zone is simulated using an advanced type of water balance tipping bucket approach, based on incoming and outgoing fluxes adjusted with drainage functions based on physical characteristics of the soil horizons (Raes et al., 2006). Incoming fluxes comprise rainfall, irrigation and capillary rise, whilst outgoing fluxes comprise runoff, evaporation, transpiration, and deep percolations (Raes et al., 2009, 2018c; Vanuytrecht, Raes, Steduto, et al., 2014).

Stress effects (water, temperature, fertility, and salt) are simulated using stress coefficients (Ks). Ks are multiplied with parameters underlying model equations (e.g. eq. 7-11 to 7-12) and range from one (no stress) to zero (full stress). Stress coefficients thereby affect multiple processes in the AquaCrop simulation scheme. Water stress indicators are based on SWC in the root zone. When SWC drops below certain critical thresholds, water stress coefficients drop below one. Water stress coefficients affect four different processes, depending on SWC thresholds: canopy expansion (Ks_{exp}), stomatal closure (Ks_{sto}), early senescence (Ks_{sen}) and adjustment of HI (f_{HI}) and root zone expansion (Raes et al., 2018c; Vanuytrecht, Raes, Steduto, et al., 2014).

$$Tr = Ks \times Ks_{Tr} \times (Kc_{Trx} \times CC^*) \times ET_0 \quad (7\text{-}11)$$

$$B = Ks_b \times WP^* \times \sum \frac{Tr}{ET_0} \quad (7\text{-}12)$$

$$Y = f_{HI} \times HI_0 \times B \quad (7\text{-}13)$$

where Tr is transpiration (mm), Ks is a water stress coefficient (0-1) being either Ks_{sto} (stomatal stress coefficient) or Ks_{aer} (aeration stress coefficient), Ks_{Tr} is the cold stress coefficient for crop transpiration (0-1), CC^* is the adjusted green canopy cover (%), $Kc_{Tr,x}$ is the maximum crop coefficient (-), ET_0 is the reference evapotranspiration as calculated by the FAO 56 method (mm), B is the aboveground dry biomass (ton DM ha^{-1}), Ks_b is the cold temperature stress coefficient (0-1), WP^* is the normalized water productivity factor (for ET_0 and CO_2 content) (g DM m^{-2} or ton DM ha^{-1}), Y is the dry yield (ton DM ha^{-1}), f_{HI} is the adjustment factor under water, heat and/or cold stress (0-1.6), HI_0 is the reference harvest index(-).

Calibration entails setting model parameters within realistic boundaries, so simulations correspond to observed values. AquaCrop includes two types of crop parameters: conservative parameters that do not change with the cultivar, time, environment and management and non-conservative parameters that are cultivar, time, environment or management specific (Steduto et al., 2012).

A detailed overview of the simulated processes is given by Hsiao et al. (2009), Raes et al. (2009) and Steduto et al. (2009). AquaCrop version v7.0 was used and newly released versions of the AquaCrop model, and corresponding changes to the modelling scheme can be found at the FAO site (FAO, 2020) and in the corresponding updated AquaCrop reference manuals.

7.2.6 Crop parameter calibration

Banana crop files were created for C1 and C2 separately and modelled successively (Table 7-1). Banana was treated as a fruit crop in AquaCrop. Phenological events in AquaCrop can be specified in days after planting (DAP) or GDD. We calibrated the model in DAP, as our database comprised only a single area. C1 was modeled until average harvest of C1 (DAP: 0-397 for FI, DAP 0-410 for RF). C2 was modelled directly following C1 harvest until average harvest of C2 (27/11/2019: DAP 744 for FI, 20/12/2019: 767 DAP for RF). C1 notes mats until harvest of C1 plants, C2 notes mats until harvest of C2 plants. Within C1 and C2, mats are composed of multiple plants. For C1, the AquaCrop option 'transplanting' was used, and for C2 the option 'regrowth' was used as plants do not germinate and recover after planting. As mats continue to grow after flowering, a mat was considered non-determinant.

The canopy curve, root growth, $WP^*$and HI_0 parameters were calibrated based on measured data from the FI plots (chapter 5 and 6), which were considered non-stressed in terms of soil moisture, fertility, and salinity. Fertility and salinity stress responses where thereby not considered in this calibration. Root water extraction patterns were taken as such that the top ¼ of the roots extracted 40% whilst the bottom ¼ of roots extracted only 10%, in line with the root water uptake patterns of banana, which is a shallow rooted crop (Carr, 2009). WP^* was determined iteratively for FI plots. Using ET_0 as calculated by the Penman-Monteith equation together with CC observations from irrigated plots in the field, Tr was calculated according to eq. 7-11 (with Kc_{Trx} 1.1 for banana, and assuming zero stress as plots were irrigated). Cumulative B observations from irrigated plots, where plotted against cumulative $\sum \frac{Tr}{ET_0}$, and the slope of this line gave an indication of WP^* for use in AquaCrop. WP^* equal to 11 g m^{-2} was used (normalized for the year 2000) during AquaCrop modelling (which becomes 12 g m^{-2} in 2018-2020). The reference harvest index (HI_0) was based on Y observations at harvest of FI which was 41-43% for both cycles. A HI_0 of 40% was chosen for calibration, as HI of C1 and C2 were close together and this led to best goodness-of-fit. Onset of flowering (flower initiation) was set 12 weeks before flower emergence, as there are 12 leaves present inside the pseudostem at the estimated time of flower initiation (Turner et al., 2007). Duration of flowering was thus set as 84 days as development of the female flowers inside the pseudostem spans 11-12 weeks in the tropics (Turner et al., 2007). Buildup of HI was set from flower initiation until harvest. Days to senescence was set as days to maturity, since new leaves are continuously formed on a mat due to its perennial nature, hence canopy decline due to senescence was not considered.

Water stress coefficients for canopy expansion (Ks_{exp}), stomatal closure (Ks_{sto}) and early senescence (Ks_{sen}) were based on literature values and adjusted iteratively until RF models achieved best model fits (but keeping all other parameter values at the values obtained in the calibration on the FI treatment) (Table 7-1). Parameters and stress coefficients were adjusted in sequence such that first CC, then SWC, then B and then Y were simulated correctly. Banana plants are affected (in leaf expansion and stomatal closure) whenever 20-35% TAW is depleted (Allen et al., 1998; Carr, 2009), thereby upper depletion thresholds for p_{exp-up} and p_{sto-up} were set at 0.30 and 0.35 respectively within that range. During stress, the ET_0 sum to be exceeded before senescence is triggered (mm) was set to 200 mm as banana plants only show signs of leaf senescence (e.g. petiole collapse) after they have been significantly stressed for a long duration. The aeration stress for banana (Ks_{aer}) was set at saturation VWC as banana growth is affected after 1-2 days of waterlogging (depending on the cultivar) (Carr, 2009).

The influence of water stress on the harvest index (f_{HI}) depends on the stage when water stress occurs. Before flowering, banana plants do not show any increase in HI due to water stress. After flower initiation, no impact of restricted vegetative growth during yield formation was set as leaves of the mother plant are already formed at bunch filling, and the bunch becomes the biggest sink (reducing the effect of vegetative growth of the daughter on bunch weights) (Robinson & Galan-Sauco, 2010).The maximum depletion threshold for pollination (p_{pol}) was set at 0.98 since bananas are parthenocarpic fruits and hence do not require pollination for flower and fruit development (Robinson & Galan-Sauco, 2010). The number of female fruits (cultivar dependent) depends on the vegetative growth preceding flower initiation as the number of flowers (fingers) is significantly correlated to pseudostem diameter in the Grande Naine cultivar (Holder & Gumbs, 1982). The effects of drought stress during the period between flower initiation and flower emergence revealed flower number to be negatively affected by drought (Holder & Gumbs, 1982). The reduction in the number of female flowers (fingers) under drought can however be offset to a certain extent by an increased filling of the remaining fingers as shown by bunch trimming experiments on Grande Naine (Bugaud et al., 2012). We chose to not consider the effect of drought on f_{HI} during pollination (flower initiation) as the effect of drought before flower initiation (vegetative growth) and the effect of drought during yield formation on f_{HI} (from flower initiation until bunch harvest) already considers the reduction of yield under drought stress and led to good yield simulation results. If we considered the effect of drought on f_{HI} during pollination, the effect of drought on f_{HI} during bunch filling (yield formation) needs to be compensated accordingly. A small negative impact on HI due to stomatal closure during yield formation was set, as bunches fill (in addition to photosynthesis during yield formation) partly from retranslocation of nutrients from the corm (Dens, Romero, et al., 2008; Robinson & Galan-Sauco, 2010).

Base and upper temperatures (14 and 38°C) were set based on Robinson & Galan-Sauco (2010). Cold and heat stress on pollination and transpiration were not considered as in the East African highlands suboptimal temperatures limiting flower number and transpiration (<16°C) were not reached.

7.2.7 Adjustment of AquaCrop model for localized drip irrigation

AquaCrop assumes the soil profile is homogenous in the horizontal plane underneath a plantation and differs only in the vertical direction. The fluxes in and out of the system are assumed to be one dimensional (vertical), and uniform over the entire field surface (upper boundary) and bottom of the root zone (lower boundary) (Raes et al., 2012b, 2015b, 2018c; Vanuytrecht, Raes, Steduto, et al., 2014).

The area where roots subtract water (A_{root}) follows the area where water is present. In the rainy season, when soil moisture is supplied by precipitation and drippers, the entire field surface (A_{field}) is wetted, and soil moisture can be considered uniformly distributed. This is no longer the case in a dry season when supplying drip irrigation, as only a fraction of the soil surface is wetted by the drippers (A_{drip}). The entire moisture subtracted from the evapotranspiring surface (A_{field}), needs to come from this root zone container (A_{root}) (eq 7-14) (Figure 7-2).

$$f_{root} = \frac{A_{root}}{A_{field}} \; with \begin{cases} A_{root} = A_{field} \; in \; rainy \; season \\ A_{root} = A_{drip} \; in \; dry \; season \end{cases}; \qquad (7\text{-}14)$$

with f_{root} is the horizontal fraction of the field surface (%) where roots subtract water, A_{root} is the horizontal area (m² mat^{-1}) where roots subtract water from the field, A_{drip} is the horizontal area (m² mat^{-1}) wetted by the drippers in the dry season and A_{field} is the total horizontal area of the field (m² mat^{-1}).

A workaround to the AquaCrop scheme was proposed to model drip irrigation (Annex V). In the rainy season or in a rainfed dry season, the soil moisture balance of the full field area was simulated, and no adjustments were necessary to the AquaCrop model scheme.

For a drip irrigated field in the dry season, the soil moisture balance in the root zone container ($A_{root} = A_{drip}$) was simulated. Adjustments to both input and output files were necessary to represent localized drip irrigation. These adjustments were:

(1) ET_0 as calculated according to the Penman-Monteith equation was adjusted by dividing the values with the fraction occupied by the roots (f_{root}). In the dry season, f_{root} was f_{drip} being 25%.

(2) Irrigation amounts (I) were expressed as an equivalent depth (in mm) applied to the root zone container, by dividing the volume of applied water in the field (in L) by the area of the root zone container (A_{root}).

(3) Soil evaporation in the dry season was considered only from A_{drip} since only evaporation can occur from the wetted field area fraction (f_{drip}). To exclude evaporation from the rest of the field, a synthetic mulch layer of (1-f_{drip}%) was added during modelling in the dry season.

Climate, irrigation, and management input files were adjusted whenever irrigation was applied in the dry seasons (Figure 7-1). Model runs were performed back-to-back linking adjusted and non-adjusted runs to cover a complete crop cycle.

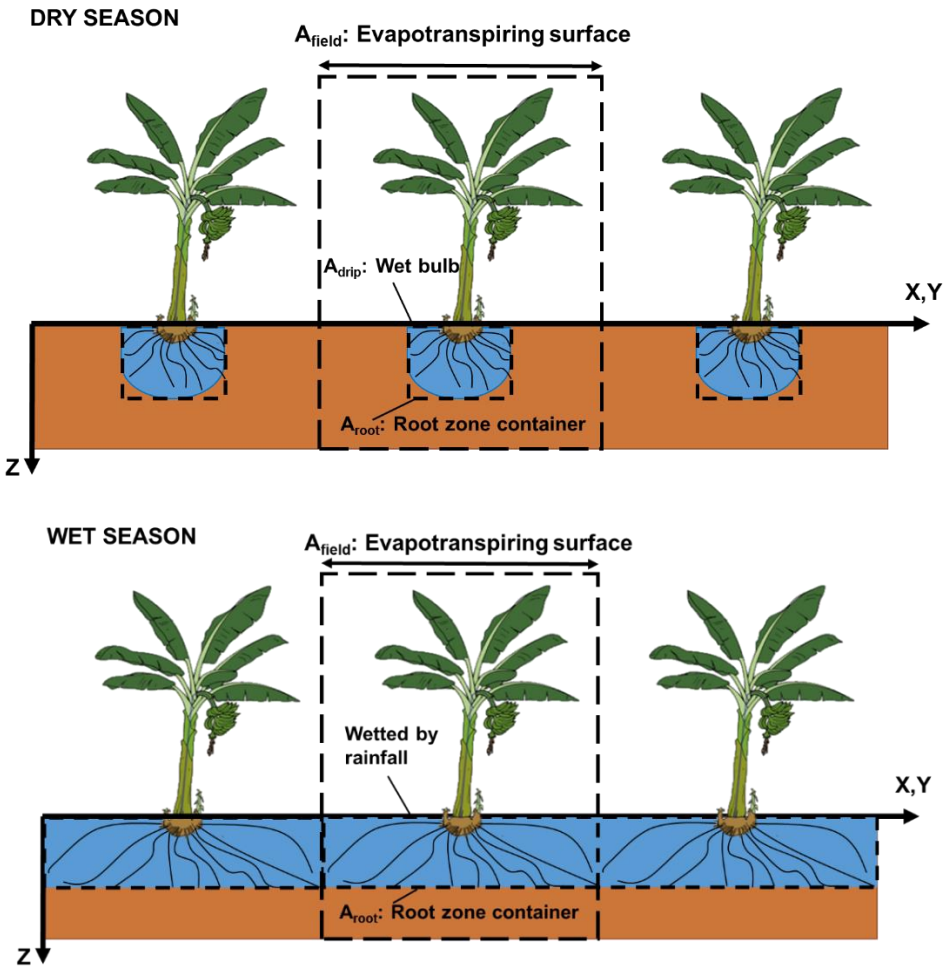


Figure 7-2: Distribution of banana plants in the field. X,Y is direction of the horizontal field surface, Z is the direction of the depth from 0 (surface) to depth Z of the soil profile. The blue area indicates the wetted area in the two seasons. Each individual mat has a region bounded by the rectangle. The wet bulb notes the area wetted by the drippers (A_{drip}). The root zone container notes the volume where roots are located, and water is subtracted being different in the wet and dry season. The evapotranspiring surface is the total area where banana plants subtract water from.

Table 7-1: Crop parameters used in AquaCrop. Crop files were created for each cycle and treatment. C1 and C2 denote cycle 1 and 2. FI denotes full irrigation, and RF denotes rainfed. Default indicates default values for a C3 fruit-grain producing crop in AquaCrop. Flowering denotes flower initiation. Flowering duration denotes time from flower initiation to flower emergence at the top of the pseudostem. Type notes whether parameters are conservative (C) or non-conservative (NC).

Parameters	Type	Description	Value				Determination
			C1-FI	C1-RF	C2-FI	C2-RF	
Settings							
Sow		Crop is sown (1), transplanted (2) or regrowth (3)	2	2	3	3	Observed
Type		Crop type (1 = leafy vegetable, 2=fruit/grain producing, 3=root/tuber, 4 = repeatedly harvested)	2	2	2	2	Observed
Det		Crop determinancy linked (1) or unlinked with flowering (0) - Banana mat is indeterminant	0	0	0	0	Observed
Depladj		Soil water depletion factors are adjusted (1) or not (0) by ET_0	0	0	0	0	Not considered
Crop development							
Canopy cover							
CC_0	NC	Initial Canopy Cover in fraction soil cover (-) (depends on plant density)	0.017	0.017	0.6	0.4	Observed
CC_s	C	Soil surface covered by an individual seedling at 90 % emergence (cm^2)	1020	1020	-	-	Observed
den	NC	Plant density in the field (plants ha^{-1})	1666	1666	1666	1666	Observed
CC_x	NC	Maximum canopy cover in fraction soil cover (-)	0.90	0.90	0.90	0.90	Calibrated
cgc	C	Canopy growth coefficient: Increase in CC (% per day)	0.027	0.027	0.021	0.021	Calibrated
cdc	C	Canopy decline coefficient: Decrease CC (% per day)	-	-	-	-	Not considered
Days to recovery	NC	From regrowth to recovering (days)	3	3	7	7	Observed
Days to senescence	NC	From regrowth to start senescence (days)	397	410	376	376	Observed
Days to maturity	NC	From regrowth to maturity (days)	397	410	376	376	Observed
Flowering and yield							
Days to onset of flowering	NC	From regrowth to onset of flowering (days)	180	180	111	150	Observed
Duration of flowering	NC	Length of the flowering stage (days)	84	84	75	75	Literature
Duration of HI_0 buildup	NC	Building up of harvest index starting at flower initiation until harvest (days)	223	238	265	226	Observed
Root deepening							
$Z_{r,min}$	NC	Minimum effective rooting depth (m)	0.1	0.1	0.6	0.6	Observed
$Z_{r,max}$	NC	Maximum effective rooting depth (m)	0.6	0.6	0.6	0.6	Observed
Days to max depth	NC	From regrowth to maximum rooting depth (days)	180	180	-	-	Observed
rt_{shp}	C	Shape factor describing root zone expansion (-)	15	15	15	15	Calibrated
Root water extraction up	NC	Maximum root water extraction (m^3 water m^{-3} soil day^{-1}) in top quarter of root zone	0.048	0.048	0.048	0.048	Literature
Root water extraction bottom	NC	Maximum root water extraction (m^3 water m^{-3} soil day^{-1}) in bottom quarter of root zone	0.012	0.012	0.012	0.012	Literature

Table 7-2: Selected crop parameters used in AquaCrop. Crop files were created for each cycle and treatment. C1 and C2 denote cycle 1 and 2. FI denotes full irrigation, and RF denotes rainfed. Default indicates default values for a C3 fruit-grain producing crop in AquaCrop. Flowering denotes flower initiation. Flowering duration denotes time from flower initiation to flower emergence at the top of the pseudostem.

Parameters	Type	Description	Value				Determination
			C1-FI	C1-RF	C2-FI	C2-RF	
$\boldsymbol{ET_0}$							
$K_{c,Trx}$	C	Crop coefficient when canopy is complete but prior to senescence (-)	1.1	1.1	1.2	1.2	Literature
Production							
WP^*	C	Water productivity normalized for ET_0 and CO2 (WP*) (g m^{-2})	15	15	15	15	Calibrated*
f_{sink}	NC	Crop performance under elevated atmospheric CO2 conditions	50	50	50	50	Default
HI_0	C	Reference harvest index (HI_0) (%)	32	32	32	32	Calibrated**
$DM\%$	NC	Dry matter content of fresh yield (%)	15	15	15	15	Observed
Response to stress							
Water							
p_{exp-up}	C	Soil water depletion factor for canopy expansion - Upper threshold	0.3	0.3	0.3	0.3	Calibrated
$p_{exp-low}$	C	Soil water depletion factor for canopy expansion - Lower threshold	0.8	0.8	0.8	0.8	Calibrated
$p_{exp-shp}$	C	Shape factor for water stress coefficient for canopy expansion (0.0 = straight line)	3	3	3	3	Calibrated
p_{sto-up}	C	Soil water depletion fraction for stomatal control - Upper threshold	0.35	0.35	0.35	0.35	Calibrated
$p_{sto-shp}$	C	Shape factor for water stress coefficient for stomatal control (0.0 = straight line)	3	3	3	3	Calibrated
p_{sen-up}	C	Soil water depletion factor for canopy senescence - Upper threshold	0.98	0.98	0.98	0.98	Calibrated
$p_{sen-shp}$	C	Shape factor for water stress coefficient for canopy senescence (0.0 = straight line)	3	3	3	3	Calibrated
$etos$	C	ET_0 sum during stress period to be exceeded before senescence is triggered (mm)	200	200	200	200	Calibrated
Ks_{aer}	C	Vol% for anaerobiotic point at which deficient aeration occurs	0	0	0	0	Literature

In our calculations a WP of 11 g m^{-2} (normalized for the year 2000) was used, but a WP* of 15 g m^{-2} is expected to be reached when considering 1) leaf removal, 2) improved $cormD$ biomass estimations, 3) growth respiration during bunch filling, 4) growth and maintenance respiration losses due to corm maintenance and recycling. **An adjustment of WP* entailed a downward adjustment of the HI0. In our calculations a HI0 of 40% was used, but this is assumed to be adjusted to 32% when using WP* of 15 g m^{-2}.

Table 7-1 (Cont.): Selected crop parameters used in AquaCrop. Crop files were created for each cycle and treatment. C1 and C2 denote cycle 1 and 2. FI denotes full irrigation, and RF denotes rainfed. Default indicates default values for a C3 fruit-grain producing crop in AquaCrop.

Parameters	Type	Description	Value				Determination
			C1-FI	C1-RF	C2-FI	C2-RF	
Harvest index effect		Effects of harvest index dependent on time of water stress					
Before flowering	C	Increase (in %) of HI due to water stress before flowering	0	0	0	0	Literature
During flowering	C	No impact on HI of restricted vegetative growth during yield flowering (-)	-9	-9	-9	-9	Not considered
Pollination effect	C	Soil water depletion factor for pollination (p - pol) - Upper threshold ($m^3\ m^{-3}$)	0.98	0.98	0.98	0.98	Calibrated
During yield formation	C	Coefficient describing negative impact on HI of stomatal closure during yield formation (flower initiation to harvest) (-) small effect	8	8	8	8	Calibrated
Temperature Stress							
T_{base}	C	Base temperature (°C) below which crop development no longer progresses (°C)	14	14	14	14	Literature
T_{up}	C	Upper temperature (°C) above which crop development no longer progresses (°C)	38	38	38	38	Literature
	C	Cold (air temperature) stress affecting pollination - not considered	-9	-9	-9	-9	Not considered
	C	Heat (air temperature) stress affecting pollination - not considered	-9	-9	-9	-9	Not considered
	C	Cold (air temperature) stress on crop transpiration not considered	-9	-9	-9	-9	Not considered
Soil Fertility stress	NC	Not considered	-9	-9	-9	-9	Not considered
Salt Stress	NC	Not considered	-9	-9	-9	-9	Not considered

7.2.8 Model evaluation

The same sets of observational data were used for calibration of crop parameters and model evaluation using goodness-of-fit values. Additional validation datasets could not be collected in this study due to the intense data collection nature of these experiments resulting in lack of time and resources for setting up validation plots.

CC, SWC, B and Y were considered in model evaluation. Observed values from the field and simulated AquaCrop outputs were compared (Figure 7-3), and goodness-of-fit characteristics used were R^2 (Pearson's correlation coefficient), Root mean square error (RMSE), Relative root mean square error (RRMSE), the Nash and Sutcliffe model efficiency (NSE) and the Wilmot's index of agreement (d) (Chapter 4,Table 4-2).

7.3 Results

Climate, irrigation, and management inputs were adjusted when drip irrigation was applied based on the horizontal root fraction f_{root}= 25%. Inputs in rainy seasons, and rainfed dry seasons were not adjusted. Together with the calibration of the crop parameters, this mostly led to good simulation for FI production, and slightly less accurate simulations for RF production, although these can still be considered good to moderate good (Table 7-3 and Figure 7-3).

Table 7-3: Goodness-of-fit values for AquaCrop simulations: R^2 (Pearson's correlation coefficient), RMSE (residual mean square error), RRMSE (relative residual mean square error), NSE (Nash and Sutcliffe model efficiency) and d (Wilmot's index of agreement). FI notes full irrigation, RF notes rainfed. CC notes canopy cover (%), SWC notes soil water content (mm), B notes aboveground dry biomass (ton ha^{-1}) and Y notes dry yield (ton ha^{-1}). 'C1' notes cycle 1, 'C2' notes cycle 2 and 'Combined' notes the two cycles together. For interpretation of values, the reader is referred to table 2. RMSE units are: % for CC, $m^3 m^{-3}$ for SWC, ton ha^{-1} for B and ton ha^{-1} for Y. RRMSE units are %.

		FI					RF				
	Parameter	**R^2**	**RMSE**	**RRMSE**	**NSE**	**d**	**R^2**	**RMSE**	**RRMSE**	**NSE**	**d**
C1+C2	CC	0.98	6.56	10	0.93	0.98	0.86	14.09	24	0.61	0.92
	SWC	0.62	30.07	12	-1.77	0.62	0.85	31.22	17	0.62	0.9
	Biomass	1	4.34	18	0.95	0.99	1	3.96	21	0.92	0.98
	Yield	0.99	1.13	15	0.98	1	0.98	1.07	22	0.95	0.99
C1											
	CC	0.93	4.89	6	0.77	0.93	0.93	13.92	26	0.76	0.95
	SWC	0.55	33.18	13	-4.65	0.52	0.97	15.86	8	0.91	0.98
	Biomass	0.99	6.9	14	0.58	0.92	0.99	2.59	27	0.9	0.97
	Yield	0.93	2.11	11	0.72	0.95	0.99	0.56	23	0.97	0.99
C2											
	CC	0.98	8.32	15	0.93	0.98	0.46	13.7	21	0.01	0.69
	SWC	0.69	27.38	11	-0.86	0.68	0.7	43.3	24	0.11	0.75
	Biomass	1	1.5	14	0.98	0.99	0.99	5.44	16	0.26	0.82
	Yield	1	0.37	13	0.99	1	0.8	1.79	17	0.24	0.84

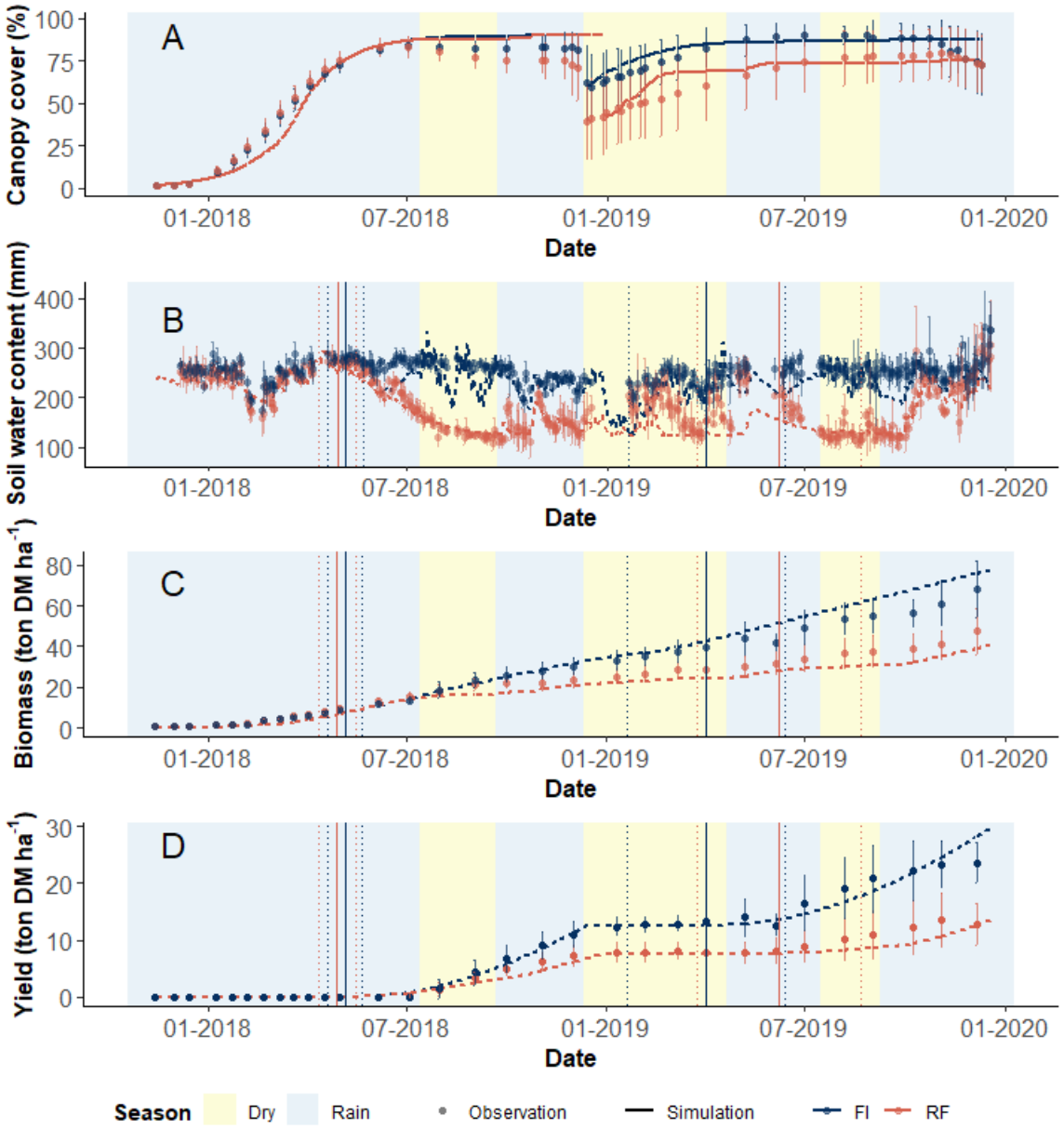


Figure 7-3: Observed and simulated values for full irrigated (FI) and rainfed (RF) plots over the course of two crop cycles for A) Canopy cover, B) Soil water content, C) Biomass and D) Yield. Vertical (bold) lines denote average flowering date of C1 and C2 in RF and FI plots, vertical dotted lines denote average flowering date-±1SD. Flowering denotes flower initiation. Observations present mean values -±1SD.

7.3.1 Canopy cover

CC simulations slightly underestimated observed CC in C1, and slightly overestimated CC in C2 for RF (Figure 7-3A). For FI all CC goodness-of-fit indicators point to (very) good model performance (Table 7-3). For both cycles combined: R^2 was greater than 0.98 (very good), RMSE was 6.56%, RRMSE was 10% (very good), NSE was 0.93 (very good) and d was 0.98 (very good). For RF goodness-of-fit indicators range from moderate good to very good. For both cycles combined: R^2 was 0.86 (very good), RMSE was 14.09%, RRMSE was 24% (moderate good), NSE was 0.61 (moderate good) and d was 0.92 (very good)(Table 7-3).

7.3.2 Soil water content

SWC in the maximum rooting zone (60 cm depth) from the output of AquaCrop were used for comparison against observed SWC calculated from TDR sensors at 0-30 cm and 30-60 cm.

SWC simulations followed patterns in observed SWC over the course of the two growing seasons (Figure 7-3B), but deviations occurred depending on the treatment and cycle. SWC observations in FI plots remained relatively stable throughout both cycles, whilst FI simulations showed increased fluctuations and were more dynamic reducing goodness of fit. Fluctuations from observed values occur mostly in the dry seasons (or in the beginning of the wet season), which indicates this can be due to the nature of the modelled drip irrigation. A smaller irrigation application dose in the dry season in FI was rapidly followed by a drop in SWC in the root zone as shown by the fluctuation around August 2018, and at the onset of the dry season in January 2019. SWC fluctuations occur rapidly in FI plots since these are accompanied by high T_r out of the root zone, faster than observed in the field. A similar pattern is observed in RF plots.

RF simulations in C1 followed observed SWC closely, yet SWC simulations in C2 did not capture two observed peaks in SWC: the rise of SWC in February 2019 (due to irrigation) and around May 2019 (due to rains). This is reflected in the RRMSE (24%) in C2 RF. This is still moderately good, but worse than RRMSE in C1 RF and C2 FI. The SWC underestimation in February 2019 is due to the increased T_r out of the root zone in the dry season which led to a faster depletion in the root zone than actually observed in the field. The observed low $SWCs$ close to PWP can be connected to the plateau of CC development in RF, which develops again when SWC rises. For FI plots, SWC remains above the lower threshold for CC expansion, thus CC development never stops.

Most goodness-of-fit indicators however point to moderately good model performance in FI (Table 7-3). For both cycles combined: R^2 was 0.62 (moderately good), RMSE was 31 $m^3\ m^{-3}$, RRMSE was 12% (good). However, NSE values were -1.77 (poor) and d values were 0.62 (moderately poor). SWC simulations over time, do follow observed moisture over time (Figure 7-3B). For RF, all goodness-of-fit indicators point to good model performance. For both cycles combined, R^2 was 0.85 (good), RMSE was 31 $m^3\ m^{-3}$, RRMSE was 17% (good), NSE was 0.62 (good) and d was 0.9 (very good).

Overall, the simulations captured observed SWC variations over time (Figure 7-3B). After shutting off irrigation in June 2018, simulated SWC in RF plots closely followed observed TDR values as the soil dried out, whilst under continuing irrigation simulated SWC also followed observations over time. The adjustment of drip irrigation however ensures fast depletion of the root zone which becomes rapidly observable when irrigation is switched off (or suboptimal) as $SWCs$ drop fast (faster than based on observations).

7.3.3 Biomass

B simulations were good to moderate good in FI and RF (Figure 7-3C and Table 7-3). For FI most goodness-of-fit indicators point to very good model performance (Table 7-3). For both cycles combined: R^2 was close to 1 (very good), RMSE was 4.34 ton DM ha^{-1}, RRMSE was 18% (good), NSE was 0.95 (very good) and d was 0.99 (very good). The simulated B runs straight through most observed B values in the field in FI, although deviates slightly in C2 (Figure 7-3C). For RF, most goodness-of-fit indicators point to good model performance (Table 7-3). For both cycles combined: R^2 was 1 (very good), RMSE was 3.96 ton DM ha^{-1}, RRMSE was 21% (moderate good), NSE was 0.92 (very good) and d was 0.98 (very good).

For C1, simulated B at harvest was 32.8 ton DM ha^{-1} (FI) and 21.9 ton DM ha^{-1} (RF). For C2, simulated B at harvest was 41.6 ton DM ha^{-1} (FI) and 19.25 ton DM ha^{-1} (RF). The simulated B shows similar patterns as the observed B over time (Figure 7-3C). From 2019, B accumulation in RF plots stops in the dry season due to soil drying, and B accumulation starts again due to increase in SWC in the rainy season. Upon reaching the dry season again, soils start drying and B accumulation halts again. This stepwise pattern is observed in both simulated in response to simulated SWC and in observed values. In RF, B simulations started to deviate slightly from observed values at the onset of soil moisture stress approximately at the start of the dry season in June 2018, when SWC in drop toward PWP (Figure 7-3B). Moisture stress immediately led to stomatal closure, resulting in a reduced biomass accumulation. Underestimation of SWC in the dry season in February 2019 and the rainy season in May 2019, led to lower simulated B than observed (Figure 7-3C). Underestimation of B simulations is thereby linked to underestimation of SWC simulations, but overall underestimation is slight.

7.3.4 Yield

Y was simulated well to very well in FI and RF in both cycles (Figure 7-3D and Table 7-3). Y buildup in the field, and in the simulations, started from flowering (flower initiation) onwards.

For FI all goodness-of-fit indicators point to very good model performance (Table 7-3). For both cycles combined, simulations were close to perfect as R^2 was 0.99 (very good), RMSE was 1.13 ton DM ha^{-1}, RRMSE was 15% (good), NSE was 0.98 (very good) and d was 1 (very good). Simulated Y ran straight through values observed in the field. For RF, all goodness-of-fit indicators also point to very good model performance (Table 7-3). For both cycles combined: R^2 was 0.98 (very good), RMSE was 1.07 ton DM ha^{-1}, RRMSE was 22% (moderately good), NSE was 0.95 (very good) and d was 0.99 (very good).

For C1, simulated Y at harvest was 12.8 ton DM ha^{-1} (FI) and 7.6 ton DM ha^{-1} (RF). For C2, simulated Y at harvest was 13.9 ton DM ha^{-1} (FI) and 5.9 ton DM ha^{-1} (RF). With a DM of 15%, and a density of 1,666 mats ha^{-1}, average simulated fresh bunch weights were 48 kg FM plant^{-1} (FI) and 30.4 kg FM plant^{-1} (RF) in C1 versus 55.6 kg plant^{-1} (FI) and 23.6 kg plant^{-1} (RF) in C2. Actual observed fresh bunch weights were 49.6 (±7.61) kg FM plant^{-1} (FI) and 33.2 (±9.1) kg FM plant^{-1} (RF) in C1 versus 52.4 (±15.2) kg FM plant^{-1} (FI) and 33.3 (±9.9) kg FM plant^{-1} (RF) in C2. Observed Y at harvest is therefore very close to simulated Y at harvest, indicating good model performance.

7.4 Discussion

The dataset for calibrating model parameters was also used for comparison with model simulations. No independent validation datasets were collected given the extensive nature of data collection and the long growth cycles in banana plantations. To fully make statements concerning model validity and efficiency and apply the model in scenario analysis, validation of independent datasets in different environments still needs to occur. Vanuytrecht, Raes, & Willems (2014) performed a sensitivity analysis determining influential and non-influential crop and soil parameters in the AquaCrop model and determined to which extent model outputs changed in response to these parameters. Influential parameters depended on environmental conditions (crop, soil, climate) for which the model was calibrated, indicating the significance of calibration conditions on parameter values. Furthermore, parameters that were influential under tested environments, might be non-influential for different environmental conditions and irrigation systems. Our study thereby provides prior parameter values with which other calibration exercises can start and compare their calibration exercises.

7.4.1 Comparison calibrated parameters with literature

Commercial Cavendish plantations produce yields between 40-50 ton FM ha^{-1}, sometimes reaching 60 ton FM ha^{-1} (FAO, 2018a). Our actual FI yields reached 82 ton FM ha^{-1} in C1 and 87 ton ha^{-1} in C2. In a well performing plantation individual plant yields rise with increasing ratoon (Robinson & Galan-Sauco, 2010). As C1 and C2 yields are so similar, we postulate that the absolute maximum yield ceiling of Cavendish was reached in C1. Taking into account the C1 and C2 cycle duration, the fresh yield was 71 ton FM ha^{-1} year^{-1} in C1 and 51 ton FM ha^{-1} year^{-1} in C2. In contrast, yields in low input rainfed East African Highlands range from 6.1-25 ton FM ha^{-1} year^{-1}, depending on the agro-ecological zone, cultivar and plantation density (Ndabamenye et al., 2012). Our fields match and even surpass production in well-managed commercial (Cavendish) plantations indicating production to be near maximum, and thus stresses to be minimal in the FI plots. Our observed fields were thereby used for calibration of non-stressed crop parameters.

7.4.1.1 WP^* and HI_0 adjustment.

A WP^* of 11 g m^{-2} (normalized for CO_2 and ET_0 in the reference year 2000; 12 g m^{-2} for the year 2018-2020) showed best model fits for banana. Normally, WP^* ranges from 15-20 g m^{-2} for C3 crops and from 30-34 g m^{-2} for C4 crops (Steduto et al., 2012). Hence, our calibrated value for WP^* is low for C3 crops. Several hypotheses exist for the low WP^* in our study:

(1) Fallen and dead leaves were continuously removed in the plantation and were not accounted for in B calculations. Including the weight of these removed leaves would increase WP^* by 10-20%. Because we did not account for this leaf removal, our simulated B is in fact standing B in the field (which is readily observable). For a farmer it is more interesting to get an indication on standing B in the field, leading to the justification of not including removed leaf weight in B calculations.

(2) $CormD$ estimations based on V_{pseudo} were suboptimal (Chapter 6) and a similar allometric model was chosen for FI and RF plants (eq. 7-7). ANCOVA analysis showed a very slight effect of treatment on allometry reducing intercept and slope in RF treatments compared to FI treatments, but this small effect was considered non-significant as 95%CI for model coefficients overlapped and goodness of fit remained similar when pooling treatment data. The effect of using treatment specific $cormD$ models (Chapter 6, Table 6-5) would increase total B at harvest in FI plants by approx. 0.2-0.3 ton DM ha^{-1} which corresponds to an increase in B (and WP^*) by 0.5-1%, which is a small increase.

(3) Growth and maintenance respiration losses are included in the WP^* and differ between plant species (Steduto et al., 2007a). Respiration is an important factor in the WP^* as between 30-60% of the carbon assimilated during photosynthesis is subsequently lost by respiration in annual and perennial crops (Amthor et al., 2019). Growth respiration losses differ between crop species because of the growth respiration losses per compound DM formed are higher for lipids, proteins and lignin than for other components (Penning De Vries et al., 1983) This is why in AquaCrop the WP^* for sunflower during the vegetative stage is 18 g m^{-2}, whilst during yield formation it becomes 11 g m^{-2} due to the high lipid content of sunflower seeds. For cotton, WP^* during the vegetative stage is 15 g m^{-2}, whilst WP^* during yield formation becomes 11 g m^{-2} due to the high protein and lipid content of cotton balls (Raes et al., 2018c). For banana, a likewise adjustment might be needed during bunch filling, but this remains speculation. The energy dense banana fruits are richer in carbohydrates, fibre, K, Fe and vitamin A than other fruits, but do not have high lipid or protein contents that require excessive energy during formation (Penning De Vries et al., 1983; Robinson & Galan-Sauco, 2010).

(4) The large standing biomass, the long growth cycle of banana and the respiration cost associated with the storage of assimilates in the belowground corm and the translocation to the aboveground bunch might lead to considerable respiration losses. The corm is an underground storage organ, and stored assimilates can be used for bunch filling and sucker development (Eckstein et al., 1995; Robinson & Galan-Sauco, 2010; Twyford & Walmsley, 1973). Maintenance of storage organs during development can account for large respiratory energy use (6-25%) and also translocation leads to respiration losses (Penning De Vries et al., 1983). The long cycle duration of banana crops may also lead to relatively high maintenance respiration losses. The maintenance respiration rate is proportional to the standing biomass, or more precise, to the quantity of N accumulated in the biomass as maintenance respiration is presumably primarily for protein turnover and other processes related to protein content (Amthor & Baldocchi, 2001). Twyford & Walmsley (1973, 1974) observed that a Cavendish banana plantation accumulates between 100 and 300 kg N ha^{-1} cycle^{-1} in its B (for a B accumulation ranging from 14-38 ton DM ha $^{-1}$). Our accumulated B was 32-41 ton DM ha^{-1} cycle^{-1} in FI, with an estimated N uptake of 300-400 kg N ha^{-1} cycle^{-1}. The large standing B and N in our banana plantations, which becomes a more or less constant standing stock with consecutive harvests compensated by new growth, potentially leads to high maintenance respiration losses compared to annual crops with a much shorter growth cycle starting from seedlings.

Of these four hypotheses, the first two would lead to an underestimation of the real WP^* of 11-22% based on our experimental data, while the 3rd and 4th would imply that the WP^* is truly low for banana. In our calculations a WP^* of 11 g m^{-2} (12 g m^{-2} in 2018-2020) was used and a HI_0 of 40%. We hypothesise that the WP^* for banana is in the range of C3 crops due to the underestimation of WP^* based on our data, but that maintenance respiration cost are quite high in a banana field indicating WP^* in banana is near the low range of C3 crops. We do propose that future modelling efforts should increase WP^* by approx. 20% to 15 g m^{-2}, whilst HI_0 should be reduced by 20% to 32%.

A WP^* of 11 g m^{-2} (12 g m^{-2} in 2018-2020) resulted in a proper simulation of standing B and fresh yields with HI_0 of 40% and a bunch DM percentage of 15% at harvest. Our HI_0 falls in the range of previously reported literature values: 20-60% in field grown EAHB Mbwazirume (Taulya, 2015), and 33% in Cavendish Williams (Eckstein et al., 1995; Robinson & Galan-Sauco, 2010). A bunch DM percentage of 15% seems accurate, as Taulya (2015) for Mbwazirume and we in Chapter 6 for Cavendish had similar bunch DM percentage. A commercial bunch is composed of fruit pulp, fruit skin and the peduncle bearing the hands. Composition of a bunch (% peduncle, skin, pulp) changes during bunch development, and as such DM% in the bunch changes over time (Robinson & Galan-Sauco, 2010). Ripe fruit pulp DM percentage is around 20-30% in Cavendish cultivars, and changes over time (Bugaud et al., 2012; Mahouachi, 2007; Robinson & Galan-Sauco, 2010). Bunch DM can thus range approx. between 10-20%, depending on the cultivar and bunch composition (% peduncle, skin and pulp) (Mahouachi, 2007; Robinson & Galan-Sauco, 2010).

7.4.2 Evaluation of model outputs

AquaCrop was able to simulate FI conditions satisfactorily based on most goodness of fit indicators for CC (R^2≥0.93; RRMSE≤15%; NSE≥0.77; d≥0.89), SWC (R^2≥0.55; RRMSE≤13%; NSE≥-4.65; d≥0.52), B (R^2≥0.99; RRMSE≤18%; NSE≥0.58; d≥0.95) and Y (R^2≥0.93; RRMSE≤15%; NSE≥0.72; d≥0.95) (Table ***7-3***), and over time similar patterns were shown between observed and simulated values (Figure 7-3). Although SWC were sometimes underestimated in FI (NSE=-4.62 in C2), values did not drop below stress thresholds for long periods of time. In FI plots, total stress over two crop cycles were 1.25% on

CC expansion, 5.17 % on stomatal closure and 0 % on senescence. This further indicates that FI plots were properly irrigated to achieve optimal production.

RF plots were more significantly stressed over two full growing seasons as SWC in simulations and observations often dropped below moisture stress thresholds in the dry seasons (Figure 7-3B). Cumulative stress was 38% on CC expansion and 42% on stomatal closure. Overall, AquaCrop performance was good to moderately good for modelling RF based on most statistical indicators: CC (R^2≥0.46; RRMSE≤26%; NSE≥0.01; d≥0.69), SWC (R^2≥0.7; RRMSE≤24%; NSE≥0.11; d≥0.75), B (R^2≥0.99; RRMSE≤27%; NSE≥0.26; d≥0.82) and Y (R^2≥0.8; RRMSE≤23%; NSE≥0.24; d≥0.84) (Table ***7-3***). Even though AquaCrop performs well for a range of crops in different environments and irrigation treatments (Steduto et al., 2011), performance has also shown to decline in conditions of water stress in simulating biomass and yields: maize (Sandhu & Irmak, 2019), sorghum (Hadebe et al., 2017), traditional leafy vegetables (Nyathi et al., 2018) and teff (Araya, Keesstra, et al., 2010; Tsegay et al., 2012).

Model fit was worse for SWC of FI compared to RF (Table 7-2). In FI, similar SWC patterns were seen between observed and simulated values, yet simulated values were often lower than observed SWC leading to a suboptimal goodness of fit compared to RF SWC simulations.

This is likely due to the nature of the drip irrigation system in AquaCrop as only a fraction of the soil surface is wetted using drip irrigation. Our moisture sensors observed the soil moisture in the wetted area underneath the drippers which can be wetter than the entire field (as modelled by AquaCrop in the rainy season). This was observed in the SWC simulation patterns as they were close to the observations (TDR sensors), but oftentimes remain lower in the rainy seasons.

Adjusting AquaCrop for drip irrigation in the dry seasons also led to a faster root zone depletion as the entire transpiration (T_r) was assumed to come from the wetted area (f_{root} = 25%). At high CC in the dry season, T_r leads to a very fast depletion of the soil moisture as the T_r needs to come entirely from the limited root zone area (limited in horizontal extent). The smaller the root zone, the faster water was subtracted to feed this T_r demand and the larger SWC fluctuations in the limited root zone. Fluxes in (irrigation) and out (drainage, transpiration) of the root zone were increased under the drip irrigation adjustment. Calibration using a drip system might thereby increase the speed with which moisture stress occurred in the root zone compared to other irrigation systems due to these larger fluxes. Using flood or furrow irrigation would more evenly wet the entire field, resulting in a more extended horizontal root proliferation, and could result in closer fits between TDR sensors and simulations, and a slower SWC depletion in the root zone. The fast depletion in the root zone can be observed by the pronounced simulated SWC fluctuations in the dry seasons in FI plots (August to November 2018 and January to March 2019)(Figure 7-3B). The suboptimal SWC simulations in C2 of the RF plots can also be linked to the drip irrigation adjustment. In the first dry season of 2019 (February to March), SWC was underestimated significantly in RF plots (Figure 7-3B) when several rainfall events took place (Figure 6-1a and Annex II, Figure S1). The horizontal root zone expansion might have been bigger than the assumed 25%, resulting in actual slower SWC subtraction than simulated.

Mabhaudhi et al., (2014a), using actual observed rooting depths of *Colocasia esculenta* L. Schott (Taro) in the field during calibration, observed an underestimation of SWC and B in AquaCrop simulations. They found that increasing rooting depth during calibration (Z_r = 0.80 m) in contrast to what was found in the field (Z_r = 0.45 m) led to a better model fit in terms of SWC and B in drought stressed

plots. For banana, horizontal root expansion was limited to a 0.7 m radius during irrigation in the dry season. However, horizontal expansion of roots in banana mats can be up to 2-3 m (Turner et al., 2007), and based on own observations roots proliferated the entire field in the rainy season. Thus the adjustment of drip irrigation in the dry season focuses all the roots within the area of the wet bulb. This led to a fast depletion of SWC (in FI and RF) and adjustment of B, faster than actually would be the case in the field as the banana plant might be able to subtract water (and thus grow) due to a bigger extended root area. The adjustment for drip irrigation in the dry season did prove to be necessary for continuously irrigated FI plots, as initial calibration for FI plots revealed a bad fit for SWC if not adjusted for drip irrigation (data not shown). Calibrating the model using a different irrigation system than a drip irrigation system (flood, sprinkler, or furrow) might lead to a better fit in terms of *SWC* due to a more even wetting of the field and thereby reduce *SWC* fluctuations in the field.

Simulated B was overestimated slightly in FI C2 and underestimated slightly in RF C2 compared to observed B. This could be due to the suboptimal $cormD$ regressions for determining total B for calibration (Chapter 6). A single model was used for determining $cormD$ in FI and RF mats (eq. 7-7) however the corm might have been different in FI and RF due to increased stress in RF plants. The effect of using treatment specific $cormD$ models (Chapter 6, Table 6-5) increased total B at harvest in FI plants and reduced total B in RF plants by approx. 0.2-0.3 ton DM ha^{-1} $cycle^{-1}$, shifting the observed B upward for an increased $cormD$ in FI, and downwards for a reduced $cormD$ in RF increasing goodness of fit (however slight). Such under and overestimations were not seen in Y as the observed Y was based on actual bunch weights, and the simulated Y was based on the simulated B that in reality could be better than observed B.

Another possible explanation for the underestimation of B in RF C2 could again be the drip irrigation adjustment. Between February to March 2019, there were rainfall events that wetted the entire field, but the drip irrigation adjustment only used the rainfall on the f_{root} (25%) in its calculations. The rainfall outside the simulated f_{root}, contributed to actual B, but not to simulated B. The underestimation of simulated SWC compared to observed SWC during this time, arrested B accumulation in simulations more than was observed in the field (Figure 7-3). In the dry seasons, SWC fell quickly to PWP in RF plots resulting in stomatal closure and impeding biomass buildup. In the rainy seasons, an increase in SWC resulted in opening of the stomata to allow for B buildup. This pattern is seen when viewing simulations and observations (Figure 7-3). Stomata in banana respond fast to soil water contents, and start to close when 20-35% of TAW is depleted (Allen et al., 1998; Carr, 2009). Our stomatal threshold was set to 0.35. The difference between the observed SWC peaks in the first dry season of 2019 (February to March) and the simulated SWC in RF (Figure 7-3B) might explain the plateau in simulated B in these periods, which did not occur as such in the field, leading to a slightly reduced B accumulation in C2. Resetting stomatal threshold values to 0.5 did not improve model fits, indicating the stress thresholds did not lie at the basis of the discrepancy between observed and simulated B values. Roots were assumed to exploit the total field area in the rainy season, and are only assumed to be limited to 25% in the dry season when wetted by drip irrigation, since roots take up water from this wetted area (Carr, 2009). In reality however, horizontal root expansion evolves over time. It takes roots some time to exploit the total field after the rainy season has started, but many die off in the dry season. Moisture outside the horizontal boundary of the root zone container assumed in the dry season can contribute to plant growth, whilst in AquaCrop this moisture was assumed to be lost.

Y simulations performed well in FI plots (R^2≥0.93; RRMSE≤14%; NSE≥0.78; d≥0.95) and in RF plots (R^2≥0.79; RRMSE≤25%; NSE≥0.17; d≥0.8) (Figure 7-3D and Table ***7-3***). In AquaCrop, Y formation occurs due to a linear buildup of the HI from flowering until harvest (after a short lag phase). In banana plants, bunches fill logistically from the onset of flower initiation (Mahouachi, 2007; Robinson & Galan-Sauco, 2010). Simulated Y at harvest only slightly deviated from actual Y for C1 and C2 in both RF and FI (Figure 7-3D) indicating AquaCrop simulated Y correctly.

7.4.3 Towards an AquaCrop banana growth model

7.4.3.1 Successive banana crop files

Back-to-back modelling of C1 and C2 plants showed promising results for modelling repeatedly harvested crops. Using cgc parameters obtained in Chapter 5, setting time to flowering and maturity based on average DTF and DTH as observed in the field (Chapter 6), and setting HI_0 and DM% as observed in FI plots in the field, led to C1 and C2 crop files that could be used successively such that simulated CC, SWC, B and Y could be accurately modelled. Nyathi et al. (2018) simulated repeatedly harvested leafy vegetables under different irrigation regimes by running such successive models with good results. Their successive crop files were similar, but in our research, crop files for C1 and C2 differed significantly for banana. cgc were set to calibrated cgc in C1 (chapter 5) but were reduced in C2 (as canopy seemed to develop slower) leading to a better goodness of fit than using similar cgc in C1 and C2.

A further difficulty in banana plantations is calibration of CC_0 in successive crop files. C2 plants already develop during C1, and CC_0 (size of the follower) in regrowth depends on the size and moment of sucker selection and the conditions under which it develops. Irrigation in C1 will have an effect on the CC_0 of C2, as LAI growth of C2 will be affected by soil moisture during growth of C1 (Chapter 5). CC_0 will be a non-conservative parameter needing local calibration – as for transplanted crops and differing in RF and FI plots between different cycles.

7.4.3.2 Phenological delay in banana

Banana crop parameters were set different between treatments (Table 7-1). AquaCrop uses the growing degree days (GDD) concept to calculate onset of phenological events (McMaster & Wilhem, 1997). GDD are daily heat units accumulated by a plant above a temperature threshold. Temperature drives development, and timing of various phenological stages can be determined after cultivar specific GDD accumulation thresholds are reached. AquaCrop assumes GDD thresholds do not differ between locations under optimal and stressed conditions. In our field, onset of flowering and harvest in RF-C2 plants started to be delayed slightly due to moisture stress (Chapter 6). Flowering can be influenced by environmental factors as soil moisture and photoperiods, and as such GDD from planting until bunch emergence may vary in different locations (Turner et al., 2007). Fortescue et al. (2011) found GDD varied between 3,000-4,200°C d between different planting dates, indicating the large effect of moisture stress and photoperiod on timing to flower emergence. Taulya (2013) likewise found GDD accumulated at flower emergence to vary from 3,000-4,500°C days (in Kawanda, Uganda) and 2,000-3,800 °C days (in Ntungamo, Uganda). Turner, Fortescue and Thomas (2007) likewise discussed the effect of planting date experiments by Lassoudiere (1979) and Turner (1987) on GDD to flower emergence which ranged between 2,500-3,500°C days. A factor other than temperature thereby affects flowering in banana, and the effect of moisture stress on GDD can be very large. Fortescue et al. (2011) showed the inclusion of a stress coefficient based on rainfall and photoperiod

in their calculation of GDD until flower emergence reduced variation in GDD from 3,000-4,200°Cd to 2,200-2,400°Cd. This indicates inclusion of a (water) stress coefficient in AquaCrop during the calculation of GDD seems necessary for banana to simulate the possible large effect of water stress on phenology. So far, the effect of soil moisture on GDD is not embedded in AquaCrop, warranting the different calibration of crop files in FI and RF plots. Calibration of time to phenological events therefore occurred separately for RF and FI plots.

7.4.3.3 Modelling mature plantations

GDD thresholds in banana are also not singular on a plantation level. Flowering and harvest occur within a narrow timeframe in young plantations, but as plantations develop over time, mats develop asynchronously due to both plant physiology (e.g. variation in flowering, sucker emergence, plant death between plants) and management practices (e.g. sucker selection strategy, plant replacement) (Tixier et al., 2004). In C1, flowering was spread over a few weeks (Figure 6-1, Chapter 6 and Figure 7-3): FI plant flowered at 258 (±16.1) DAP, and RF plants flowered at 251 (±17.4) DAP (Chapter 6). In C2, flowering was spread over a few months (Figure 6-1, Chapter 6 and Figure 7-3): FI plants flowered at 589 (±72.6) DAP and RF plants flowered at 656 (±75) DAP (Chapter 6). With increasing cycle, the variation in flowering and harvest increases (Tixier et al., 2004), and a fully mature banana plantation will be composed of individual mats which flower at their own rate, and where harvest occurs year round. Following variation in flowering and harvest, individual mats will also show more variation with increasing cycle in terms of LAI (CC), B and Y as shown by the increase in variance (errorbar) with increasing plantation age (Figure 7-3).

The single flowering and harvest times in our banana C1 and C2 crop files, will thereby be of limited use in a fully mature plantation with plants of all ages. The number of plants flowering and harvested each month will reach a steady state condition under asynchronous sucker selection strategy, or will become highly seasonal under synchronous sucker selection strategy (Tixier et al., 2004). Mature plantations thereby behave more like repeatedly harvested ratoon crops, than flowering plants. In mature plantations characterized by variation in size and phenology, AquaCrop needs to be calibrated as a repeatedly harvested leafy vegetable (as opposed to a fruit crop) as a small fraction of plants are continuously harvested over a full growing season. As such, our crop files which were calibrated as a fruit crop, can only be used for initial plantations. The parameters relating to ET_0 ($Kc_{Tr,x}$) , production ($WP^* *$ and HI_0) , response to water (stress coefficients), harvest index stress effects and temperature (T_{base} and T_{up}) (Table 7-1) are expected to remain valid even in mature plantations, the parameters describing CC, time to flowering and yield and root deepening will need adjustment in mature plantations.

7.5 Conclusion and recommendation

Our study provides a first set of estimates of parameters underlying the AquaCrop growth model for banana modelling, based on field data of two crop cycles under drip irrigated and rainfed conditions. AquaCrop accurately simulated two banana crop cycles for irrigated and rainfed plants across all parameters: CC, SWC, B and Y, although validation against independent datasets still needs to occur to assess if the calibration of conservative parameters was achieved properly. An observed WP^* of 11 g m^{-2} (12 g m-2 for 2018-2020)did seem on the low side for C3 crops, but this value is hypothesized to be closer to 15 g m^{-2} considering: (1) cutting of old leaves, (2) imperfect corm biomass estimation, (3) energy use during bunch filling and (4) large maintenance respiration of stored assimilates and imperfect assimilate cycling between corm and bunch. Stress coefficients for canopy expansion,

stomatal closure and senescence were within reported literature values. Crop files differed between C1 and C2, due to the nature of banana plantations, and differed between FI and RF due to the bananas' phenological delay under drought, which is more pronounced than in other crops. As shown here, successive modelling of banana cycles as a fruit crop, can be used in initial plantations characterized by a narrow flowering and harvest timeframe. This is very helpful for setting up plantations and assessment of risks during the first year, as the first cycle in banana always takes the longest to fulfill. Furthermore, for commercial purposes, plantations are often restarted to achieve harvest peaks when necessary. In mature plantations, calibration as a fruit crop no longer can be used, as plants of all ages and sizes are present, and plantations behave more as repeatedly harvested ratoon crops. However most parameters as $Kc_{Tr,x}$, WP^* and HI_0 and the effect of water and temperature stresses are expected to remain similar in mature plantations. This indicates our crop files are useful even for mature plantations, as data collection underlying parameterization is especially cumbersome and labor intensive given the bananas long cycle duration.

Further research needs to accurately monitor root zones of banana, and soil moisture across the entire field under drip irrigation to further obtain insights in water use and fine tune the drip irrigation adjustment as put forward here. Additional validation on independent datasets for initial plantations needs to occur to show the performance of the AquaCrop banana model as put forward here and assess its use across environments.

In conclusion, AquaCrop has potential for modelling banana plantations and the simple nature of the model provides benefits for wide adoption. Based on our findings, the following recommendations are put forward to increase the use of AquaCrop for banana:

- Validation on independent datasets under different environmental and irrigation systems for young plantations
- Delay of flowering/maturity and other phenological stages due to water stress
- Banana simulated as a repeatedly harvested leafy vegetable in mature plantations.
- A crop module that can combine successive crop files can be included in AquaCrop
- A further fine-tuning of the AquaCrop scheme for drip irrigation as proposed in this study
- An adjustment of the root growth module whereby horizontal root zone expansion is also considered

8 General discussion and conclusions

8.1 Introduction

Water deficit is one of the biggest challenges facing banana production worldwide (Carr, 2009). Irrigation is necessary to reach yield potentials in areas with suboptimal rainfall amounts and to bridge dry periods which, due to the long cycle duration, occur frequently in most banana plantations. In most banana producing regions, rainfed production needs to be supplemented by irrigation to limit drought stress. Fresh water is a finite resource, of which 70% of worldwide supplies are already used for agriculture (Foley et al., 2011; IPCC, 2019). In the banana sector, 99% of water use corresponds to the agricultural production phase (FAO, 2017). Adjustments at the field scale are therefore necessary to reduce water footprints, and production needs to become more robust under increasingly variable climatic conditions. In order to properly guide irrigation, farmers need more certainty of the outcome when investing in irrigation and when changing irrigation schedules. Crop simulation models can assist in assessing production of banana under a wide range of different production scenarios, but previous models were either too mechanistic to be used by farmers, or too inaccurate. Therefore, a new accurate but practical model is necessary to reliably simulate banana production and water balances.

The goal of this thesis was to explore the applicability of the AquaCrop model for banana under optimal and drought stressed conditions. This required a good understanding of the growth behavior of banana under drought, specifically of its growth components canopy cover (Chapter 5), phenology, biomass, and yield (Chapter 6). In Arusha, Tanzania where experiments took place, total yearly rainfall amounts are suboptimal to fully cover a banana's demand, hence rainfed fields experience drought stress. These insights and field data led to a large database with which for the first time, AquaCrop could be calibrated and evaluated for banana (Chapter 7).

The discussion put forward here aims to answer the research questions addressed in the work packages (WP) dealing with the research objectives as put forward in Chapter 1. Firstly, the overall growth behavior of banana plants in the field under irrigated and rainfed conditions was discussed and insights presented to address water stress. Then our AquaCrop banana modelling was discussed in terms of its goodness of fit and adaptation to drip irrigation and the banana growth structure. Next, AquaCrop's applicability and limitations were presented and compared with previous banana models. Finally future research suggestions were presented.

8.2 Effect of drought on field grown banana

Assessment: Irrigated plots were close to optimal production, whereas rainfed plots were not, based on: (1) soil moisture values over the course of the experiment, (2) ratios between moisture received and ET_0 and (3) plant growth parameters and production.

Soil moisture values in the irrigated plots remained close to FC during most of the time of the field trial in both cultivars: Huti Green Bell (HG) and Grande Naine (GN) (Figure 5-2, Figure 6-1 and Figure 7-3). Only HG C1 might have been slightly drought stressed between planting and flower emergence (Chapter 6, Table 6-2) based on the ratio between moisture added (rainfall and irrigation) and ET_0 during this period (R_{PF}). An R_{PF} of 0.743 was reached in HG C1. However, between planting and harvest, total R_{PH} remained above 1 for all irrigated plots, and as such large yields were obtained in both cultivars in both cycles.

Fresh bunch weights in HG FI plots were 25.4 kg plant^{-1} (32.07 ton ha^{-1} year^{-1}) for C1 and 40.8 kg plant^{-1} (45.4 ton ha^{-1} year^{-1}) for C2 (Chapter 6, Table 6-2). HG bunches surpassed rainfed optimally fertilized yields of (Meya, 2021)(Submitted) by 20% in C1 and 8% in C2 working on HG plants in the same area (Tengeru). They reached 27.24 ton ha^{-1} year^{-1} in C1, and 37.78 ton ha^{-1} year^{-1} in C2. Fresh bunch weights in GN FI were 49.6 kg plant^{-1} (71.8 ton ha^{-1} year^{-1}) for C1 and 52.4 kg plant^{-1} (52.1 ton ha^{-1} year^{-1}) for C2 (Chapter 6, Table 6-2). GN yields well surpassed commercial Cavendish plantations of 40-50 ton ha^{-1} year^{-1}(FAO, 2018a).

In well producing plantations, individual plant yields rise between C1 and C2 (Robinson & Galan-Sauco, 2010), which is the case for HG, but not for GN which indicates that GN under the current treatment reached immediately its potential in C1. Given the very high production values in our field, we state that we are close to optimal production. Chapter 7 gives support to this conclusion, as AquaCrop simulations of FI plots revealed very slight total stresses over two crop cycles based on soil moisture values: 2.3 % on CC expansion and 5.8 % on stomatal closure.

In contrast, soil moisture in RF plots often dropped below FC and even reached PWP in the dry seasons leading to drought stress (Figure 5-2, Figure 6-1, and Figure 7-2). Received moisture in RF plots was suboptimal (935 mm year^{-1} for HG and 1,297 mm year^{-1} for GN) compared to optimal values for banana production (1,100 to 2,650 mm year^{-1})(Van Asten et al., 2011) and not evenly spread leading to significant dry periods (Chapter 6, Figure 6-1 and Annex II, Figure S1). In the Arusha region this leads to an estimated annual requirement of 680 to 1,520 mm year-1 evenly distributed moisture (**Figure 2-5**). The ratio between moisture received and ET_0 was thereby suboptimal in RF plots compared to FI plots (R_{FH}<1.1 during bunch filling and R_{PF}< 0.6-0.8 during vegetative growth) although ratios in RF plots were at times optimal too when growth stages coinciding with rain seasons (e.g. R_{FH} > 1.1 in HG-C1 since bunch filling coincided with rainy season)(**Table 6-2**). Overall**,** vegetative growth (e.g. CC, LAI, V_{pseudo}, $ABGVD$, $cormD$), bunch growth (e.g. N_{finger}, N_{hand}, V_{finger}, $bunchF$) and phenology (e.g. time from planting/suckering to bunch harvest) were affected by drought stress in RF plots (**Table 6-2**).

Fresh bunch weights in RF plots were 19.6 kg plant^{-1} (23.3 ton ha^{-1} year^{-1}) for HG C1 and 24.4 kg plant^{-1} (22.4 ton ha^{-1} year^{-1}) for HG C2, and 33.2 kg plant^{-1} (49.24 ton ha^{-1} year^{-1}) for GN C1 and 33.3 kg plant^{-1} (31.84 ton ha^{-1} year^{-1}) for GN C2 (Chapter 6, Table 6-2). Hence yields in RF fields were 27% lower in C1 and 51% lower in C2 for HG, and 31% lower in C1 and 39% lower in C2 for GN. Chapter 7 supports this conclusion, as AquaCrop simulations revealed cumulative stress was 38% on CC expansion and 42% on stomatal closure leading to pronounced water stress.

8.2.1 Effect of drought on canopy cover

Assessment: The CC in banana plantations reacted quickly to moisture stress: (1) over the course of a growing season and (2) diurnally.

In both HG and GN, drought quickly affected leaves as shown by a reduction in LAI and CC in RF, much before plants showed visible signs of drought stress as petiole collapse (Chapter 5, Figure 5-3 and Figure 5-7). LAI and CC at the plot scale started to deviate between RF and FI plots 8-9 weeks after soil moisture in RF plots first diverged from FI values. Deviation of CC from optimal growth curves is an indication of drought stress. Under drought, the cgc in AquaCrop will be reduced through multiplication with the stress coefficient K_{exp}, resulting in a reduction of the cgc parameter (cgc adjusted) which can also lead to a lower CC_x. This was the case for HG, due to onset of moisture stress

during the vegetative growth of C1 (Table 5-4). For GN, cgc was slightly higher in RF treatments, which was due to non-differing moisture regimes during vegetative growth in C1 (Chapter 5, Figure 5-2 and Chapter 6, Table 6-2), leading to similar CC growth curves between FI and RF treatments until flower emergence, still CC_x was lower in RF plots (Chapter 5, Figure 5-3).

CC and LAI development depend on the plant cultivar, used plant density and management. The diploid HG is taller and characterized by narrower more erect leaves (Perrier et al., 2019) than the triploid GN which is shorter, broader and has more horizontal leaves (Ploetz et al., 2007). This was reflected in (1) a lower laf factor for HG (0.66) compared to GN (0.75), (2) a lower extinction coefficient (b) in the CC-LAI curves for HG (0.51) than GN (0.67) (Chapter 5, Figure 5-8) and (3) significantly differing CC growth curves (cgc) between cultivars (Chapter 5, Figure 5-3). At a same spacing, GN plants will cover the ground faster than HG (Chapter 5, Table 5-3). The cgc is considered a conservative parameter in AquaCrop when expressed in GDD (Raes et al., 2018c; Steduto et al., 2012). However, conservative parameters might require adjustment for different cultivar groups (Steduto et al., 2012). This indicates that cgc at a same plant density might be smaller for diploid cultivars, than for triploid cultivars. Our research provides indicative values for both diploid and triploid banana varieties for cgc in AquaCrop modelling. Commonly used plant densities in banana plantations are 2 × 2 m (2,500 plants ha^{-1}) for HG, and 3 × 2.5 m (1,333 plants ha^{-1}) for GN which differ from the studied planting density (1,667 plants ha^{-1}). These commonly used plant densities would result in different CC growth curves, CC-LAI curves and cgc coefficients in AquaCrop, whereby differences between cultivars might be less pronounced.

CC also showed a diurnal pattern in both cultivars under high ET_0, which was increased under soil moisture depletion (Chapter 5: Figure 5-4, Figure 5-5 and Figure 5-6). This diurnal canopy pattern is probably linked to diurnal turgor pressure of the leaves. Turgor pressure reacts quickly to drought in the rooting zone (Zimmermann et al., 2010). Under drought a root derived ABA signal is triggered which is sent to the leaves and results in a reduced stomatal conductance and transpiration (Van Wesemael et al., 2019). Under dry soils, when plants are unable to take up and supply enough moisture to the leaves, turgor pressure drops in the leaf and stomata close. Under optimal irrigation, leaf turgor pressure drops less and recovers during the late afternoon/night, whilst under sub-optimal irrigation leaf turgor pressure drops are more pronounced during the day and may not recover overnight. Leaf folding may thereby be an active process (as opposed to leaf wilting) based on turgor pressure (like leaf rolling in grasses (Baret et al., 2018)), which is enhanced under drought, and is thought to help regulate leaf temperature by reducing solar radiation interception. Further research determining CC in parallel with leaf patch clamps as used by Zimmermann et al. (2010), could prove this hypothesis. Van Wesemael et al. (2019) found transpiration rates of 32 potted banana cultivars in greenhouse conditions to show a marked decrease in the afternoon compared to morning values. Even though all cultivars showed a transpiration decline, timing of stomatal closure, transpiration and leaf gas exchange reduction was cultivar dependent and two groups could be identified: risk takers that close stomata relatively late compared to risk averse cultivars closing stomata earlier in the day. However, the decrease in daily CO_2 assimilation was small compared to the decrease in stomatal conductance indicating more CO_2 was taken up per molecule of water transpired leading to an afternoon increase in WP. Banana thereby seems to contain multiple diurnal water saving mechanisms. Given distinct cultivar groups exist in their daily stomatal closure response, we hypothesize there are cultivar groups differing in their leaf folding response under drought.

8.2.2 Effect of drought on other vegetative, generative and phenological parameters

Assessment: Vegetative parameters, generative parameters and phenological events were all affected by drought depending on the onset of moisture stress.

Drought during the vegetative stage closes stomata, reduces leaf area (Chapter 5: Figure 5-3 and Figure 5-7), resulting in a slower pseudostem growth (V_{rate}) and lower vegetative biomass ($ABGVD$ and $cormD$) (Chapter 6: Figure 6-2 and Table 6-2). This has an effect on bunch yields through a reduced photosynthetic and translocation potential for bunch filling (Dens, Romero, et al., 2008; Eckstein & Robinson, 1995; Robinson & Galan-Sauco, 2010; Twyford & Walmsley, 1973). Drought during the generative phase further reduced yields by affecting bunch components like N_{hand}, N_{finger} (set at flower initiation) and weight ($fingerF$) and volume (V_{finger}) of individual fingers (determined mostly from flower emergence until bunch harvest) (Chapter 6, Figure 6-2 and Table 6-2). The time to flower emergence and time to harvest started to be extended in RF compared to FI plots, leading to longer growing seasons under drought (Chapter 6, Table 6-2). Flower cycle duration was similar in HG, whilst delayed by 14% in GN RF. Harvest cycle duration was delayed by 21% in HG RF, whilst delayed by 5% in GN RF compared to FI plots. As such, cycle duration is affected significantly, and it contributed to the yield differences expressed in units of ton ha^{-1} year^{-1}. This pattern was present in calendar days and GDD after planting in line with findings of Fortescue et al. (2011).

As drought reduced all components governing production in a banana plantation, we checked if allometry was significantly affected under drought. As allometric relationships often underlie crop modelling efforts, allometric plasticity under drought needed to be assessed.

Assessment: Allometric relationships for $ABGVD$ and $cormD$ did not differ significantly between treatments. Allometry based on pseudostem volume (V_{pseudo}) is promising for non-destructive biomass estimation of $ABGVD$, yet $cormD$ remains challenging as it is positioned under the ground.

V_{pseudo} seems a promising indicator for allometry in banana plantations, as it is linked to all components of vegetative growth (Annex IV, Figure S2) and V_{rate} is also linked to bunch growth rates (B_{rate}) (Chapter 6, Figure 6-2, and Figure 6-3). This indicates the universal nature of V_{pseudo} in contrast with earlier allometric equations using only height or girth at base (Nyombi et al., 2009; Wairegi et al., 2009).

Based on V_{pseudo}, $ABGVD$ could be estimated using a single allometric formula for both cultivars and treatments. V_{pseudo} did not seem accurate for properly estimating underground $cormD$ (Chapter 6, Table 6-4), and new research should include corm based parameters (e.g. corm height, corm circumference, number of suckers produced) because a corm stores a lot of biomass. It has to be noted that due to the subterranean position of the corm, such characteristics are hard to measure except during destructive measurements. An option would consist of calculating $cormD$ based on V_{pseudo} and phenology as $cormD$ is a storage organ that shrinks and grows depending to the phenological stage (Taulya, 2013). This would entail first a detailed periodic destructive sampling of a large number of plants to calculate the correlation between $cormD$, aboveground parameters and phenology.

Treatment effects on $ABGVD$ and $cormD$ allometric equations were statistically significant following ANCOVA (reducing intercept and/or slope in RF equations), but these were small as 95%CI overlapped for the model coefficients and goodness of fit remained similar pooling treatments (Chapter 6, Table 6-5). Thereby we concluded drought to not affect allometry significantly for $ABGVD$ and $cormD$. It

could be that V_{pseudo} already reflects differences in DM allocation under drought, such that relationships between V_{pseudo} and $ABGVD$ and $cormD$ remain similar. Van Wesemael et al. (2019) found several banana cultivars to invest more in root growth than in leaf growth under osmotic drought stress in the greenhouse, indicating allometric plasticity under severe stress. Furthermore, Taulya (2013) investigated DM allocation plasticity between above and belowground biomass in response to drought stress, K and N deficiencies. Drought stressed highland banana only increased DM allocation to the corm under K deficient conditions. Their overall bunch yields in plots receiving K and growing under wet conditions (>1,100 mm year^{-1}) were 8-15 ton ha^{-1} year^{-1}, already pointing to severe stress. Drought stress in our fields could not be severe enough to lead to allometric plasticity in the field, as even drought stressed fresh yields remained above 22 ton ha^{-1} year^{-1} for HG and above 31 ton ha^{-1} year^{-1} for GN. Allometric relationships might thus be different in more drought stressed and under nutrient deficient conditions increasing DM partitioning to the corm. This fits with the hypothesis that investment in corm DM is a survival response, which is also observed in tuber crops. Twyford & Walmsley (1973) found additionally that $cormD$ could be increasingly used under stress to fill the bunch, in contrast to non-stressed conditions relying more on newly created photosynthetic DM for bunch filling. Under stress, the $cormD$ could thereby also be negatively affected. The total effects of these stresses (and the stage in which plants are affected) on the estimation of $ABGVD$ and $cormD$ deserves more attention. Future studies calibrating AquaCrop for severely nutrient and drought stressed banana should thereby assess allometry based on an interaction of these stresses for the cultivars used.

Assessment: allometric equations forecasting $bunchF$ based on V_{pseudo} differed significantly between treatments and cultivars due to differences during bunch filling. Forecasting at flowering could estimate potential bunch weights

Allometric relationships for bunch weight ($bunchF$) are cultivar-specific due to differences in DM partitioning between cultivars (Niklas, 2004; Ploetz et al., 2007). The ratio between vegetative biomass and yield at harvest will differ between cultivars as harvest index (HI) ranges between 20-60% (Robinson & Galan-Sauco, 2010). This warrants the use of cultivar specific allometric equations for bunch estimation and thus care needs to be taken when extrapolating existing relationships to other cultivars.

Allometric plasticity occurred under drought in $bunchF$ forecasting models based on $V_{pseudo,flower}$ in both cultivars (Chapter 6: Table 6-5). At similar $V_{pseudo,flower}$, lower $bunchF$ were reached in RF plants due to suboptimal bunch formation under drought (R_{FH} <1.1). R_{FH} was significant in cycles where R_{FH} for RF plants was <1.1, whilst R_{FH} was not significant when both RF and FI plants developed under optimal conditions (R_{FH} >1.1-1.2)(Chapter 6: Table 6-6). A suboptimal R_{FH} during bunch filling reduces $bunchF$ significantly, which is not reflected in $V_{pseudo,flower}$. The distinction between "potential" and "actual" weights is a critical distinction that needs to occur in yield forecasting. Nyombi (2010) and Wairegi et al. (2009) stated that girth at base measured at flower emergence can be used to estimate bunch fresh weights on farm. As drought during bunch filling is not reflected in the $V_{pseudo,flower}$, this is not valid for estimating actual bunch weights. To estimate 'actual' bunch weights, the environmental effects during bunch filling need to be incorporated either directly (e.g., as R_{FH}) or indirectly (incorporating bunch characteristics as e.g. V_{finger}). Our FI allometric equations provides indicative values of the yield to be reached when management after flower emergence is optimal.

Comparing bunch yield potentials based on $V_{pseudo,flower}$ with actual bunch weights in the field, allows farmers to quantify yield losses due to poor management. This can assist farmers in making decisions on whether increased management is justified when comparing to possible yield gains by such management. Economic yield forecasting can also occur in banana fields based on $V_{pseudo,flower}$ for market predictions. Accurate information on banana yields in smallholder farms is lacking (Wairegi et al., 2009).

8.2.3 How to spot and address drought stress in smallholder fields?

Our research shows plantation production is affected significantly by drought. More and more aerial photography is being used in precision agriculture to spot stresses (drought, nutrients, weeds and pathogens) as it allows to quickly assess entire fields in contrast to ground-based observations requiring more sampling points, time and resources (Maes & Steppe, 2019). In banana fields, we have shown CC to be influenced by drought both (1) over the course of a growing season and (2) diurnally, which indicates drone photography can be helpful in assessing drought stress in the field. However, several issues need to be addressed before drones can assist in irrigation scheduling.

Firstly, as CC is highly influenced by cultivar, plant spacing and management it becomes difficult to assess when CC growth curves start deviating from the optimum. In our research, only two cultivars were assessed under one planting density. Changing planting densities and using different cultivars would influence optimal CC curve growth significantly (Nielsen et al., 2012). Optimum curves would be different. Deviations from these optimums cannot be assessed without the presence of a reference plot that is optimally irrigated (something that cannot be assured in farmers' fields). In the Arusha region, banana leaves are also often pruned and used as fodder (Meya, 2021)(submitted), and as CC depends on LAI, leaf management of a plantation also affects CC curves significantly.

A more promising indicator seems to be the diurnal CC variation as this occurred in both cultivars on the same dates. However, CC shows stronger diurnal patterns in response to ET_0 than to soil moisture deficit, and only when comparing drought stressed plots to fully irrigated plots does soil moisture stress becomes apparent due to a more significant and prolonged leaf folding. Drone technology can help spot drought in the field, through leaf folding, but the real strength in spotting drought is the usage of drones with other sensors than the commercial RGB cameras such as modified-RGB cameras measuring NIR, multispectral cameras, hyperspectral cameras, and thermal cameras. Previous drought stress detection using aerial photography mainly relied on thermal images (Maes & Steppe, 2019), and this might also work in banana plantations. Van Wesemael (2015), Vantyghem et al. (2020) and Uwimana et al. (2021) used handheld thermal cameras on plants in Arusha under different moisture conditions and observed plant leaf temperature rising under drought stress due to a drop in transpiration. Vantyghem et al. (2020) evaluated the use of stable carbon isotope ratios ($\delta\ ^{13}C$) and leaf temperature as indicators for stress in the same fields of this thesis. They found significantly higher $\delta\ ^{13}C$ values in RF plots indicating more drought stress. Similarly, during the day, RF banana plant leaf temperature increased by 7°C more than under FI, yet at dawn leaf temperatures were similar. Leaf temperature followed a diurnal pattern, with higher temperatures being reached in RF plants due to closing of the stomata. Even under leaf folding, temperatures rose more in RF leaves. Leaf folding under drought might be a technique by which plants actively aim to reduce temperature when stomata close, but as leaf temperature still increased, this mechanism is an incomplete solution.

When sensors and cameras become increasingly smaller and cheaper, handheld commercial drones can be used to quickly assess drought in the field. Further research could thereby assess the canopy

folding pattern simultaneously with sensors measuring multiple wavelengths and plant thermal regimes. These sensors might also provide insight in plant stress under low ET_0 conditions.

Currently, irrigation scheduling based on visible plant characteristics is considered too late to limit yield losses in banana (Carr, 2009; Surendar et al., 2013). Irrigation can also be applied based on soil moisture in the root zone as this reflects drought sooner than based on plant characteristics. Soil moisture sensors should be positioned in the effective rooting zone of banana where most water absorption takes place (approx. top 0.6 m), and in the region wetted by the dripper heads (approx. 0.2-0.5 m distance from dripper heads supplying 4L hr^{-1}) (Bassoi et al., 2004; Carr, 2009; Coelho et al., 2010). This ensures users of knowing the exact soil moisture in a banana field. However this is too technical and capital intensive for smallholder farmers.

Irrigation can also be performed based on estimated crop water requirements in the field. An indicator can be the ratio between moisture addition and ET_0, in line with the crop development stage. When R < 0.6–0.8 (vegetative stage), and R < 1.1–1.2 (generative stage) plants are affected in the field (Chapter 6, Figure 6-2 and Table 6-2) (Allen et al., 1998; Carr, 2009). Based on daily or weekly ET_0 (estimated based on weather data through the FAO 56 method or through evaporation pans in the field) irrigation can be scheduled indicatively to the plant's need. Irrigation schedules based on R do however not include estimates on soil water storage, which can contribute significantly to irrigation. Carr (2009) reviewed multiple irrigation studies in banana performed in the Tropics, Subtropics and Mediterranean linking crop water use (transpiration) to estimates of ET_0. Transpiration was linearly linked to ET_0, with crop coefficients differing according to location, season, and plant growth stage. Taking this into account, simple irrigation calendars can be created based on crop type, growth stage and climate data in a region. Boesveld et al. (2011) using a simple irrigation calendar for cabbage production in farmers' field trials in Nepal and Zambia, showed a significant reduction in irrigation amounts whilst keeping similar production levels compared to regular farmer practices and regional extension guidelines.

Irrigation schedules based on R can be extended to smallholders through in person meetings, but increasingly digital tools are used. A study in 2016 in Tanzania revealed radio to be the most cost-effective extension service in increasing smallholder participation in legume-based sustainable agriculture, whilst SMS campaigns further increased adoption and awareness when combined with radio campaigns (Silvestri et al., 2020). Mobile phones are not very well spread among farming communities in SSA but smartphone usage is rapidly increasing, allowing to develop internet infrastructure without landlines and moving beyond just normal communication (Kabbiri et al., 2018). In the future when smartphone adoption by farming communities becomes widespread, meteorological services could send daily ET_0 and precipitation updates to smartphones through a wide range of agricultural and meteorological apps to assisting in real time irrigation scheduling (Ferreira et al., 2020).

Most smallholders still rely on intuition for irrigation scheduling. Furthermore, irrigation application in smallholder fields is determined by access to irrigation water which can be suboptimal due to seasonal droughts, sharing of resources between many stakeholders and lack of financial means (Mbonile, 2005). In rainfed agriculture paradigm shifts are necessary and other management interventions need to be tested beyond irrigation scheduling e.g. techniques which might save water in the field, reduce crop water demand, or increase production with suboptimal (physical and/or economic) irrigation amounts (Rockström et al., 2010). A well-calibrated model like AquaCrop can

assist in calculating crop water requirements and developing irrigation calendars whilst also for estimating the effects of water saving management techniques in the field.

8.3 AquaCrop calibration of irrigated and drought stressed banana

Assessment: AquaCrop was able to model the first two cycles of a banana plantation in terms of CC, SWC, and Y in both FI and RF plots.

AquaCrop was set up for the GN cultivar only, as data of two complete growth cycles were collected. Indeed this was not possible for HG, as a storm on 01-01-2019 lead to toppling of a significant number of plants in both RF and FI. As AquaCrop, through its CC, is a population model, toppling of plants affected CC significantly such that data could no longer be used for model calibration after this storm. This resulted in loss of replications of C1 and C2 plants.

Minimally needed components for calibration of AquaCrop (among which periodic measurements of Z_r, CC, SWC, B and Y) (Steduto et al., 2012) were monitored over the course of two crop cycles. We lacked data on actual transpiration (T_r) in the field due to the plant size making a comparison against simulated T_r values impossible. Future experiments with lysimeters could provide T_r data for testing the AquaCrop growth engine under field conditions. Other techniques such as sap-flow meters in banana (Liu et al., 2008), are not practical for field use on fully grown banana plants as they damage plant tissue and need to be calibrated and moved frequently due to the rapid growth of the plant. High resolution dendrometers (stem radius sensors) can also be used to assess transpiration as stem radius variations can be linked to corresponding tree water use (Drew & Downes, 2009; Zweifel, 2016). Zweifel et al. (2001) for example used dendrometers to assess daily stem fluctuations of potted 8 year old Norway spruce, which were linked to whole tree transpiration. While dendrometers are interesting, there remain challenges in turning raw dendrometer measurements into transpiration data (Zweifel, 2016). Also most dendrometer applications have been used in forestry. Tree stems contain bark and woody material, which is very different from the banana pseudostem composed of leaf sheaths. Its pseudostem is fleshy, contains 95% water, a lot of air pockets and is non-woody (Robinson & Galan-Sauco, 2010; Swennen & Rosales, 1994). Dendrometers have yet to be used in banana research, and firstly need to be adjusted to the banana herbaceous pseudostem before transpiration research can even be conceived (Steppe, personal communication). Secondly, dendrometer stem radius changes need to be assessed in parallel to actual transpiration measurement in greenhouse pot trials. Leaf patch clamps (Zimmermann et al., 2008; Zimmermann et al., 2010) can also be used in measuring diurnal water fluxes in the leaf, and could similarly as dendrometer readings be used to assess whole plant transpiration. However, this technology is still considered too experimental for field use to assess actual transpiration rates. In the future, novel techniques to measure T_r which are less expensive than lysimeters, and more accurate than sap-flow meters, dendrometers and leaf patch clamps, should be used to get indicative values of whole field transpiration.

Stresses other than drought were avoided. Fertilizers and manure were added, plots were weeded monthly, no pests were present, temperature stress was not present and due to optimal EC_e values of irrigation water, and no inherent high salt content in the soil profile, salt stress was not present. Plants might have been affected by Black Sigatoka (*Pseudocercospora fijiensis*) in the long wet season of 2018. However since maximum physiological activity occurs in the last two to five emerged leaves for Grande Naine cultivars (Carr, 2009), and only the oldest leaves showing symptoms were cut, together with high production levels in FI plots, we conclude stress caused by diseases was minimal.

AquaCrop was able to simulate dynamically CC, SWC, B and Y during the first two cycles of a banana plantation (Chapter 7, Table ***7-3*** and Figure 7-3). FI plots were simulated satisfactorily for CC (R^2≥0.93; RRMSE≤15%; NSE≥0.77; d≥0.89), SWC (R^2≥0.55; RRMSE≤13%; NSE≥-4.65; d≥0.52), B (R^2≥0.99; RRMSE≤18%; NSE≥0.58; d≥0.95) and Y (R^2≥0.93; RRMSE≤15%; NSE≥0.72; d≥0.95) (Chapter 7, Table 7-2), and over time similar patterns were shown between observed and simulated values (Figure 7-3). RF plots were likewise simulated with good accuracy CC (R^2≥0.46; RRMSE≤26%; NSE≥0.01; d≥0.69), SWC (R^2≥0.7; RRMSE≤24%; NSE≥0.11; d≥0.75), B (R^2≥0.99; RRMSE≤27%; NSE≥0.26; d≥0.82) and Y (R^2≥0.8; RRMSE≤23%; NSE≥0.24; d≥0.84) (Chapter 7, Table 7-2).

Adaptations to the AquaCrop model proved necessary: (1) adjustments for drip irrigation and (2) adjustments because of the multi-cycle banana growth structure.

8.3.1 Drip irrigation adjustments

Assessment: Adjustments to the AquaCrop modelling scheme were necessary to model drip irrigation in a plantation setting, yet lead to a fast depletion of moisture in the rooting zone

Drip irrigation in the dry season only wets a portion of the soil, leading to a large horizontal heterogeneity of the soil moisture content. Yet AquaCrop assumes a homogeneous soil profile in the horizontal direction (Raes et al., 2018c). As banana roots only take up water from the wet area in the dry season (Carr, 2009; Robinson & Galan-Sauco, 2010), this entailed an adjustment to the AquaCrop model structure (Chapter 7, Figure 7-2 and Annex VI).

Our adjustment assumed roots to be present over the entire horizontal field in the rainy season and limited to the area wetted by the drippers in the dry season (Chapter 7, Figure 7-2). Alternation between rainy and drip irrigated dry seasons in AquaCrop assumed rooting zones to be adjusted overnight, which is never the case under field conditions. This could have contributed to the underestimation of $SWCs$ in FI and RF plots. By focusing all the roots within the wet bulb in the dry season, SWC depletions occurred faster than observed in the field. Fluxes in (irrigation) and out (drainage, transpiration) of the root zone were increased under the drip irrigation adjustment. Calibration using a drip system could increase the speed with which moisture stress occurs in the root zone compared to other irrigation systems due to these larger fluxes. Using flood or furrow irrigation would more evenly wet the entire field, resulting in a more extended horizontal root proliferation, and could result in closer fits between moisture observations and simulations, and a slower SWC depletion in the root zone. Precipitation events during the dry season also wetted the area outside the wet bulb, but this moisture was assumed to be irrelevant using our modelling scheme. The underestimation of SWC is linked to the underestimation of simulated B in RF plots. Based on underestimated $SWCs$ adjustments of B might have occurred faster than observed in the field, as banana might have been able to subtract water beyond this area.

More improvements can be made in the future by considering a dynamic horizontal root zone in AquaCrop based on actual root dynamics in the rainy and dry seasons. Root studies, drip irrigation studies and TDR grid measurements and modelling of the 3D water flow and root water uptake should complement one another in assessing the zones where banana subtract moisture in the dry and rainy season. Such studies can show the region where roots are active to determine the fraction where roots subtract water for input in the drip irrigation adjustment. This seems to be more relevant than trenching methods, as these reveal the presence of roots, but do not provide an indication on root activity.

8.3.2 Crop parameter sets for the first two cycles of a banana plantation

Assessment: Calibrated banana crop parameters differ between cycles and treatments. Non-conservative parameters might still require local-calibration, whereas conservative parameters can be considered as calibrated – yet validation still needs to occur.

During the calibration process, banana was treated as a fruit crop which was harvested twice. Crop parameter files were created for C1 and C2 separately (Chapter 7, Table 7-1). Our results show that AquaCrop can accurately capture such plantation dynamics in a banana field for the first two growth cycles by successive modelling of C1 and C2 crop files. Back-to-back modelling of successive cycles was also accurately done by Nyathi et al. (2018) simulating alfalfa. Their C1 and C2 files were similar, but in banana several parameters differ between C1 and C2.

AquaCrop makes a distinction between conservative crop parameters (parameters that do not require local calibration) and non-conservative crop parameters (parameters that change with the cultivar, management, and environmental conditions) (Chapter 7, Table 7-1 and Annex I, Table S1). Generally, conservative parameters should be calibrated only once and are expected to remain constant under different growing conditions and water regimes (Steduto et al., 2012).

Conservative parameters governing transpiration ($Kc_{Tr,x}$), biomass production (WP^* and HI_0) and the effect of stress (water stress thresholds) are the most important. A WP^* of 11 g m^{-2} (12 g m^{-2} for the year 2018-2020) showed best model fits for banana. WP^* in C3 crops ranges from 15-20 g m^{-2} (Raes et al., 2018a; Steduto et al., 2012). Our WP^* thereby seems low for a C3 crop, but with this calibrated value for WP^* we achieved good model for results for B and Y in the field. Several hypotheses exist for a possible underestimation of the WP* in our experiments: (1) removal of old leaves and (2) imperfect corm biomass estimation. Other hypotheses imply the WP^* for banana should be truly on the low side for C3 crops: (3) energy use during bunch filling lowering WP^* and (4) considerable respiration losses due to assimilate cycling between corm and bunch, and maintenance respiration. We thereby suggest future research to increase WP^* by 10-20% to 15 g m^{-2} (lower range of C3 crops), whilst simultaneously reducing HI_0 by 10-20%. Based on observed data, a HI_0 of 40% and a bunch DM % of 15 was set in AquaCrop leading to proper Y simulation in FI plots. HI_0 is within the range of observed literature values for banana (Robinson & Galan-Sauco, 2010), whilst a DM% of 15% was similarly reached by Taulya (2015) for EAHB.

Water stress coefficient indicators were set based on literature values and adjusted iteratively to achieve good model fits. p_{exp-up} for canopy expansion was set at a depletion of 30% TAW, whilst p_{sto} for stomatal closure, was set at a depletion of 35% TAW, which is within reported literature values (Allen et al., 1998; Carr, 2009). RF simulations underestimated B very slightly but resetting stomatal thresholds to 50% TAW did not improve model fit, indicating stress coefficients are not at the basis of this discrepancy. Instead the underestimations of B were linked to underestimations in SWC. Conservative parameters were set similarly for both C1 and C2 (except for $Kc_{Tr,x}$).

There are indications that the conservative *WP** parameter and water stress coefficient settings might still differ between groups of banana cultivars. The relative contribution of the B genome seems to lead to increased drought stress resistance in banana plants (Carr, 2009; Kissel et al., 2015; Van Wesemael et al., 2019). Kissel et al. (2015) studied transpiration efficiency (dry matter accumulated per liter water transpired) of six banana cultivars in greenhouse conditions and found cultivars containing a B genome had a higher transpiration efficiency under drought (pF < 2.8). Van Wesemael

et al. (2019) studied growth performance of 32 banana cultivars under non-stressed and osmotic drought stress in pots in the greenhouse. Cultivar performance (aboveground biomass accumulation) differed significantly between cultivars under both control and osmotic stress conditions. Transpiration rates also differed between cultivar groups: some cultivars closed stomata earlier in the day reducing daily transpiration, whilst other cultivars kept stomata open longer leading to a higher daily transpiration. The large transpiration reduction in the afternoon did not lead to such a pronounced difference in CO_2 assimilation and water use efficiency thereby increased in the afternoon when stomata close. Different cultivars thereby show differences in daily Tr and water use efficiency. Whether differences are still pronounced in the field needs to be investigated, as the previous research was conducted on potted plants in screenhouses.

Non-conservative parameters describing root deepening, CC development and phenology are cultivar, management and soil dependent and thus require local fine tuning. Soil type and restrictive layers significantly influence banana root growth (Carr, 2009), but on average roots mostly subtract water between 0.4-0.6 m depth. Our root parameters ($Z_{r,min}$ and $Z_{r,max}$) can be taken as a starting point and need only to be fine-tuned under soil conditions which are very different from our current experimental conditions.

With other cultivars, plant densities and a different sucker selection strategy, an additional fine-tuning of CC parameters would be required. The CCs of a seedling is considered conservative (Steduto et al., 2012), yet the CC_0 and CC_x of a plantation depend strongly on cultivar, plant spacing (which is non-conservative according to Steduto et al., (2012)) and management (Chapter 5). Furthermore, CC_0 of cycles beyond C1 is much higher than in C1 due to the development of these cycles already during the development of previous cycles. CC_0 of successive cycles needs to be adjusted based on the total stresses (on leaf extension and stomatal closure) received during the previous growth cycle as these will determine LAI and CC of the following cycle (Chapter 5). CC_0 of C2 also depends on the sucker selection strategy of the farmer. Suckers in our field were selected at the same time (4 MAP) at a same side of the banana mat to keep plantation lines (Annex II). Consequently not always the most vigorous sucker was selected. If the most vigorous sucker would have been selected a faster CC growth could have been possible. Harvest dynamics in the field also determine CC patterns in the field. If many plants are harvested in a short time interval, the CC would decline rapidly unlike when harvesting would be spread over a longer time. This provides a challenge in setting accurate CC_0 values in succeeding cycles, hence the need to calibrate this non-conservative parameter to local conditions. In fully mature plantations, with a more heterogeneous plantation structure and a more continuous harvest, a stable CC may be reached (see further).

Calibration of banana as a fruit crop entailed the setting of phenological events based on observed flower emergence and harvest maturity (Chapter 7, Table 7-1). Phenological events are non-conservative in AquaCrop (Steduto et al., 2012) and vary between different cultivars, cycles, and treatments (Chapter 6). Figure 8-1 shows flower emergence and harvest peaks expressed in GDD after planting for both cultivars and treatments based on collected data for flower emergence and harvest dates in Chapter 6. It shows flower emergence and harvest peaks for C1 and C2 in HG and GN differ significantly. This reveals that the setting of cultivar and cycle specific phenological thresholds in banana is not as straightforward as in other crops. Care has to be taken to reach conclusions on HG-C2 flower emergence and harvest as a large portion of plants toppled in the field before they could be measured. The presented data are from data collected before the storm or from non-toppled plants in the field.

Assessment: as drought delays flowering and maturity, singular GDD thresholds underlying the AquaCrop model need to be adjusted for moisture stress through specific Ks coefficients. Furthermore, singular GDD thresholds will no longer be valid in a mature plantation as flowering and harvest become continuous with increasing cycling

The growth cycle of banana started to be extended under RF conditions in both cultivars (Chapter 6, Table 6-2). This entailed the setting of phenological events differently in the different treatments (Chapter 7, Table 7-1). It appears flower emergence and harvest peaks of RF plants started to be delayed (in days and in GDD) (Figure 8-1). A stress coefficient based on soil moisture (as incorporated in the STICS and LINTUL models) could be used in GDD calculation in AquaCrop such that this behavior is accounted for.

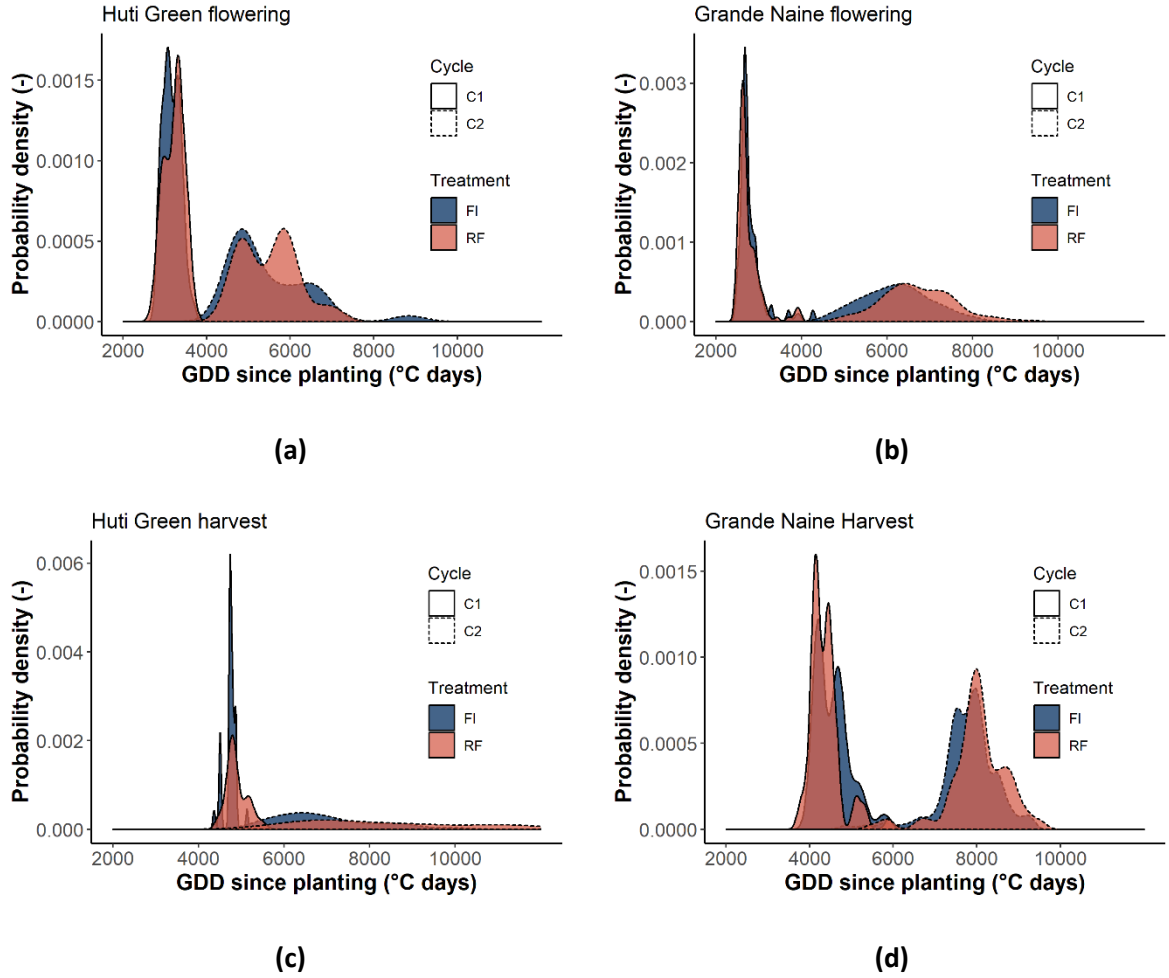


Figure 8-1: Probability density functions of the time expressed in growing degree days (GDD) of banana mats in a plantation flowering and harvest-ready: a) flowering of Huti green Bell plants, b) flowering of Grande Naine plants, c) harvest of Huti Green plants, d) harvest of Grande Naine plants. Time is expressed in GDD since planting of cycle 1. Only harvest ready plants were included in the calculation of probability density. Flowering notes flower emergence. FI notes fully irrigated, RF notes rainfed. C1 denotes cycle 1, C2 denotes cycle 2.

Not only is there a cultivar and treatment effect, there also seems to be a cycle effect. Flower emergence and harvest in C1 occurred within a narrower timeframe than flowering and harvest in C2 in both FI and RF plots as shown by an increased standard deviation in these values (Chapter 6, Figure 6-1c and Table 6-2). This is also shown when expressed in GDD since planting as peaks for flower emergence and harvest are higher and within a narrower timeframe in C1 than C2 (Figure 8-1). This

increased variation in phenology with cycling, together with phenology delay under drought, will result in a heterogeneous plantation over time (Lamour et al., 2020; Tixier et al., 2004). Choosing a different sucker selection strategy in which the most vigorous suckers are selected might reduce the variation and spread of flowering and harvest in C2, yet over time a heterogeneous plantation would still result. This indicates that singular GDD thresholds can only be used in young plantations and are no longer useful in mature banana plantations. Mature banana plantations thus need another modelling method.

8.3.3 Modelling mature banana plantations

According to Tixier et al. (2004) the number of bunches harvested per week evolves from significant harvest peaks in the initial cycle, to a steady state system in later cycles depending on the sucker selection strategy (Figure 8-2). Harvest peak dynamics in Figure 8-2 were outputs of SIMBA-POP which was calibrated based on data from fields in Guadeloupe and Martinique growing Grande Naine with no major stress present (hurricanes, drought or pests) (Tixier et al., 2004). An asynchronous sucker selection strategy, whereby best suckers are selected from each mat, regardless of their position and time of suckering, is mostly used by smallholder farmers, and leads to a fully heterogeneous plantation structure where plants of all ages are present in the field. Farmers do that to secure food security during the year unlike commercial plantations which would rather prefer to have peak harvests when prices are high and use a synchronous sucker strategy, selecting suckers of similar height.. Robinson and Galan-Sauco (2010) mention flowering and harvest peaks also depend on environment. In the humid tropics, with relatively stable temperatures and light conditions year round, plantations develop a stable steady state system whereby flowering and harvest become uniform year round. In the subtropics, where seasonality in temperature, light and rainfall is more pronounced, time to flowering and harvest will become highly seasonal. Harvest dynamics in the field are thereby dependent on sucker selection strategy, temperature, lighting, and moisture received during growth.

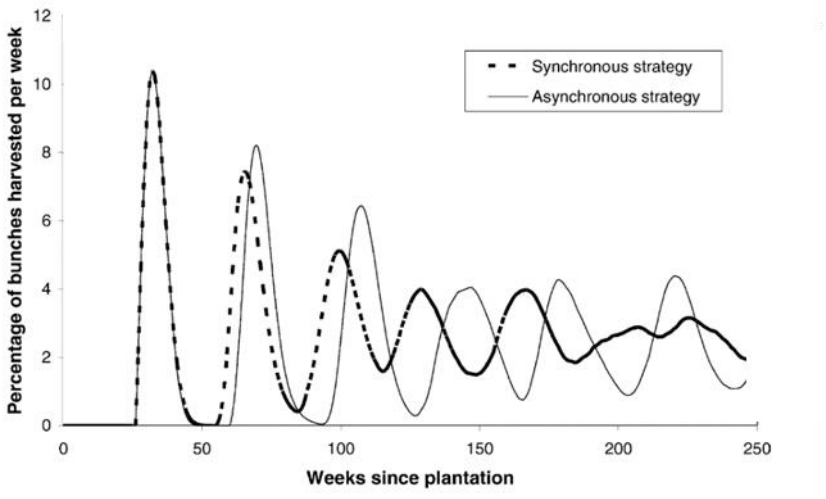


Figure 8-2: Number of bunches harvested per week (% of total plantation) for 2 sucker selection strategies. Source: Tixier et al. (2004).

In contrast to fruit crops being harvested once or twice over the course of a season, mature banana plantations could be calibrated as a repeatedly harvested vegetable/forage crop in AquaCrop, similarly to procedures used for simulation of perennial herbaceous forage crops (Raes et al., 2020). Perennial herbaceous forage crops are characterized by a relatively stable CC and rooting depth Z_r, and are cut

multiple times over the course of a growing season. These cuttings are specified in AquaCrop, and the B cut away is converted to actual forage to feed animals (Y). The frequency of cutting events, and the amount of cut away CC, B and Y are inputs in such a model and need to be assessed in mature banana plantations.

It is assumed that in a plantation in the humid tropics, the frequency of harvest (% plants harvested per week) evolves towards 1-5% per week with a synchronous sucker strategy, and about 2-3% per week with an asynchronous sucker strategy (Figure 8-2). Taking an asynchronous sucker strategy, the CC is expected to reach a steady state level. Turner et al. (2007) indicated LAI values of > 5 m² m^{-2} to be reached in mature plantations. At such LAI values, CC is close to maximum for both HG and GN based on our CC-LAI curves (Chapter 5, Figure 5-8). Assuming similar harvest fractions of approx. 2% per week over the course of a year (Tixier et al., 2004), would lead to less than 2% reduction in LAI, leading to negligible CC fluctuations. The CC_0 after harvest and CC_x before cutting would then be similar. T_r and B could be calculated based on this steady state CC, and adjusted to stresses (e.g. moisture stress) according to the calculation procedures in AquaCrop. Weekly Y could be simulated by multiplying the total B in the field with the HI of a mature mat (adjusted by stresses), and the percentage of mature mats harvested in the field each week (which is assumed to be relatively stable in the humid tropics).

In a plantation in the subtropics (or a synchronous sucker selection strategy in the humid tropics), the frequency of harvest would become more seasonal. The seasonal nature of harvest would lead to more pronounced CC fluctuations since a large number of harvested plants in a short timeframe would lead to a more pronounced CC drop after harvest. In that situation, CC_0 after harvest and CC_x before cutting may no longer be similar and would follow a seasonal pattern. T_r, B and Y could then also be calculated based on this seasonal CC according to the calculation procedures in AquaCrop. Weekly Y could again be simulated multiplying the total B in the field with the HI of a mature mat (adjusted by stresses), and the percentage of mature mats harvested in the field each week (which now would be seasonal in the subtropics).

To model mature plantations with AquaCrop, one would require to correctly predict the harvest dynamics, i.e. the faction of plants harvested each week in a given year. Harvest dynamics in mature plantations are the key for the next step in AquaCrop modelling. These need to be studied in light of moisture stress in the field. Banana delays phenological events under drought compared to non-stressed conditions (Fortescue et al., 2011; Robinson & Galan-Sauco, 2010; Turner et al., 2007) and this was also observed in our experiments. Therefore, the effect of drought on harvest dynamics in a mature field needs to be assessed. In a humid environment with stable rainfall amounts over time and an asynchronous sucker selection strategy, harvest dynamics are expected to become stable over time. In a sub-humid environment with pronounced dry seasons, harvest dynamics in rainfed fields are expected to become highly seasonal, compared to irrigated fields where dynamics will be more stable over time. Actual monitoring of mature plantations (in the tropics and subtropics) on CC, SWC, B and Y in combination with flowering and harvest dynamics of irrigated and rainfed fields needs to occur to gather a database for further modelling with AquaCrop.

8.4 AquaCrop usefulness and applicability

8.4.1 AquaCrop validation and performance

To gain a robust set of well performing crop parameters for the banana plant, additional validation on independent datasets needs to occur in multi-year and multi-location trials under different water regimes (Hsiao et al., 2009; Vanuytrecht, Raes, Steduto, et al., 2014).

Modeling with AquaCrop has been carried out for a multitude of crops under different environmental conditions under different levels of irrigation regimes and water stress (e.g. wheat in Northern China (Iqbal et al., 2014) and Iran (Andarzian et al., 2011), quinoa in the Bolivian Altiplano (Sam Geerts et al., 2009), maize in Texas, California, Spain (Steduto et al., 2011), soybean in Nigeria (Adeboye et al., 2019) and Lebanon (Abi Saab et al., 2014), and many others). At the moment 15 crops are embedded in the AquaCrop model of which most are annual. Major crop types are cereals (maize, wheat, rice, barley, quinoa, sorghum), tubers (potato, sugar beet), vegetable crops (tomato), legumes (soybean, Bambara groundnut, alfalfa) and grasses (sugarcane, teff). Hence perennial crops are underrepresented. Performance of AquaCrop was shown to vary for different crops and production scenarios. Simulations are often satisfactory, but performance is suboptimal under environments when very different from the ones of original calibration (Steduto et al., 2011). Model performance has been shown to decline in conditions of severe water stress in multiple studies using multiple crops: maize (Abedinpour et al., 2012; Sandhu & Irmak, 2019), sorghum (Hadebe et al., 2017), traditional leafy vegetables (Nyathi et al., 2018), teff (Araya, Keesstra, et al., 2010; Tsegay et al., 2012), wheat (Castañeda-Vera et al., 2015). Water stress in AquaCrop assumes that water is distributed homogenously over the horizontal rooting zone, which is not always the case (especially under drip irrigation as shown in Chapter 7). Introducing heterogeneous horizontal soil moisture distribution in AquaCrop (as proposed in chapter 7) could better represent drought in the rooting zone in the field but increases complexity in the model which may lead to suboptimal moisture balances. A finetuning of our proposed adaptation for drip irrigation, considering dynamic horizontal root distribution and water uptake could lead to better performance.

Multiple sensitivity analyses for the AquaCrop model also revealed influential parameters depend on environmental conditions (crop, soil, climate) in which the model is used. Depending on the production situation, some parameters can be more sensitive in the calibration process (i.e. affect simulation outputs with small changes in the parameter values) whilst others can be less sensitive (i.e. its values could change significantly without influencing simulations) (Guo et al., 2020; Jin et al., 2018; Silvestro et al., 2017; Steduto et al., 2011; Vanuytrecht, Raes, & Willems, 2014). This warrants the need for further local calibration of crop parameters and particularly validation of model outputs under different environments. Upon validation of our crop parameter set, particular attention should be paid to the most sensitive conservative parameters as identified by Vanuytrecht, Raes, & Willems (2014).

Non-conservative crop parameters (Chapter 7, Table 7-2) are cultivar dependent. When using cultivars different from our study, they always need fine tuning (Steduto et al., 2012). Thus, model parameters as proposed in our study could deviate in other banana cultivars warranting cultivar-specific calibration of non-conservative parameters. Dépigny et al. (2017) showed crop parameters in their AAB simulation model to vary between different plantain cultivars. Their model parameter values could be divided into distinct cultivar groups. Calibrating AquaCrop for more cultivars might similarly reveal cultivar or ploidy group parameter sets.

8.4.2 AquaCrop-banana usefulness for agriculture in SSA

Our research provides parameter sets for Cavendish production in the East African Highlands. Using our proposed crop parameter values will allow the user to get indicative simulation results in this area and provides a start for additional validation under different conditions.

Agriculture in SSA is mostly rainfed, and where irrigation is applied in smallholder fields, this is mostly through traditional techniques as flood or furrow irrigation or manual application by collecting water from village pumps (Mbonile, 2005; Xie et al., 2014). In the upper-Pangani Basin, where this research was conducted, 80% of irrigation systems are smallholder furrow irrigation schemes (Mbonile, 2005). A wide range of agricultural practices in banana plantations can be simulated in AquaCrop: crop management, soil management, weed and nutrient management, application of mulches and other field management practices (Steduto et al., 2012; Vanuytrecht, Raes, Steduto, et al., 2014). However, AquaCrop does not simulate the effect of pests and diseases on production, which may be significant in smallholder production situations (Ploetz et al., 2015). Given AquaCrop is a water-driven/crop water productivity software, rainfed production and/or multiple irrigation types (flood, furrow, sprinkler or drip irrigation) and schedules can be modelled with the same software (Vanuytrecht, Raes, Steduto, et al., 2014). As such, our calibrated banana crop parameters could be used to model diverse banana production scenarios. Simulation outputs from AquaCrop could be used in a variety of ways e.g. developing irrigation schedules (full, deficit and supplemental) (Linker et al., 2016), determining the influence of field management on soil moisture and production in rainfed plantations (e.g. application of mulches)(Adeboye et al., 2019), assessing the effect of planting density on CC, water use and yield (Wellens et al., 2013) and determining impact of climate change on yield, assess economic risks and possible adaptation strategies (Bird et al., 2016). Simulations would provide users with a first assessment of how production can be increased in banana plantations.

8.4.3 AquaCrop versus other banana models

8.4.3.1 Model structure comparison

A comparison of AquaCrop with previous modelling efforts in banana reveals several key features of AquaCrop. Models differ substantially in their degree of complexity, adjustment to the banana cropping structure, growth engine and intended use (Table 8-1). AquaCrop distinguishes itself from other presented crop models as it: (1) has a daily simulation time step, (2) uses *CC* instead of *LAI* for growth, (3) has a water driven growth engine (*WP*), (4) has an extensive soil moisture balance, field management and irrigation scheduling component and (5) uses a relatively low number of easily intuitive model parameters (Abdalhi & Jia, 2018; Vanuytrecht, Raes, Steduto, et al., 2014). We now discuss each of these seven points below.

(1) Most models use a daily simulation timestep except for SIMBA and the AAB plantain model (weekly) and CENTURY (monthly). Transpiration and growth can already be affected when soil moisture drops below thresholds on a daily timeframe (Carr, 2009; Zimmermann et al., 2010). A weekly or monthly time step becomes suboptimal in simulating soil moisture balances and irrigation scheduling. For example, irrigation frequency in drip irrigated fields may be daily or twice-daily to limit drought stress, thereby limiting the use of crop models with a weekly or monthly time step for such a scenario.

(2) AquaCrop uses CC as an indicator for growth, whereas other models use LAI. Using LAI has benefits as LAI can easily be separated for each cycle by calculating LAI of C1, LAI of C2 and LAI of

C3 (Chapter 5), whilst CC cannot be separated between cycles. This separation of LAI per cycle allows the simulation of the DM production in each plant on a mat separately by modelling LAI of plants individually and calculating the fraction of light intercepted by the different canopy layers. LAI allowed STICS, SIMBA, LINTUL and AAB plantain models to describe biomass buildup and allocation across cycles and organs in a very elaborate manner.

Using CC in AquaCrop simplifies the model structure. It is easier to estimate CC than LAI in the field. However, CC cannot be separated between the different cycles. As AquaCrop uses CC, it acts as a field population model that models banana mats instead of individual cycles. This makes more sense because DM partitioning occurs across cycles on the same corm individual cycles on a mat are naturally connected. DM partitioning is even found to occur across cycles (Dens, Romero, et al., 2008). Total DM of a mat could later be allocated to the different cycles in AquaCrop through partitioning coefficients.

(3) Previous modelling efforts used a radiation-driven growth engine based on the intercepted light by the *LAI* based on the *LUE* of the canopy (Chapter 3). AquaCrop uses a different approach and relies on the link between Tr and B based on the WP of the crop. The use of WP has benefits over LUE. A WP_b^* (normalized for CO_2 and ET_0) can be used across climates, growth conditions and similar crop cultivars (Steduto et al., 2007a). In contrast LUE factors vary with cultivar, age, water deficit, leaf nitrogen content, temperature and other stresses (Sinclair & Muchow, 1999; Steduto, 2006; Van Ittersum et al., 2003). Using the *WP* concept puts water limited production at the core of modelling in AquaCrop.

(4) Incorporation of water-stress occurs in all models containing a water balance component (STICS, SIMBA, LINTUL2) through the use of water stress coefficients (K_s) based on the soil water balance. All models that include a soil moisture balance component, considered the soil as a water reservoir where fluxes in (capillary rise, irrigation, rainfall, and subsurface flow) and out (runoff, deep percolation, transpiration, evaporation, and subsurface flow) determine the amount of water in the rooting zone. The description, considered water fluxes and corresponding detail of the water balance varies in the presented models and is most detailed in AquaCrop. All models in Table 8-1 do not simulate subsurface flow. AquaCrop simulates all other fluxes whereas e.g. STICS, SIMBA-WAT and LINTUL2 do not incorporate capillary rise which can be significant depending on the location of groundwater. The soil layer description is also different in the models and most detailed in AquaCrop. Where LINTUL allows users to only create a single soil layer (bounded by the rooting depth), AquaCrop allows the user to create soil layers of up to five horizons (which can further be subdivided by the model for calculation purposes) and uses more extensive soil water balance calculations than a simple tipping bucket approach mostly used in other models.

Table 8-4: Model structure and adaptations to the banana structure of previous crop modelling efforts on Banana and AquaCrop.

	CENTURY	**STICS**	**SIMBA**	**LINTUL**	**AAB plantain**	**AquaCrop**
Source	(Woomer et al., 1998)	(Brisson & Dorel, 1998)	(Tixier et al., 2008)	(Nyombi, 2010; Taulya, 2015)	(Dépigny et al., 2017)	(this study)
Model structure						
Daily timestep		x		x		x
Radiation driven (LUE)	x	x	x	x	x	
Water driven (WUE)						x
Canopy cover based						x
Soil-water balance/stress effect		x	x	x		x*
Nutrient balance/stress effect		x	x			x
Irrigation management component		x	x	x		x
Extensive calibration, model structure and difficulty in parameterization	x	x	x	x	x	
Adjustments to banana structure						
Multiple cycles			x	x		x
Phenology (GDD) adjustment to stress		x		x		**
Singular GDD phenology thresholds		x		x	x	x
Log-normal GDD phenology thresholds			x			***

Note: *extensive soil water balance, **proposed adjustment for incorporation of phenology stress effect on GDD, ***proposed adjustment to incorporate heterogeneous mat (GDD) structure (mature plantations)

In line with the more detailed soil description and soil-water balance in AquaCrop, the model also incorporates a more detailed irrigation management component where type (rainfed, flood, furrow, sprinkler, dripper), amount and frequency of irrigation application can be added. The AquaCrop software is thus built specifically for modelling water-limited production and irrigation scheduling. Other models (STICS, SIMBA, LINTUL) also contain water application components: STICS allows to describe irrigation application and type (over canopy, under canopy and drip irrigation), SIMBA-WAT does not incorporate a specific irrigation application module, but irrigation amounts need to be added to incoming rainfall, whilst LINTUL2 allows to incorporate irrigation amounts and frequency, but not irrigation type. Irrigation application can thus be modelled in the field in many models, but where some models can only describe irrigation as inputs and provide rough irrigation guidelines as outputs (e.g. water application needed to keep soil at FC), AquaCrop can create more extended irrigation schedules (deficit, supplemental, and optimal) as model outputs, thereby increasing user friendliness.

(5) AquaCrop uses a relatively low number of easily intuitive input variables in contrast with other crop models. Model comparison studies (Abi Saab et al., 2015; Todorovic et al., 2009a; Van Gaelen, 2011, 2016) have shown AquaCrop to require less input than e.g. CERES, STICS, WOFOST and CropSyst. This increases the model applicability especially in data sparse regions (Castañeda-Vera et al., 2015).

8.4.3.2 Adjustment to the banana cropping structure

Models differ in their adjustment to the banana growth structure. Banana differs foremost from other crops in that it is (1) perennial, (2) multiple cycles grow on the same mat, (3) neighboring mats in the field are different and (4) phenology is delayed under drought. CENTURY and STICS only simulated the growth of one cycle, whilst the others tried to incorporate the multi-cycle nature of banana. SIMBA is most adjusted to the banana growth structure. These models incorporate the perennial and multi-cycle cropping structure in their models. SIMBA-POP incorporated sucker development, flowering and harvest using a log-normal distribution in GDD (Tixier et al., 2004). In SIMBA, these distributions drive the development of heterogeneity as neighboring mats become dissimilar over time (Figure 8-2), but a delay under drought stress on these distributions is not included. LINTUL and the AAB plantain model can also simulated multiple cycles on the same mat, yet assumed all mats in the field to be homogenous (Dépigny et al., 2017; Nyombi, 2010; Taulya, 2015). Sucker emergence, flowering and harvest were all assumed to occur after a set singular GDD threshold was reached, which is not accurate in banana (Figure 8-1). Their theoretical multiple cycling behavior was furthermore only used to simulate a single banana cycle. Our AquaCrop-banana model simulating C1 and C2 follows the LINTUL system in that it assumes singular thresholds for flowering and harvest, which remains valid in young banana plantations, but no longer in mature plantations. Our suggestion put forward for modelling mature plantations incorporates the heterogeneity of mats in AquaCrop yet would remain simpler than the extensive SIMBA structure. This would allow the parsimonious nature of AquaCrop to remain valid for future modelling. The delay of phenology under drought was incorporated in STICS and LINTUL2 as these models incorporated a drought stress coefficient that was multiplied with daily GDD calculation when stress occurred.

8.4.3.3 Model performance comparison

Performance of banana crop models varies significantly (Table 8-2). Overall, AquaCrop performance in our study was evaluated in terms of CC, SWC, B and Y; components of water limited production. Other crop models differ in terms of evaluated variables during banana simulation. Some models did not compare any model simulations with actual observations in the field (CENTURY, LINTUL1), such

that their performance cannot be assessed. These models were theoretical explorations of the potential for modelling banana plantations.

STICS, SIMBA, LINTUL2 and AAB model provided a subset of simulated outputs for comparison against observed values (Table 8-2). However, many model simulation outputs were not compared with actual field observations.

Table 8-5: Model performance comparison between different banana modelling exercises. Simulated variables note simulation outputs of the model: leaf area index (LAI), canopy cover (CC), biomass (B), soil water content (SWC) and yield (Y).

Model	Simulated variable	Evaluation	Data source
CENTURY	B	-	(Woomer et al., 1998)
STICS	LAI	Graphically good fit	(Brisson & Dorel, 1998)
	SWC	Graphically suboptimal fit	(Brisson & Dorel, 1998)
SIMBA models			
SIMBA-POP	Date of harvest peaks	R^2=0.99	(Tixier et al., 2004)
SIMBA-GROW	LAI	-	(Tixier et al., 2008)
	B	-	(Tixier et al., 2008)
	Y	R^2=0.55-0.72 and RRMSE=26.3%	(Tixier et al., 2008)
SIMBA-WAT	SWC	RRMSE=20.6%	(Tixier et al., 2008)
LINTUL model			
LINTUL1	Potential LAI, B and Y	-	(Nyombi, 2010)
LINTUL2	LAI	-	(Taulya, 2015)
	SWC	R^2=0.05-0.15 and RRMSE=3-8%; Graphically suboptimal	(Taulya, 2015)
	B	R^2= 0.87-0.89 and RRMSE=7-8%; Graphically suboptimal	(Taulya, 2015)
	Y	2-3 times higher than observed Y	(Taulya, 2015)
AAB plantain	LAI	Cultivar dependent model fit; graphically	(Dépigny et al., 2017)
	B	Cultivar dependent model fit; graphically	(Dépigny et al., 2017)
	Y	Cultivar dependent model fit; RRMSE=3.1-50.3%	(Dépigny et al., 2017)
AquaCrop			
FI treatment	CC	R^2=0.98 and RRMSE=10%	This study
	SWC	R^2=0.62 and RRMSE=12%	This study
	B	R^2=1 and RRMSE=18%	This study
	Y	R^2=0.99 and RRMSE=15%	This study
RF treatment	CC	R^2=0.86 and RRMSE=24%	This study
	SWC	R^2=0.85 and RRMSE=17%	This study
	B	R^2=1 and RRMSE=21%	This study
	Y	R^2=0.98 and RRMSE=22%	This study

Note: "-" notes parameters whose performance was not or could not be evaluated

The STICS model can e.g. simulate LAI, B, DM allocation to organs, root growth, SWC and Y. Brisson & Dorel (1998) used STICS for modelling banana growth, but only compared simulations and observations for LAI, root growth and SWC. Root growth (root length density, RLD) was overestimation in STICS (0.25 $cm^3 cm^{-3}$) compared to maximum observed RLD in banana in their fields (0.12 cm^3 cm^{-3}). For irrigated treatments, Brisson & Dorel (1998) mention the SWC in the root zone was accurately simulated in the root zone in the beginning of the growth season but simulated SWC started to deviate significantly (was excessive) from observed values when the crop started to cover

the soil. This could not be checked since graphs and goodness-of-fit indicators were not presented for SWC in irrigated treatments. For RF treatments, a graph of SWC observations and simulations was presented. SWC simulations followed partially the variations in observed SWC variations due to rains. Often higher or lower SWC were observed in the field compared to simulations indicating suboptimal performance. LAI was modelled satisfactorily as LAI simulations and observations coincided almost completely. In general, performance of the model could not properly be assessed. Goodness-of-fit indicators for RLD, SWC and LAI were lacking and performance could thus only assessed be assessed visually. Visually, LAI appeared to be simulated accurately, but RLD and SWC were suboptimal. No simulations and observations were presented for B and Y.

SIMBA is composed of many sub-models. These submodules were previously assessed in terms of performance separately (Table 8-2). For simulating banana production under water deficit, we were only interested in assessing model performance of sub-models handling on phenology (SIMBA-POP), plant growth (SIMBA-GROWTH) and water balance (SIMBA-WAT).

SIMBA-POP performs accurately. Validation of the model was carried out on harvest data from seven field plots in Guadeloupe. The model estimated the cumulative number of harvested bunches very accurately (R^2 = 0.98, n=1058), and the model was able to accurately predict 29 harvest peaks within 3 weeks of the observed peak. The model becomes less accurate in observing harvest peaks over time (beyond cycle 3), but this is because harvest peaks become more spread out over time evolving to a steady state scenario. SIMBA-GROW (like STICS) can model LAI, B, DM allocation to plant organs and Y, but model performance was only assessed for Y at harvest (Tixier et al., 2008). Validation was performed based on independent data collected from a field survey in Guadeloupe in 2000. Y (ton DM ha^{-1} $year^{-1}$) was simulated moderately good to moderately poor based on R^2 (0.55-0.72) and RRMSE (26.3%). Other validation outputs of the SIMBA-GROW module (LAI, B) were not published in their research. SIMBA-WAT, the sub-model simulating water balances, was calibrated for fields (soil conditions) of Guadeloupe based on collected rainfall, run-off, and water potential (SWC) measurements over the course of 12 months. Validation on independent data in fields of Guadeloupe revealed SWC (soil water potential) was simulated moderately good (RRMSE 20.6%). The creators of the SIMBA model themselves mention that SIMBA performance cannot be validated in its entirety. Whether good individual sub-model performance leads to proper total model performance when the sub-models are linked cannot be certain. It is unsure how accurate water-limited production of banana can be simulated by linking SIMBA-POP, SIMBA-GROW and SIMBA-WAT. An extensive evaluation of these linked models needs to occur first.

LINTUL2 added a water balance to LINTUL1 to assess water-limited production of the EAHB Kisansa in the field. LINTUL2 was calibrated and validated in 2 regions in Uganda (Ntungamo and Kawanda). LINTUL2 performance was evaluated in terms of SWC, B (total DM of organs) and Y (bunch DM). The model was validated on 24 and 27 plants in Ntungamo and Kawanda, respectively. Performance of the calibrated model was quantitatively evaluated using 1:1 plots of predicted vs. observed values for SWC and B (total DM) and used goodness-of-fit indicators were R^2 and RRMSE. B simulations showed good model fit in terms of R^2 (0.87-0.89) and RRMSE (7-8%), yet a graphical comparison showed B simulations to differ significantly from observed values from planting to harvest. Comparing these graphs with goodness-of-fit results leads to considerable doubt on the accuracy of the presented goodness-of-fit results for B. Total SWC showed very poor to poor model fit in terms of R^2 (-0.05 – 0.15), yet very good model fit in terms of RRMSE (3-8%). However, simulated SWC showed to differ extensively from observed SWC over time. SWC simulations showed similar patterns than

observations, but SWC was continuously overestimated in Kawanda and underestimated in Ntungamo compared to actual SWC. Difference testing further revealed that all observed B components at harvest (leaves, pseudostem, bunch, corm) were significantly different from simulated values (p<0.05). The simulated Y (6.5 ±0.3 kg DM plant^{-1}) was 2 to 3 times higher than observed bunch weights in the field (2.7±0.2 kg DM plant^{-1}). Model performance in simulating SWC, B, and Y were thus poor.

The AAB plantain model did not incorporate a soil water balance and only modelled potential production under optimal conditions. Model performance was evaluated graphically in terms of LAI and B. Overall the model described the LAI trend accurately, although several cultivars showed slight under-and overestimations of the LAI curve. A similar pattern was observed for B. Model accuracy of the AAB model was next evaluated quantitatively by comparing observed and simulated Y at harvest (bunch DM kg plant^{-1}) in terms of RRMSE. For the different cultivars RRMSE ranged from 3.1% (very good) to 50.3% (very poor), revealing cultivar dependent performance of the model. In the cultivar groups with better fit (RRMSE<25%) LAI and B were simulated accurately. In the cultivar groups with worse fit (RRMSE >25%), LAI and B simulations showed deviations from observed values. Poor results could also be explained due to a difference in growth behavior and allocation patterns between cultivars which might have been described too basic in the model structure.

Comparing the performance of AquaCrop with other model performance assessments then reveals: (1) that this study using AquaCrop assessed multiple indicators (CC, SWC, B and Y) for water limited growth as opposed to other models and (2) model fit of AquaCrop for these indicators is often better than other models (e.g. LINTUL2). To fully compare model performance of AquaCrop with other models a comparison study should be undertaken. A field experiment should be performed under water limited conditions where banana production data (e.g. periodic CC, LAI, SWC, B and Y) is compared to simulations using different models (e.g. AquaCrop, SIMBA, LINTUL2).

8.4.4 Recommendations for future research on AquaCrop

Our research focused on banana plantations during its first two cycles and on well fertilized plants. Our research only focused on water limited production of banana. In order to simulate nutrient-limited growth, a database on nutrient stressed plots needs to be gathered as well. Future research should also involve mature plantations from commercial banana plantations or farmers' fields to calibrate AquaCrop for heterogeneous plantations. Given the detailed nature of this experiment, validation plots in other areas could not be set up to assess the value of our models across sites – this naturally still needs to occur to assess the validity of model parameters as put forward here. These efforts should lead to the ongoing development of an AquaCrop model on banana with wider applicability. Building on the list of proposed research suggestions in Chapter 7, our overall recommendations for future research are:

- Validation of parameter sets on independent data needs to occur in multi-year, multi-location trials using different irrigation systems and schedules.
- More fine-tuning of the AquaCrop scheme for drip irrigation can be done by inclusion of a horizontal root zone expansion and water uptake module in AquaCrop.
- The AquaCrop model performance needs to be assessed for other cultivars (under different plant densities and sucker selection strategies). Preferably cultivars that show promise for withstanding drought stress better (B genome) and that are commercially or locally

important. This will lead to a check of non-conservative parameter sets and assess whether they differ among cultivar groups.

- Delay of flowering, maturity and other phenological stages due to water stress in banana can be embedded in AquaCrop by a new GDD calculation scheme as used currently in STICS and LINTUL models.
- In mature plantations, banana can be treated as a repeatedly harvested leafy vegetable. Calibration (and subsequent validation) on mature banana plantations, in parallel with flower emergence and harvest dynamic research, should lead to an AquaCrop banana model for plantations beyond the first cycles.

References

Abdalhi, M. A. M., & Jia, Z. (2018). Crop yield and water saving potential for AquaCrop model under full and deficit irrigation managements. *Italian Journal of Agronomy*, *13*(4), 267–278. https://doi.org/10.4081/ija.2018.1288

Abedinpour, M., Sarangi, A., Rajput, T. B. S., Singh, M., Pathak, H., & Ahmad, T. (2012). Performance evaluation of AquaCrop model for maize crop in a semi-arid environment. *Agricultural Water Management*, *110*, 55–66. https://doi.org/10.1016/j.agwat.2012.04.001

Abele, S., Twine, E. E., & Legg, C. (2007). Food Security in Eastern Africa and the Great Lakes Technical Report. In *USAID crop crisis control project*. International Institute of Tropical Agriculture.

Abi Saab, M. T., Albrizio, R., Nangia, V., Karam, F., & Rouphael, Y. (2014). Developing scenarios to assess sunflower and soybean yield under different sowing dates and water regimes in the Bekaa valley (Lebanon): Simulations with Aquacrop. *International Journal of Plant Production*, *8*(4), 457–482.

Abi Saab, M. T., Todorovic, M., & Albrizio, R. (2015). Comparing aquaCrop and cropSyst models in simulating barley growth and yield under different water and nitrogen regimes: Does calibration year influence the performance of crop growth models? *Agricultural Water Management*, *147*, 21–33. https://doi.org/10.1016/j.agwat.2014.08.001

Abràmoff, M. D., Magalhães, P. J., & Ram, S. J. (2004). Image processing with imageJ. *Biophotonics International*, *11*(7), 36–42.

Adeboye, O. B., Schultz, B., Adekalu, K. O., & Prasad, K. C. (2019). Performance evaluation of AquaCrop in simulating soil water storage, yield, and water productivity of rainfed soybeans (Glycine max L. merr) in Ile-Ife, Nigeria. *Agricultural Water Management*, *213*, 1130–1146. https://doi.org/10.1016/j.agwat.2018.11.006

Adhikari, U., Nejadhashemi, A. P., & Woznicki, S. A. (2015). Climate change and eastern Africa: A review of impact on major crops. *Food and Energy Security*, *4*(2), 110–132. https://doi.org/10.1002/fes3.61

Ali, M. H., & Talukder, M. S. U. (2008). Increasing water productivity in crop production-A synthesis. *Agricultural Water Management*, *95*(11), 1201–1213. https://doi.org/10.1016/j.agwat.2008.06.008

Allen, R. G., Pereira, L. S. L. S., Raes, D., & Smith, M. (1998). Crop Evapotranspiration: Guidelines for computing crop water requirements. In *FAO Irrigation and Drainage Paper 56* (Vol. 56). https://doi.org/10.1016/j.eja.2010.12.001

Amthor, J. S., & Baldocchi, D. D. (2001). Chapter 3: Terrestrial Higher Plant Respiration and Net Primary Production. In *Terrestrial Global Productivity* (pp. 33–59). https://doi.org/10.1016/b978-012505290-0/50004-1

Amthor, J. S., Bar-Even, A., Hanson, A. D., Millar, A. H., Stitt, M., Sweetlove, L. J., & Tyerman, S. D. (2019). Engineering strategies to boost crop productivity by cutting respiratory carbon loss. *Plant Cell*, *31*(2), 297–314. https://doi.org/10.1105/tpc.18.00743

Andarzian, B., Bannayan, M., Steduto, P., Mazraeh, H., Barati, M. E., Barati, M. A., & Rahnama, A. (2011). Validation and testing of the AquaCrop model under full and deficit irrigated wheat production in Iran. *Agricultural Water Management*, *100*(1), 1–8. https://doi.org/10.1016/j.agwat.2011.08.023

Araya, A., Habtu, S., Hadgu, K. M., Kebede, A., & Dejene, T. (2010). Test of AquaCrop model in simulating biomass and yield of water deficient and irrigated barley (Hordeum vulgare).

Agricultural Water Management, *97*(11), 1838–1846. https://doi.org/10.1016/j.agwat.2010.06.021

Araya, A., Keesstra, S. D., & Stroosnijder, L. (2010). Simulating yield response to water of Teff (Eragrostis tef) with FAO's AquaCrop model. *Field Crops Research*, *116*, 196–204. https://doi.org/10.1016/j.fcr.2009.12.010

Bahmani, O., & Eghbalian, S. (2018). Simulating the Response of Sugarcane Production to Water Deficit Irrigation Using the AquaCrop Model. *Agricultural Research*, *7*(2), 158–166. https://doi.org/10.1007/s40003-018-0311-0

Baret, F., Madec, S., Irfan, K., Lopez, J., Comar, A., Hemmerlé, M., Praud, S., & Tixier, M. H. (2018). Leaf-rolling in maize crops: from leaf scoring to canopy-level measurements for phenotyping. *Journal of Experimental Botany*, *69*(10), 2705–2716. https://doi.org/doi:10.1093/jxb/ery071

Bassoi, L. H., Teixeira, A. H. D. C., Lima Filho, J. M. P., Silva, J. A. M. E., Silva, E. E. G. Da, Ramos, C. M. C., & Sediyama, G. C. (2004). Guidelines for irrigation scheduling of banana crop in São Francisco Valley, Brazil. II - Water consumption, crop coefficient, and physiologycal behavior. *Revista Brasileira de Fruticultura*, *26*(3), 464–467. https://doi.org/10.1590/S0100-29452004000300022

Bello, Z. A., & Walker, S. (2017). Evaluating AquaCrop model for simulating production of amaranthus (Amaranthus cruentus) a leafy vegetable, under irrigation and rainfed conditions. *Agricultural and Forest Meteorology*, *247*, 300–310. https://doi.org/10.1016/j.agrformet.2017.08.003

Bergez, J. E., Leenhardt, D., Colomb, B., Dury, J., Carpani, M., Casagrande, M., Charron, M. H., Guillaume, S., Therond, O., & Willaume, M. (2012). Computer-model tools for a better agricultural water management: Tackling managers' issues at different scales - A contribution from systemic agronomists. *Computers and Electronics in Agriculture*, *86*, 89–99. https://doi.org/10.1016/j.compag.2012.04.005

Bird, D. N., Benabdallah, S., Gouda, N., Hummel, F., Koeberl, J., La Jeunesse, I., Meyer, S., Prettenthaler, F., Soddu, A., & Woess-Gallasch, S. (2016). Modelling climate change impacts on and adaptation strategies for agriculture in Sardinia and Tunisia using AquaCrop and value-at-risk. *Science of the Total Environment*, *543*, 1019–1027. https://doi.org/10.1016/j.scitotenv.2015.07.035

Blomme, G., Draye, X., Rufyikiri, G., Declerck, D., De Waele, D., Tenkouano, A., & Swennen, R. (2000). Progress in understanding the roots of Musa spp. *In Inibap Annual Report 1999*, *9*, 14–19.

Blomme, G., Swennen, R., & Tenkouano, A. (1999). Assessment of variability in the root system characteristics of banana (Musa spp.) according to genome group and ploidy level. *Infomusa*, *9*(2), 4–7.

Blomme, G., & Tenkouano, A. (1998). Effect of plant age and ploidy on estimated and actual leaf area of banana plants. *Infomusa*, *7*(2), 6–7.

Bodner, G., Nakhforoosh, A., & Kaul, H. P. (2015). Management of crop water under drought: a review. *Agronomy for Sustainable Development*, *35*, 401–442. https://doi.org/10.1007/s13593-015-0283-4

Boesveld, H., Zisengwe, L. S., & Yakami, S. (2011). Drip Planner Chart: A simple irrigation scheduling tool for smallholder drip farmers. *Irrigation and Drainage Systems*, *25*, 323–333. https://doi.org/10.1007/s10795-012-9127-4

Bouman, B. A. M., Van Keulen, H., Van Laar, H. H., & Rabbinge, R. (1996). The "School of de Wit" crop growth simulation models: A pedigree and historical overview. *Agricultural Systems*, *52*(2–3), 171–198. https://doi.org/10.1016/0308-521X(96)00011-X

Brisson, N., & Dorel, M. (1998). Effects of soil management and water regime on banana growth between planting and flowering. *Acta Horticulturae*, *490*, 229–238.

Brisson, N., Gary, C., Justes, E., Roche, R., Mary, B., Ripoche, D., Zimmer, D., Sierra, J., Bertuzzi, P., Burger, P., Bussière, F., Cabidoche, Y. M., Cellier, P., Debaeke, P., Gaudillère, J. P., Hénault, C., Maraux, F., Seguin, B., & Sinoquet, H. (2003). An overview of the crop model STICS. *European Journal of Agronomy*, *18*, 309–332. https://doi.org/10.1016/S1161-0301(02)00110-7

Brown, A., Tumuhimbise, R., Amah, D., Uwimana, B., Nyine, M., Mduma, H., Talengera, D., Karamura, D., Kuriba, J., & Rony, S. (2017). Bananas and Plantains (Musa spp.). In *Genetic Improvement of Tropical Crops* (pp. 219–240). https://doi.org/10.1007/978-3-319-59819-2

Bugaud, C., Belleil, T., Daribo, M. O., & Génard, M. (2012). Does bunch trimming affect dry matter content in banana? *Scientia Horticulturae*, *144*, 125–129. https://doi.org/10.1016/j.scienta.2012.06.035

Carr, M. K. V. (2009). The water relations and irrigation requirements of banana (Musa spp.). *Experimental Agriculture*, *45*(1), 333–371. https://doi.org/10.1017/S001447970900787X

Castañeda-Vera, A., Leffelaar, P. A., Álvaro-Fuentes, J., Cantero-Martínez, C., & Mínguez, M. I. (2015). Selecting crop models for decision making in wheat insurance. *European Journal of Agronomy*, *68*, 97–116. https://doi.org/10.1016/j.eja.2015.04.008

Champion, J. (1963). *Le bananier*. G.P.-Maisonneuve & Larose.

Chaves, B. C., Cayón, G. S., & Jones, J. W. (2009). Modeling plantain (Musa AAB Simmonds) potential yield. *Agronomía Colombiana*, *27*(3), 359–366.

Christelová, P., De Langhe, E., Hřibová, E., Čížková, J., Sardos, J., Hušáková, M., Van den houwe, I., Sutanto, A., Kepler, A. K., Swennen, R., Roux, N., & Doležel, J. (2017). Molecular and cytological characterization of the global Musa germplasm collection provides insights into the treasure of banana diversity. *Biodiversity and Conservation*, *26*, 801–824. https://doi.org/10.1007/s10531-016-1273-9

Coelho, E. F., Da Silva, A. J. P., & De Miranda, J. H. (2010). Sensor placement for soil water monitoring in banana crop irrigated by drip irrigation systems. *Eng. Agríc. Jaboticabal*, *30*(4), 608–618.

Damour, G., Ozier-Lafontaine, H., & Dorel, M. (2012). Simulation of the growth of banana (Musa spp.) cultivated on cover-crop with simplified indicators of soil water and nitrogen availability and integrated plant traits. *Field Crops Research*, *130*, 99–108. https://doi.org/10.1016/j.fcr.2012.02.013

Darko, R. O., Yuan, S. Q., Yan, H. F., Liu, J. P., & Abbey, A. (2016). Calibration and validation of aquacrop for deficit and full irrigation of tomato. *International Journal of Agricultural and Biological Engineering*, *9*(3), 104–110. https://doi.org/10.3965/j.ijabe.20160903.1812

De Buck, S., & Swennen, R. (2016). Bananas: the green gold of the South. In *VIB Fact Series*. https://doi.org/D/2016/12.267/3

De Langhe, E., Hřibová, E., Carpentier, S., Doleel, J., & Swennen, R. (2010). Did backcrossing contribute to the origin of hybrid edible bananas? *Annals of Botany*, *106*, 849–857. https://doi.org/10.1093/aob/mcq187

De Langhe, Edmond. (1995). Banana and Plantain: the Earliest Fruit Crops? In *INIBAP Annual Report 1995*.

de Wit, C. T., Brouwer, R., & de Vries, F. W. T. (1970). The simulation of photosynthetic systems. *Proceedings of the IBP/PP Technical Meeting, Trebon, 14-21 September 1969*, 47–70.

Dens, K. R., Romero, R. A., Swennen, R., & Turner, D. W. (2008). Removal of bunch, leaves, or pseudostem alone, or in combination, influences growth and bunch weight of ratoon crops in two banana cultivars. *Journal of Horticultural Science & Biotechnology*, *83*(1), 113–119. https://doi.org/10.1080/14620316.2008.11512355

Dens, K. R., Swennen, R. L., Romero, R. A., & Turner, D. W. (2008). Simulation of Banana Plant Growth (Musa spp. AAA, Cavendish Sub- Group) Based on Temperature and Ontogeny. *Acta Horticulturae*, *803*, 181–186.

Dépigny, S., Lescot, T., Achard, R., Diouf, O., Cote, F. X., Fonbah, C., Sadom, L., & Tixier, P. (2017). Model-based benchmarking of the production potential of plantains (Musa spp., AAB): Application to five real plantain and four plantain-like hybrid varieties in Cameroon. *Journal of Agricultural Science*, *155*, 888–901. https://doi.org/10.1017/S0021859616000964

Dorel, M. (2001). Effet des pratiques culturales sur les propriétés physiques des sols volcaniques de Guadeloupe et influence sur l'enracinement du bananier [Université catholique de Louvain]. In *Thèse de doctorat*. https://agritrop.cirad.fr/485591/

Dorel, M., Achard, R., & Tixier, P. (2008). SIMBA-N: Modeling nitrogen dynamics in banana populations in wet tropical climate. Application to fertilization management in the Caribbean. *European Journal of Agronomy*, *29*(1), 38–45. https://doi.org/10.1016/j.eja.2008.02.004

Draye, X., Delvaux, B., & Swennen, R. (1999). Distribution of Lateral Root Primordia in Root Tips of Musa. *Annals of Botany*, *84*, 393–400. https://doi.org/0305-7365/99/090393

Drew, D. M., & Downes, G. M. (2009). The use of precision dendrometers in research on daily stem size and wood property variation: A review. *Dendrochronologia*, *27*, 159–172. https://doi.org/10.1016/j.dendro.2009.06.008

Eckstein, K., & Robinson, J. C. (1995). Physiological responses of banana (Musa AAA; Cavendish sub-group) in the subtropics. II. Influence of climatic conditions on seasonal and diurnal variations in gas exchange of banana leaves. *Journal of Horticultural Science*, *70*(1), 157–167. https://doi.org/10.1080/14620316.1995.11515285

Eckstein, K., Robinson, J. C., & Davie, S. J. (1995). Physiological responses of banana (Musa AAA; Cavendish sub-group) in the subtropics. III. Gas exchange, growth analysis and source-sink interaction over a complete crop cycle. *Journal of Horticultural Science*, *70*(1), 169–180. https://doi.org/10.1080/14620316.1995.11515286

Eisenhauer, J. G. (2003). Regression through the Origin. *Teaching Statistics*, *25*(3), 76–80.

Ekanayake, I. J., Ortiz, R., & Vuylsteke, D. R. (1994). Influence of Leaf Age, Soil Moisture, VPD and Time of Day on Leaf Conductance of Various Musa Genotypes in a Humid Forest - Moist Savanna Transition Site. *Annals of Botany*, *74*, 173–178.

Ekanayake, I. J., Ortiz, R., & Vuylsteke, D. R. (1998). Leaf stomatal conductance and stomatal morphology of Musa germplasm. *Euphytica*, *99*, 221–229. https://doi.org/10.1023/A:1018311912407

Emerman, S. H. (1996). The tipping bucket equations as a model for macropore flow. *Journal of Hydrology*, *174*(1), 23–47.

Eyland, D., Breton, C., Sardos, J., Kallow, S., Panis, B., Paofa, J., Tardieu, F., Welcker, C., & Janssens, S. B. (2020). Filling in the gaps in Gene Banks: Collecting, Characterizing and Phenotyping Wild Banana Relatives of Papua New Guinea. *Crop Science*, *Adapting agriculture to climate change: a walk on the wild side*. https://doi.org/10.1002/csc2.20320.

FAO. (1978). *Report on the agro-ecological zones project - V1: Results for Africa. World soil resources report 48/1*.

FAO. (1996). *Agro-ecological zoning guidelines. FAO Soils Bulletin 73.* FAO Soils Bulletin; FAO. http://www.fao.org/3/W2962E/W2962E00.htm (Last accessed 12/01/2020)

FAO. (2012). *GAEZ: Global Agro-Ecological Zones*. Food and Agricultural Organisation. http://www.fao.org/nr/gaez/en/ (Last accessed 12/01/2020)

FAO. (2014). *Water withdrawal by sector, around 2007*. AQUASTAT Database. http://www.fao.org/nr/aquastat (Last accessed 12/01/2020)

FAO. (2015). *Banana Facts: world banana production, exports and imports*. FAO Infographics. http://www.fao.org/resources/infographics/infographics-details/en/c/297695/ (Last accessed 12/01/2020)

FAO. (2017). Water footprint of the banana industry. In *World Banana Forum*. http://www.fao.org/3/a-i6914e.pdf

FAO. (2018a). *Banana facts and figures*. FAOSTAT EST: Banana Facts. http://www.fao.org/economic/est/est-commodities/bananas/bananafacts/en/#.W--lHTgzbIU%0A (Last accessed 12/01/2020)

FAO. (2018b). *The future of food and agriculture – Alternative pathways to 2050*. http://www.fao.org/3/I8429EN/i8429en.pdf

FAO. (2020). *AquaCrop*. AquaCrop. http://www.fao.org/aquacrop/en/ (Last accessed 12/01/2020)

FAO, IFAD, UNICEF, WFP, & WHO. (2018). The State of Food Security and Nutrition in the World 2018. Building Climate Resilience for Food Security and Nutrition. In *State of the world*. https://doi.org/10.1093/cjres/rst006

FAOSTAT. (2019). *Banana and plantain production data*. http://www.fao.org/faostat/en/#data/ (Last accessed 12/01/2020)

Farahani, H. J., Izzi, G., & Oweis, T. Y. (2009). Parameterization and evaluation of the aquacrop model for full and deficit irrigated cotton. *Agronomy Journal*, *101*(3), 469–476. https://doi.org/10.2134/agronj2008.0182s

Ferreira, L. B., da Cunha, F. F., de Oliveira, R. A., & Rodrigues, T. F. (2020). A smartphone APP for weather-based irrigation scheduling using artificial neural networks. *Pesquisa Agropecuaria Brasileira*, *55*, 1–10. https://doi.org/10.1590/S1678-3921.PAB2020.V55.01839

Foley, J. A., Ramankutty, N., Brauman, K. A., Cassidy, E. S., Gerber, J. S., Johnston, M., Mueller, N. D., O'Connell, C., Ray, D. K., West, P. C., Balzer, C., Bennett, E. M., Carpenter, S. R., Hill, J., Monfreda, C., Polasky, S., Rockström, J., Sheehan, J., Siebert, S., … Zaks, D. P. M. (2011). Solutions for a cultivated planet. *Nature*, *478*, 337–342. https://doi.org/10.1038/nature10452

Fortescue, J. A., & Turner, D. W. (2005). Growth and development of ovules of banana, plantain and enset (Musaceae). *Scientia Horticulturae*, *104*, 463–478. https://doi.org/10.1016/j.scienta.2005.01.007

Fortescue, J. A., Turner, D. W., & Romero, R. (2011). Evidence that banana (Musa spp.), a tropical monocotyledon, has a facultative long-day response to photoperiod. *Functional Plant Biology*, *38*, 867–878. https://doi.org/10.1071/FP11128

Gagnard, J., Gautier, P., & Martin-prevel, P. (1984). *Plant Analysis: As a Guide to the Nutrient Requirements of Temperate and Tropical Crops.* Lavoisier.

Ganry, J. (1976). Recherche d'une relation entre température mesurée sous abri et température agissant au niveau des zones de croissance du bananier. Aplication au calcul d'une vitesse de développement. *Fruits*, *31*(10), 587–598.

Garnett, T., Appleby, M. C., Balmford, A., Bateman, I. J., Benton, T. G., Bloomer, P., Burlingame, B., Dawkins, M., Dolan, L., Fraser, D., Herrero, M., Hoffmann, I., Smith, P., Thornton, P. K., Toulmin, C., Vermeulen, S. J., & Godfray, H. C. J. (2013). Sustainable intensification in agriculture: Premises and policies. *Science*, *341*, 33–34. https://doi.org/10.1126/science.1234485

Geerts, S., & Raes, D. (2009). Deficit irrigation as an on-farm strategy to maximize crop water

productivity in dry areas. *Agricultural Water Management*, *96*, 1275–1284. https://doi.org/10.1016/j.agwat.2009.04.009

Geerts, S., Raes, D., & Garcia, M. (2010). Using AquaCrop to derive deficit irrigation schedules. *Agricultural Water Management*, *98*, 213–216. https://doi.org/10.1016/j.agwat.2010.07.003

Geerts, Sam, Raes, D., Garcia, M., Miranda, R., Cusicanqui, J. A., Taboada, C., Mendoza, J., Huanca, R., Mamani, A., Condori, O., Mamani, J., Morales, B., Osco, V., & Steduto, P. (2009). Simulating yield response of quinoa to water availability with aquacrop. *Agronomy Journal*, *101*(3), 499–508. https://doi.org/10.2134/agronj2008.0137s

German Calberto, G., Staver, C., & Siles, P. (2015). An assessment of global banana production and suitability under climate change scenarios. In A. Elbehri (Ed.), *Climate change and food systems: global assessments and implications for food security and trade* (pp. 266–291). Food Agriculture Organization of the United Nations (FAO).

Grieser, J., Gommes, R., & Bernardi, M. (2006). New LocClim - the Local Climate Estimator of FAO. *Geophysical Research Abstracts*, *8*, 08305. ftp://ext-ftp.fao.org/SD/SDR/Agromet/New_LocClim

Guo, D., Zhao, R., Xing, X., & Ma, X. (2020). Global sensitivity and uncertainty analysis of the AquaCrop model for maize under different irrigation and fertilizer management conditions. *Archives of Agronomy and Soil Science*, *66*(8), 1115–1133. https://doi.org/10.1080/03650340.2019.1657845

Hadebe, S. T., Modi, A. T., & Mabhaudhi, T. (2017). Calibration and testing of AquaCrop for selected sorghum genotypes. *Water SA*, *43*(2), 209–221. https://doi.org/10.4314/wsa.v43i2.05

Haifa. (2020). *Crop Guide: Banana Fertilizer Recommendations*. Banana Fertilizer. https://www.haifa-group.com/banana-fertilizer/crop-guide-banana-fertilizer-recommendations (Last accessed 12/01/2020)

Hamdy, A., Ragab, R., & Scarascia-Mugnozza, E. (2003). Coping with water scarcity: Water saving and increasing water productivity. *Irrigation and Drainage*, *52*, 3–20. https://doi.org/10.1002/ird.73

Heng, L. K., Hsiao, T., Evett, S., Howell, T., & Steduto, P. (2009). Validating the FAO aquacrop model for irrigated and water defi cient field maize. *Agronomy Journal*, *101*(3), 488–498. https://doi.org/10.2134/agronj2008.0029xs

Henry, M., Picard, N., Trotta, C., Manlay, R. J., Valentini, R., Bernoux, M., & Saint-André, L. (2011). Estimating tree biomass of sub-Saharan African forests: A review of available allometric equations. *Silva Fennica*, *45*(3), 477–569. https://doi.org/10.14214/sf.38

Holder, G. D., & Gumbs, F. A. (1982). Effects of irrigation at critical stages of ontogeny of the banana cv. “Robusta” on growth and yield. *Tropical Agriculture*, *59*(3), 221–226.

Hoogenboom, G., White, J. W., & Messina, C. D. (2004). From genome to crop: Integration through simulation modeling. *Field Crops Research*, *90*, 145–163. https://doi.org/10.1016/j.fcr.2004.07.014

Hsiao, T. C., Heng, L., Steduto, P., Rojas-Lara, B., Raes, D., & Fereres, E. (2009). Aquacrop-The FAO crop model to simulate yield response to water: III. Parameterization and testing for maize. *Agronomy Journal*, *101*(3), 448–459. https://doi.org/10.2134/agronj2008.0218s

Hunter, M. C., Smith, R. G., Schipanski, M. E., Atwood, L. W., & Mortensen, D. A. (2017). Agriculture in 2050: Recalibrating targets for sustainable intensification. *BioScience*, *67*(4), 386–391. https://doi.org/10.1093/biosci/bix010

IPCC. (2019). Summary for Policymakers. *Climate Change and Land: An IPCC Special Report on Climate Change, Land Degradation, Sustainable Land Management, Food Security and Greenhouse Gas Fluxes in Terrestrial Ecosystems*, 1–15. https://doi.org/10.1002/9781118786352.wbieg0538

Iqbal, M. A., Shen, Y., Stricevic, R., Pei, H., Sun, H., Amiri, E., Penas, A., & del Rio, S. (2014). Evaluation of the FAO AquaCrop model for winter wheat on the North China Plain under deficit irrigation from field experiment to regional yield simulation. *Agricultural Water Management*, *135*, 61–72. https://doi.org/10.1016/j.agwat.2013.12.012

IUSS Working Group WRB. (2014). World reference base for soil resources 2014. International soil classification system for naming soils and creating legends for soil maps. In *World Soil Resources Reports No. 106*. FAO. https://doi.org/10.1017/S0014479706394902

Jacovides, C. P., & Kontoyiannis, H. (1995). Statistical procedures for the evaluation of evapotranspiration computing models. *Agricultural Water Management*, *27*, 365–371. https://doi.org/10.1016/0378-3774(95)01152-9

Jamieson, P. D. (1991). A test of the computer simulation model ARCWHEAT1 on wheat crops grown in New Zealand. *Field Crops Research*, *27*, 337–350.

Jannoyer, M. (1995). Déterminisme du nombre d'organes reproducteurs d'une inflorescence de bananier (Musa acuminata, cv `Grande Naine') [Institut national agronomique]. In *Thèse 3e cycle*. https://agritrop.cirad.fr/326802/

Jennings, S. B., Brown, N. D., & Sheil, D. (1999). Assessing forest canopies and understorey illumination: canopy closure, canopy cover and other measures. *Forestry*, *72*(1), 59–73. https://doi.org/10.1093/forestry/72.1.59

Jin, X., Li, Z., Nie, C., Xu, X., Feng, H., Guo, W., & Wang, J. (2018). Parameter sensitivity analysis of the AquaCrop model based on extended fourier amplitude sensitivity under different agro-meteorological conditions and application. *Field Crops Research*, *226*, 1–15. https://doi.org/10.1016/j.fcr.2018.07.002

Kabbiri, R., Dora, M., Kumar, V., Elepu, G., & Gellynck, X. (2018). Mobile phone adoption in agri-food sector: Are farmers in Sub-Saharan Africa connected? *Technological Forecasting and Social Change*, *131*, 253–261. https://doi.org/10.1016/j.techfore.2017.12.010

Kadioglu, A., Terzi, R., Saruhan, N., & Saglam, A. (2012). Current advances in the investigation of leaf rolling caused by biotic and abiotic stress factors. *Plant Science*, *182*, 42–48. https://doi.org/10.1016/j.plantsci.2011.01.013

Kallarackal, J., Milburn, J., & Baker, D. (1990). Water Relations of the Banana. III. Effects of Controlled Water Stress on Water Potential, Transpiration, Photosynthesis and Leaf Growth. *Australian Journal of Plant Physiology*, *17*(1), 79–90. https://doi.org/10.1071/PP9900079

Karamura, D., Frison, E., Karamura, D. A., & Sharrock, S. (1998). Banana production systems in eastern and southern Africa. In *Bananas and Food Security.* (pp. 401–412).

Karunaratne, A. S., Azam-Ali, S. N., Izzi, G., & Steduto, P. (2011). Calibration and validation of fao-aquacrop model for irrigated and water deficient bambara groundnut. *Experimental Agriculture*, *47*(3), 509–527. https://doi.org/10.1017/S0014479711000111

Kebede, B., & Soromessa, T. (2018). Allometric equations for aboveground biomass estimation of Olea europaea L. subsp. cuspidata in Mana Angetu Forest. *Ecosystem Health and Sustainability*, *4*(1), 1–12. https://doi.org/10.1080/20964129.2018.1433951

Kissel, E., van Asten, P., Swennen, R., Lorenzen, J., & Carpentier, S. C. (2015). Transpiration efficiency versus growth: Exploring the banana biodiversity for drought tolerance. *Scientia Horticulturae*, *185*, 175–182. https://doi.org/10.1016/j.scienta.2015.01.035

Krause, P., Boyle, D. P., & Bäse, F. (2005). Comparison of different efficiency criteria for hydrological model assessment. *Advances in Geosciences*, *5*, 89–97. https://doi.org/10.5194/adgeo-5-89-2005

Lacointe, A. (2000). Carbon allocation among tree organs: A review of basic processes and representation in functional-structural tree models. *Annals of Forest Science*, *57*, 521–533. https://doi.org/10.1051/forest:2000139

Lamour, J., Le Moguédec, G., Naud, O., Lechaudel, M., Taylor, J., & Tisseyre, B. (2020). Evaluating the drivers of banana flowering cycle duration using a stochastic model and on farm production data. *Precision Agriculture*, *Online*. https://doi.org/10.1007/s11119-020-09762-y

Lassoudiere, A. (1979). Comportement du bananier Poyo au second cycle. I. Rejetonnage et multiplication vegetative. *Fruits*, *34*(11), 645–658.

Lassoudière, A. (1980). Comportement du bananier Poyo au second cycle. III. Etude d'une population. *Fruits*, *35*(1), 3–17.

Lassoudière, A. (2007). *Le bananier et sa culture*. Savoir faire.

Le Roux, X., Lacointe, A., Escobar-Gutierrez, A., & Le Dizès, S. (2001). Carbon-based models of individual tree growth: A critical appraisal. *Annals of Forest Science*, *58*, 469–506. https://doi.org/10.1051/forest:2001140

Lehmann, N., Finger, R., Klein, T., Calanca, P., & Walter, A. (2013). Adapting crop management practices to climate change: Modeling optimal solutions at the field scale. *Agricultural Systems*, *117*, 55–65. https://doi.org/10.1016/j.agsy.2012.12.011

Linker, R., Ioslovich, I., Sylaios, G., Plauborg, F., & Battilani, A. (2016). Optimal model-based deficit irrigation scheduling using AquaCrop: A simulation study with cotton, potato and tomato. *Agricultural Water Management*, *163*, 236–243. https://doi.org/10.1016/j.agwat.2015.09.011

Liu, H. J., Cohen, S., Tanny, J., Lemcoff, J. H., & Huang, G. (2008). Transpiration estimation of banana (Musa sp.) plants with the thermal dissipation method. *Plant and Soil*, *308*, 227–238. https://doi.org/10.1007/s11104-008-9622-4

Lu, P., Woo, K.-C., & Liu, Z.-T. (2002). Estimation of whole-plant transpiration of bananas using sap flow measurements. *Journal of Experimental Botany*, *53*(375), 1771–1779. https://doi.org/10.1093/jxb/erf019

Mabhaudhi, T., Modi, A. T., & Beletse, Y. G. (2014a). Parameterisation and evaluation of the FAO-AquaCrop model for a South African taro (Colocasia esculenta L. Schott) landrace. *Agricultural and Forest Meteorology*, *192–193*, 132–139. https://doi.org/10.1016/j.agrformet.2014.03.013

Mabhaudhi, T., Modi, A. T., & Beletse, Y. G. (2014b). Parameterization and testing of AquaCrop for a South African bambara groundnut landrace. *Agronomy Journal*, *106*(1), 243–251. https://doi.org/10.2134/agronj2013.0355

Maes, W. H., & Steppe, K. (2019). Perspectives for Remote Sensing with Unmanned Aerial Vehicles in Precision Agriculture. *Trends in Plant Science*, *24*(2), 152–164. https://doi.org/10.1016/j.tplants.2018.11.007

Mahouachi, J. (2007). Growth and mineral nutrient content of developing fruit on banana plants (Musa acuminata AAA, 'Grand Nain') subjected to water stress and recovery. *Journal of Horticultural Science and Biotechnology*, *82*(6), 839–844. https://doi.org/10.1080/14620316.2007.11512315

Maniruzzaman, M., Talukder, M. S. U., Khan, M. H., Biswas, J. C., & Nemes, A. (2015). Validation of the AquaCrop model for irrigated rice production under varied water regimes in Bangladesh. *Agricultural Water Management*, *159*, 331–340. https://doi.org/10.1016/j.agwat.2015.06.022

Mbonile, M. J. (2005). Migration and intensification of water conflicts in the Pangani Basin, Tanzania. *Habitat International*, *29*, 41–67. https://doi.org/10.1016/S0197-3975(03)00061-4

McClymont, L., Goodwin, I., O'Connell, M. G., & Whitfield, D. M. (2011). Variation in within-block

orchard canopy cover - Implications for crop water requirement and irrigation management. *Acta Horticulturae*, *889*, 233–240.

McMaster, G. S., White, J. W., Hunt, L. A., Jamieson, P. D., Dhillon, S. S., & Ortiz-Monasterio, J. I. (2008). Simulating the influence of vernalization, photoperiod and optimum temperature on wheat developmental rates. *Annals of Botany*, *102*, 561–569. https://doi.org/10.1093/aob/mcn115

McMaster, G. S., & Wilhem, W. W. (1997). Growing degree-days: One equation, two interpretations. *Agricultural and Forest Meteorology*, *87*, 291–300. https://doi.org/10.1016/S0168-1923(97)00027-0

Mekwatanakarn, W., & Turner, D. W. (1989). A simple model to estimate the rate of leaf production in bananas in the subtropics. *Scientia Horticulturae*, *40*(1), 53–62. https://doi.org/10.1016/0304-4238(89)90007-1

Metherell, A. K., Harding, L. A., Cole, V. C., & Parton, W. J. (1993). CENTURY soil organic Matter Model Environment. *Great Plains System Research Unit Technical Report*, *4*, 1–18.

Meya, A. (2021). Nutrient use efficiency of selected varieties of bananas and beans in association on three representative soil types of the Upper Pangani Basin, Tanzania. In *PhD Thesis (Submitted)*. KULeuven, Belgium.

Meya, A. I., Ndakidemi, P. A., Mtei, K. M., Swennen, R., & Merckx, R. (2020). Optimizing soil fertility management strategies to enhance banana production in volcanic soils of the Northern Highlands, Tanzania. *Agronomy*, *289*(10), 1–21. https://doi.org/doi:10.3390/agronomy10020289

Milburn, J. A., Kallarackal, J., & Baker, D. A. (1990). Water Relations of the Banana. I. Predicting the Water Relations of the Field-Grown Banana Using the Exuding Latex. *Australian Journal of Plant Physiology*, *17*, 57–68. https://doi.org/10.1071/PP9900057

Mindzie, C. M., Doutrelepont, H., Vrydaghs, L., Swennen, R. L., Swennen, R. J., Beeckman, H., de Langhe, E., & de Maret, P. (2001). First archaeological evidence of banana cultivation in central Africa during the third millenium before present. *Vegetation History and Archaeobotany*, *10*, 1–6.

Molden, D. (2007). Water Security for Food Security: Findings of the Comprehensive Assessment for Sub - Saharan Africa. In *Water for Food, Water for Life: A Comprehensive Assessment of Water Management in Agriculture*.

Molden, D., Oweis, T., Steduto, P., Bindraban, P., Hanjra, M. A., & Kijne, J. (2010). Improving agricultural water productivity: Between optimism and caution. *Agricultural Water Management*, *97*, 528–535. https://doi.org/10.1016/j.agwat.2009.03.023

Monteith, J. L., & Moss, C. J. (1977). Climate and the Efficiency of Crop Production in Britain [and Discussion]. *Philosophical Transactions of the Royal Society of Biological Sciences*, *281*(1), 277–294. https://doi.org/10.1098/rstb.1977.0140

Mukasa, H. H., Ocan, D., Rubaihayo, P. R., & Blomme, G. (2005). Relationships between bunch weight and plant growth characteristics of Musa spp. assessed at farm level. *MusAfrica*, *16*, 2–3.

NARO. (2001). *Banana production manual*. NARO, Uganda.

Nash, J. E., & Sutcliffe, J. V. (1970). River flow forecasting through conceptual models part I - A discussion of principles. *Journal of Hydrology*, *10*(3), 282–290. https://doi.org/10.1016/0022-1694(70)90255-6

Ndabamenye, T., Van Asten, P. J. A., Vanhoudt, N., Blomme, G., Swennen, R., Annandale, J. G., & Barnard, R. O. (2012). Ecological characteristics influence farmer selection of on-farm plant density and bunch mass of low input East African highland banana (Musa spp.) cropping systems.

Field Crops Research, *135*, 126–136. https://doi.org/10.1016/j.fcr.2012.06.018

Negash, M., Starr, M., & Kanninen, M. (2013). Allometric equations for biomass estimation of Enset (Ensete ventricosum) grown in indigenous agroforestry systems in the Rift Valley escarpment of southern-eastern Ethiopia. *Agroforestry Systems*, *87*, 571–581. https://doi.org/10.1007/s10457-012-9577-6

Nielsen, D. C., Miceli-Garcia, J. J., & Lyon, D. J. (2012). Canopy cover and leaf area index relationships for wheat, triticale, and corn. *Agronomy Journal*, *104*(6), 1569–1573. https://doi.org/10.2134/agronj2012.0107n

Niklas, K. J. (2004). Plant allometry: is there a grand unifying theory? *Biological Review*, *79*, 871–889. https://doi.org/10.1017/S1464793104006499

Nyathi, M. K., van Halsema, G. E., Annandale, J. G., & Struik, P. C. (2018). Calibration and validation of the AquaCrop model for repeatedly harvested leafy vegetables grown under different irrigation regimes. *Agricultural Water Management*, *208*, 107–119. https://doi.org/10.1016/j.agwat.2018.06.012

Nyine, M., Uwimana, B., Akech, V., Brown, A., Ortiz, R., Doležel, J., Lorenzen, J., & Swennen, R. (2019). Association genetics of bunch weight and its component traits in East African highland banana (Musa spp . AAA group). *Theoretical and Applied Genetics*, *132*, 3295–3308. https://doi.org/10.1007/s00122-019-03425-x

Nyombi, K. (2010). Understanding growth of East Africa highland banana: experiments and simulation. In *PhD Thesis*. Wageningen University.

Nyombi, K., van Asten, P. J. A., Corbeels, M., Taulya, G., Leffelaar, P. A., & Giller, K. E. (2010). Mineral fertilizer response and nutrient use efficiencies of East African highland banana (Musa spp., AAA-EAHB, cv. Kisansa). *Field Crops Research*, *117*(1), 38–50. https://doi.org/10.1016/j.fcr.2010.01.011

Nyombi, K., Van Asten, P. J. A., Leffelaar, P. A., Corbeels, M., Kaizzi, C. K., & Giller, K. E. (2009). Allometric growth relationships of East Africa highland bananas (Musa AAA-EAHB) cv. Kisansa and Mbwazirume. *Annals of Applied Biology*, *155*(3), 403–418. https://doi.org/10.1111/j.1744-7348.2009.00353.x

Obiefuna, J. C., & Ndubizu, T. O. . (1979). Estimating Leaf Area of Plantain. *Scientia Horticulturae*, *11*, 31–36.

Paredes, P., de Melo-Abreu, J. P., Alves, I., & Pereira, L. S. (2014). Assessing the performance of the FAO AquaCrop model to estimate maize yields and water use under full and deficit irrigation with focus on model parameterization. *Agricultural Water Management*, *144*, 81–97. https://doi.org/10.1016/j.agwat.2014.06.002

Paredes, Paula, & Torres, M. O. (2017). Parameterization of AquaCrop model for vining pea biomass and yield predictions and assessing impacts of irrigation strategies considering various sowing dates. *Irrigation Science*, *35*(1), 27–41. https://doi.org/10.1007/s00271-016-0520-x

Parton, W. J., Schimel, D. S., Cole, C. V., & Ojima, D. S. (1987). Analysis of Factors Controlling Soil Organic Matter Levels in Great Plains Grasslands1. *Soil Science Society of America Journal*, *51*(5), 1173–1179. https://doi.org/10.2136/sssaj1987.03615995005100050015x

Passioura, J. (2006). Increasing crop productivity when water is scarce - From breeding to field management. *Agricultural Water Management*, *80*(1–3), 176–196. https://doi.org/10.1016/j.agwat.2005.07.012

Peng, B., Guan, K., Tang, J., Ainsworth, E. A., Asseng, S., Bernacchi, C. J., Cooper, M., Delucia, E. H., Elliott, J. W., Ewert, F., Grant, R. F., Gustafson, D. I., Hammer, G. L., Jin, Z., Jones, J. W., Kimm, H.,

Lawrence, D. M., Li, Y., Lombardozzi, D. L., … Zhou, W. (2020). Towards a multiscale crop modelling framework for climate change adaptation assessment. *Nature Plants*, *6*, 338–348. https://doi.org/10.1038/s41477-020-0625-3

Penman, H. L. (1948). Evaporation from open water, bare soils and grass. *Proceedings of the Royal Society. Series A. Mathematical, Physical And Engineering Sciences*, *193*(1032), 120–145. https://doi.org/https://doi.org/10.1098/rspa.1948.0037

Penning De Vries, F. W. T., Vanlaar, H. H., & Chardon, M. C. M. (1983). Bioenergetics of Growth of Seeds, Fruits, and Storage Organs in Potential Productivity of Field Crops under different Environments. In *Potential Productivity Of Field Crops Under Different Environments* (pp. 37–59). IRRI.

Pereira, L. S., Oweis, T., & Zairi, A. (2002). Irrigation management under water scarcity. *Agricultural Water Management*, *57*(3), 175–206. https://doi.org/10.1016/S0378-3774(02)00075-6

Perrier, X., Jenny, C., Bakry, F., Karamura, D., Kitavi, M., Dubois, C., Hervouet, C., Philippson, G., De Langhe, E., & Langhe, E. De. (2019). East African diploid and triploid bananas: a genetic complex transported from South-East Asia. *Annals of Botany*, *123*(1), 19–36. https://doi.org/10.1093/aob/mcy156

Picard, N., Saint-André, L., & Henry, M. (2012). *Manual for building tree volume and biomass allometric equations: From field measurement to prediction. Food and Agricultural Organization of the United Nations, Rome, and Centre de Coopération Internationale en Recherche Agronomique pour le Développement*. http://www.fao.org/3/i3058e/i3058e.pdf

Pinheiro, J., Bates, D., DebRoy, S., Sarkar, D., & R core team. (2019). *nlme: Linear and Nonlinear Mixed Effects Models.* (R package version 3.1-141). https://cran.r-project.org/package=nlme (Last accessed 12/01/2020)

Ploetz, R. C., Kema, G. H. J., & Ma, L.-J. (2015). Impact of diseases on export and smallholder production of banana. *Annual Review of Phytopathology*, *53*(1), 269–288. https://doi.org/10.1146/annurev-phyto-080614-120305

Ploetz, R. C., Kepler, A. K., Daniells, J., & Nelson, S. C. (2007). Banana and plantain — an overview with emphasis on Pacific island cultivars. Musaceae (banana family). In C. R. Elevitch (Ed.), *Traditional Trees of the Pacific Islands - Species Profiles for Pacific Island Agroforestry* (pp. 531–562). Permanent Agriculture Resources.

Poorter, H., & Nagel, O. (2000). The role of biomass allocation in the growth response of plants to different levels of light, CO2, nutrients and water: a quantitative review. *Australian Journal of Plant Physiology*, *27*(6), 595–607. https://doi.org/10.1071/PP99173

R Core Team. (2017). *R: A language and environment for statistical computing* (3.4.3). R Foundation for Statistical Computing.

Raes, D., Geerts, S., Kipkorir, E., Wellens, J., & Sahli, A. (2006). Simulation of yield decline as a result of water stress with a robust soil water balance model. *Agricultural Water Management*, *81*(3), 335–357. https://doi.org/10.1016/j.agwat.2005.04.006

Raes, D., Steduto, P., Hsiao, T. C., & Fereres, E. (2009). Aquacrop-The FAO crop model to simulate yield response to water: II. Main algorithms and software description. *Agronomy Journal*, *101*(3), 438–447. https://doi.org/10.2134/agronj2008.0140s

Raes, D., Steduto, P., Hsiao, T. C., & Fereres, E. (2012a). Chapter 2: Users guide. In *AquaCrop Reference manual version 4.0* (p. 200). Food and Agricultural Organisation of the United Nations.

Raes, D., Steduto, P., Hsiao, T. C., & Fereres, E. (2012b). Chapter 3: Calculation Procedures. In *Aquacrop Reference Manual version 4.0* (p. 125). Food and Agricultural Organisation of the United Nations.

Raes, D., Steduto, P., Hsiao, T. C., & Fereres, E. (2015a). Chapter 2: Users guide. In *AquaCrop Reference manual version 5.0* (p. 275). Food and Agricultural Organisation of the United Nations.

Raes, D., Steduto, P., Hsiao, T. C., & Fereres, E. (2015b). Chapter 3: Calculation procedures. In *AquaCrop Reference manual version 5.0* (p. 124). Food and Agricultural Organisation of the United Nations.

Raes, D., Steduto, P., Hsiao, T. C., & Fereres, E. (2018a). Chapter 1 FAO crop-water productivity model to simulate yield response to water. In *Aquacrop Reference Manual version 6.0* (p. 18). Food and Agricultural Organisation of the United Nations.

Raes, D., Steduto, P., Hsiao, T. C., & Fereres, E. (2018b). Chapter 2 Users Guide. In *Aquacrop Reference Manual version 6.0* (p. 301). Food and Agricultural Organisation of the United Nations.

Raes, D., Steduto, P., Hsiao, T. C., & Fereres, E. (2018c). Chapter 3: Calculation Procedures. In *Aquacrop Reference Manual version 6.0* (p. 138). Food and Agricultural Organisation of the United Nations.

Raes, D., Steduto, P., Hsiao, T. C., & Fereres, E. (2020). Simulation of perennial herbaceous forage crops. In *Aquacrop Reference Manual version 7.0*.(In process)

Ripoche, A., Achard, R., Laurens, A., Tixier, P., Lavigne, C., Alvarez, S., Gauquier, A., Blanchard, M., Ripoche, A., Achard, R., Laurens, A., & Tixier, P. (2012). Modeling spatial partitioning of light and nitrogen resources in banana cover-cropping systems. *European Journal of Agronomy*, *41*(2), 81–91. https://doi.org/10.1016/j.eja.2012.04.001

Ritz, C., & Streibig, J. C. (2008). *Nonlinear Regression with R* (R. Gentleman & K. Hornik (eds.)). Springer, New York, NY. https://doi.org/10.1007/978-0-387-09616-2

Robinson, J. C., & Alberts, A. J. (1986). Growth and yield Responses of Banana (Cultivar 'Williams') to drip irrigation under Drought and Normal Rainfall Conditions in the Subtropics. *Scientia Horticulturae*, *30*(3), 187–202. https://doi.org/10.1016/0304-4238(86)90097-X

Robinson, J. C., & Galan-Sauco, V. (2010). Bananas and Plantains. In *Crop production science in horticulture* (2nd ed.). Longmans, UK. http://www.scopus.com/inward/record.url?eid=2-s2.0-84890136438&partnerID=tZOtx3y1

Robinson, J. C., & Nel, D. J. (1989). Plant density studies with banana (cv. Williams) in a subtropical climate. II. Components of yield and seasonal distribution of yield. *Journal of Horticultural Science*, *64*(2), 211–222.

Rockström, J., Karlberg, L., Wani, S. P., Barron, J., Hatibu, N., Oweis, T., Bruggeman, A., Farahani, J., & Qiang, Z. (2010). Managing water in rainfed agriculture-The need for a paradigm shift. *Agricultural Water Management*, *97*(4), 543–550. https://doi.org/10.1016/j.agwat.2009.09.009

Rockström, J., Steffen, W., Noone, K., Persson, Å., Chapin, F. S., Lambin6, E. F., Lenton, T. M., Scheffer, M., Folke, C., Schellnhuber, H. J., Nykvist, B., Wit, C. A. de, Hughes, T., Leeuw, S. van der, Rodhe, H., Sörlin, S., Snyder, P. K., Costanza, R., Svedin, U., … Foley, J. A. (2009). A safe operating space for humanity. *Nature*, *461*, 472–475.

Rodrigo, V. H. L., Stirling, C. M., Teklehaimanot, Z., & Nugawela, A. (1997). The effect of planting density on growth and development of component crops in rubber/banana intercropping systems. *Field Crops Research*, *52*(1–2), 95–108. https://doi.org/DOI: 10.1016/S0378-4290(96)01069-6

Sandhu, R., & Irmak, S. (2019). Performance of AquaCrop model in simulating maize growth, yield, and evapotranspiration under rainfed, limited and full irrigation. *Agricultural Water Management*, *223*, 105687. https://doi.org/10.1016/j.agwat.2019.105687

Satter, R. L., & Galston, A. W. (1981). Mechanism Of Control Of Leaf Movements. *Ann. Rev. Plant Physiol.*, *32*, 83–110.

Silvestri, S., Richard, M., Edward, B., Dharmesh, G., & Dannie, R. (2020). Going digital in agriculture: how radio and SMS can scale-up smallholder participation in legume-based sustainable agricultural intensification practices and technologies in Tanzania. *International Journal of Agricultural Sustainability*, *Online*, 1–12. https://doi.org/10.1080/14735903.2020.1750796

Silvestro, P. C., Pignatti, S., Yang, H., Yang, G., Pascucci, S., Castaldi, F., & Casa, R. (2017). Sensitivity analysis of the Aquacrop and SAFYE crop models for the assessment of water limited winter wheat yield in regional scale applications. *PLoS ONE*, *12*(11), e0187485. https://doi.org/10.1371/journal.pone.0187485

Sinclair, T. R., & Muchow, R. C. (1999). Radiation Use Efficiency. *Advances in Agronomy*, *65*, 215–265. https://doi.org/10.1016/S0065-2113(08)60914-1

Soares, J. D. R., Pasqual, M., Lacerda, W. S., Silva, S. O., & Donato, S. L. R. (2014). Comparison of techniques used in the prediction of yield in banana plants. *Scientia Horticulturae*, *167*, 84–90. https://doi.org/10.1016/j.scienta.2013.12.012

Spitters, C. J. ., & Schapendonk, A. H. C. M. (1990). Evaluation of breeding strategies for drought tolerance in potato by means of crop growth simulation. *Plant and Soil*, *123*, 193–203.

Spitters, C. J. T. (1990). Crop Growth Models: Their usefulness and limitations. *Acta Horticulturae*, *267*, 349–368. https://doi.org/10.17660/ActaHortic.1990.267.42

Steduto, P. (2006). Biomass Water-Productivity: Comparing the Growth-Engines of Crop Models. *WUEMED Training Course "Integrated Approaches to Improve Drought Tolerance in Crops,"* 1–17.

Steduto, P., Hsiao, T. C., & Fereres, E. (2007a). On the conservative behavior of biomass water productivity. *Irrigation Science*, *25*, 189–207. https://doi.org/10.1007/s00271-007-0064-1

Steduto, P., Hsiao, T. C., & Fereres, E. (2007b). On the conservative behavior of biomass water productivity. *Irrigation Science*, *25*(3), 189–207. https://doi.org/10.1007/s00271-007-0064-1

Steduto, P., Hsiao, T. C., Fereres, E., & Raes, D. (2012). Crop yield response to water. In *FAO Irrigation and Drainage Paper 66*. FAO.

Steduto, P., Hsiao, T. C., Raes, D., & Fereres, E. (2009). Aquacrop-the FAO crop model to simulate yield response to water: I. concepts and underlying principles. *Agronomy Journal*, *101*(3), 426–437. https://doi.org/10.2134/agronj2008.0139s

Steduto, P., Hsiao, T. C., Raes, D., Fereres, E., Izzi, G., Heng, L., & Hoogeveen, J. (2011). Performance review of AquaCrop - The FAO crop-water productivity model. *ICID 21st International Congress on Irrigation and Drainage*, 231–248.

Steduto, P., Raes, D., Hsiao, T. C., & Fereres, E. (2008). AquaCrop: a new model for crop prediction under water deficit conditions. In A. Lopez-Francos (Ed.), *Drought management: scientific and technological innovations* (pp. 285–292). Zaragoza: CIHEAM. http://om.ciheam.org/om/pdf/a80/00800453.pdf

Stevens, B., Diels, J., Brown, A., Stanley, B., Ndakidemi, P. A., & Swennen, R. (2020). Banana biomass estimation and yield forecasting from non-destructive measurements for two contrasting cultivars and irrigation treatments. *Agronomy*, *10*(9), 1435. https://doi.org/10.3390/agronomy10091435

Stevens, B., Diels, J., Vanuytrecht, E., Brown, A., Bayo, S., Rujweka, A., Richard, E., Ndakidemi, P., & Swennen, R. (2020). Canopy cover evolution , diurnal patterns and leaf area index relationships in a Mchare and Cavendish banana cultivar under different soil moisture regimes. *Scientia Horticulturae*, *272*, 109328. https://doi.org/10.1016/j.scienta.2020.109328

Stover, R. H., & Simmonds, N. W. (1987). Bananas. In *Tropical Agriculture Series*. Longman Scientific &

Technical.

Stricevic, R., Cosic, M., Djurovic, N., Pejic, B., & Maksimovic, L. (2011). Assessment of the FAO AquaCrop model in the simulation of rainfed and supplementally irrigated maize, sugar beet and sunflower. *Agricultural Water Management*, *98*(10), 1615–1621. https://doi.org/10.1016/j.agwat.2011.05.011

Surendar, K. K., Devi, D. D., Ravi, I., Krishnakumar, S., Kumar, S. R., & Velayudham, K. (2013). Water Stress in Banana- A Review. *Bulletin of Environment Pharmacology and Life Sciences*, *2*(6), 1–18.

Swennen, R. (1984a). A physiological study of the suckering behaviour in Plantain (Musa cv AAB). Part I State of the Art. In *PhD Thesis*. KULeuven, Belgium.

Swennen, R. (1984b). A physiological study of the suckering behaviour in Plantain (Musa cv AAB). Part II Observations and experiments. In *PhD Thesis*. KULeuven, Belgium.

Swennen, R., & De Langhe, E. (1985). Growth Parameters of Yield of Plantain (Musa cv. AAB). *Annals of Botany*, *65*, 197–204.

Swennen, R., & Rosales, F. E. (1994). Bananas. In *Encyclopedia of Agricultural Science* (Vol. 1, pp. 215–232). Academic Press.

Taiz, L., & Zeiger, E. (2010). *Plant Physiology, Fifth Edition* (Vol. 1). Sinauer Associates.

Taulya, G. (2013). East African highland bananas (Musa spp. AAA-EA) “worry” more about potassium deficiency than drought stress. *Field Crops Research*, *151*, 45–55. https://doi.org/10.1016/j.fcr.2013.07.010

Taulya, G. (2015). Ky’osimba Onaanya: Understanding productivity of East African highland banana. In *PhD Thesis*. Wageningen University.

Taulya, G., van Asten, P. J. A., Leffelaar, P. A., & Giller, K. E. (2014). Phenological development of East African highland banana involves trade-offs between physiological age and chronological age. *European Journal of Agronomy*, *60*, 41–53. https://doi.org/10.1016/j.eja.2014.07.006

Tenkouano, A., Vuylsteke, D., & Swennen, R. (2007). Sink competition and desuckering effects on field performance of triploid and tetraploid plantain genotypes. *Journal of Crop Improvement*, *20*(1–2), 31–51. https://doi.org/10.1300/J411v20n01_02

Thomas, D. S., & Turner, D. W. (1998). Leaf gas exchange of droughted and irrigated banana cv. Williams (Musa spp.) growing in hot, arid conditions. *The Journal of Horticultural Science and Biotechnology*, *73*(3), 419–429. https://doi.org/10.1080/14620316.1998.11510994

Thomas, D. S., & Turner, D. W. (2001). Banana (Musa sp.) leaf gas exchange and chlorophyll fluorescence in response to soil drought, shading and lamina folding. *Scientia Horticulturae*, *90*(1–2), 93–108. https://doi.org/10.1016/S0304-4238(00)00260-0

Thomas, D. S., Turner, D. W., & Eamus, D. (1998). Independent effects of the environment on the leaf gas exchange of three banana (Musa sp.) cultivars of different genomic constitution. *Scientia Horticulturae*, *75*(1), 41–57. https://doi.org/10.1016/S0304-4238(98)00114-9

Tixier, P., Lavigne, C., Alvarez, S., Gauquier, A., Blanchard, M., Ripoche, A., & Achard, R. (2011). Model evaluation of cover crops, application to eleven species for banana cropping systems. *European Journal of Agronomy*, *34*(2), 53–61. https://doi.org/10.1016/j.eja.2010.10.004

Tixier, P., Malezieux, E., Dorel, M., Malézieux, E., Dorel, M., & Wery, J. (2004). SIMBA-POP: A cohort population model for long-term simulation of banana crop harvest. *Ecological Modelling*, *180*(2–3), 407–417. https://doi.org/10.1016/j.ecolmodel.2004.04.028

Tixier, P., Malézieux, E., Dorel, M., & Wery, J. (2008). SIMBA, a model for designing sustainable banana-based cropping systems. *Agricultural Systems*, *97*(3), 139–150.

https://doi.org/10.1016/j.agsy.2008.02.003

Tixier, P., Risède, J. M., Dorel, M., & Malézieux, E. (2006). Modelling population dynamics of banana plant-parasitic nematodes: A contribution to the design of sustainable cropping systems. *Ecological Modelling*, *198*(3–4), 321–331. https://doi.org/10.1016/j.ecolmodel.2006.05.003

Todorovic, M., Albrizio, R., Zivotic, L., Abi Saab, M. T., Stöckle, C., & Steduto, P. (2009a). Assessment of aquacrop, cropsyst, and WOFOST models in the simulation of sunfl ower growth under different water regimes. *Agronomy Journal*, *101*(3), 509–521. https://doi.org/10.2134/agronj2008.0166s

Todorovic, M., Albrizio, R., Zivotic, L., Abi Saab, M. T., Stöckle, C., & Steduto, P. (2009b). Assessment of aquacrop, cropsyst, and WOFOST models in the simulation of sunflower growth under different water regimes. *Agronomy Journal*, *101*(3), 509–521. https://doi.org/10.2134/agronj2008.0166s

Tsegay, A., Raes, D., Geerts, S., Vanuytrecht, E., Abraha, B., Deckers, J., Bauer, H., & Gebrehiwot, K. (2012). Unravelling Crop Water Productivity of Tef (Eragrostis Tef (Zucc.) Trotter) Through Aquacrop in Northern Ethiopia. *Experimental Agriculture*, *48*(2), 222–237. https://doi.org/10.1017/S0014479711001153

Turner, D. W. (1972). Dry matter production, leaf area and growth analvsis. *Australian Journal of Experimental Agriculture and Animal Husbandry*, *12*, 216–224.

Turner, D. W. (1998). Ecophysiology Of Bananas: The Generation and Functioning Of The Leaf Canopy. *Acta Horticulturae*, *490*, 211–221.

Turner, D. W., Fortescue, J. A., Ocimati, W., & Blomme, G. (2016). Plantain cultivars (Musa spp. AAB) grown at different altitudes demonstrate cool temperature and photoperiod responses relevant to genetic improvement. *Field Crops Research*, *194*, 103–111. https://doi.org/10.1016/j.fcr.2016.02.006

Turner, D. W., Fortescue, J. A., & Thomas, D. S. (2007). Environmental physiology of the bananas (Musa spp.). *Brazilian Journal of Plant Physiology*, *19*(4), 463–484. https://doi.org/10.1590/S1677-04202007000400013

Turner, D. W., & Hunt, N. (1987). Planting Date and Defoliation Influence the Time of Harvest of Bananas. *Scientia Horticulturae*, *32*, 233–248.

Turner, D. W., & Thomas, D. S. (1998). Measurements of plant and soil water status and their association with leaf gas exchange in banana (Musa spp.): A laticiferous plant. *Scientia Horticulturae*, *77*(3–4), 177–193. https://doi.org/10.1016/S0304-4238(98)00168-X

Twyford, I. T., & Walmsley, D. (1973). The mineral composition of the Robusta banana plant: I. Methods and plant growth studies. *Plant and Soil*, *39*(2), 227–243.

Twyford, I. T., & Walmsley, D. (1974). The mineral composition of the Robusta banana plant: III. Uptake and distribution of mineral constituents. *Plant and Soil*, *41*(3), 471–491.

United Nations. (2019). World Population Prospects 2019 Highlights. In *World Population Prospects 2019.* http://www.ncbi.nlm.nih.gov/pubmed/12283219

Uwimana, B., Zorrilla-Fontanesi, Y., Van Wesemael, J., Mduma, H., Brown, A., Carpentier, S., & Swennen, R. (2021). Effect of seasonal drought on the agronomic performance of four banana genotypes (Musa spp.) in the East African highlands. *Agronomy*, *11*(1), 4. https://doi.org/10.3390/agronomy11010004

Van Asten, P. J. A., Fermont, A. M., & Taulya, G. (2011). Drought is a major yield loss factor for rainfed East African highland banana. *Agricultural Water Management*, *98*(4), 541–552. https://doi.org/10.1016/j.agwat.2010.10.005

Van Den Bergh, I., Ramirez, J., Staver, C., W. Turner, D., Jarvis, A., & Brown, D. (2012). Climate change in the subtropics: The impacts of projected averages and variability on banana productivity. *Acta Horticulturae*, *928*, 89–100. https://doi.org/10.17660/actahortic.2012.928.9

Van Gaelen, H. (2011). Simulating yield response of barley to weed infestation in AquaCrop: case study Tigray, Northern Ethiopia. In *Msc. Thesis*. KU Leuven, Belgium.

Van Gaelen, H. (2016). Evaluating agricultural management from field to catchment scale Development of a parsimonious agro-hydrological model. In *PhD Thesis*. KU Leuven, Belgium.

Van Gaelen, H., Delbecque, N., Abrha, B., Tsegay, A., & Raes, D. (2016). Simulation of crop production in weed-infested fields for data-scarce regions. *Journal of Agricultural Science*, *154*(6), 1026–1039. https://doi.org/10.1017/S0021859615000982

Van Gaelen, H., Tsegay, A., Delbecque, N., Shrestha, N., Garcia, M., Fajardo, H., Miranda, R., Vanuytrecht, E., Abrha, B., Diels, J., & Raes, D. (2015). A semi-quantitative approach for modelling crop response to soil fertility: Evaluation of the AquaCrop procedure. *Journal of Agricultural Science*, *153*(7), 1218–1233. https://doi.org/10.1017/S0021859614000872

Van Ittersum, M. K., Leffelaar, P. A., Van Keulen, H., Kropff, M. J., Bastiaans, L., & Goudriaan, J. (2003). On approaches and applications of the Wageningen crop models. *European Journal of Agronomy*, *18*(3–4), 201–234. https://doi.org/10.1016/S1161-0301(02)00106-5

Van Wesemael, J. (2015). Saving banana from thirst : identification of stress inducible promoters and genes related to drought. In *Msc. Thesis*. KULeuven.

Van Wesemael, J. (2019). Mining the Musa biodiversity. In *PhD Thesis*. KULeuven, Belgium.

Van Wesemael, J., Kissel, E., Eyland, D., Lawson, T., Swennen, R., & Carpentier, S. (2019). Using Growth and Transpiration Phenotyping Under Controlled Conditions to Select Water Efficient Banana Genotypes. *Frontiers in Plant Science*, *10*, 352. https://doi.org/10.3389/fpls.2019.00352

Vantyghem, M., Merckx, R., Hood-Nowotny, R., Stevens, B., Resch, C., Roman, G., & Dercon, G. (2020). Innovative physiological indicators for drought stress in banana. *EGU General Assembly*, online. https://doi.org/https://doi.org/10.5194/egusphere-egu2020-4844

Vanuytrecht, E., Raes, D., Steduto, P., Hsiao, T. C., Fereres, E., Heng, L. K., Garcia Vila, M., & Mejias Moreno, P. (2014). AquaCrop: FAO's crop water productivity and yield response model. *Environmental Modelling and Software*, *62*, 351–360. https://doi.org/10.1016/j.envsoft.2014.08.005

Vanuytrecht, E., Raes, D., & Willems, P. (2011). Considering sink strength to model crop production under elevated atmospheric CO2. *Agricultural and Forest Meteorology*, *151*(12), 1753–1762. https://doi.org/10.1016/j.agrformet.2011.07.011

Vanuytrecht, E., Raes, D., & Willems, P. (2014). Global sensitivity analysis of yield output from the water productivity model. *Environmental Modelling and Software*, *51*, 323–332. https://doi.org/10.1016/j.envsoft.2013.10.017

Varma, V., & Bebber, D. P. (2019). Climate change impacts on banana yields around the world. *Nature Climate Change*, *9*, 752–757. https://doi.org/https://doi.org/10.1038/s41558-019-0559-9

Wairegi, L., Van Asten, P., Tenywa, M., & Bekunda, M. (2009). Quantifying bunch weights of the East African Highland bananas (Musa spp. AAA-EA) using non-destructive field observations. *Scientia Horticulturae*, *121*(1), 63–72. https://doi.org/10.1016/j.scienta.2009.01.005

Wairegi, L., Van Asten, P., Tenywa, M., & Bekunda, M. (2010). Abiotic constraints override biotic constraints in East African highland banana systems. *Field Crops Research*, *117*(1), 146–153. https://doi.org/10.1016/j.fcr.2010.02.010

Wairegi, Lydia, & van Asten, P. (2011). Norms for multivariate diagnosis of nutrient imbalance in the East African Highland bananas (Musa spp. AAA). *Journal of Plant Nutrition*, *34*(10), 1453–1472. https://doi.org/10.1080/01904167.2011.585203

Weiner, J. (2004). Allocation , plasticity and allometry in plants. *Perspectives in Plant Ecology, Evolution and Systematics*, *6*, 207–215.

Weiss, M., Baret, F., Smith, G. J., Jonckheere, I., & Coppin, P. (2004). Review of methods for in situ leaf area index (LAI) determination. *Agricultural and Forest Meteorology*, *121*(1–2), 37–53. https://doi.org/10.1016/j.agrformet.2003.08.001

Wellens, J., Raes, D., Traore, F., Denis, A., Djaby, B., & Tychon, B. (2013). Performance assessment of the FAO AquaCrop model for irrigated cabbage on farmer plots in a semi-arid environment. *Agricultural Water Management*, *127*, 40–47. https://doi.org/10.1016/j.agwat.2013.05.012

Wellens, J., Raes, D., Tychon, B., Wellens, J., Raes, D., & Tychon, B. (2017). On the Use of Decision-Support Tools for Improved Irrigation Management: AquaCrop-Based Applications. In *Current Perspective on Irrigation and Drainage* (pp. 53–67). Intech. https://doi.org/10.5772/109528

Wickham, H. (2016). *ggplot2: Elegant Graphics for Data Analysis*. Springer-Verlag New York. https://ggplot2.tidyverse.org

Willmott, C. J. (1981). On the validation of models. *Physical Geography*, *2*(2), 184–194. https://doi.org/10.1080/02723646.1981.10642213

Wolka, K., Mulder, J., & Biazin, B. (2018). Effects of soil and water conservation techniques on crop yield, runoff and soil loss in Sub-Saharan Africa: A review. *Agricultural Water Management*, *207*, 67–79. https://doi.org/10.1016/j.agwat.2018.05.016

Woomer, P. L., Bekunda, M. A., & Nkalubo, S. T. (1999). Estimation of Banana Yield Based on Bunch Phenology. *African Crop Science Journal*, *7*(4), 341–347.

Woomer, P. L., Bekunda, M., & Bwamiki, D. (1998). Modelling Banana Growth and Soil Organic Matter Dynamics With The Century Model. *African Crop Science Journal*, *6*(2), 205–214.

World Economic Forum. (2018). Global Risks Report 2018. In *Global risks report* (Vol. 13, Issue 1). https://doi.org/978-1-944835-15-6

Xie, H., You, L., Wielgosz, B., & Ringler, C. (2014). Estimating the potential for expanding smallholder irrigation in Sub-Saharan Africa. *Agricultural Water Management*, *131*, 183–193. https://doi.org/10.1016/j.agwat.2013.08.011

Yamaguchi, J., & Araki, S. (2004). Biomass production of banana plants in the indigenous farming system of the East African Highland A case study on the Kamachumu Plateau in northwest Tanzania. *Agriculture, Ecosystems and Environment*, *102*, 93–111. https://doi.org/10.1016/S0167-8809(03)00230-5

Zeleke, K. T., Luckett, D., & Cowley, R. (2011). Calibration and testing of the FAO AquaCrop model for canola. *Agronomy Journal*, *103*(6), 1610–1618. https://doi.org/10.2134/agronj2011.0150

Zimmermann, D., Reuss, R., Westhoff, M., Geßner, P., Bauer, W., Bamberg, E., Bentrup, F. W., & Zimmermann, U. (2008). A novel, non-invasive, online-monitoring, versatile and easy plant-based probe for measuring leaf water status. *Journal of Experimental Botany*, *59*(11), 3157–3167. https://doi.org/10.1093/jxb/ern171

Zimmermann, U., Rüger, S., Shapira, O., Westhoff, M., Wegner, L. H., Reuss, R., Gessner, P., Zimmermann, G., Israeli, Y., Zhou, A., Schwartz, A., Bamberg, E., & Zimmermann, D. (2010). Effects of environmental parameters and irrigation on the turgor pressure of banana plants measured using the non-invasive, online monitoring leaf patch clamp pressure probe. *Plant Biology*, *12*(3), 424–436. https://doi.org/10.1111/j.1438-8677.2009.00235.x

Zotz, G., & Bader, M. Y. (2009). Agricultural Crop models: Concepts of Resource Acquisition and Assimilate partitioning. In *Progress in Botany* (Vol. 70, pp. 147–170).

Zweifel, R. (2016). Radial stem variations - a source of tree physiological information not fully exploited yet. *Plant, Cell and Environment*, *39*(2), 231–232. https://doi.org/10.1111/pce.12613

Zweifel, R., Item, H., & Hasler, R. (2001). Link between diurnal stem radius changes and tree water relations. *Tree Physiology*, *21*(12–13), 869–877. https://doi.org/10.1093/treephys/21.12-13.869

Annex I: AquaCrop Parameters

Table S1: AquaCrop crop parameters. Type C notes conservative parameters whilst NC notes non-conservative parameters. Condition notes parameters that describe crops under non-limiting conditions (nl), or conditions with water (w), temperature (t), soil fertility (f) and soil salinity (s) stress or under elevated CO2 conditions (co).

Type	Parameter	Description	unit	Condition
Settings				
	m	Determination of crop cycle: by calendar days (1) or by growing degree days (0)		
	sow	Crop is (1) sown (1), (2) transplanted (2) or (3) regrowing		
	$type$	Crop type (1= leafy vegetable, 2= fruit/grain producing, 3 = root/tuber, 4= repeatedly harvested)		
	det	Crop determinacy linked (1) or unlinked (0) with flowering		
	$depladj$	Soil water depletion factors are adjusted by ET_0 (1) or not (0)		
Canopy development				
C	cc_s	Soil surface covered by an individual seedling at 90% emergence	cm^2	nl
C	cc_{sr}	Canopy size of individual plant (re-growth) at 1st day	cm^2	nl
C	cdc	Decrease in canopy cover	$m^2 m^{-2}$ GDD^{-1} or m^2 m^{-2} d^{-1}	nl
C	cgc	Increase in canopy cover	$m^2 m^{-2}$ GDD^{-1} or m^2 m^{-2} d^{-1}	nl
NC	CC_0	Initial canopy cover	%	nl
NC	CC_x	Maximum canopy cover	%	nl
NC	den	Number of plants per hectare	plants ha^{-1}	nl
NC	eme	Period from sowing to emergence	GDD or d	nl
NC	mat	Total length of crop cycle from sowing to maturity	GDD or d	nl
NC	sen	Period from sowing to start senescence	GDD or d	nl
C	$etos$	ET_0-sum to be exceeded during stress period before senescence is triggered mm	mm	w
C	$p_{exp-low}$	Soil water depletion factor for canopy expansion - lower threshold	%TAW	w
C	$p_{exp-shp}$	Shape factor for water stress coefficient for canopy expansion (0.0 = straight line)	(-)	w
C	p_{exp-up}	Soil water depletion factor for canopy expansion - upper threshold	%TAW	w
C	p_{sen}	Soil water depletion factor for canopy senescence - upper threshold	%TAW	w
C	$p_{sen-shp}$	Shape factor for water stress coefficient for canopy senescence (0.0 = straight line)	(-)	w

Table S1: *AquaCrop crop parameters. Type C notes conservative parameters whilst NC notes non-conservative parameters. Condition notes parameters that describe crops under non-limiting conditions (nl), or conditions with water (w), temperature (t), soil fertility (f) and soil salinity (s) stress or under elevated CO2 conditions (co).* (Cont.)

Type	Parameter	Description	unit	Condition
C	T_{base}	Base temperature below which crop development does not progress	°C	t
C	T_{up}	Upper temperature above which crop development no longer increases with an increase in temperature	°C	t
NC	$s_{CCx_{shp}}$	Shape factor for soil fertility/salinity stress coefficient for maximum canopy cover	(-)	f/s
NC	$s_{dec_{shp}}$	Shape factor for the response of decline of canopy cover to soil fertility/salinity stress	(-)	f/s
NC	$s_{ex_{shp}}$	Shape factor for soil fertility/salinity stress coefficient for canopy expansion	(-)	f/s
Evapotranspiration				
C	$evardc$	Effect of canopy cover in reducing soil evaporation in late season stage	(-)	nl
C	Kc_{dcl}	Decline of crop transpiration coefficient as a result of ageing and senescence	% d^{-1}	nl
C	Kc_x	Maximum crop transpiration coefficient when canopy is complete but prior to senescence	(-)	nl
C	p_{sto}	Soil water depletion fraction for stomatal control - upper threshold	%TAW	w
C	$p_{sto,shp}$	Shape factor for water stress coefficient for stomatal control (0.0 = straight line)	(-)	w
NC	$anaer$	Anaerobic point at which deficient aeration occurs	VWC% below θ_{sat}	w
NC	$s_{sto,shp}$	Shape factor for soil salinity stress coefficient for stomatal closure	(-)	s
C	K_{sb}	Cold (air temperature) stress on crop transpiration	°C	
Biomass production				
C	f_{wpy}	Ratio of water productivity normalized for ET_0 and CO_2 during yield formation	%	nl
C	WP^*	Crop water productivity normalized for ET_0 and CO_2	g m^{-2}	nl
NC	f_{sink}	Crop performance under elevated atmospheric CO_2 concentration	%	co
C	$stbio$	Minimum growing degrees required for full biomass production	°C d^{-1}	t
NC	s_{wpshp}	Shape factor for soil fertility stress coefficient for crop water productivity	(-)	f
C	EC_x	Maximum electrical conductivity of saturated soil-paste extract at which a crop can no longer grow	dS m^{-1}	s
C	EC_{min}	Minimum electrical conductivity of saturated soil-paste extract at which a crop starts to be affected by soil salinity	ds m^{-1}	s
NC	$s_{b,shp}$	Shape factor for soil salinity stress coefficient for biomass production	(-)	s
Yield formation				
C	exc	Excess of potential fruits	%	nl
C	$hilen$	Period of harvest index building-up during yield formation	GDD or d	nl

Table S1: *AquaCrop crop parameters. Type C notes conservative parameters whilst NC notes non-conservative parameters. Condition notes parameters that describe crops under non-limiting conditions (nl), or conditions with water (w), temperature (t), soil fertility (f) and soil salinity (s) stress or under elevated CO2 conditions (Cont.)*

Type	Type	Type	Type	
C	HI_0	Reference harvest index	%	nl
NC	flo	Period from sowing to flowering/tuber formation	GDD or d	nl
NC	$flolen$	Length of flowering	GDD or d	nl
C	$polmn$	Minimum air temperature below which pollination starts to fail (cold stress)	°C	t
C	$polmx$	Maximum air temperature above which pollination starts to fail (heat stress)	°C	t
C	$hinc$	Allowable maximum increase of specified harvest index	%	w
C	$hingsto$	Coefficient describing negative impact on harvest index of stomatal closure during yield formation		w
C	$hipsflo$	Possible increase of harvest index due to water stress before flowering	%	w
C	$hipsveg$	Coefficient describing positive impact on harvest index of restricted vegetative growth during yield formation		w
C	p_{pol}	Soil water depletion factor for pollination - upper threshold	%TAW	w
NC	WP_Y^*	Water Productivity normalized for ET_0 and CO_2 during yield formation (as % WP*)	% WP^*	
NC	DM	Dry matter content of fresh yield	%	nl
Root zone development				
C	rt_{shp}	Shape factor describing root zone expansion		
NC	$root$	Period from sowing to maximum rooting depth	GDD or d	nl
NC	$rtexlw$	Maximum root water extraction in bottom quarter of root zone	$m^3\ m^{-3}$ soil d^{-1}	nl
NC	$rtexup$	Maximum root water extraction in top quarter of root zone	$m^3\ m^{-3}$ soil d^{-1}	nl
NC	$Z_{r,x}$	Maximum effective rooting depth	m	nl
NC	$Z_{r,min}$	Minimum effective rooting depth	m	nl
NC	$Z_{r,min-rg}$	Minimum effective rooting depth (m) in first year - required only in case of regrowth	m	

Annex II: Experimental design overview

1. Climatic conditions in the field

An automated weather station (TAHMO weather station: Decagon DS-2 sonic anemometer with pyranometer, REC-1 rain gauge, and VP-4 thermometer and humidity sensor with a solar-powered and GPRS-enabled EM50G), located at the edge of the field, measured air temperature (°C), wind speed at 2 m height (m s^{-1}), relative humidity (%), precipitation (mm) and solar radiation (MJ m^{-2} min^{-1}) at a 5 minute interval. Daily reference evapotranspiration (ET_0) was computed using the FAO Penman-Monteith approach (Allen et al. 1998).

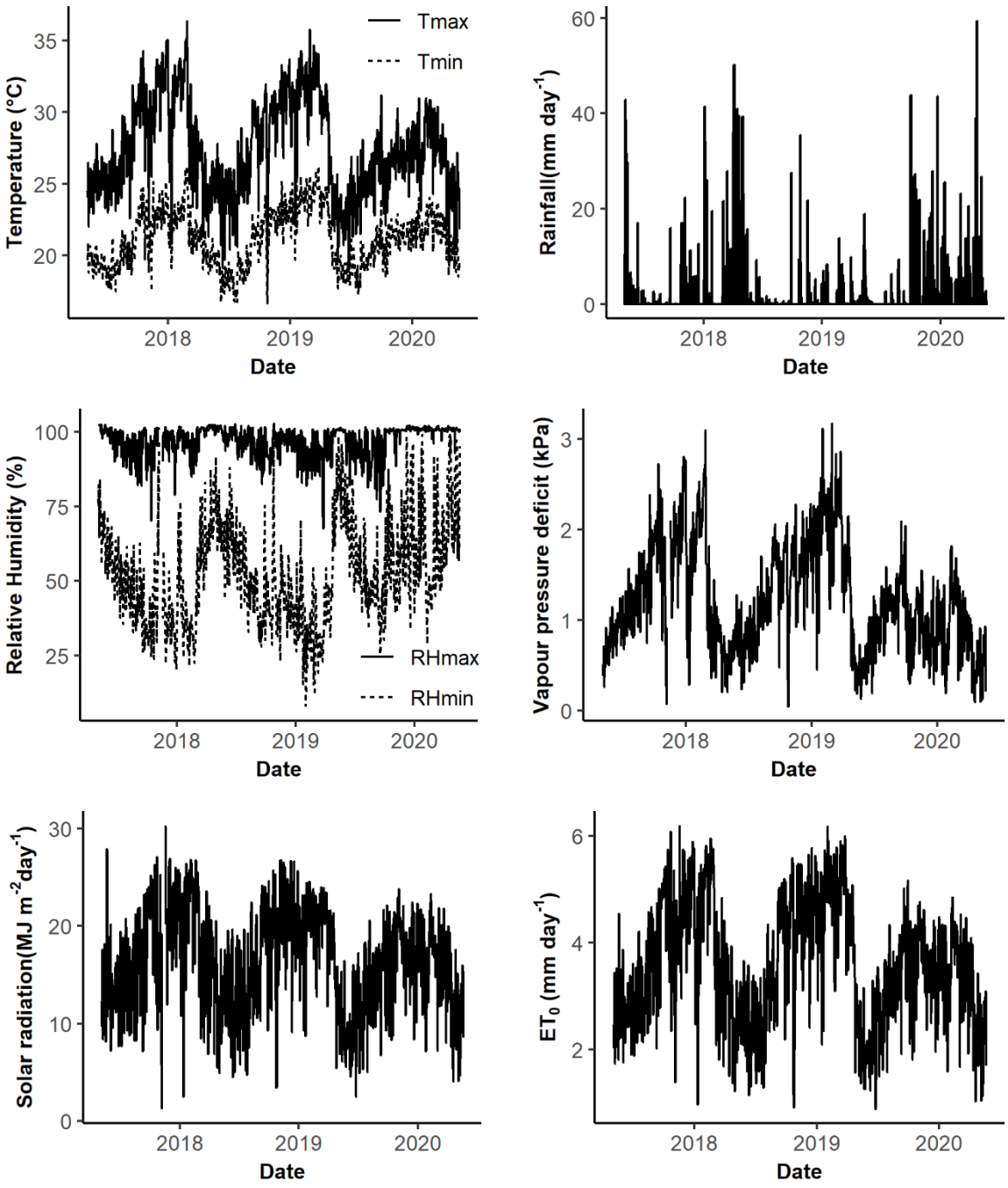


Figure S1: Weather data at the Nelson Mandela African Institution of Science and Technology 2017 - 2020.

2. Field Layout

Fields were established at the joint research farm of the Nelson Mandela African Institution of Science and Technology (NM-AIST) and the International Institute of Tropical Agriculture (IITA) in Arusha, Tanzania (3° 23′ 58″ S, 36° 47′ 48″ E). The experiments were conducted on fields with no recent history of banana cultivation. Two cultivars (experiments) were planted: Mchare cv. Huti Green Bell (HG) and Cavendish cv. Grande Naine (GN). Treatments applied were irrigation regimes: "Full irrigation" (FI) and "Rainfed" (RF).

The design was a blocked design with drip irrigation as treatment but given the infrastructure the irrigation treatments could not be randomized (Annex II, Figure S2).

In experiment 1, two blocks were planted with HG on 3-05-2017. Each block contained five rows of 15 mats, subdivided in three plots of 25 mats (5×5), of which the central nine mats (3×3) were used for continuous non-destructive data collection. Each block was a different irrigation treatment, as valves to shut off irrigation were installed at the front of each block. For HG, there were three plots for each treatment. Border mats were used for periodic destructive sampling.

In experiment 2, four blocks were planted with GN on 13-11-2017. Each block contained five rows of 14 mats, subdivided in two plots of 35 mats (7×5), receiving two different irrigation treatments. Valves were installed in the middle of a plant row (between mat 7 and 8); therefore, two irrigation treatments were present in a block. The central nine mats (3×3) were used for growth data collection, leading to four replications (plots) per treatment. The first and last two mats of each row (2×5 mats) together with the border rows were used for destructive sampling. Each treatment was replicated four times across the blocks.

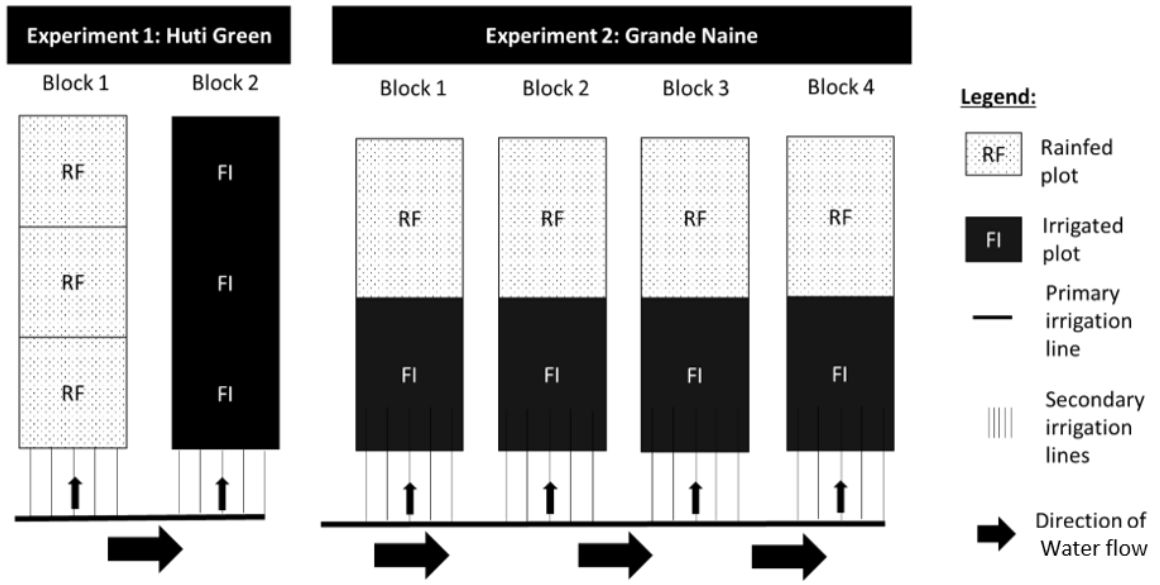


Figure S2: Diagram of experimental design for experiment 1 on Huti Green Bell, and experiment 2 on Grande Naine. A plot constitutes of 5x5 plants in Huti Green Bell, and of 7x5 plants in Grande Naine. There are 3 plots per treatment for Huti Green Bell, and 4 plots per treatment for Grande Naine.

3. Irrigation treatment design and application

Each banana row was fitted with two driplines, at each side of a banana mat that supply irrigation water. Originally each mat's position was fitted with two drippers (one at each side of the mat). Each dripper supplies approx. 4L hr^{-1}. Two extra drippers were installed on 6 June 2018. For the HG experiment, this was at 57 WAP and for the GN experiment at 29 WAP.

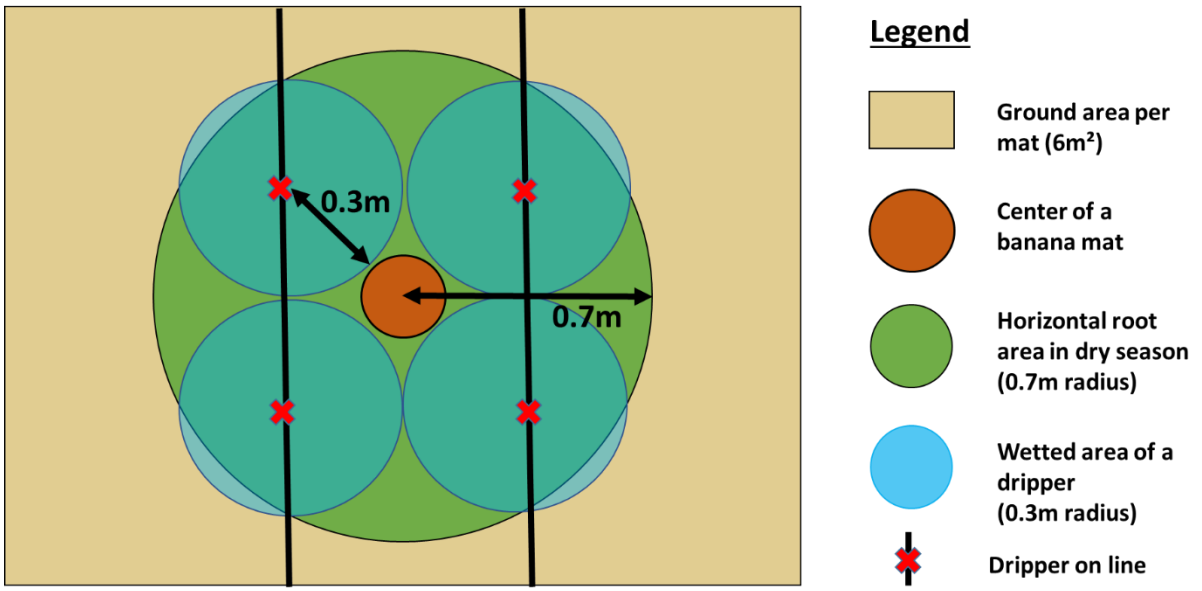


Figure S3: Single banana mat diagram.

Uniformity of the driplines was assessed, and regardless of the position (front: position 1 vs. end: position 15) of a dripline, drippers supplied approx. 4 L hr^{-1} and no patterns in discharge rate were found with position in the line (Annex II, Figure S4). Irrigation discharge also showed no systematic pattern such that blocks closer to the irrigation pump (block 1) received more than the ones further away (block 4) (Annex II, Figure S2 and Figure S4). Differences in discharge between the blocks were possibly due to small leaks in the driplines, and not due to a systematic pressure drop along the dripline.

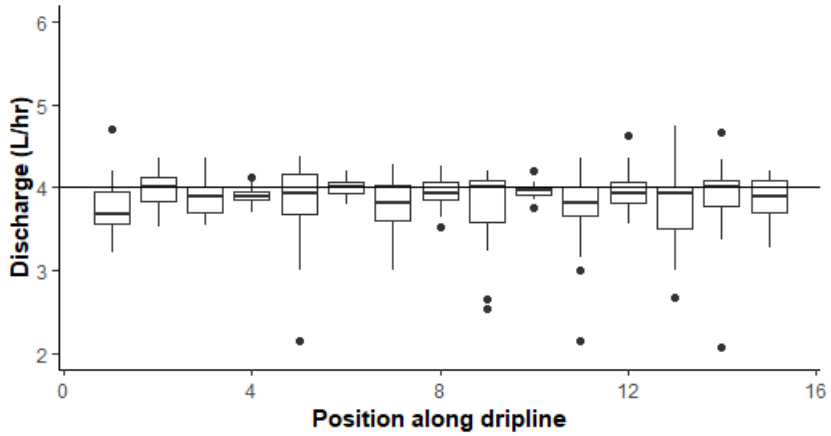


Figure S4: Dripper discharge rates according to the position of the dripper in the line. Position 1 is close to the main feeder line, whilst position 15 is furthest away (~50m from the main line). Data from discharge measurements in November 2017.

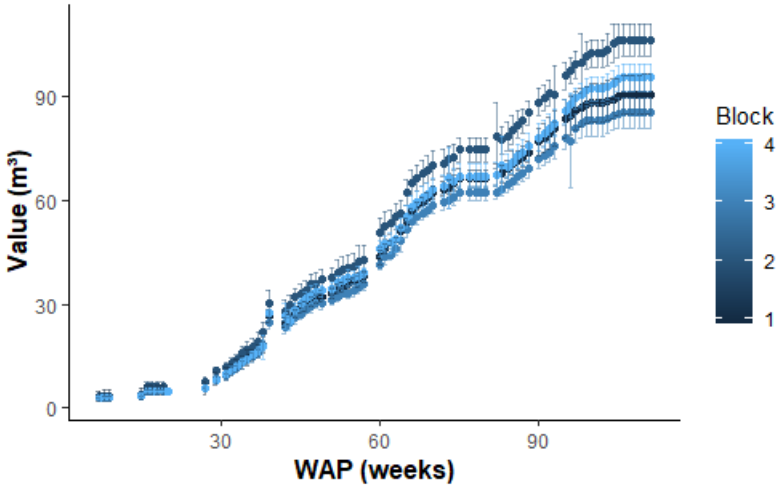


Figure S5: Discharge amounts over time for different GN blocks which are always irrigated similarly.

Discharge rates of drippers depend strongly on the applied water pressure in the lines which could not be assessed because of the nature of the irrigation system and the multitude of different irrigation sections in the entire field (of which our experiment was only a small section). If the water pressure in the driplines was high enough, each dripper head applied 4L hr^{-1} due to the specifications of the dripper head (Annex II, Figure S4). Since the entire irrigation system was designed such that a full 100 m line would be irrigated, we assumed the pressure in the first 50 m of the lines to fully supply the discharge rate. Furthermore, the positioning of irrigation valves in our driplines when shutting off the RF plots further lead to increased pressure in the irrigated lines. This would ensure the irrigation valves to reach the needed pressure to supply 4L hr^{-1} in the FI plots.

4. Soil description

Soils were Endocalcic Phaeozems (Geoabruptic, Clayic, Humic) (IUSS Working Group WRB, 2014) or Udertic to Vertic Haplustols (USDA, 1999) on gently sloping land (3%) located at the foothill of Mt. Meru at an altitude of 1,188 m. asl. Soils were moderately shallow to deep (90-120 cm), well structured, well drained with a silty clay loam to silty clay texture (Annex II, Table S1).

Table S1: Physico-chemical properties specified per soil horizon, for the soil at the Nelson Mandela African Institution of Science and Technology (NM-AIST). Texture: Sand, silt, and clay (%) and corresponding soil class; pH-H_2O: pH as measured in distilled water H_2O; P-Olsen: available phosphorus content; TOC: total organic carbon; TN: total nitrogen; BS: base saturation (%); CEC: cation exchange capacity; Ca, Mg, Na, K and P: acetic acid extractable Calcium, Magnesium, Potassium, Sodium.

					Physico-chemical properties									
Soil horizon				**Textural properties**						**Chemical properties**				
Depth	**Sand**	**Silt**	**Clay**	**Class**	**pH H20**	**P-Olsen**	**TOC**	**TN**	**BS**	**CEC**	**Ca**	**Mg**	**K**	**Na**
cm	----------%----------			-	-	mg/100g	----------%----------			----------cmolc/kg----------				
0 - 15	8.5	57.7	33.8	Silt clay loam	7.2	5.4	4.24	0.38	78.75	69.37	4.01	0.28	4.2	4.7
15 - 55	5.3	54.1	40.6	Silt clay	7.5	4.4	1.51	0.14	90.00	63.37	4.80	0.34	1.5	3.6
55-95	4.7	48.8	46.5	Silt clay	7.4	0.4	1.65	0.15	86.25	76.71	5.46	0.28	1.7	3.5
95-112	50.4	22	27.6	Sandy clay loam	7.5	0.5	4.28	0.37	90.00	74.70	4.78	0.26	4.6	5.9
112-140	32.6	22.6	44.8	Loam	7.6	0.8	4.06	0.35	93.75	70.04	5.80	0.31	4.5	5.7
140 -	84.6	3.9	11.5	Loamy sand	7.8	0.1	6.04	0.58	100	60.03	5.39	0.17	6.6	7.4

Soil water holding capacity (WHC) was determined based on a pF curve analysis of the soil (Annex II, Figure S6).

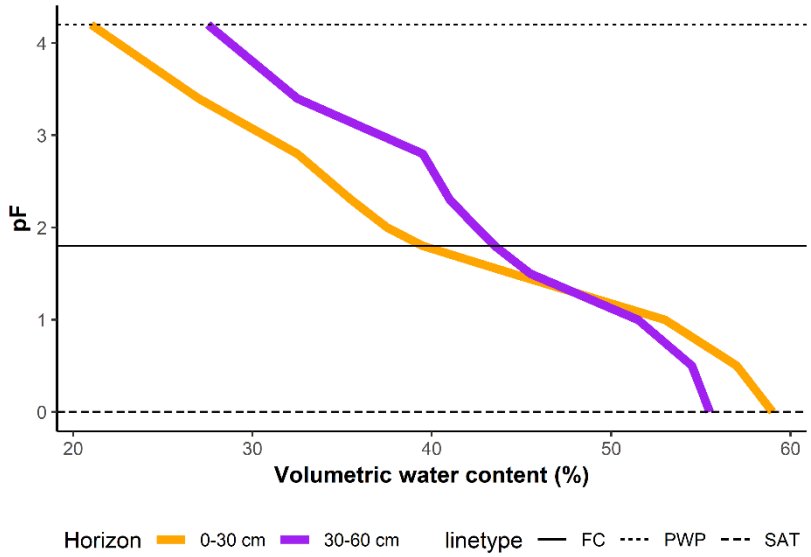


Figure S6: pF curve of the soil horizons (0-30 cm and 30-60 cm). FC notes field capacity (pF 1.8), PWP notes permanent wilting point (pF 4.2) and SAT notes saturation (pF 0).

5. Soil moisture measurements

Soil moisture was monitored daily by Time Domain Reflectometry (TDR) in the root zone. Within each plot (Annex II, Figure S2), the central banana mat was fitted with two TDR probes installed vertically at different depths: 0-30 cm (horizon 1) and 30-60 cm (horizon 2). Probes were installed in the area wetted by the drippers (Annex II, Figure S3), at 50 cm from the central mat and read out each morning before irrigation by a TDR-200 (Campbell scientific, Inc.). Daily moisture depletion, Dr (mm), was calculated at the plot level as:

$$Dr, i = 1000(\theta_{FC} - \theta_i) \times Z_r \quad (1)$$

with Dr, i being depletion on day i, θ_{FC} being the volumetric water content (VWC) at field capacity (FC, [m³ m-³]), θ_i being the actual VWC at day i (m³ m-³) and Z_r being the rooting depth (m). The rooting depth was estimated as a logistical interpolation between the depth at 10 days after planting (0.1 m) and at flowering (0.6 m). Rooting depths were checked every three months over the course of the growing season through root trenching methods. Banana reaches a maximum rooting depth at flowering (Turner et al., 2007), and trenches revealed that roots were continually present until depths of 1 m after flowering in both HG and GN mats, as the soil profile was bounded by a saprolite hardpan layer at 1m. Roots were present up to 1 m depth from flowering onwards, but number of roots declined substantially below 60 cm depth. The effective maximum rooting depth (Zr_x) was taken as 0.6 m following own observations and literature (Carr, 2009; Turner et al., 2007).

Depletion values are negative when water contents are below FC and positive when values are above FC.

Daily depletion values were compared against the readily available water (RAW [mm]), as an indicator of moisture deficit. RAW was calculated as:

$$RAW = 1000\left(\theta_{FC} - \theta_{pwp}\right) \times Z_r \times p = TAW \times p_{adj} \quad (2)$$

with θ_{pwp} being the VWC at Permanent wilting point ($m^3\ m^{-3}$), p_{adj} being a depletion factor (-) and TAW being the total available water (mm). The value of p_{adj} was chosen to be the generic factor *p* of 0.35 for banana as given by Allen et al. (1998), adjusted for reference evapotranspiration (ET_0) according to Raes et al. (2018). When the $D_{r,i} < RAW$, plants are assumed to experience moisture deficit.

All mats received irrigation until 4 MAP (establishment period). Thereafter, two irrigation treatments were installed: optimal "full" irrigation (FI) and rainfed (RF). In the FI treatment, mats received water whenever more than 25% TAW was about to be depleted in the first or second soil horizon (based on VWC contents read out by the TDR sensors. Water in the RF treatment was shut off after 4 MAP.

6. Fertilizer application

Mats received a mixture of mineral fertilizers and manure. Mineral fertilizers were split applied: 153 kg N ha^{-1} $year^{-1}$ (urea), 206 kg K ha^{-1} $year^{-1}$ (muriate of potash), 19.26 kg Mg ha^{-1} $year^{-1}$ and 25.6 kg S ha^{-1} $year^{-1}$ (MgSO4) were applied monthly in the rainy season and every two months in the dry season, while 40.2 kg P ha^{-1} $year^{-1}$ (triple super phosphate) was applied every five months. Twenty L of fresh farmyard cow manure was applied per mat twice yearly before the start of the rainy season.

7. Plantation management

All suckers were allowed to grow until approx. four months after planting (MAP), at which time one sucker of approx. 30-50 cm height was selected (depending on the existing suckers around a plant) and the others pruned. For HG this was at 2017-09-14, and for GN this was at 2018-03-20. Suckers were chosen amongst the existing suckers around a plant: 1) at a similar side around the mother plant to ensure plantation lines to be kept similar, 2) of a similar height. This ensured suckers at a similar position were selected, but these were not always the most vigorous suckers.

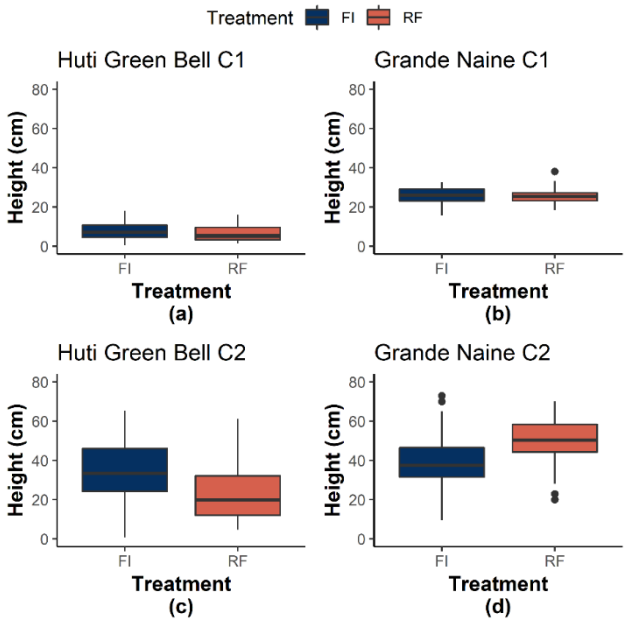


Figure S7: Initial plant heights for planting materials (a) Initial plant height for Huti Green Bell in cycle 1 (C1) (b) Initial plant height for Grande Naine in C1, (c) Initial plant height for Huti Green Bell in cycle 2 (C2)and (d) Initial plant height for Grande Naine in C2

Each banana mat thereafter was composed of C1 and C2, and de-suckering was carried out afterwards on a monthly basis. During bunch filling, a sucker around C2 was chosen in a similar fashion: (1) at a similar position around C2 and (2) of similar height.

Additional leaf pruning events occurred due to the development of Black Sigatoka (*Pseudocercospora fijiensis*) in the long wet season of 2018 at 2018-05-21 (P1), 2018-06-05 (P2), and 2018-07-30 (P3). At P1 and P2, only the oldest leaves with symptoms of the fungus (yellowing and petiole collapse) were cut. At P3 the oldest six leaves of each plant were cut away to retain the spread of the fungus affecting the older leaves.

8. Plant growth data collection

Non-destructive plant growth data were measured monthly at the plot level (3×3 mats), on individual plants (C1 and C2) present on the mat until harvest of C1 as this corresponds to a CC growth cycle. Measured variables and variables calculated from growth measurements are listed in Annex II, Table S2.

Destructive data entailed destructive sampling of full mats. Every three months, mats (n=3) were selected in each treatment in both experiments for destructive sampling. Non-destructive plant growth data were measured from these plants, together with the biomass of the different cycles and components (Annex II, Table S2).

Harvest entailed harvesting plants when these became ready based on first yellowing of fingers on a bunch. Non-destructive plant growth data were collected from these plants together with harvest data (Annex II, Table S2).

Table S6: Growth measurements collected from banana plots

Parameter	Unit	Abbreviation	Level of measurement	Timing
Non-destructive growth measurements				
Pseudostem Height	cm	H	Individual plants on a mat, central 9 plants of each plot	PM/DS/H
Pseudostem Girth at base	cm	$Gbase$	Individual plants on a mat, central 9 plants of each plot	PM/DS/H
Pseudostem Girth at mid	cm	$Gmid$	Individual plants on a mat, central 9 plants of each plot	PM/DS/H
Pseudostem Girth at 1m	cm	$G1m$	Individual plants on a mat, central 9 plants of each plot	PM/DS/H
Leaf length of 3rd functional leaf	cm	$LL3$	Individual plants on a mat, central 9 plants of each plot	PM/DS/H
Leaf width of 3rd functional leaf	cm	$LW3$	Individual plants on a mat, central 9 plants of each plot	PM/DS/H
Functional leaves	Nr	$functL$	Individual plants on a mat, central 9 plants of each plot	PM/DS/H
Dead Leaves	nr	$deadL$	Individual plants on a mat, central 9 plants of each plot	PM/DS/H
Canopy cover	%	CC	Individual mats, central 9 mats of each plot†, Plot level‡	PM/DS/H
Destructive growth measurements				
Leaf length	cm	LL	Destructively sampled plant, individual leaves	DS/H
Leaf width	cm	LW	Destructively sampled plant, individual leaves	DS/H

Table S6-*Cont.*: Growth measurements collected from banana plots

Parameter	Unit	Abbreviation	Level of measurement	Timing
Functional leaves	nr	$funct L$	Individual plants on a mat	DS/H
Dead leaves	nr	$dead L$	Individual plants on a mat	DS/H
Leaf area	m²	$LA_{measured}$	Destructively sampled plant, individual leaves	DS/H
Total leaf area plant	m²	$LA_{plant,measured}$	Destructively sampled plant, all leaves combined	DS/H
Leaf weight	kg	$leaf F$	Destructively sampled plant	DS/H
Pseudostem weight	kg	$pseudostem F$	Destructively sampled plant	DS/H
Petiole weight	kg	$petiole F$	Destructively sampled plant	DS/H
Destructive: only at periodic sampling				
Corm weight	kg	$corm F$	Destructively sampled plant	DS
Destructive only at harvest				
Bunch weight	kg	$bunch F$	Destructively sampled plant	H
Peduncle weight	kg	$peduncle F$	Destructively sampled plant	H
Number of hands	nr	N_{hand}	Destructively sampled plant	H
Number of fingers per hand	nr	N_{finger}	Destructively sampled plant	H
Weight per hand	kg	$hands F$	Destructively sampled plant	H
Finger length of 5 fingers from hand 2,5 and 8	cm	$finger L$	Destructively sampled plant	H
Finger circumference of 5 fingers from hand 2,5 and 8	cm	$finger C$	Destructively sampled plant	H
Fresh finger weight of 5 fingers from hand 2,5 and 8	kg	$finger F$	Destructively sampled plant	H
Calculated growth measurements based on non-destructive and destructive growth measurements				
Leaf area factor	-	laf	individual leaf	DS
Leaf area plant	m²	LA_{plant}	Individual plant	PM/DS/H
Leaf area mat	m²	LA_{mat}	Individual mat	PM/DS/H
Leaf area index, plant	m^2m^{-2}	LAI_{plant}	Individual plant	PM/DS/H
Leaf area index, mat	m^2m^{-2}	LAI_{mat}	Individual mat	PM/DS/H

Note: †For Huti Green plants before the drone arrived, ‡With the drone. PM stands for Periodic Monthly; DS stands for Destructive sampling; H stands for Harvest.

Annex III: Canopy cover supplementary data

Supplementary Figures

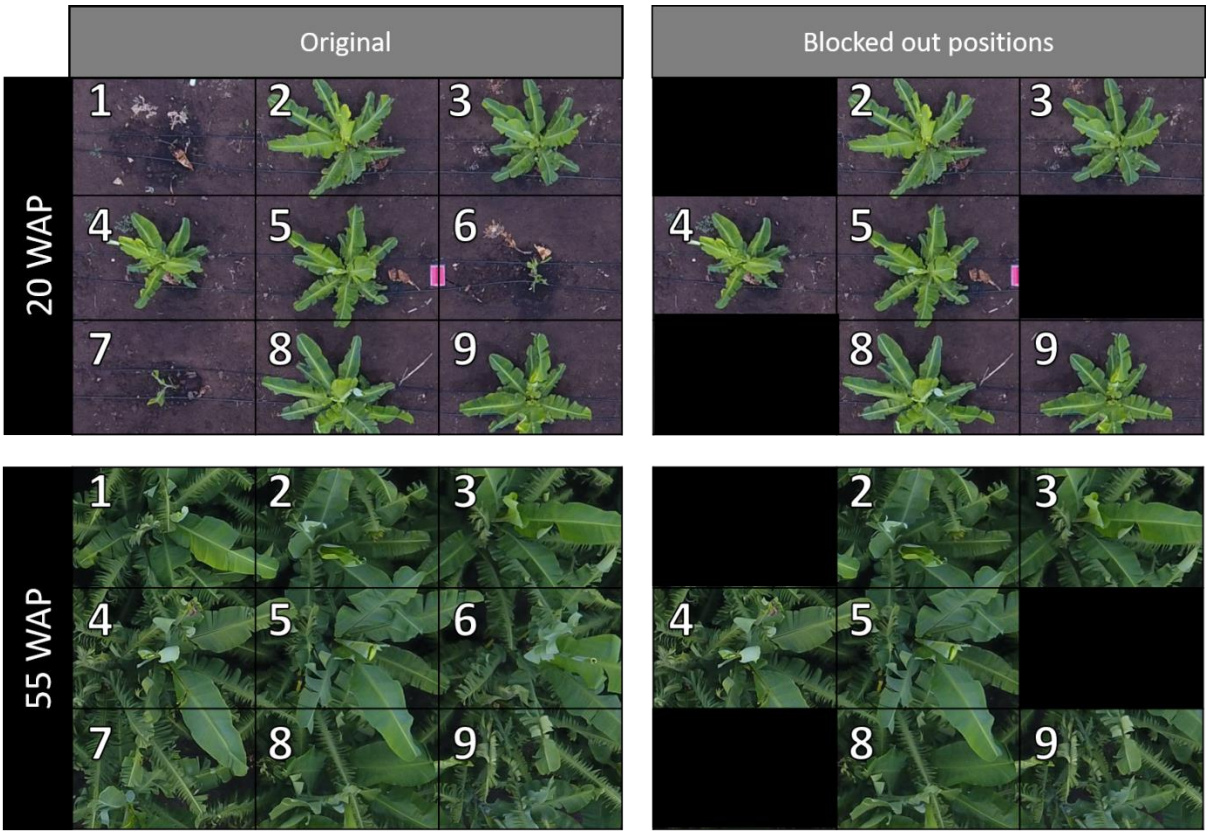


Figure S1: Adapting CC values for missing plant positions. Original picture with original plants (left), picture after blocking out missing plant positions (right).

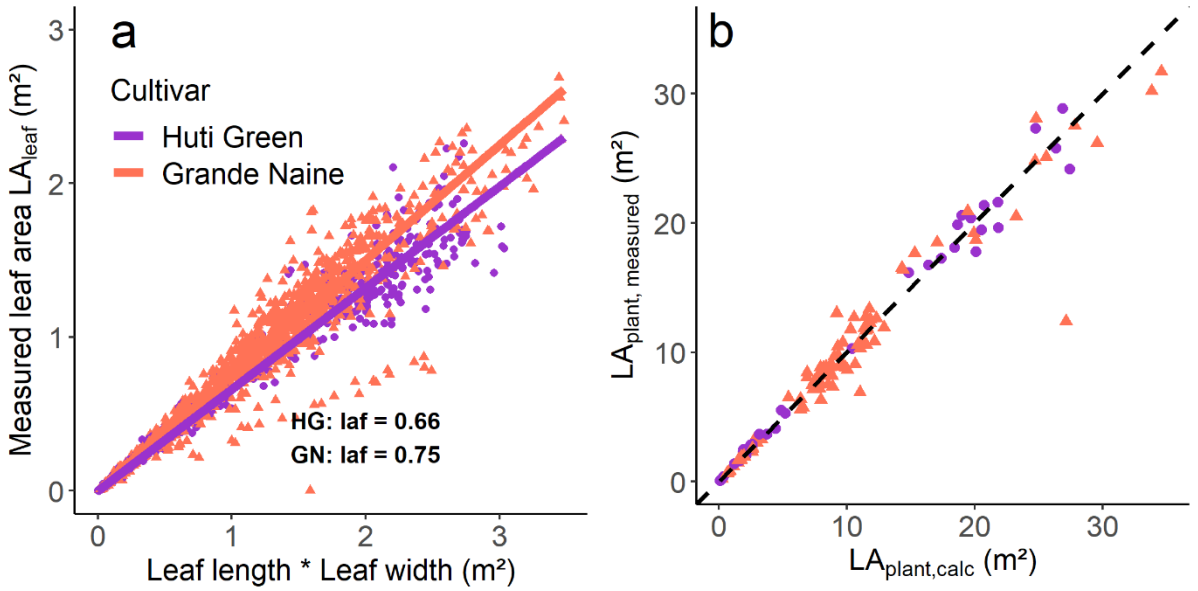


Figure S2: a) Leaf area factor for HG: Mchare – Huti Green and GN: Cavendish – Grande Naine. Measured leaf area LA_{leaf} vs. leaf length (LL) x leaf width (LW). The slope of the curve gives the leaf area factor (laf). b) Total plant leaf area as measured at destructive sampling through image analysis ($LA_{plant,\ measured}$) vs. total plant leaf area calculated based on summing up all leaf areas present on a plant, whereby leaf areas are calculated using the laf for the two banana cultivars (HG: Mchare - Huti Green Bell and GN: Cavendish - Grande Naine).

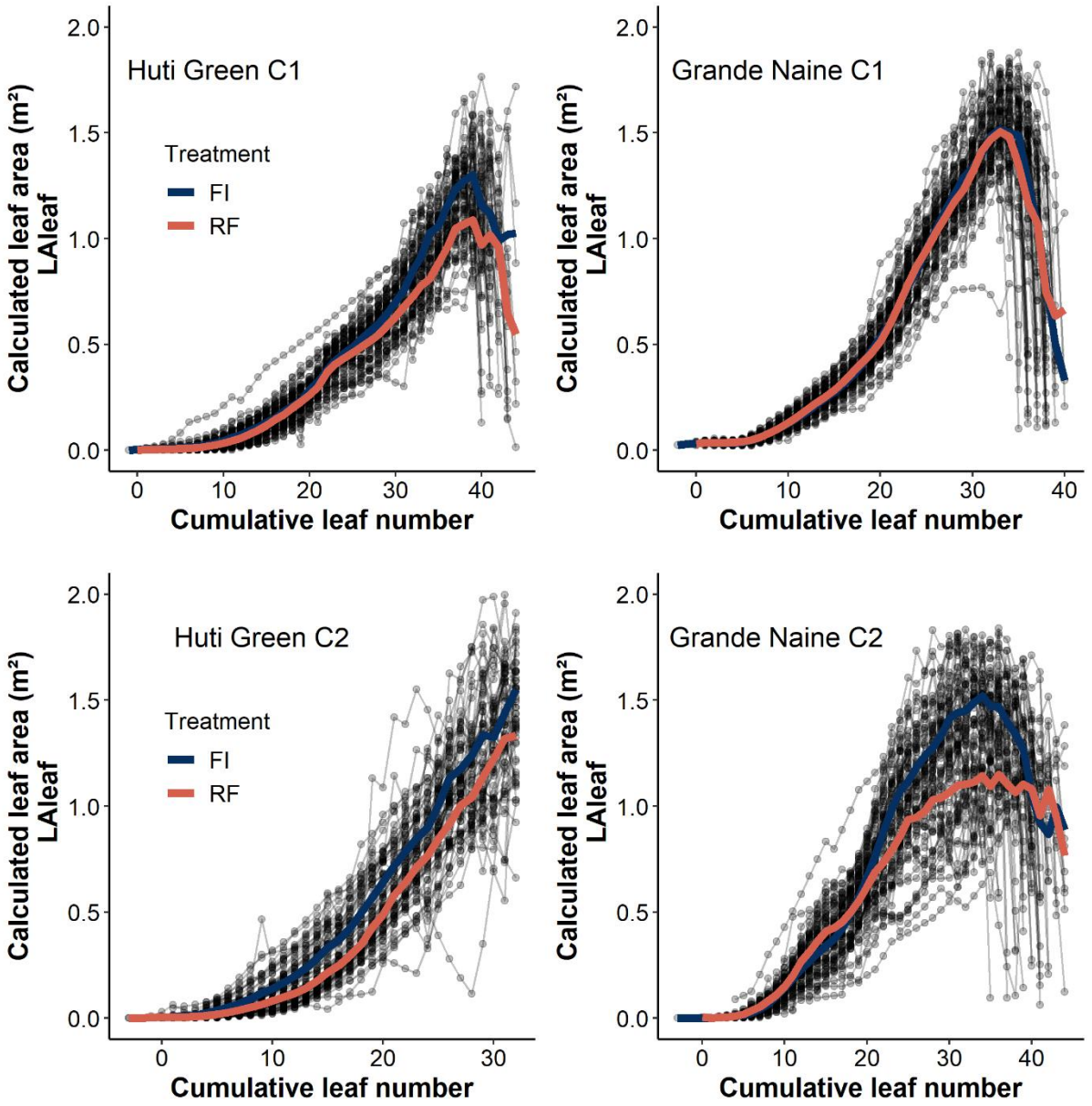


Figure S3: Leaf area database for cumulatively developed leaves of banana cultivars HG: Mchare - Huti Green and GN: Cavendish - Grande Naine under two irrigation treatments (FI: full irrigation and RF: rainfed). Leaf area increases exponentially until approx. leaf 30 to 40, thereafter the leaf area drops until the last leaf before harvest. Grey points and lines note leaf areas for each cumulative leaf measured on plant level. The orange and blue line note the average of all leaf area for each cumulative leaf per treatment.

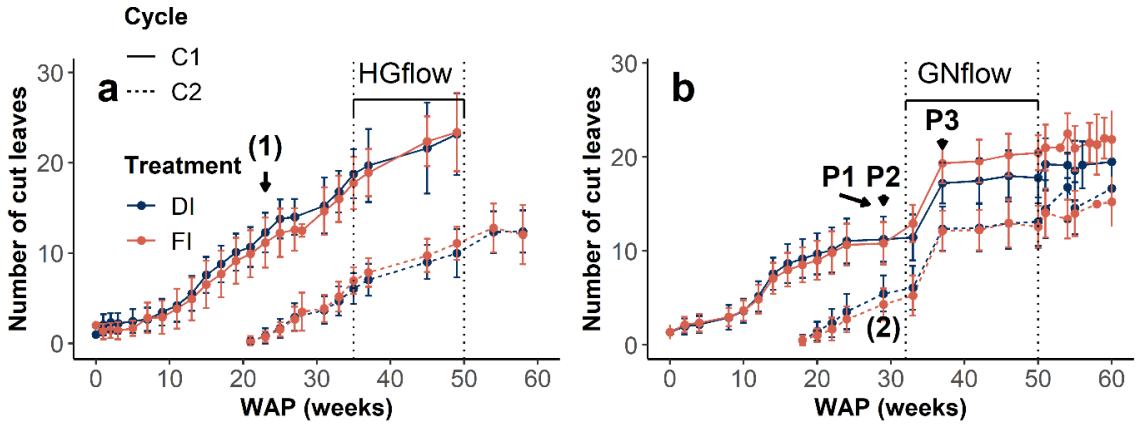


Figure S4: Leaf cutting over time (WAP: weeks after planting) for two experiments a) HG: Mchare - Huti Green and b) GN: Cavendish - Grande Naine under two irrigation regimes (FI: full irrigation and RF: rainfed). Points denote cumulative leaf number cut, error bars denote mean +/-standard deviation as determined at plot level (n=3 for HG and n=4 for GN). HGflow indicates period of flowering of cycle 1 in HG experiment. GNflow indicates period of flowering of cycle 1 in GN experiment; (1) denotes the onset of moisture divergence in HG experiment, whilst (2) denotes the onset of moisture divergence in GN experiment. '*' indicates a statistically significant ($p < 0.005$) difference between FI and RF. P1, P2 and P3 indicate the different leaf pruning events.

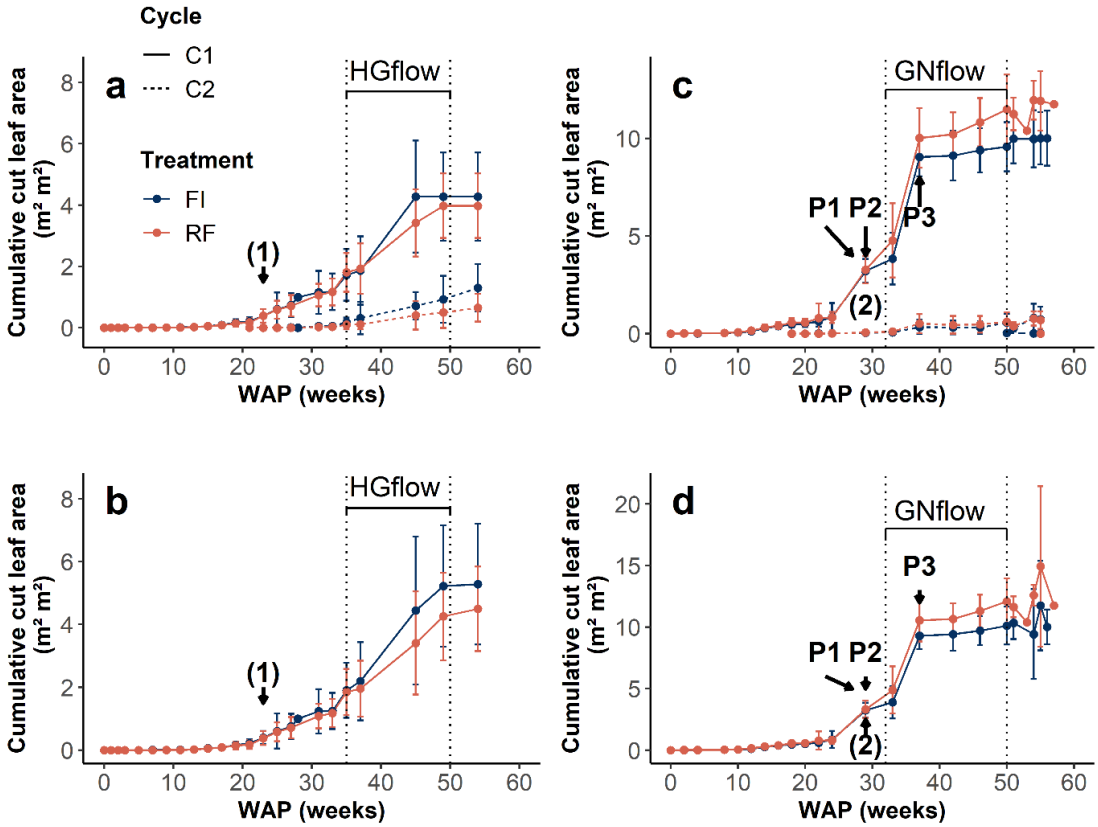


Figure S5: Cumulative leaf area cut over time (WAP: weeks after planting) for two experiments HG: Mchare - Huti Green and GN: Cavendish - Grande Naine under two irrigation regimes (FI: full irrigation and RF: rainfed). a) HG leaf area cut for cycle 1 (C1) and cycle 2 (C2), b) HG leaf area cut on mat level c) GN leaf area cut for cycle 1 (C1) and cycle 2 (C2), d) GN leaf area cut on mat level. Points denote cumulative leaf area cut, error bars denote mean +/-standard deviation as determined at plot level (n=3 for HG and n=4 for GN). HGflow indicates period of flowering of cycle 1 in HG experiment. GNflow indicates period of flowering of cycle 1 in GN experiment; (1) denotes the onset of moisture divergence in HG experiment, whilst (2) denotes the onset of moisture divergence in GN experiment. '*' indicates a statistically significant ($p < 0.005$) difference between FI and RF. P1, P2 and P3 indicate the different leaf pruning events.

Supplementary ANCOVA model outputs

Treatment specific logistical model comparison

Huti Green Bell comparison

Table S1: Huti Green ANCOVA output. Comparison of model with no treatment specific parameters (m.null) and a model with all parameters treatment specific (m.all).

ANCOVA 1: anova(m.null,m.all) # indicates there is a treatment effect							
Analysis of variance table							
Model 1: CC ~ CC_x * CC_0* exp(R * days)/(CC_x + CC_0* (exp(R * days) - 1))							
Model 2: CC ~ CC_x [tr] * CC_0 [tr] * exp(R[tr] * days)/(CC_x [tr] + CC_0* (exp(R[tr] * days) - 1))							
	Res.Df	RSS	Df	SS	F value	Pr(>F)	sign
1	95	2920.6					
2	92	1982.1	3	938.56	14.521	8.05E-08	***
Signif. codes: 0 ‘***’ 0.001 ‘**’ 0.01 ‘*’ 0.05 ‘.’ 0.1 ‘ ’ 1							

Table S2: Huti Green ANCOVA output. Comparison of model with treatment specific parameter r (m.R) and a model with all parameters treatment specific (m.all).

ANCOVA 2: anova(m.all,m.R) # indicates no difference between models differing in all and differing in only R							
Analysis of variance table							
Model 1: CC ~ CC_x [tr] * CC_0 [tr] * exp(R[tr] * days)/(CC_x [tr] + CC_0 * (exp(R[tr] * days) - 1))							
Model 2: CC ~ CC_x * CC_0 * exp(R[tr] * days)/(CC_x + CC_0 * (exp(R[tr] * days) - 1))							
	Res.Df	RSS	Df	SS	F value	Pr(>F)	sign
1	92	1982.1					
2	94	2050.5	-2	-68.431	1.5881	0.2099	
Signif. codes: 0 ‘***’ 0.001 ‘**’ 0.01 ‘*’ 0.05 ‘.’ 0.1 ‘ ’ 1							

Grande Naine comparison

Table S3: Grande Naine ANCOVA output. Comparison of model with no treatment specific parameters (m.null) and a model with all parameters treatment specific (m.all).

> ANCOVA 1: anova(m.null,m.all) # indicates there is a treatment effect

Analysis of variance table

Model 1: CC ~ CC_x * CC_0 * exp(R * days)/(CC_x + CC_0 * (exp(R * days) - 1))

Model 2: CC ~ CC_x [tr] * CC_0 [tr] * exp(R[tr] * days)/(CC_x [tr] + CC_0 * (exp(R[tr] * days) - 1))

	Res.Df	RSS	Df	SS	F value	Pr(>F)	sign
1	81	662.06					
2	78	583.43	3	78.63	3.5041	0.01922	*

Signif. codes: 0 '***' 0.001 '**' 0.01 '*' 0.05 '.' 0.1 ' ' 1

Table S4: Grande Naine ANCOVA output. Comparison of model with treatment specific parameter R (m.R) and a model with all parameters treatment specific (m.all).

> ANCOVA 2: anova(m.R, m.all) #A model where only R differs between treatments is not ok

Analysis of variance table

Model 1: CC ~ CC_x * CC_0 * exp(R[tr] * days)/(CC_x + CC_0 * (exp(R[tr] * days) - 1))

Model 2: CC ~ CC_x [tr] * CC_0 [tr] * exp(R[tr] * days)/(CC_x [tr] + CC_0 * (exp(R[tr] * days) - 1))

	Res.Df	RSS	Df	SS	F value	Pr(>F)	sign
1	80	647.91					
2	78	583.43	2	64.479	4.3101	0.01677	*

Signif. codes: 0 '***' 0.001 '**' 0.01 '*' 0.05 '.' 0.1 ' ' 1

Table S5: Grande Naine ANCOVA output. Comparison of model with treatment specific parameters R and CC_x (m.R. CC_x) and a model with all parameters treatment specific (m.all).

>ANCOVA 3: anova(m.R. CC_x, m.all) # A model where R and CC_x differ is ok

Analysis of variance table

Model 1: CC ~ CC_x [tr] * CC_0 * exp(R[tr] * days)/(CC_x [tr] + CC_0 * (exp(R[tr] * days) - 1))

Model 2: CC ~ CC_x [tr] * CC_0 [tr] * exp(R[tr] * days)/(CC_x [tr] + CC_0 * (exp(R[tr] * days) - 1))

	Res.Df	RSS	Df	SS	F value	Pr(>F)	sign
1	79	584.03					
2	78	583.43	1	0.59728	0.0799	0.7782	

Signif. codes: 0 '***' 0.001 '**' 0.01 '*' 0.05 '.' 0.1 ' ' 1

Treatment specific AquaCrop model comparison

Huti Green Bell comparison

AquaCrop equation Part 1

Table S6: Huti Green Bell ANCOVA output. Comparison of aquacrop regression models for equation part 1 with no treatment specific parameters (m.null) and a model with all parameters treatment specific (m.all).

> ANCOVA 1: anova(m.null,m.all) # indicates there is NOT a treatment effect in the first equation

Analysis of variance table

Model 1: CC ~ cc0 * exp(days * cgc)

Model 2: CC ~ cc0 * exp(days * cgc[tr])

	Res.Df	RSS	Df	SS	F value	Pr(>F)	sign
1	56	1951.3					
2	55	1947.6	1	3.6926	0.1043	0.748	

Signif. codes: 0 '***' 0.001 '**' 0.01 '*' 0.05 '.' 0.1 ' ' 1

AquaCrop equation Part 2

Table S7: Huti Green Bell ANCOVA output. Comparison of aquacrop regression models for equation part 2 with no treatment specific parameters (m.null) and a model with all parameters treatment specific (m.all).

> ANCOVA 1: anova(m.null,m.all) # indicates there is a treatment effect

Analysis of variance table

Model 1: CC ~ CC_x - 0.25 * (CC_x ^2)/cc0 * exp(-1 * days * cgc)

Model 2: CC ~ CC_x [tr] - 0.25 * (CC_x [tr]^2)/cc0 * exp(-1 * days * cgc[tr])

	Res.Df	RSS	Df	SS	F value	Pr(>F)	sign
1	39	2191					
2	37	1079.2	2	1111.8	19.06	2.04E-06	***

Signif. codes: 0 '***' 0.001 '**' 0.01 '*' 0.05 '.' 0.1 ' ' 1

Table S8: Huti Green Bell ANCOVA output. Comparison of aquacrop regression models for equation part 2 with treatment specific parameter canopy growth coefficient (m.cgc) and a model with all parameters treatment specific (m.all).

> ANCOVA 2: anova(m.cgc,m.all) # indicates only an effect of treatment on cgc is not enough, CC_x is also affected by treatment

Analysis of variance table

Model 1: CC ~ CC_x - 0.25 * (CC_x ^2)/cc0 * exp(-1 * days * cgc[tr])

Model 2: CC ~ CC_x [tr] - 0.25 * (CC_x [tr]^2)/cc0 * exp(-1 * days * cgc[tr])

	Res.Df	RSS	Df	SS	F value	Pr(>F)	sign
1	39	1286.2					
2	37	1079.2	2	207.05	3.5495	0.03889	*

Signif. codes: 0 '***' 0.001 '**' 0.01 '*' 0.05 '.' 0.1 ' ' 1

Grande Naine comparison

AquaCrop equation Part 1

Table S9: Grande Naine ANCOVA output. Comparison of aquacrop regression models for equation part 1 with no treatment specific parameters (m.null) and a model with all parameters treatment specific (m.all).

> ANCOVA 1: anova(m.null,m.all) # indicates there is no treatment effect in equation part 1							
Analysis of variance table							
Model 1: CC ~ cc0 * exp(days * cgc)							
Model 2: CC ~ cc0 * exp(days * cgc[tr])							
	Res.Df	RSS	Df	SS	F value	Pr(>F)	sign
1	42	167.82					
2	41	167.75	1	0.066931	0.0164	0.8989	
Signif. codes: 0 '***' 0.001 '**' 0.01 '*' 0.05 '.' 0.1 ' ' 1							

AquaCrop equation Part 2

Table S10: Grande Naine ANCOVA output. Comparison of aquacrop regression models for equation part 2 with no treatment specific parameters (m.null) and a model with all parameters treatment specific (m.all).

>ANCOVA 1: anova(m.null,m.all) # indicates there is a treatment effect in equation part 2							
Analysis of variance table							
Model 1: CC ~ CC_x - 0.25 * (CC_x ^2)/cc0 * exp(-1 * days * cgc)							
Model 2: CC ~ CC_x [tr] - 0.25 * (CC_x [tr]^2)/cc0 * exp(-1 * days * cgc[tr])							
	Res.Df	RSS	Df	SS	F value	Pr(>F)	sign
1	39	763.47					
2	37	531.13	2	232.34	8.0927	0.001215	**
Signif. codes: 0 '***' 0.001 '**' 0.01 '*' 0.05 '.' 0.1 ' ' 1							

Table S11: Grande Naine ANCOVA output. Comparison of aquacrop regression models for equation part 2 with treatment specific parameters canopy growth coefficient (m.cgc) and a model with all parameters treatment specific (m.all).

> ANCOVA 2: anova(m.cgc, m.all) # indicates differing cgc is not enough							
Analysis of variance table							
Model 1: CC ~ CC_x - 0.25 * (CC_x ^2)/cc0 * exp(-1 * days * cgc[tr])							
Model 2: CC ~ CC_x [tr] - 0.25 * (CC_x [tr]^2)/cc0 * exp(-1 * days * cgc[tr])							
	Res.Df	RSS	Df	SS	F value	Pr(>F)	sign
1	39	765.99					
2	37	531.13	2	234.86	8.1805	0.001143	**
Signif. codes: 0 '***' 0.001 '**' 0.01 '*' 0.05 '.' 0.1 ' ' 1							

Table S12: Grande Naine ANCOVA output. Comparison of aquacrop regression models for equation part 2 with treatment specific parameters maximum Canopy cover (m. CC_x) and a model with all parameters treatment specific (m.all).

> ANCOVA 3: anova(m. CC_x, m.all) #indicates differing CC_x is not enough

Analysis of variance table

Model 1: CC ~ CC_x [tr] - 0.25 * (CC_x [tr]^2)/cc0 * exp(-1 * days * cgc)

Model 2: CC ~ CC_x [tr] - 0.25 * (CC_x [tr]^2)/cc0 * exp(-1 * days * cgc[tr])

	Res.Df	RSS	Df	SS	F	value	Pr(>F)	sign
1	39	747.92						
2	37	531.13	2	216.79		7.551	0.001778	**

Signif. codes: 0 '***' 0.001 '**' 0.01 '*' 0.05 '.' 0.1 ' ' 1

Annex IV: Allometry supplementary data

Supplementary figures

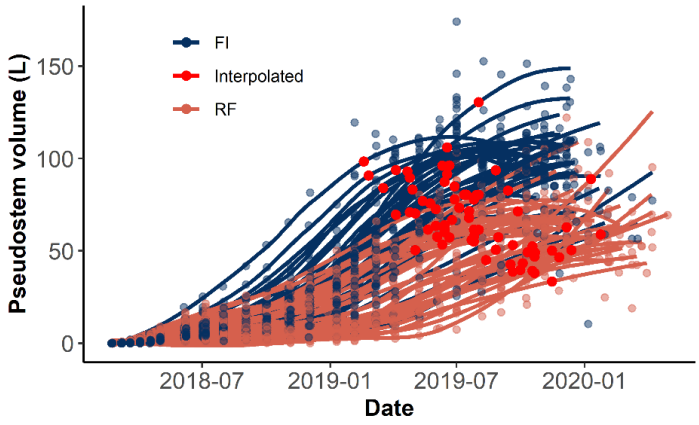


Figure S1: Growth of pseudostem volume (L) over time in Grande Naine of individual plants in cycle 2 (C2). Dots indicate actual growing measurements, lines indicate local non-parametric regression curves of individual plants under full irrigation (FI) and Rainfed (RF). Red dots indicate the intersection of the regression curves with the date of flowering of C2 and show the interpolated $V_{pseudo,flower}$.

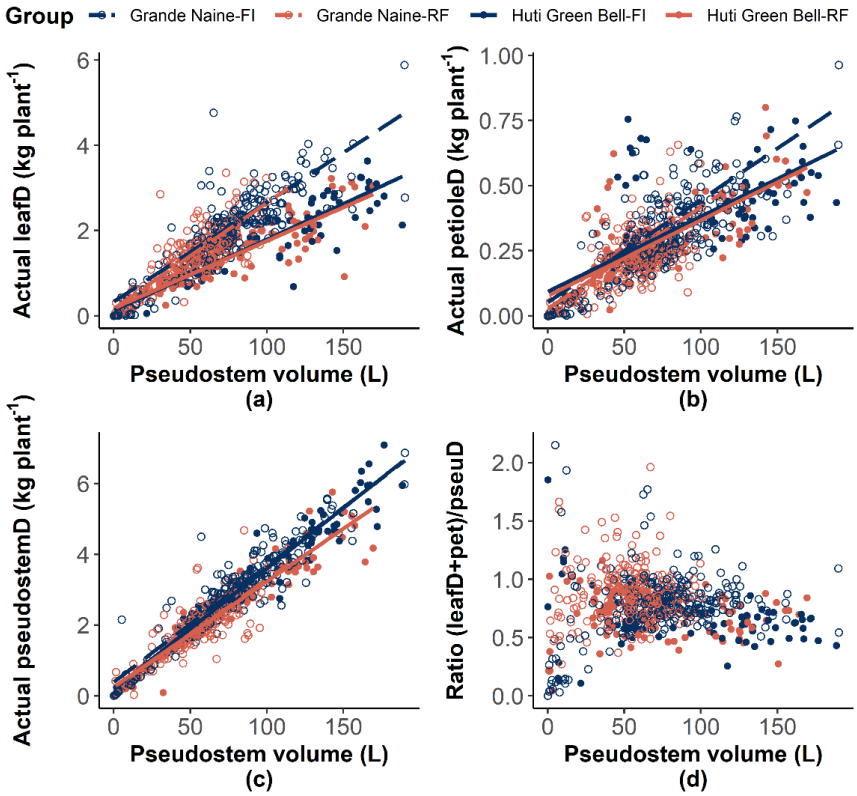


Figure S2: Components of aboveground vegetative dry biomass ($ABGVD$, kg plant $^{-1}$). (a) Leaf dry weight ($leafD$, kg plant^{-1}) versus pseudostem volume (L); (b) Petiole dry weight ($petioleD$, kg plant^{-1}) versus pseudostem volume (L); (c) Pseudostem dry weight ($pseudostemD$, kg plant^{-1}) versus pseudostem volume (L). Used regression models in (a), (b) and (c) were specific models for treatment and cultivar using pseudostem volume as predictor. (d) Ratio between sum of $leafD$ and $petioleD$ to $pseudostemD$. FI denotes full irrigation, RF denotes rainfed.

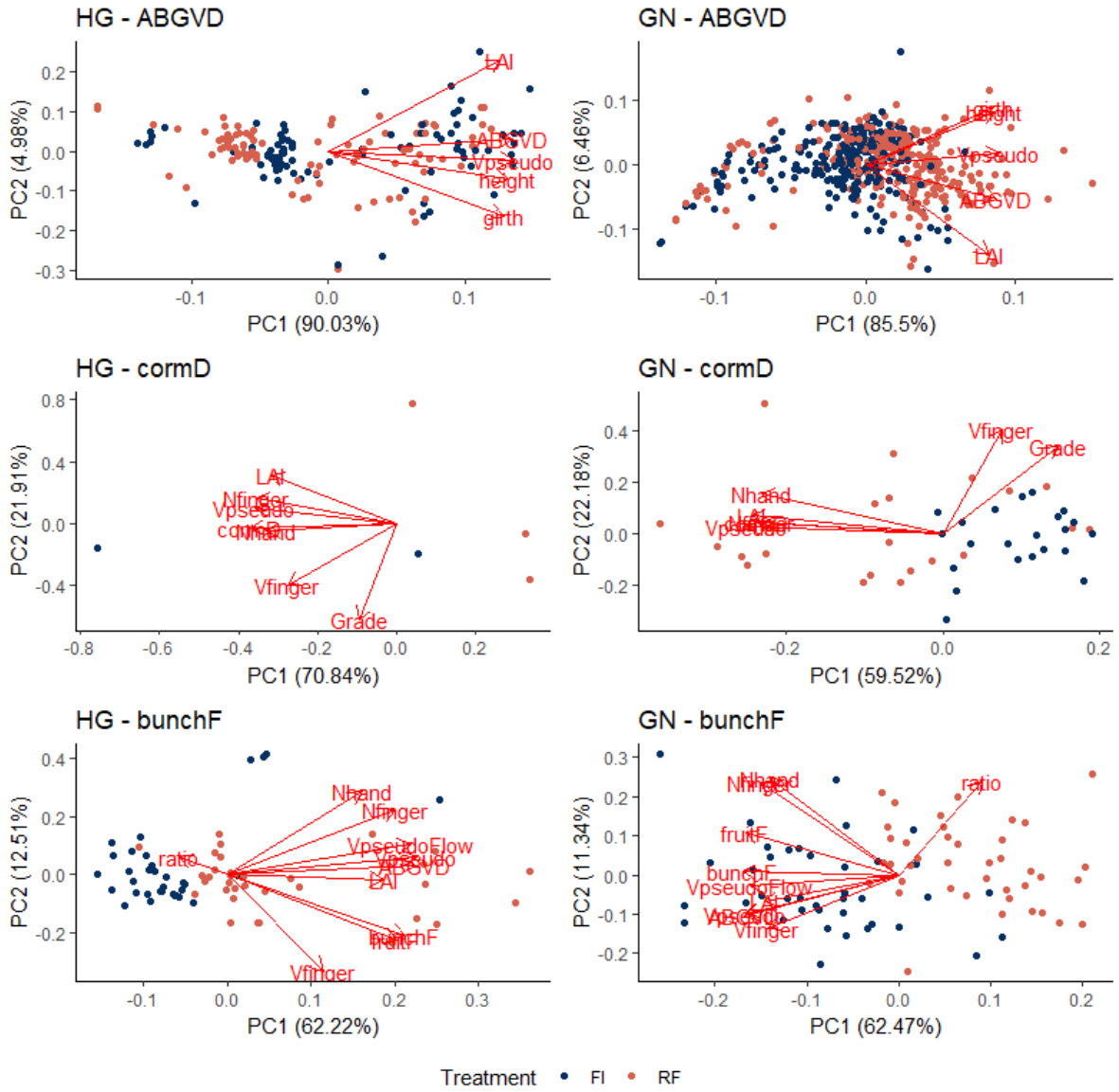


Figure S3: Principal component analysis (scaled and centered) biplots for datasets used in regression. $ABGVD$: dataset for Aboveground vegetative dry matter regression, $cormD$ data: dataset for corm dry matter $cormD$ regression and $bunchF$ data: dataset for bunch fresh weight regression. PC1 is principal component 1, PC2 is principal component 2. Dots indicate observations in the first 2 principal component axes and red arrows indicate the PC loadings for the used variables in the PC analysis. Loadings that are close to each other (in a similar or opposite direction) and have a similar length are considered to be correlated. Abbreviations of the loadings are given in table 6-1 in Chapter 6.

PCA analysis reveals $ABGVD$ is correlated to vegetative parameters (V_{pseudo}, LAI), $cormD$ is correlated to V_{pseudo} , and $bunchF$ is correlated to V_{pseudo} , $V_{pseudo,floweirng}$, LAI, $ABGVD$ and V_{finger} as the loadings vectors point in a similar direction and have a similar length.

PCA analysis further reveals the number of hands and the number of fingers are positively correlated, whilst the V_{finger} is not correlated to the N_{hand} and N_{finger}. However, $bunchF$ is correlated to both V_{finger}, N_{finger} and N_{finger}.

Supplementary tables

Table S1: Dry matter (DM, g dry matter g fresh weight^{-1}) (mean and sd) of the plant organs obtained in the field trial. Moisture contents were determined from subsamples of plant organs taken at harvest from the different cycles. Treatment differences were not significant (*p<0.05*), leading to the pooling of data across the treatments (FI: full irrigation and RF: rainfed) per cycle (C1, C2 and C3) to obtain a dry matter percentage per organ per cycle.

		Huti Green Bell			Grande Naine		
Organ	**Cycle**	**N**	**Mean**	**sd**	**N**	**Mean**	**sd**
Male bud	C1	20	0.10	0.05	36	0.10	0.05
Male bud	C2	20	0.10	0.06	47	0.09	0.04
Male bud	C3	7	0.08	0.01	14	0.09	0.02
Fruit	C1	48	0.25	0.09	18	0.14	0.11
Fruit	C2	18	0.18	0.23	37	0.21	0.17
Peduncle	C1	77	0.08	0.04	20	0.06	0.01
Peduncle	C2	54	0.07	0.04	42	0.07	0.08
Pseudostem	C1	80	0.07	0.02	68	0.07	0.04
Pseudostem	C2	24	0.08	0.05	63	0.06	0.04
Pseudostem	C3				10	0.05	0.02
Petiole	C1	74	0.11	0.03	65	0.09	0.03
Petiole	C2	24	0.11	0.03	57	0.09	0.07
Petiole	C3				7	0.09	0.01
Leaf	C1	54	0.22	0.04	64	0.17	0.05
Leaf	C2	25	0.16	0.05	60	0.18	0.09
Corm	C1	10	0.11	0.04	34	0.13	0.05
Corm	C2	5	0.15	0.07	28	0.13	0.07
Corm	C3	4	0.12	0.08	11	0.14	0.07

Annex V: AquaCrop model supplementary data

Table S1: soil input file specified in the AquaCrop model (Arusha.SOL file).

Soil horizon		Volumetric Water content						Physical properties			
Name	**Depth**	**SAT**	**FC**	**PWP**	**TAW**	K^{*}_{sat}	K^{**}_{sat}	**Penetrability**	**Gravel**	**Cr_a**	**Cr_b**
	cm	----------**%**----------			m^3m^{-3}	mm day^{-1}	mm day^{-1}	----------%----------			
Ahp	0 - 15	60	39	18	21	617	150	100	0	-0.143	2.621
C1	15 - 55	57	40	21	19	125	125	100	0	-0.5366	1.493
C2	55-100	55	43	27	16	500	110	100	0	-0.2366	2.472

*based on pedo-transfer function of Saxton and Rawls (2006) based on percentages of sand, silt, clay, and organic matter content (OM) for each soil horizon (if OM rises: Ksat rises).** based on AquaCrop default proposed values and Saxton and Rawls (2006) values unadjusted for OM.

Results do not change significantly when using the K^{*}_{sat} from Saxton and Rawls (2006) and the K^{**}_{sat} from AquaCrop for both FI and RF simulations (data not shown). Therefore K_{sat}^{**} in AquaCrop was used.

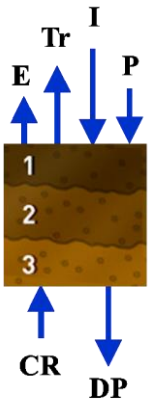
Annex VI: Adjustment for simulating drip irrigation

Note composed by Dirk RAES, Jan DIELS and Eline VANUYTRECHT.

Department of Earth and Environmental Sciences, KU Leuven University, Belgium

June 2017.

Part of the reality that is simulated (system)



The interacting between crop and soil is the part of the reality (system) that is simulated in AquaCrop. By keeping track of incoming and outgoing water fluxes at the boundaries of the system, AquaCrop calculates by means of a soil water balance, the amount of water retained in the root zone, the root zone depletion and the corresponding water stresses affecting canopy development, crop transpiration and production (Fig. S1). The fluxes in and out of the system are assumed to be one dimensional (vertical upwards or downwards), and uniform over the entire field surface (upper boundary) and bottom of the root zone (lower boundary). They are expressed as an equivalent depth (mm water) per unit time step (day).

1 mm of water is equivalent to 1 liter per m^2 or 10 m^3 per hectare.

Figure S1: Uniform movement of water in and out of the simulated system. Water is lost by soil evaporation (E), crop transpiration (Tr), and deep percolation (DP), and gained by irrigation (I), rainfall (P) and capillary rise (CR)

Characteristics of localized (drip) irrigation

Specific characteristics of drip irrigation that should be considered in a simulation:

- small irrigation application doses, which are frequently applied (specified in the *Irrigation management* menu);
- small fraction of the soil surface that is wetted by drip irrigation (e.g. 30%, and even nihil with subsurface drip). AquaCrop simulates the reduction in soil evaporation after an irrigation event, by considering only the wetted fraction (f_w) of the field surface (specified as input in the *Irrigation management* menu);
- high soil water content (close to Field Capacity) that is maintained in the root zone by a frequent application of water. Irrigation is scheduled when only a small fraction of the total available water (TAW) is depleted out of the root zone (one of the available time criteria for the generate of an irrigation schedule in the *Irrigation management* menu);
- limited root deepening in the absence of significant rainfall during the season. When the soil profile is dry at the start of the simulation (specified in the *Initial conditions* menu), only the top part of the soil profile is wetted by drip irrigation (small irrigation application doses). Since in AquaCrop root zone deepening is limited in a dry subsoil, roots will concentrate in the wetted top soil. This results in an increase of root density in the shallow root zone, which is simulated in AquaCrop by an automatic increase of the maximum root water extraction rate.

Herbaceous crops with high plant density

When the crop is fully developed, the canopy will cover (nearly) the total field surface (CC close to 100%). The root zone can be regarded as a huge (leaky) container which occupies the total soil profile (Fig. S2).

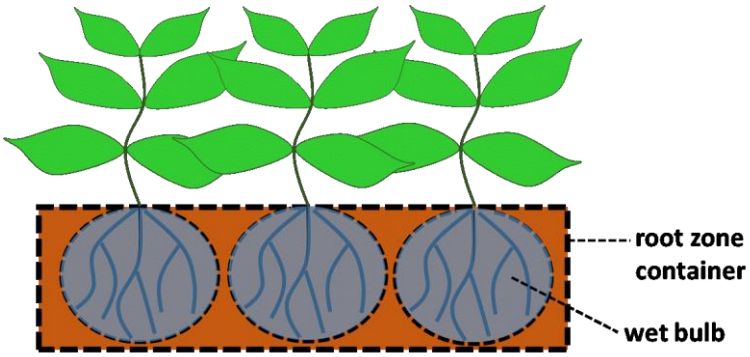


Figure S2: Root zone depicted as a huge container occupying the total soil profile

Although only a fraction of the soil surface is wetted by drip irrigation, the irrigation water is stored below the surface, in relatively large wet bulbs. As a result of rain, the relatively high plant density, and the relatively large wet bulbs, it can be assumed that the roots are well distributed in the total soil profile (if not so, rainwater that infiltrated outside the wet bulbs, will move between irrigation applications to the roots by matrix forces). A uniform movement of water at the boundaries of the soil profile is valid.

Orchards in a dry environment, also valid for herbaceous crops with large row spacing in a dry environment young orchards in their first year(s)

If rainfall is limited, the roots remain concentrated in wet bulbs which occupy only a part of the total soil profile (Fig. S3).

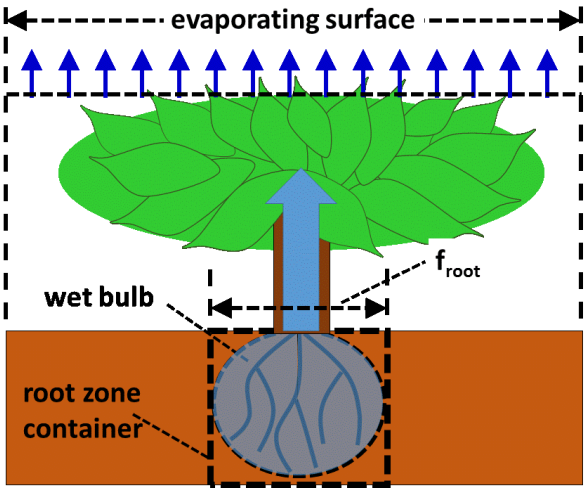


Figure S3: Wet bulb and root zone container in an orchard occupying only a fraction (f_{root}) of the soil profile

Due to the large distance between the individual plants or trees (low plant density) and the localized application of irrigation water by drip, the size of the effective root zone is relatively small (Fig. S3).

Since the water fluxes in and out of the root zone are quite different from the fluxes in and out of the non-rooted part of the soil profile, the fluxes are no longer uniform at the boundaries of the entire soil profile.

By restricting the simulation of the soil water balance to the root zone, the fluxes in and out of the simulated system remain uniform. The effective root zone (system) is considered as a (leaky) container, which occupies only a fraction (f_{root}) of the total soil profile (e.g. 30% or f_{root} = 0.333). What happens in the non-rooted part of the soil profile, outside the container, is of no interest. Infiltration and evaporation of water from occasional rain events in that part, do not contribute to transpiration and crop production, and can be disregarded. Although the effective root zone occupies only a fraction of the soil profile, the driving force for water extraction out of the system is the evaporative demand over the entire field surface.

Solution 1: adjustment of the evapotranspiration

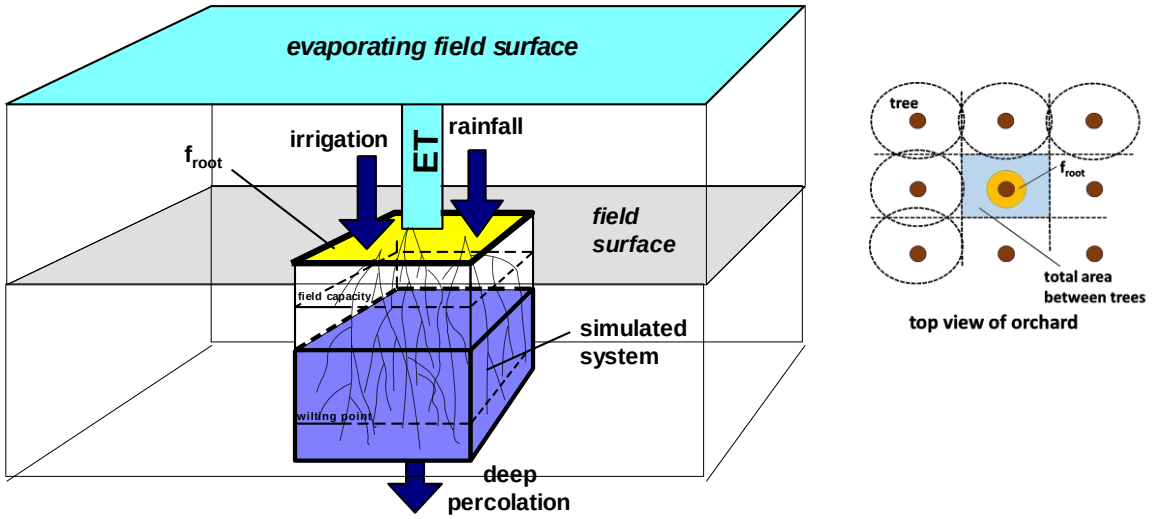


Figure S4: Solution 1, in which the evapotranspiration (ET) out of the system (root zone container) is adjusted to the evaporating surface (field surface)

The size of the evaporating field surface does not correspond with the fraction of the field surface occupied by the system, which is the root zone container (Fig. S4). Since all the water lost by evapotranspiration (expressed as an equivalent depth: mm of water or liter per m^2 of field surface) is extracted out of a small part of the soil profile (mm of water or liter per m^2 of the root zone), a correction is required. The adjustment consists in increasing the reference evapotranspiration (ETo).

Adjustments of the input required in AquaCrop:

- The adjustment of the reference evapotranspiration (ETo) is done in the *ETo file* by dividing the ETo values with the fraction (f_{root}) of the soil profile that is rooted. Reference evapotranspiration in the ETo file becomes [ETo/f_{root}]. If f_{root} is one third of the field surface (f_{root} = 0.333), the evaporative demand of the atmosphere out of the container (which must supply all of the water) is three times larger than ETo;
- The upper and lower thresholds for soil water depletion, together with the shape of the stress function, determine the magnitude of the soil water stress affecting one or another process for specific soil water contents in the root. Since the thresholds are automatically adjusted in AquaCrop to the evaporating demand of the atmosphere, the high assumed ETo values might result in a too quick response to soil water depletion. Although a lot of water needs to be extracted

out of a small part of the soil profile, the root density in that part is also high. To avoid an overreaction to the increased values of ETo, (i) switch of the correction to ETo (select 'none' for the adjustment by ETo, in the various tab sheets of the responses to water stresses in the *Crop characteristics* menu) or (preferably) (ii) decrease the sensitivity of the adjustment to ETo (which is a program parameter which can be adjusted in the *Program settings: Crop parameters* menu);

- Soil evaporation (E) out of the system will be very small since the canopy cover shelters completely the surface of the root zone container, and irrigation water is applied locally. Evaporation after rainfall from the soil surface not belonging to the system, is no part of the soil water balance, and should not be accounted for. To minimize or switch off soil evaporation after rainfall as well as after irrigation, consider in the *Field management* menu a 90 to 100 % cover by mulches. The mulches are 'user specified' and should reduce evaporation by 95 to 100%;
- The specified amount of rainfall in the PLU file, needs not to be corrected, since it is expressed as an equivalent depth in mm/day and assumed to infiltrate uniformly all over the total field surface (minus eventually the fraction lost by surface runoff);
- In AquaCrop the (net) irrigation application dose is expressed in mm (equivalent depth). The area of the root zone container (m^2), should be considered to convert the volume (liter) of applied irrigation water to an equivalent depth in mm. If for example, the drip irrigation replenishes daily the 5 mm/day of water lost by evapotranspiration (from the entire field surface), then the required net volume of irrigation water (which is concentrated in the root zone container) is $5/f_{root}$ mm. If f_{root} is one third of the field surface (f_{root} = 0.333), the net irrigation application dose that needs to be specified in the *Irrigation management* menu is (5/0.333 =) 15 mm. Since all the irrigation water is stored in only 1 third of the soil profile, the irrigation application dose is 3 times the amount of water lost by evapotranspiration.

Water extracted by crop transpiration (mm/day) from the root zone container is [Tr,system]:

$$Tr = Ks\ Ks_{Tr}\ Kc_{Tr} \left[\frac{ETo}{f_{root}} \right] \qquad \text{(Eq. 1)}$$

where Ks is the coefficient for soil water stress, Ks_{Tr} the coefficient for cold stress, Kc_{Tr} the crop transpiration coefficient, ETo the reference evapotranspiration (mm/day) and f_{root} the fraction of the field surface occupied by the root zone container. The crop transpiration coefficient is:

$$Kc_{Tr} = CC^*\ Kc_{Tr,x} \qquad \text{(Eq. 2)}$$

where CC* is the canopy cover corrected for micro-advection (when incomplete canopy cover), and $Kc_{Tr,x}$ is the coefficient for maximum crop transpiration (well-watered-soil and complete canopy, CC = 1). For most crops $Kc_{Tr,x}$ is about 1.05 up to 1.20.

Since the small reservoir must cope with the evaporative demand of the total field surface, water stresses will swiftly arise in the absence of a frequent application of water. While running a simulation, Ks is adjusted daily by considering the water stress in the root zone container. The available growing-degree days determine the occurrence of cold stress and Ks_{Tr}. The coefficients Ks and Ks_{Tr} vary between 1 (no stress) and zero (full stress).

Adjustments of the output required in AquaCrop:

- The simulated crop transpiration (Tr_{system}) is extracted out of the root zone container (system). Since the non-rooted part does not transpire, the amount of water lost from the entire field surface by crop transpiration (Tr_{field}) is f_{root} times Tr_{system}. If f_{root} is one third of the field surface (f_{root} = 0.333), Tr_{field} is only one third of the value (Tr_{system}) reported in the output file;

- The simulated deep percolation (DP_{system}) drains entirely out of the system (root zone container). In the absence of significant rainfall during the growth cycle, the deep percolation losses from the non-rooted part will be negligible. The amount of water that drains to the ground water table (DP_{field}), is f_{root} times DP_{system} If f_{root} is one third of the field surface (f_{root} = 0.333), DP_{field} is only one third of the value (DP_{system}) reported in the output file.

Table S1: Calculation of the soil water balance for solution 1.

Characteristics:

- ☐ Climate: P = 0; ETo = 5 mm/day; no cold stress
- ☐ Crop: Distance between trees = 2.0 m, distance between rows = 3.5 m; Kc_{Tr} = 1.0; Zr (effective rooting depth) = 0.7 m; when 25% of TAW is depleted, water stress starts to affect leaf expansion; when 50% of TAW is depleted, water stress starts to affect crop transpiration;
- ☐ Soil profile (fine soil fraction): θ_{SAT} = 0.50, θ_{FC} = 0.30 and θ_{PWP} = 0.10 m^3/m^3;
- ☐ Irrigation: each time 15 % of TAW is depleted, 49 liter of water is applied to each tree; f_{root} is 1/3 of the field surface or f_{root} = 0.333;

☐ Initial soil water content in root zone (Wr_{ini}): Field capacity.

$Wr_{ini} = Wr_{FC} = 1000\ (\theta_{FC})\ Zr = 210$ mm;

$TAW = 1000\ (\theta_{FC} - \theta_{PWP})\ Zr = 140$ mm;

Allowable depletion = 0.15 TAW = 21 mm. Irrigation should be applied when:

- root zone depletion ≥ 21 mm at the end of the day, or
- soil water content in root zone (Wr) ≤ Wr_{FC} – 21 = 210 – 21 = 189 mm at end of the day;

Irrigation dose is 49 litre per tree. Irrigation is concentrated on 1/3 of (2.0m × 3.5m) = $7m^2$, which is on 2.333 m^2 (surface of system). The equivalent depth for the system = 49 litre per 2.333 m^2 or I = (49/2.333) = 21 mm;

DP = 0 if Wr ≤ Wr_{FC} = 210 mm;

Transpiration starts to be affected when 0.5 TAW = 70 mm is depleted. If root zone depletion ≤ 70 mm or Wr ≥ 210 – 70 = 140 mm, Ks = 1 and $Tr = Kc_{Tr}$ (ETo/3) = 15 mm/day.

Day	Wr_{start} (mm)	Wr at end of the day without irrigation $Wr_t = Wr_{start} + P - E - Tr - DP$ (mm)	Irrigation ? $Wr_t \leq 189$ mm	I (mm)	$Wr_{end} = Wr_t + I$ (mm)
ini					210
1	210	210 + 0 – 0 – 15 – 0 = 195	no	0	195 + 0 = 195
2	195	195 + 0 – 0 – 15 – 0 = 180	yes	21	180 + 21 = 201
3	201	201 + 0 – 0 – 15 – 0 = 186	yes	21	186 + 21 = 207
4	207	207 + 0 – 0 – 15 – 0 = 192	no	0	192 + 0 = 192
5	192	192 + 0 – 0 – 15 – 0 = 177	yes	21	177 + 21 =198
6	198	198 + 0 – 0 – 15 – 0 = 183	yes	21	183 + 21 = 204
7	204	204 + 0 – 0 – 15 – 0 = 189	yes	21	189 + 21 = 210

Solution 2: adjustment of the storage capacity of the soil profile

In this option, the system is stretched till it covers the entire soil profile. The adjustment consists in bringing the storage capacity of the entire soil profile in line with the limited storage capacity of the actual root zone (Fig. S5).

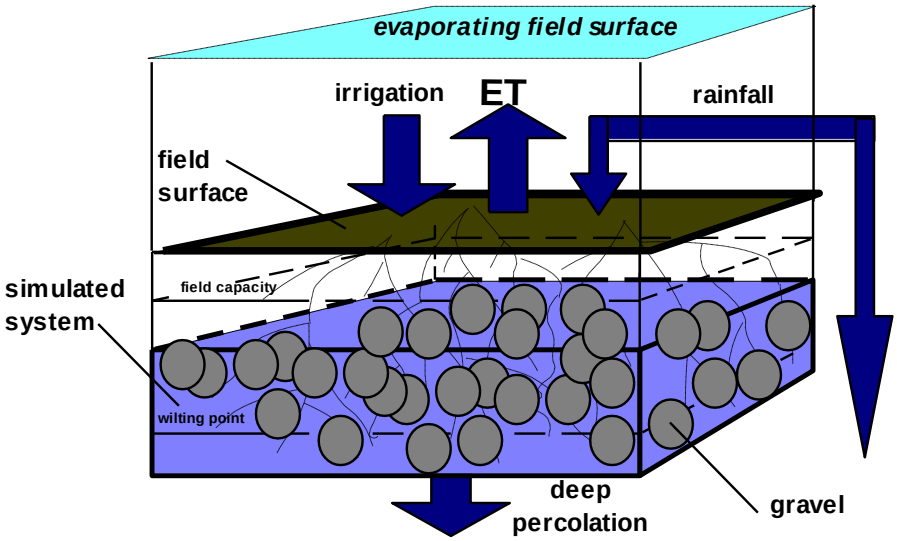


Figure S5: Solution 2, in which the root zone container (system) covers the entire soil profile, and its storage capacity is reduced with the help of gravel

Adjustments of the input required in AquaCrop:

- Match the storage capacity (TAW: total available soil water) of the total soil profile, to the storage capacity of the root zone container. This can be obtained by assuming the presence of gravel in the total soil profile. By specifying the mass percentage of gravel in the *Soil profile characteristic* menu, AquaCrop converts it to the volume percentage of gravel, and display the adjusted TAW and the percentage of the plant available water. The volume percentage should be 100 f_{root}, where f_{root} is the fraction of the soil profile that is rooted;
- Since the container (system) and the evaporating field surface have the same dimensions (Fig. 5), ETo correctly expresses the evaporating demand of the atmosphere;
- Although the container (system) and the evaporating field surface have the same dimensions, only a fraction of the observed rainfall infiltrates in the root-zone container. The amount (mm) of rainfall (P) in the *PLU file* needs to be reduced, by multiplying the values with the fraction f_{root}: it becomes [$f_{root} \times P$]. If f_{root} is one third of the field surface ($f_{root} = 0.333$), the amount of rainfall that infiltrates in the container is only one third of the observed rainfall;
- To minimalize or inhibit soil evaporation (see justification in solution 1), consider in the *Field management* menu a 90 to 100 % cover by mulches. The mulches are 'user specified' and should reduce evaporation by 95 to 100%;
- In AquaCrop the (net) irrigation application dose is expressed in mm (equivalent depth). The surface (m^2) of the root zone container (which is in this solution the total field surface), should be considered to convert the volume (litre) of applied irrigation water to an equivalent depth in mm. If for example, the drip irrigation replenishes daily the 5 mm/day of water lost by evapotranspiration, then the net irrigation application dose that needs to be specified in the *Irrigation management* menu is 5 mm as well. All the irrigation water is stored in the total soil profile (which storage capacity is however reduced to only 1 third of its original storage, if f_{root} is 0.333).

Water extracted by transpiration (mm/day) from the root zone is:

$$Tr = Ks\ Ks_{Tr}\ Kc_{Tr}\ ETo \qquad \text{(Eq. 3)}$$

where Ks is the coefficient for soil water stress, Ks_{Tr} the coefficient for cold stress, Kc_{Tr} the crop transpiration coefficient, and ETo the reference evapotranspiration (mm/day).

Due to the limited storage capacity of the soil profile, water stresses will swiftly arise in the absence of a frequent application of water. While running a simulation, Ks is adjusted daily by considering the water stress in the soil profile. The available growing-degree days determine the occurrence of cold stress and Ks_{Tr}. The coefficients Ks and Ks_{Tr} vary between 1 (no stress) and zero (full stress).

Adjustments of the output required in AquaCrop:

Since the container (system) and the evaporating field surface have the same dimensions, the fluxes (expressed as an equivalent depth) in the output files, need not be adjusted to the field surface.

Table S2: Calculation of the soil water balance for solution 2.

Characteristics: see Table S1					
For a 80 mass% of gravel, the plant available water drops to 33.33 %. Or the vol % of gravel is 66.66% (equations to convert mass to volume percent of gravel are given in the reference manual of AquaCrop). Or $(1 - vol\%_{gravel}/100) = 0.333 = f_{root}$.					
$Wr_{ini} = Wr_{FC} = 1000\ (\theta_{FC})\ Zr\ (1 - vol\%_{gravel}/100) = 70$ mm; $TAW = 1000\ (\theta_{FC} - \theta_{PWP})\ Zr\ (1 - vol\%_{gravel}/100) = 46.66$ mm; Allowable depletion = 0.15 TAW = 7 mm. Irrigation should be applied when: – root zone depletion ≥ 7 mm at the end of the day, or – soil water content in root zone (Wr) ≤ Wr_{FC} - 7 = 70 – 7 = 63 mm at end of the day; Irrigation dose is 49 litre per tree, which expressed as an equivalent depth (mm) for the field surface (system) is 49 litre per (2m × 3.5m) = 7 m^2 or 7 litre per m^2 which is I = 7 mm; DP = 0 if Wr ≤ Wr_{FC} = 70 mm; Transpiration starts to be affected when 0.5 TAW = 23.33 mm is depleted. If root zone depletion ≤ 23.33 mm or Wr ≥ 70 – 23.33 = 46.66 mm, Ks = 1 and $Tr = Kc_{Tr}\ ET = 5$ mm/day.					
Day	Wr_{start} (mm)	Wr at end of the day without irrigation $Wr_t = Wr_{start} + P - E - Tr - DP$ (mm)	Irrigation ? $Wr_t \leq 63$ mm	I (mm)	$Wr_{end} = Wr_t + I$ (mm)
ini					70
1	70	70 + 0 – 0 – 5 – 0 = 65	no	0	65 + 0 = 65 mm
2	65	65 + 0 – 0 – 5 – 0 = 60	yes	7	60 + 7 = 67 mm
3	67	67 + 0 – 0 – 5 – 0 = 62	yes	7	62 + 7 = 69 mm
4	69	69 + 0 – 0 – 5 – 0 = 64	no	0	64 + 0 = 64 mm
5	64	64 + 0 – 0 – 5 – 0 = 59	yes	7	59 + 7 = 66 mm
6	66	66 + 0 – 0 – 5 – 0 = 61	yes	7	61 + 7 = 68 mm
7	68	68 + 0 – 0 – 5 – 0 = 63	yes	7	63 + 7 = 70 mm

Non-irrigated orchards

In the absence of localized irrigation, roots will occupy the entire or major part of the soil profile. The ratio f_{root} is much larger than in drip irrigated orchards in a dry environment. If f_{root} is not close to 1 (e.g. because of large spacing), one of the solutions discussed above can be applied to simulate the soil water balance.

Orchards irrigated only during dry season

During the rainy season, water is extracted by the roots out of the entire, or major part of the soil profile in response to evapotranspiration (f_{root} is 1, or close to 1). When irrigation is locally applied (drip) in the dry season, only a small fraction of the soil profile is wetted and contribute to ET (f_{root} is small). Hence the simulated system, which is the part of the soil profile in which incoming and outgoing water are simulated as uniform fluxes over the boundaries, cannot be considered as the same in the rainy and dry season (Fig. 6).

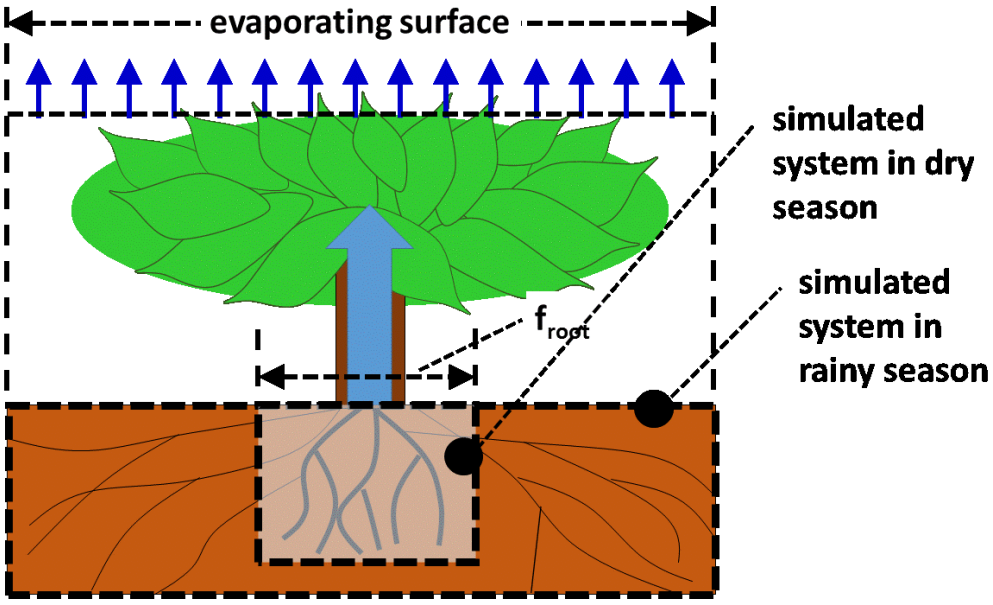


Figure S6: Simulated systems in dry and rainy season

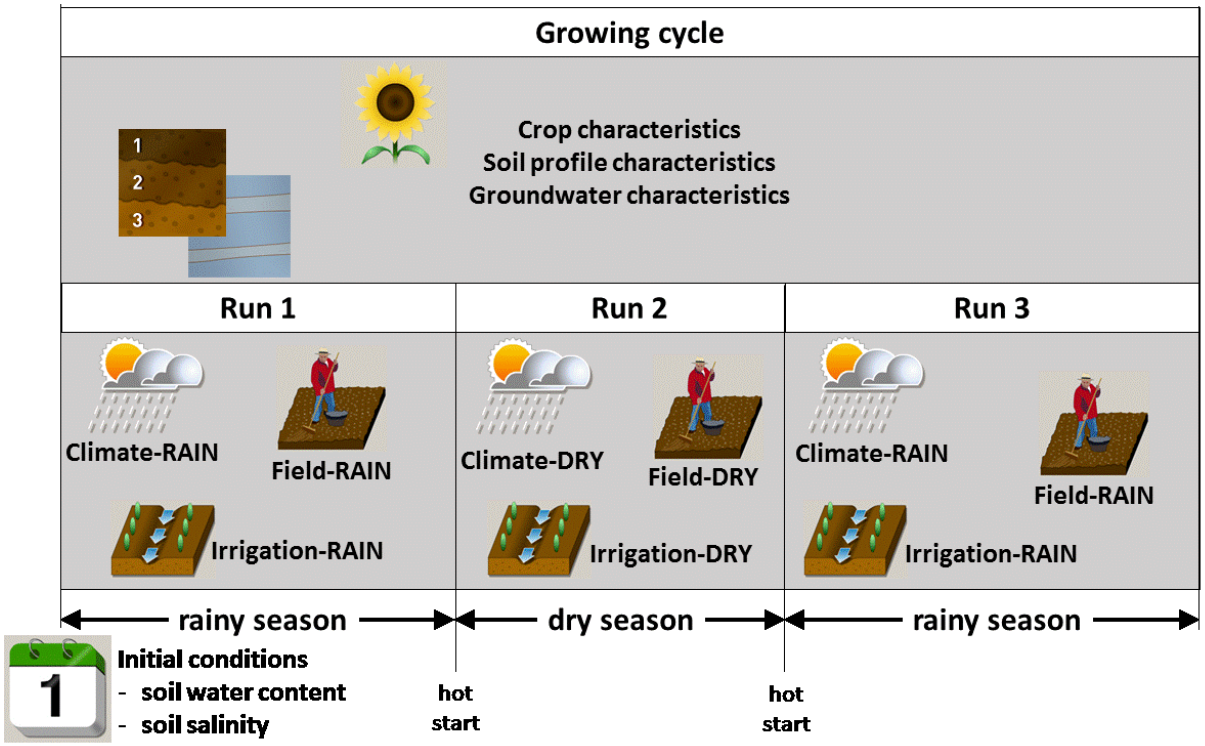
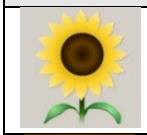


Figure S7: Successive simulations within one growing cycle, each which its own Climate, Field management and Irrigation management file

It can be assumed that at the end of the rainy season (switch from Run 1 to Run 2) the soil water content in the entire soil profile (simulated system in Run 1) is comparable to the soil water content in the root zone container (simulated system in Run 2). Since at the end of the dry season (switch from Run 2 to Run 3), the soil water content in the root zone container (simulated system in Run 2) is assumed to be comparable to the soil water content in the entire soil profile (simulated system in Run 3), the switch from dry to rainy season can only occur when the top of the entire soil profile is already sufficiently wetted by rainfall. If required, it is possible to update in AquaCrop the soil water content during a simulation run.

Table S3: Content of the files for the successive simulations depicted in Figure S6

File		Content
Growing cycle		
	Crop	Conservative and cultivar specific crop parameters, and non-conservative crop parameters fine-tuned to the environment
	Soil profile	Soil physical characteristics, stoniness and penetrability of the different horizons
	Ground-water	Groundwater table characteristics (if the water table is less than 4 meter below rooting depth): the characteristics (depth and quality of the groundwater) can vary throughout the season
	Initial Conditions	Status of the soil water and salt content, canopy and root development, and biomass production at the start of the first day of the simulation period
Rainy season (Run 1 and 3)		
	Climate	– Minimum and maximum air temperature (Tnx) – Reference evapotranspiration (ETo) – Rainfall (PLU) – Mean annual atmospheric CO2
	Field management	If applicable specify: – limited soil fertility – field surface practices affecting surface runoff – weed infestation
	Irrigation management	None (rainfed cropping)
Dry season (Run 2)		
	Climate	– Minimum and maximum air temperature (Tnx) – Reference evapotranspiration adjusted to system (ETo/f_{root}) – Rainfall (PLU) – Mean annual atmospheric CO2
	Field management	Mulches (to inhibit/reduce soil evaporation in the system) If applicable specify: – limited soil fertility
	Irrigation management	Irrigation schedule (see Table 1 for the computation of the net irrigation application dose)